TREATMENT OF HOSPITAL WASTEWATER USING ACTIVATED CARBON FROM NEEM *(AZADIRACHTA INDICA)* HUSK AND SEED CAKE

By

KENNETH KUKHIYEP ALAU

DEPARTMENT OF CHEMISTRY
AHMADU BELLO UNIVERSITY, ZARIA
NIGERIA.

JANUARY, 2016

TREATMENT OF HOSPITAL WASTEWATER USING ACTIVATED CARBON FROM NEEM *(AZADIRACHTA INDICA)* HUSK AND SEED CAKE

By

Kenneth Kukhiyep ALAU, B.Sc. (Hons.) 2005, M.Sc. 2010, (A.B.U.)

PhD/Sci/12644/2010-2011

A PhD THESIS SUBMITTED TO THE SCHOOL OF POSTGRADUATE STUDIES, AHMADU BELLO UNIVERSITY

IN PARTIAL FULFILLMENT OF THE REQUIREMENTS FOR THE AWARD OF DOCTORATE DEGREE IN ANALYTICAL CHEMISTRY

DEPARTMENT OF CHEMISTRY
AHMADU BELLO UNIVERSITY, ZARIA
NIGERIA

JANUARY, 2016

DECLARATION

I declare that the work in the Thesis entitled "**PRODUCTION OF ACTIVATED CARBON FROM NEEM *(AZADIRACHTA INDICA)* HUSK AND CAKE FOR THE TREATMENT OF HOSPITAL WASTEWATER**" has been performed by me in the Department of Chemistry, Ahmadu Bello University, Zaria. The information derived from the literature has been duly acknowledged in the text and a list of references provided. No part of this thesis was previously presented for another degree or diploma in this or any other institution.

_____	_____	_____
Name of Student	Signature	Date

CERTIFICATION

This Thesis entitled "**PRODUCTION OF ACTIVATED CARBON FROM NEEM *(AZADIRACHTA INDICA)* HUSK AND CAKE FOR THE TREATMENT OF HOSPITAL WASTEWATER**" by Kenneth Kukhiyep ALAU meets the regulations governing the award of the degree of Doctor of Philosophy in Analytical Chemistry of Ahmadu Bello University, and is approved for its contribution to knowledge and literary presentation.

	_____	_____
Professor C.E. Gimba Chairman, Supervisory Committee	Signature	Date
	_____	_____
Professor E.B. Agbaji Member, Supervisory Committee	Signature	Date
	_____	_____
Dr. S.E. Abechi Member, Supervisory Committee	Signature	Date
	_____	_____
Professor V.O. Ajibola Head of Department	Signature	Date
	_____	_____
Professor K. Bala Dean, School of Post Graduate Studies	Signature	Date

DEDICATION

This research work is dedicated to the Almighty God, the Alpha and Omega, the Author and Finisher of my Faith.

ACKNOWLEDGEMENT

All glory, honour, power and majesty to Almighty God, Jesus Christ and the Holy Spirit, whose power working in me performed infinitely more than I can ever ask or imagine and especially for guiding, keeping and protecting me throughout my study period, I am most grateful.

Special gratitude goes to my able supervisors: Prof. Casmir Emmanuel Gimba, Prof. Edith Bolanle Agbaji and Dr. Stephen Eyije Abechi who, despite their tight schedules, still had time for me. I must confess that I am thrilled and humbled by the confidence and trust bestowed on me. I am grateful for the corrections, advice, encouragement and above all the love and concern you showered on me despite my weakness. I pray that the good Lord will preserve, bless and be gracious to you all.

My appreciation also goes to Mr. Marcus Kasai of NARICT who despite the scarcity of the sample as at the time of the collection went extra mile to assist in obtaining the sample. Special thanks to the management of the Abuja University Teaching Hospital and especially the Medical Director, Hospital Ethical Committee, Engr. Mabas Bala Mangut, Mr. Isa Adamu and all those that supported me in the wastewater collection and ethical approval. I also appreciate Mr. Oche Ochibo, Mr. Ekwuribe Silas, staff of Multi-Purpose Laboratory and the analyst in the Department of Soil Science for their support in analyzing my sample. Special thanks to Dr. Moses Yilleng for liaising with Queens University Belfast, UK in analyzing most of my samples.

I wish to express my sincere appreciation and love to all the academic and technical staff and students of the great Department of Chemistry, A.B.U., Samaru, Zaria. This study cannot be complete without the able support of a friend and brother, in the person of Dr. Emeka Nwankwere, who stood by me despite his tight schedule. I pray God to bless you specially. I cannot forget my roommate and friend, John Anyam who supported me in the struggle. I thank God especially for my parents, Dr. and Mrs. Donatus Alau, for their continuous support, encouragement and parental love, care and concern to see me successful. I pray God to reward you in a very special way and may

you be honored. To my brothers and sister, Cornelius, Douglas, Amos and Caroline, thanks for tolerating and accommodating my deficiencies. May the good Lord uphold you and may His love and peace continue to bind us all as a family. To my lovely wife, Fatima Faustina Kulak Alau and my precious children Joseph Tisan Alau and Justina Chat Alau who sacrificed their time and stood by me during the course of my work, may God grant you your heart desires. I wish to express my sincere gratitude and appreciation to my uncle, Dr. Daniel Kajang for his immense contribution in making me who I am, I pray God to continue to bless him and his family. I will not forget Mr. and Mrs. Joseph Patrick, Mr. and Mrs. Tobias John, Mr. and Mrs. Silver Mathias, Mr. and Mrs. Enoch Asimya for their immense support, encouragement and advice.

This will not be complete without the mention of my late supervisors, Prof. G.F.S. Harrison and Prof. J.A. Kagbu for their positive impact in my life. I also pray for the soul of late Prof. J.F. Iyun, may their souls and souls of all the faithful departed rest in peace. Amen.

ABSTRACT

Management of hospital wastes remains a subject of public health interest due to their hazardous nature. Most of the hospital wastes are not easily degradable by natural phenomena of biochemical decomposition. However, they can be attenuated by adsorption on a suitable medium and recovered or isolated through various treatment techniques. Commercial adsorbents are expensive and not readily available locally although activated carbon has been developed from natural materials. The need to further research on these wastes to convert them into adsorbent in order to reduce waste and conserve cost is the key to the research work. The present research produced and used activated carbon from neem *(Azadirachta indica)* husk and seed cake to treat hospital wastewater. The wastewater sample used was obtained from the University of Abuja Teaching Hospital (UATH) wastewater treatment plant after certification and approval by the Hospital Ethical Committee (HEC). The raw neem husk and seed cake were carbonized at 400^{o}C and activated with $ZnCl_2$ and H_3PO_4 at 500^{o}C and 550^{o}C respectively. The moisture content of the Raw Neem Husk (RNH) and Raw Neem Cake (RNC) were found to be 4.45% and 8.95% respectively. The microstructural, structural and thermal properties of the adsorbents were studied using nitrogen gas adsorption analysis, SEM, FTIR and TGA. The surface areas and pore size of the neem activated carbons are in this order: NCH (352 m^2g; 34.26 Å)> NCZ (252.18 m^2g; 24.16 Å) > NHZ (238.56 m^2g; 22.46 Å) >NHH (230.79 m^2g; 22.22 Å). The FTIR results showed slight changes in the absorption band of the raw neem material compared to that of the activated neem carbon. This showed that the activation process was successful. The TGA results showed that the activated carbon were hydrophobic and thermally stable up to 450^{o}C. The adsorbent has been found to be effective and efficient in reducing the

investigated parameters in a multi component system. The adsorbents (Neem Cake activated with H_3PO_4 (NCH), Neem Cake activated with $ZnCl_2$ (NCZ), Neem Husk activated with $ZnCl_2$ (NHZ) and Neem Husk activated with H_3PO_4 (NHH)) reduced nitrates and chloride ions by 100%, phosphate ions by 95%, total bacterial load by 99%, total fungal load by 90%, chromium ion by 82%, lead ion by 70%, nickel ion by 61%, zinc ion by 59% and cadmium ion by 36%. The kinetic data were fed into the pseudo-second-order rate and the Weber and Morris intraparticle diffusion models. The results showed that the mechanism of removal of the pollutants was by chemisorption and that intraparticle diffusion was not the only rate determining step in the process. The Equilibria results were modelled using the Langmuir and Freundlich isotherm models. The adsorption pattern fitted into the two models but more favourably described by the Langmuir isotherm than the Freundlich isotherm, suggesting the adsorption was predominantly monolayer rather than multilayer. Column studies showed that the adsorption of nickel ion onto neem husk activated with H_3PO_4 (NHH) depends on flow rate, inlet concentration and bed height. This was analyzed using the Admas–Bohart model. Studies on regeneration and reuse of the adsorbent on the wastewater showed that the adsorbents can be reused up to the fifth cycle.

Table of Content

DECLARATION ii

CERTIFICATION iii

DEDICATION iv

ACKNOWLEDGEMENT v

ABSTRACT vii

Table of Content ix

List of Appendices xvi

List of Figures xvii

List of Tables xxiii

List of Abbreviations xxiv

CHAPTER ONE 1

1.0 INTRODUCTION 1

1.1 Origin of Wastewater 2

1.1.1 Wastewater constituents 2

1.1.2 Effect of untreated wastewater on the environment 3

1.1.3. Hospital wastewater 4

1.2 Statement of the Problem 6

1.3 Justification 7

1.4 Aim and Objectives 7

CHAPTER TWO 9

2.0 LITERATURE REVIEW 9

2.1 History of Activated Carbon **9**

2.2 Structure of Activated carbon **11**

2.3 Sources of Activated Carbon **13**

2.4 Adsorptive Properties of Activated Carbon **14**

2.5 Preparation of Activated Carbon **15**

2.5.1 Carbonization 15

2.5.2 Activation 17

2.6 General Uses of Activated Carbon **20**

2.7 Application of Activated Carbon in Environmental Pollution Studies **21**

2.7.1 Activated carbon in drinking water treatment 21

2.7.2 Municipal wastewater treatment 22

2.7.3. Industrial wastewater treatment 23

2.7.4. Hospital wastewater treatment 23

2.8 Activated Carbon Adsorption **25**

2.9 Theory of adsorption **25**

2.9.1 Types of adsorption 26

2.9.2 Extent of adsorption 27

2.9.3 Adsorption equilibria and the adsorption isotherm 27

2.9.4 Types of adsorption isotherms 27

2.9.5 Langmuir adsorption isotherm: 31

2.9.6 Freundlich adsorption isotherm 31

2.9.7 Factors affecting adsorption 33

2.10 Adsorption Process 34

2.11 Modeling of Column Study Results: Bohart–Adams Model 36

2.12 The Pseudo-Second Order Rate Kinetic Model 37

2.13 The Weber-Morris Intraparticle Diffusion Model 38

CHAPTER THREE 39

3.0 MATERIALS AND METHODS 39

3.1 Materials 39

3.2 Sample Collection 39

3.2.1 Neem sample collection 39

3.2.2 Wastewater sample collection 39

3.2.3 Description of wastewater sampling area 40

3.3 Neem Sample Preparation 42

3.4 Carbonization of Neem samples 42

3.5 Chemical Activation of the Carbon 43

3.6 Physico-chemical Characterization of Raw and Modified Neem Samples 43

3.6.1 Moisture and dry matter content 44

3.6.2 Ash content 44

3.6.3 Volatile matter content 45

3.6.4 Fixed carbon content 45

3.6.5 Density and bulk density 46

3.7 Structural and Morphological Characterization **46**

3.7.1 Brunauer Emmet Teller (BET) surface area 47

3.7.2 Fourier Transform Infrared Spectroscopy (FTIR) analysis 48

3.7.3 Scanning Electron Microscopy (SEM) analysis 48

3.7.4 Thermal Gravimetric Analysis (TGA) 48

3.8 Physico-Chemical Parameters of Wastewater **49**

3.8.1 pH 49

3.8.2 Turbidity Test 49

3.8.3 Conductivity 50

3.8.4 Biological Oxygen Demand (BOD) 50

3.8.5 Chemical Oxygen Demand (COD) 50

3.8.6 Total Dissolved Solid (TDS) 51

3.8.7 Total Solids (TS) 52

3.8.8 Determination of metal ions 52

3.8.9 Nitrate, Phosphate and Sulphate 53

3.8.10 Microbial Analysis and Enumeration 53

3.9 Column Adsorption Studies **54**

3.9.1 Column breakthrough studies 55

3.9.2 The effect of contact time 57

3.9.3 The effect of wastewater volume 57

3.9.4 Regeneration Studies 57

CHAPTER FOUR 58

4.0 RESULTS 58

4.1 Physicochemical Properties of Raw Neem and the Prepared Activated Carbons 58

4.2 The BET Surface Area and Pore Characterization of the prepared Activated Carbon 58

4.3 Fourier Transform Infrared (FTIR) Analysis 67

4.4 Scanning Electron Microscope (SEM) 67

4.5 Thermal-Analytical Studies 79

4.6 Physicochemical Characteristics of the Hospital Wastewater Before and After Treatment 79

4.7 Kinetic Studies 91

4.8 Pseudo-Second-Order Rate Models 110

4.9 Weber and Morris Intraparticle Diffusion Models 110

4.10 Effect of initial wastewater volume on physicochemical parameters of the wastewater 129

4.11 Langmuir Adsorption Isotherm 129

4.12 Freundlich Adsorption Isotherm 158

4.13: Regeneration and Reuse Studies 158

4.14 Bohart Adams Adsorption Model 169

CHAPTER FIVE 174

5.0 DISCUSSION 174

5.1 Physicochemical properties of raw neem and the prepared activated carbons **174**

5.2 Carbonization of Neem Husk and Cake **175**

5.3 Activation of Neem Husk and Cake **176**

5.4 BET Surface Area and Pore Characterization of the Prepared Activated Carbon **176**

5.5 Fourier Transform Infrared (FTIR) Analysis **177**

5.6 Scanning Electron Microscope (SEM) **179**

5.7 Thermoanalytical Studies **180**

5.8 Physicochemical Characteristics of the Hospital Wastewater Before Treatment **181**

5.9 Physicochemical parameters of the treated Water **182**

5.9.1 pH 183

5.9.3 Turbidity 184

5.9.4 Total Hardness (TH) 184

5.9.5 Chemical Oxygen Demand (COD) 185

5.9.6 Biochemical Oxygen Demand (BOD) 185

5.9.7 Dissolved Oxygen (DO) 186

5.9.8 Nitrate 186

5.9.9 Phosphates 187

5.9.10 Chloride 187

5.9.11 Heavy metals 188

5.10 Microbial load reduction activities of Neem Activated Carbon 189

5.11 The Pseudo-Second-Order Rate Kinetic Model 190

5.12 The Weber-Morris Intraparticle Diffusion Model 191

5.13 Equilibrium Adsorption Studies 192

5.13.1 Effect of initial wastewater volume on physicochemical parameters of the wastewater 192

5.14 The Langmuir Sorption Isotherm 194

5.15 Freundlich Adsorption Isotherm 195

5.16 Regeneration and Reuse Studies 195

5.17 Bohart Adams Model 196

CHAPTER SIX 197

6.0 SUMMARY, CONCLUSION AND RECOMMENDATION 197

6.1 Summary 197

6.2 Conclusion 198

6.3 Recommendation 200

REFERENCES 201

APPENDICES 212

List of Appendices

Appendix I: Ethical Approval 212

Appendix II: Physicochemical Properties of Hospital wastewater before and after treatment with adsorbents 213

Appendix III: Effect of bed height on breakthrough time 214

Appendix IV: Federal Environmental Protection Agency (Maximum Permissible Limit) 215

List of Figures

Figure 2.1: BET classification of the different types of adsorption isotherms 28

Figure 2.2: Fixed and Expanded Adsorption bed 34

Figure 2.3: Comparism between fixed-bed adsorbers in series and parallel 35

Figure 3.1: Map of Abuja indicating the location of University of Abuja Teaching Hospital 41

Figure 3.2: Schematic of laboratory column adsorption filter setup 55

Figure 4. 1: Effect of carbonization temperature on methylene(MB) adsorption 60

Figure 4. 2: Effect of activation temperature on methylene blue (MB) adsorption 61

Figure 4. 3: Nitrogen adsorption isotherm plot for neem cake activated with $ZnCl_2$ (NCZ) 63

Figure 4. 4: Nitrogen adsorption isotherm plot for neem husk activated with $ZnCl_2$ (NHZ) 64

Figure 4. 5: Nitrogen adsorption isotherm plot for neem husk activated with H_3PO_4 (NHH) 65

Figure 4. 6: Nitrogen adsorption isotherm plot for neem cake activated with H_3PO_4 (NCH) 66

Figure 4. 7: Fourier Transform Infrared Spectroscopy of the Raw Neem Husk (RNH) 68

Figure 4. 8: Fourier Transform Infrared Spectroscopy of Neem Husk activated with $ZnCl_2$ (NHZ) 69

Figure 4. 9: Fourier Transform Infrared Spectroscopy of Neem Husk activated with H_3PO_4 (NHH) 70

Figure 4. 10: Fourier Transform Infrared Spectroscopy of the Raw Neem Cake (RNC) 71

Figure 4. 11: Fourier Transform Infrared Spectroscopy of the Neem Carbon activated with H_3PO_4 (NCH) 72

Figure 4. 12: Fourier Transform Infrared Spectroscopy of Neem Cake activated with $ZnCl_2$ (NCZ) 73

Figure 4. 13: Micrograph of the transverse section of Neem Cake activated with $ZnCl_2$ (NCZ) 75

Figure 4. 14: Micrograph of the transverse section of Neem Husk activated with $ZnCl_2$ (NHZ) 76

Figure 4. 15: Micrograph of the transverse section of Neem Husk activated with H_3PO_4 (NHH) 77

Figure 4. 16: Micrograph of the transverse section of Neem Cake activated with H_3PO_4 (NCH) 78

Figure 4. 17: Thermogram of Neem Cake activated with $ZnCL_2$ (NCZ) 80

Figure 4. 18: Thermogram of Neem Cake activated with H_3PO_4 (NCH) 81

Figure 4. 19: Thermogram of Neem Husk activated with $ZnCl_2$ (NHZ) 82

Figure 4. 20: Thermogram of Neem Husk activated with H_3PO_4 (NHH) 83

Figure 4. 21: Effect of Treatment of wastewater with prepared neem carbons on COD, BOD and DO 85

Figure 4. 22: Effect of Treatment of wastewater with prepared neem carbons on Turbidity, conductivity and pH 86

Figure 4. 23: Effect of Treatment of wastewater with prepared neem carbons on hardness and total dissolved solids 87

Figure 4. 24: Effect of Treatment of wastewater with prepared neem carbons on nitrates, phosphates and chloride ions 88

Figure 4. 25: Adsorption Capacities of sorbent for heavy metal ion 89

Figure 4. 26: Effect of Treatment of wastewater with prepared neem carbons on bacterial and fungal count 90
Figure 4. 27: The effect of contact time on conductivity of treated water 92
Figure 4. 28: The effect of contact time on pH of treated water 93
Figure 4. 29: The effect of contact time on turbidity of treated water 94
Figure 4. 30: The effect of contact time on COD of treated water 95
Figure 4. 31: The effect of contact time on BOD of treated water 96
Figure 4. 32: The effect of contact time on DO of treated water 97
Figure 4. 33: The effect of contact time on TDS of treated water 98
Figure 4. 34: The effect of contact time on hardness of treated water 99
Figure 4. 35: The effect of contact time on nitrate concentration of treated water 100
Figure 4. 36: Effect of contact time on phosphate concentration of treated water 101
Figure 4. 37: Effect of contact time on chloride concentration of treated water 102
Figure 4. 38: Effect of contact time on cadmium ion of treated water 103
Figure 4. 39: The effect of contact time on chromium ion in treated water 104
Figure 4. 40: Effect of contact time on nickel ion in treated water 105
Figure 4. 41: Effect of contact time on lead ion in treated water 106
Figure 4. 42: Effect of contact time on zinc ion in treated water 107
Figure 4. 43: Effect of contact time on bacterial load in treated water 108
Figure 4. 44: Effect of contact time on fungal load in treated water 109
Figure 4.45: The pseudo-second order plot for chloride ions removal 111
Figure 4. 46: The pseudo-second order plot for nitrate ion removal 112
Figure 4. 47: The pseudo-second order plot for phosphate ion removal 113
Figure 4. 48: The pseudo-second order plot for cadmium ion removal 114
Figure 4. 49: The pseudo-second order plot for chromium ion removal 115

Figure 4. 50: The pseudo-second order plot for zinc ion removal 116

Figure 4. 51: The pseudo-second order plot for nickel ion removal 117

Figure 4. 52: The pseudo-second order plot for lead ion removal 118

Figure 4. 53: Weber and Morris diffusion models plot for chloride ion 120

Figure 4. 54: Weber and Morris diffusion models plot for nitrates ion 121

Figure 4. 55: Weber and Morris diffusion models plot for phosphates ion 122

Figure 4. 56: Weber and Morris diffusion models plot for nickel ion 123

Figure 4. 57: Weber and Morris diffusion models plot for zinc ion 124

Figure 4. 58: Weber and Morris diffusion models plot for chromium ion 125

Figure 4. 59: Weber and Morris diffusion model plot for cadmium ion 126

Figure 4. 60: Weber and Morris diffusion model plot for lead ion 127

Figure 4. 61: Effect of initial volume of wastewater on pH of treated water 131

Figure 4. 62: Effect of initial volume of wastewater on conductivity of treated water 132

Figure 4. 63: Effect of initial volume of wastewater on TDS of treated water 133

Figure 4. 64: Effect of initial volume of wastewater on turbidity of treated water 134

Figure 4. 65: Effect of initial volume of wastewater on hardness of treated water 135

Figure 4. 66: Effect of initial volume of wastewater on COD of treated water 136

Figure 4. 67: Effect of initial volume on BOD level of treated wastewater 137

Figure 4. 68: Effect of initial volume of wastewater on DO of treated water 138

Figure 4. 69: Effect of initial volume of wastewater on chloride ion conc. of treated water 139

Figure 4. 70: Effect of initial volume of wastewater on nitrate ion conc. of treated water 140

Figure 4. 71: Effect of initial volume of wastewater on phospate ion conc. of treated water 141

Figure 4. 72: Effect of initial volume of wastewater on cadmium ion conc. of treated water 142
Figure 4. 73: Effect of initial volume of wastewater on chromium ion conc. of treated water 143
Figure 4. 74: Effect of initial volume of wastewater on zinc ion conc. of treated water 144
Figure 4. 75: Effect of initial volume of wastewater on nickel ion conc. of treated water 145
Figure 4. 76: Effect of initial volume of wastewater on lead ion conc. of treated water 146
Figure 4. 77: Effect of initial volume of wastewater on bacterial load of treated water 147
Figure 4. 78: Effect of initial volume of wastewater on fungal load of treated water 148
Figure 4. 79: Langmuir adsorption model for chloride ion 149
Figure 4. 80: Langmuir adsorption model for nitrate ion 150
Figure 4. 81: Langmuir adsorption model for phosphate ion 151
Figure 4. 82: Langmuir adsorption model for cadmium ion 152
Figure 4. 83: Langmuir adsorption model for chromium ion 153
Figure 4. 84 : Langmuir adsorption model for lead ion 154
Figure 4. 85: Langmuir adsorption model for zinc ion 155
Figure 4. 86: Langmuir adsorption model for nickel ion 156
Figure 4. 87: Freundlich Isotherm models for chloride ion 159
Figure 4. 88: Freundlich Isotherm models for nitrate ion 160
Figure 4. 89: Freundlich Isotherm models for phosphate ion 161
Figure 4. 90: Freundlich Isotherm models for chromium ion 162

Figure 4. 91: Freundlich Isotherm models for zinc ion 163

Figure 4. 92: Freundlich Isotherm models for cadmium ion 164

Figure 4. 93: Freundlich Isotherm models for lead ion 165

Figure 4. 94: Freundlich Isotherm models for nickel ion 166

Figure 4. 95: The Breakthrough curve for nickel ion adsorption on NHH 170

Figure 4. 96: The effect of bed height on the adsorption capacity ($Q_{0.5}$) 171

Figure 4. 97: Effect of bed height on the breakthrough time 172

List of Tables

Table 4. 1 Physicochemical parameters of the raw and activated neem (*Azadirachta indica*) husk and cake: 59

Table 4. 2 BET Surface Area and Pore characterization of the activated carbon 62

Table 4. 3 FTIR Table of assignment for the raw and activated neem carbon 74

Table 4. 4 Thermal Gravimetric Analysis of the neem activated carbon 84

Table 4. 5 The Pseudo-second-order rate equation constant for neem carbon on wastewater 119

Table 4. 6 The Weber and Morris Difussion model constants 128

Table 4. 7 The Langmuir isotherm equation constants 157

Table 4. 8 Freundlich Isotherm model constants 167

Table 4. 9 Efficiency of regeneration and reuse of the activated carbon (NHH) 168

Table 4. 10 Bohart Adams Parameters from Ni (II) adsorption in wastewater 173

List of Abbreviations

AC	Activated Carbon
ACt	Ash Content
ANOVA	Analysis of Variance
BD	Bulk Density
BET	Brunauer-Emmet-Teller
Conc	Concentration
DTG	Differential Thermal Gravimetry
K_f	Freundlich Constant
MC	Moisture content
NCZ	Neem Cake activated with $ZnCl_2$
NCH	Neem Cake activated with H_3PO_4
NHZ	Neem Husk activated with $ZnCl_2$
NHH	Neem Husk activated with H_3PO_4
PSOR	Pseudo-second-order rate
Qe	Equilibrium sorption Capacity
Qo	Initial sorbate concentration
RNH	Raw Neem Husks
RNS	Raw Neem Seed
R^2	Coefficient of Regression
R_L	Langmuir separation factor
SA	Surface Area

TGA/DSC	Thermal Gravimetric Analysis/Differential scanning Calorimetry
UNDP	United Nation Development Program
USEPA	United States Environmental Protection Agency
VMC	Volatile Matter Content
WMIDM	Weber and Morris Intra Diffusion Model

CHAPTER ONE

1.0 INTRODUCTION

The world economy is focusing on better waste management policies so as to reduce wastes and to protect the environment (Tchnohanoglous *et al*., 1979). The present generation has an obligation to leave the next generation a more habitable environment than a surrounding littered with pollutants. This is in recognition that the world is finite and the continued pollution of the environment will, if not controlled, be difficult to rectify in the future. In Nigeria, it has been reported that poor management of waste cost the Nation roughly US$5 billion annually (Christen, 1996). Much of the damage results from oil exploration and oil spills in the Niger Delta region, poor agricultural practices, grazing, hospital waste and habitat destruction (Christen, 1996). Indiscriminate waste disposal remains a contentious issue with no end in sight. Refuse is thrown onto roadways, spread on pedestrian walkways or even dumped into gutters. The problem becomes compounded during the rainy season; water, no longer flowing freely along the gutters, remains stagnant, creating the conducive conditions for mosquitoes and vector borne diseases like malaria (Coker, 2009).

Wastewater is any water that has been adversely affected in quality by anthropogenic influence (Akter *et al*., 1999). Municipal wastewater is usually conveyed in a combined sewer or sanitary sewer, and treated at a wastewater treatment plant. The treated wastewater is then discharged into receiving water via an effluent sewer. Wastewaters generated in areas without access to centralized sewer systems rely on on-site wastewater systems. These typically comprise a septic tank, drain field, and optionally an on-site treatment unit (USEPA, 2008).

1.1 Origin of Wastewater

Some of the origins of wastewater or sewage include: human waste (used toilet paper or wipes, urine, or other bodily fluids), also known as blackwater, usually from lavatories; Cesspit leakage; Septic tank discharge; Sewage treatment plant discharge; washing water (personal, clothes, floors and dishes), also known as greywater or sullage; rainfall collected on roofs, yards, hard-standings (generally clean with traces of oils and fuel); Groundwater infiltrated into sewage; Surplus manufactured liquids from domestic sources (drinks, cooking oil, pesticides, lubricating oil, paint and cleaning liquids); Urban rainfall runoff from roads, carparks, roofs, sidewalks/pavements (contains oils, animal faeces, litter, gasoline/petrol, diesel or rubber residues, soapscum, metals from vehicle exhausts); hospital waste; Industrial waste; Industrial site drainage which include; silt, sand, alkali, oil, chemical residues (USEPA, 2008).

1.1.1 Wastewater constituents

The composition of wastewater varies widely; a partial list of these constituents are: (i) Water (more than 95 percent), which is often added during flushing to carry waste down a drain; (ii) Pathogens such as bacteria, viruses, prions and parasitic worms; (iii) Non-pathogenic bacteria; Organic particles such as faeces, hairs, food, vomit, paper fibres, plant material and humus; (iv) Soluble organic material such as urea, fruit sugars, soluble proteins, drugs, pharmaceuticals; (v) Inorganic particles such as sand, grit, metal particles, ceramics; (vi) Soluble inorganic material such as ammonia, road-salt, sea-salt, chloride, cyanide, hydrogen sulfide, nitrite, thiocyanates, thiosulfates, phosphate; (vii) Animals such as protozoa, insects, arthropods, small fish; (viii) Macro-solids such as sanitary napkins, nappies/diapers, condoms, needles, children's toys, dead animals or plants; (ix) Gases such as hydrogen sulfide, carbon dioxide, methane; (x) Emulsions

such as paints, adhesives, mayonnaise, hair colorants, emulsified oils; (xi) Toxins such as pesticides, poisons, herbicides; Pharmaceuticals and hormones (USEPA, 2008).

1.1.2 Effect of untreated wastewater on the environment

Management of healthcare wastes (HCW) should be considered as an integral part of hospital hygiene and infection control (David *et al*., 2012). The HCW generated within a healthcare facility should always follow an appropriate and well define treatment process starting from their point of generation until their final disposal (David *et al*., 2012). The poor segregation, handling and disposal practices of many hospitals, clinics and health centres are likely representatives of practices throughout Nigeria and pose serious health hazards to people living in the vicinity of healthcare institutions (Ferreira and Veiga, 2003; Da Silver *et al*., 2005; Tudor *et al*., 2005; Ndidi *et al*., 2009).

Untreated wastewater may drain directly into major watersheds, this can have serious impacts on the quality of an environment and on the health of people. Pathogens contained in such water can cause a variety of illnesses. Some chemicals pose risks even at very low concentrations and can remain a threat for long periods of time because of bioaccumulation in animal or human tissue and a significant portion of the waste management is non-degradable (Clescerl *et al*., 2010). It was reported that some health care institutions dispose of all wastes to municipal dumpsites without pre-treatment, leading to an unhealthy and hazardous environment around the health institutions, affecting patients, staff and the community Stephen and Elija (2011). Same findings have been reported by Al-Khatib *et al*. (2009) in Palestine, Akinwale *et al*. (2010) in Nigeria and Mesfin *et al*. (2011) in Ethopia. Studies have shown that infectious stools or bodily fluids that are not treated before being disposed can create and even extend epidemics (Rhodes *et al*., 2000). Mumtaz and Mirza (2014) reported that the absence of

proper sterilization procedures is believed to have increased the severity and size of cholera epidemics in Africa during the last decade.

1.1.3. Hospital wastewater

Hospital waste in simple term is any waste generated during the diagnosis, treatment, or immunization of human beings or animals or in research activities in these fields (Ogunlowo *et. al.,* 1991). It may include items like disposables, anatomical waste, cultures, discarded medicines, chemicals, disposable syringes, swabs, bandages, body fluids, human and excreta. This waste are highly infectious and can be a serious threat to human health if not managed in a scientific and discriminate manner. It had been roughly estimated that of the 4 kg of waste generated in a hospital at least 1kg would be infectious (Ogunlowo *et al*., 1991).

Hospital waste can be classified into infectious and non-infectious wastes (Patil and Shekdar, 2001). Infectious wastes contain pathogens in quantities sufficient to transmit infectious diseases on exposure to them. Health care waste is also categorized as non hazardous (non risky) and hazardous (risky) wastes (Pruss *et al*., 1999). A hazardous waste may be toxic, genotoxic, corrosive, shock sensitive, flammable, reactive, explosive, radioactive, containing infectious agents and/or sharps (Pruss *et al*., 1999). In 1999, WHO classified healthcare waste into two broad categories, the first is the communal waste which comprises of all solid waste not including infectious, chemical, or radioactive waste. This waste stream can include items such as packaging materials and office supplies. Generally, this stream can be disposed of in a communal land fill or other such arrangement. Segregation of materials which are able to be reused or recycled will greatly reduce the impact burden of this waste stream. The second category is called the special waste which consists of several different subcategories:

Infectious: Discarded materials from health-care activities on humans or animals which have the potential of transmitting infectious agents to humans. These include discarded materials or equipment from the diagnosis, treatment and prevention of disease, assessment of health status or identification purposes, that have been in contact with blood and its derivatives, tissues, tissue fluids or excreta, or wastes from infection isolation wards. Such wastes shall include, but are not limited to, cultures and stocks; tissues; dressings, swabs or other items soaked with blood; syringe needles; scalpels; diapers; blood bags. Incontinence material from nursing homes, home treatment or from specialized health-care establishments which do not routinely treat infectious diseases (e.g. psychiatric clinics) is an exception to this definition and are not considered as infectious health-care waste. Sharps, whether contaminated or not, should be considered as a subgroup of infectious health-care waste includes: Syringe needles, scalpels, infusion sets, knives, blades, broken glass.

Anatomic: consists of recognizable body parts.

Pharmaceutical: Consisting of/or containing pharmaceuticals, including: expired, no longer needed; containers and/or packaging, items contaminated by or containing pharmaceuticals (bottles, boxes).

Genotoxic: Consisting of, or containing substances with genotoxic properties, including cytotoxic and antineoplasic drugs; genotoxic chemicals.

Chemical: Consisting of, or containing chemical substances, including: laboratory chemicals; film developer; disinfectants expired or no longer needed; solvents, cleaning agents and others.

Heavy Metals: Consisting of both materials and equipment with heavy metals and derivatives, including: batteries, thermometers, manometers.

Pressurized containers: Consisting of full or empty containers with pressurized liquids, gas, or powdered materials, including gas containers and aerosol cans.

Radioactive materials: Includes: unused liquids from radiotherapy or laboratory research; contaminated glassware, packages or absorbent paper; urine and excreta from patients treated or tested with unsealed radionuclides; sealed sources (WHO, 1999).

1.2 Statement of the Problem

It has been reported that several hundreds of tonnes of HCWs are deposited in open dumpsites untreated alongside non-hazardous solid wastes (Alagoz and Kocasay, 2007), Abah and Ohimain, 2010) which pose health risks to health workers, cleaning staff, patients, visitors, waste collectors, disposal site staff, waste pickers, drug addicts and those who knowingly or unknowingly use "recycled" contaminated syringes and needles. A study conducted by Wyasu and Okereke (2011) established that hospital wastewater from Ahmadu Bello University Teaching Hospital contained significant amount of the following parameters; micro organisms, nitrate, sulphate and phosphate, heavy metals and organic contaminants which can cause serious health hazard to humans, aquatic biota, euthrophication of the water bodies, depreciation of land values, and other environmental challenges if left untreated or improper treatment. This is contrary to the international policy on waste management which states that the generator of waste is responsible for the proper management, treatment and disposal of waste (Ngwuluka *et al*., 2009). The World Health Organization estimates that each year there are about 8 to 16 million new cases of Hepatitis B virus (HBV), 2.3 to 4.7 million cases of Hepatitis C virus (HCV) and 80,000 to 160,000 cases of human immune deficiency virus (HIV) due to unsafe injections and mostly due to very poor waste management systems (WHO, 1999; Townend and Cheeseman, 2005). Recent studies in Nigeria have estimated waste generation of between 0.562 to 0.670 kg/bed/day (Longe

and Williams, 2006). Most of this hospital wastes are difficult to be degraded by natural phenomena of biochemical decomposition and the processes are expensive.

1.3 Justification

In a largely agrarian country such as Nigeria, there are so many agricultural by-products lying waste, littering and polluting the environment. The National Research Institute for Chemical Technology (NARICT) Bassawa, Zaria conducted series of researches on the neem tree (*Azadirachta indica)* and produced biodiesel and organic fertilizers from the neem kernel. Neem husk and seed cake are waste from the process. Several conventional techniques have been employed to treat wastewater in the past but all of these methods suffer from one or more limitations (efficiency, cost-effectiveness and availability) except adsorption Hajira and Muhammed (2008). It is known that the commercially made adsorbents are expensive. To this effect, within the last decade, several methods were developed to modify natural local materials and convert them to adsorbent to treat and adsorb waste and pollutants from effluents. The need to further research on these wastes to convert them into agents of environmental control in order to reduce waste and conserve cost is the key to the present research work.

1.4 Aim and Objectives

The aim of this research is to activate neem (*Azadirachta indica*) husk and seed cake with H_3PO_4 and $ZnCl_2$ and apply the prepared adsorbents for treatment of wastewater from hospital in a multi-component system. This aim was achieved through the following objectives;

i. to carry out physicochemical and structural characterization on the raw and modified neem (*Azadirachta indica)* husks and cakes using standard analytical techniques;

ii. to prepare activated carbon (AC) from neem (*Azadirachta indica)* husks and cakes by carbonization and impregnation methods using $ZnCl_2$ and H_3PO_4 as activating agents;

iii. to determine the structural and morphological characteristics of the raw and modified neem carbon by gravimetric, thermal and spectrometric methods;

iv. to determine the optimum carbonization and activation temperatures;

v. to study the effect of contact time and initial volume of the adsorbents and the adsorbates;

vi. to characterize the wastewater obtained from the hospital by determining the level of selected heavy metal ions (chromium, cadmium, nickel, lead and zinc), anions, DO, COD, BOD and other physicochemical parameters before and after treatment;

vii. to evaluate the efficiency of the activated carbon in a multi-component system;

viii. to investigate the adsorptive capacity of the adsorbent on microbial parameters (bacterial and fungal load); and

ix. to investigate the regeneration and reuse of the adsorbent on waste water.

CHAPTER TWO

2.0 LITERATURE REVIEW

2.1 History of Activated Carbon

Activated carbon is broadly defined to include a wide range of amorphous carbon-based materials prepared in such a way that they exhibit a high degree of porosity and an extended surface area (Bansal and Goyal, 2005). The use of activated carbon in its current form has only a short history. On the other hand, according to records, the use of carbon itself dates back to ancient times. The earliest known use of carbon in the form of wood chars (charcoal) by the Egyptians and Sumerians was in 3750 BC (Inglezakis and Poulopoulos, 2006). At that time, charcoal was used for various purposes such as reduction of ores in the manufacture of bronze, domestic smokeless fuel, and medicinal applications (Menendez-Diaz and Gullon, 2006). The ancient Greeks used charcoal to ease the symptoms of food poisoning due to its ability to adsorbed toxins emitted by ingested bacteria, thereby reducing their toxic effects (Menendez-Diaz and Gullon, 2006). Hindu documents dating to 450 BC refer to the use of sand and charcoal filters for the purification of drinking water (Hung *et al*., 2005). In the time of Hippocrates (ca. 460 –370 BC) and Pliny the Elder (AD 23–79) wood chars were employed for medicinal purposes (Hassler, 1974). In about 157 BC carbons of vegetable and animal origin were applied in the treatment of many diseases (Inglezakis and Poulopoulos, 2006). In the fifteenth century, during the time of Columbus, sailors used to blacken the insides of wooden water barrels with fire, since they observed that the water would stay fresh much longer. It is likely that people at that time proceeded by intuition only,

without having any insight into the mechanisms of the effect; these mechanisms were recognized beginning from the eighteenth century.

In the eighteenth century, carbons made from blood, wood, and animals were used for the purification of liquids. In 1805, wood charcoal was used in a large-scale sugar refining facility in France for decolorizing syrups, and by 1808 all sugar refineries in Europe were using charcoal as a decolorizer (Hung *et al*., 2005). In 1865 Hunter discovered the excellent gas adsorption properties of carbons derived from coconut shells (Hung *et al*., 2005). It is remarkable that the term 'adsorption' was first introduced by Kayser in 1881 to describe the uptake of gases by carbons (Hung *et al*., 2005).

Activated carbon was first produced on an industrial scale at the beginning of the twentieth century, and major developments then took place in Europe. However, at the beginning of the twentieth century activated carbon was only available in the form of powdered activated carbon (PAC). The Swedish chemist von Ostreijko obtained two patents, in 1900 and 1901, covering the basic concepts of chemical and thermal (or physical) activation of carbon, with metal chlorides and with carbon dioxide and steam, respectively (Sontheimer *et al*., 1988). In 1909, a plant named 'Chemische Werke' was built to manufacture, for the first time on a commercial scale, the powdered activated carbon Eponits from wood, adopting von Ostrejko's gasification approach (Dabrowski, 1998).

The NORIT Company, a manufacturer in Holland, first appeared in about 1911 and became widely known in the sugar industry (Hassler, 1974). The powdered activated carbons were used at that time mainly for decolorizing solutions in the chemical and food industries. On an industrial scale, the process of chemical activation of sawdust with zinc chloride was carried out for the first time in an Austrian plant at Aussing in

1914, and also in the dye plant of Bayer in 1915 (Dabrowski, 1998). This type of activation involved pyrolytical heating of the carbonaceous material in the presence of dehydrating chemicals such as zinc chloride or phosphoric acid (Purcell, 2006). In parallel to the developments in Europe, in the United States the first activated carbon was produced from black ash, a waste product of soda production, after it was accidentally discovered that the ash was effective in decolorizing liquids (Hassler, 1974). The first commercial production of activated carbon in the United States took place in 1913 (Hendricks, 2006). The use of poisonous gases in the First World War paved the way for the development and large-scale production of granular activated carbon (GAC). These carbons were used in gas masks for the adsorption of poisonous gases. Subsequently, they were used for water treatment, solvent recovery, and air purification (Hendricks, 2006). After the First World War, considerable progress was made in Europe in the manufacture of activated carbons using new raw carbonaceous materials such as coconut and almond shells. The treatment with zinc chloride yielded activated carbons with high mechanical strength and high adsorptive capacities for gases and vapors. Later, in 1935–1940, pelletized carbons were produced from sawdust by zinc chloride activation for the recovery of volatile solvents and the removal of benzene from town gas (Hung *et al.*, 2005). Nowadays, so many materials have been used as activated carbons and so many chemicals have as well been used as activating agents.

2.2 Structure of Activated carbon

Active carbons have a microcrystalline structure that starts to build up during the carbonization process (Hassler, 1974). However, the active carbon microcrystalline structure differs from that of graphite with respect to the interlayer spacing, which is 0.335 nm in the case of graphite and ranges between 0.34 and 0.35 nm in active carbons

(Bansal and Goyal 2005). The orientation of the microcrystallite layers is also different, being less ordered in active carbons. The volume of the pores in activated carbons is generally defined as being greater than 0.2ml/g and the internal surface area is generally larger than $400m^2/g$ as measured by the nitrogen BET method (Bansal and Goyal, 2005). The width of the pores varies from 3Å to several thousand angstroms, and the pores are generally classified for convenience in terms of their diameter:

Macropores	500 to 20000 **Å**
Transitional pores (mesopores)	100 to 500 **Å**
Micropores	8 to 100 **Å**

The pores appear to be cylindrical or rectangular in shape, but can also occur in a variety of irregular shapes (Bansal and Goyal, 2005). Pores may also have constrictions or bottleneck macropores, which generally contribute very little to the total internal surface area of the product, depend mainly on the nature of the carbonaceous raw material employed and the preliminary manufacturing process, viz grinding and agglomeration of the raw material (Hassler, 1974).

The pores serve as transport arteries that make the internal parts of the carbon granules readily accessible to the molecules being adsorbed (Mozammel *et al.*, 2002). The transitional pores account for about 5 per cent, and the micropores for about 95 per cent, of the internal surface area (Bansal and Goyal, 2005). The micropores are largely the product of the activation process. Activated carbons are commercially available in numerous forms: powders, granular chips in various size ranges, and shaped or moulded products extruded into rod-like shapes, which are commonly 0.8 to 6 mm in diameter by 3 to 10 mm in length (Mozammel *et al*., 2002).

X-ray diffraction studies show that the structure of activated carbon is similar to that of graphite (Bansal and Goyal, 2005). Ideal graphite consists of layers of fused hexagons

held approximately 3,35 Å apart by Van der Waals forces, so that the carbon atoms in any plane lie above the centres of the hexagons in the layer immediately below it. The structure of thermally activated carbon is believed to be composed of tiny graphite-like platelets, only a few carbon atoms thick, which form the walls of open cavities of molecular dimensions i.e. the pore system (Bansal and Goyal, 2005). However, the hexagonal carbon rings have undergone cleavage, and are randomly orientated, and lack the directional relationship with one another that is present in single graphite crystals. The overall structure is therefore very disordered, and is often referred to as *turbostrati*c (Bansal and Goyal, 2005). Furthermore, the separation between the layers is greater than that found in graphite, viz 3.60 Å. Because of the high level of structural imperfections in activated carbons, there are many possibilities for reactions with carbon atoms at the edges of the planar layers (Mattson and Mark, 1971). As a result, oxygen-containing organic functional groups, which are located mostly at the edges of broken graphitic ring systems, are present on the surface of the carbon makes the carbon to have both hydrophobic and hydrophilic tendencies (Mattson and Mark, 1971).

2.3 Sources of Activated Carbon

A wide variety of carbons have been prepared from agricultural wastes; bamboo dust, groundnut shell, rice husk and straw (Kannan and Meepkshisundaram, 2001); coconut shell and groundnut shell (Gimba, 2001); coconut husk and goat hair (Babarinde, 2002); Hazelnut shell (Demirbas *et al*., 2002); silk cotton ball, coconut tree sawdust, maize cob and banana pith (Kadirvelu *et al*., 2003); pecan shells (Bansode *et al*., 2003); walnut shell (Abeche, 2006); *Delonix regia Pods* and *Khaya senegalensis* Fruits (Ocholi, 2006). The conversion of this agricultural waste into activated carbons in waste water purification or the treatment of industrial and municipal effluents provides a potential and cheap alternative to existing commercial carbons.

Activated carbon derived from coconut tree sawdust was reportedly used to remove Cr (VI) from aqueous solution (Selvi *et al*. 2001). Activated carbon developed from a rapidly renewable bio-source was used for the removal of cadmium (II) and nickel (II) from dilute aqueous solutions (Bass *et al*., 2002). Cane from *Arundo donax*, a rapid growing plant was employed and converted to activated carbon by activating it with phosphoric acid. The carbons showed surface areas and total pore volumes of approximately 1100m^2/g and 1ml/g respectively. Study on agricultural waste from corn cob activated with $ZnCl_2$ produced an adsorbent with excellent microporous (Tsai *et al*., 2001). It has also been established that activated carbon can also be sourced from neem husk (Alau *et al.,* 2011).

2.4 Adsorptive Properties of Activated Carbon

These properties are indices representing the efficacy and efficiency of a particular activated carbon in function. The primary properties include; capacity, hardness, permeability, solubility and bulk density while the secondary properties include; pH, moisture and ash content (Abram, 1973). It is generally conceded that activated carbon owes its adsorptive properties primarily to its larger internal surface area, as well as to its *pore-size* distribution, and that the external surface area and the nature of the surface oxides play minor roles (Cheremisinoff and Ellerbusch, 1978). The size of the pores developed during activation therefore has an important influence on the adsorption behavior because the pores act as a screen. This screen prevents the adsorption of large molecules, but promotes the adsorption of an adsorbate that fits snugly into the pores, making the maximum number of contacts with the adsorbed molecule, and thus maximizing ΔH as defined mathematically in Equation 2.1.

$$\Delta H = \Delta G + T\,\Delta S \qquad 2.1$$

Where:

ΔH is the change in enthalpy, ΔG is the change in free energy, ΔS is the change in entropy, and T is the temperature of the system.

The external surface can provide only a certain amount of access to the inner pores, and it is likely that the main role of the surface oxides is to impart a hydrophilic character to the predominantly hydrophobic carbon skeleton. This would account for the affinity of activated carbon for many polar and non-polar organic and inorganic species. Adsorption occurs as a result of an imbalance of the forces that act upon the carbon atoms constituting the surface of the pore wall, such an imbalance is inherent in all surfaces and, in an attempt to rectify it molecules are adsorbed from the gaseous or aqueous phases, and are attracted and held to the surface. Surface adsorption, regardless of the energy of the interaction, must always proceed with a negative change in free energy (ΔG), as well as a decrease in entropy (ΔS), which according to above equation, must result in a negative change in free enthalpy (ΔH). Hence adsorption is always an exothermic process (Mattson and Mark., 1971).

2.5 Preparation of Activated Carbon

The most important steps in the preparation of activated carbon include:

2.5.1 Carbonization

Carbonization is the thermal conversion of cellulosic materials to char carbon (Mattson and Mark, 1971). The basic purpose of the carbonization process is to produce a carbonaceous char with a rudimentary pore system, which can be further developed by activation (Mattson and Mark, 1971). It involves heating the sample at an appropriate temperature, in an atmosphere of limited supply of oxygen. Here, most of the volatile

components are burned out leaving the char. The weight loss is usually 60 to 70% (Sun *et al.,* 1997; Diaz-Teran *et al.,* 2001). During carbonization, CO_2 and H_2O (g) which are the principal volatile products are expelled around 200-300°C Loo (1974). CO-complex and to some extent hydrogen, most likely gaseous products remaining, are only decomposed at higher temperature which means that relatively higher amounts of volatiles are given off initially Loo (1974). The removal of volatiles component as carbonization proceeds usually leads to the development of a structure, which may be significantly *micropores* and are initially accessible only to small molecules during adsorption and as carbonization continues, this pore structure may expand to give rise a *macropore*, which admit larger molecules (Bansal and Goyal, 2005). However, as carbonization proceed for longer periods at increased temperatures, it may lead to progressive closure of pore orifices and some cavities may be completely sealed off due to collapse of structure (Bansal and Goyal, 2005). At higher temperatures of carbonization and prolonged heating time, there will be further conversion of char carbon to CO or CO_2 in presence of oxygen, thus decreasing the weight of carbon at equilibrium as presented in Equations 2.2 and 2.3.

$$C_x + O_2 \longrightarrow 2CO + C_{x-2} \text{ Or} \qquad 2.2$$

$$C_x + O_2 \longrightarrow CO_2 + C_{x-1} \qquad 2.3$$

C_x = Char carbon

2.5.2 Activation

Activation is the process by which the chosen raw material or carbonized raw material is converted into finely crystalline form of carbon that is permeated by the greatest possible number of randomly distributed pores of various shapes and sizes (Mattson and Mark, 1971). The optimum pore structure was obtained when the sample were subjected to chemical activation followed by pyrolysis. These pores give rise to the extended internal surface area. In the preparation of activated carbon, it is desirable to develop the maximum accessible surface area that is commensurate with economic viability and product application (Mcdougall *et al.,* 1982). Activated carbon is made by the thermal decomposition of various carbonaceous material followed by an activation process. This is done to increase the adsorptive capacity of the carbonized materials. It involves heating the 'char' with activating agent(s) at high temperatures and cooling as fast as possible (Mozammel *et al.,* 2002). The aim of activation is to widen the pores of the charcoal to be used and hence, increasing the effective sites for adsorption. In chemical activation, the char is impregnated with an activating agent and fired to high temperatures. The activating agent(s) corrodes the carbon to form the pore structure (Mozammel *et al.,* 2002). Dehydrating salts, such as $CaCl_2$, MgCl, $ZnCl_2$, H_3PO_4 etc. are used to catalyze the carbonization process. The chars produced by carbonization have relatively little internal surface for adsorption applications (Cheremisinoff and Ellerbusch, 1978). To increase the surface area, the carbon is activated by the action of oxidizing agent, such as steam, air, or CO_2 at elevated temperature. The oxidizing gases attack the more readily oxidizable portions of the char resulting in the development of a porous structure and an extensive internal surface. (Cheremisinoff and Ellerbusch, 1978).

Activation of the carbon could involve gas activation or chemical activation. The gas activation process first involves heating in the absence of air to drive off volatile materials and to form small pores, this is followed by activation usually at a higher temperature. During the activation process, the edge group of the micro crystallite is burnt off to form macro pores followed by the burning off of the micro crystallite plane to form micro pores (Thomas and Crittenden, 1998). In the chemical activation process, dehydrating agents such as phosphoric acid, zinc chloride, sulphuric acid are commonly used to produce an activated carbon directly from the raw materials. Here, the porosity is developed by the action of the dehydrating chemical on the cellulosic structure of the starting material, or by the action of the oxidizing gases generated in the process (Abram, 1973). The effects of different activation methods on the adsorption characteristics of activated carbon from *Khaya senegalensis* fruit and *Delonix regia pods* were reported by (Turoti *et al*., 2007). The result showed that out of the four methods employed, two-step activation method is the most effective, this was followed closely by microwave method then impregnation method while one-step is the least.

A wide range of activating agents have be used in the past, these include; acids, inorganic salts, organic salts, bases, steam and carbon-dioxide. Others are: boric acid, calcium hydroxide, calcium phosphate, chlorine, cyanides, dolomite, ferric chloride, manganese chloride, manganese dioxide, manganese sulphate, nitric acid, phosphoric acid, potassium carbonate, potassium sulfide, potassium thiocyanate, sodium hydroxide, sodium phosphate, sodium sulphate, sulphur, sulphur dioxide, sulfuric acid and zinc chloride (Yehaskel, 1978). Recently, others used ethylenediamine tetraacetic acid ferric monosodium salt, ferrous oxalate, cobalt sulphate and cupric nitrate salt, (Gimba *et al*., 2004). Lartey *et al.*, 1999 activated different carbonaceous materials with oxidizing

gases such as air, steam or carbon dioxide in the presence of $ZnCl_2$, $MgCl_2$, $CaCl_2$ and H_3PO_4.

Activated carbon is produced by three methods: physical, chemical and combined (physical and chemical) procedures Qasem (1997). Physical activation involves carbonization followed by gasification at high temperatures, whereas in chemical activation, the raw material is impregnated with chemical reagent such as KCl, $ZnCl_2$ or H_3PO_4 then heat-treated at moderate temperatures (Lafi, 2001). In general, the methods most commonly employed for the manufacture of activated carbon are of two main types:

Low temperature chemical dehydration and charring of a carbonaceous substance: Temperature between 200 and 650℃ are normally employed. The most commonly used

dehydrating chemicals are: Phosphoric acid, zinc chloride and sulphuric acid. In this process, the porosity is developed by the action of the dehydrating chemicals on the cellulosic structure of the starting material or by the action of the oxidizing gas generated in the process, the raw material or charred material is impregnated with chemical reagent such as KCl, $ZnCl_2$ or H_3PO_4 then heat-treated at moderate temperature (Lafi, 2001). Activation with phosphoric acid requires temperatures in the range 375 to 500°C, and the reagent is readily recovered by leaching with water. Activation with zinc chloride occurs in the temperature range 550 to 650°C and, although most of the zinc chloride is recovered by leaching with dilute hydrochloric acid, The activated carbon produced with phosphoric acid and zinc chloride can be dried with little, if any, loss of adsorptive capacity (McDougall *et al*., 1982).

High temperature oxidation of a previously charred carbonaceous substance:

In this process, a porous structure of the starting material by controlled oxidation at temperatures between 800 and 950°C with steam or flue gas. The first step in the production of activated carbon by this method involves the carbonization, which is the formation of a char from the source material. Carbonization is generally accomplished by heating of the source material-as lumps or pre-sized material, or in moulded form, e.g. as briquettes or extrudates-in an inert atmosphere such as flue gas to a temperature that must not exceed 700°C so that dehydration and devolatilization of many of the carbon atoms can occur in a controlled manner. The main purpose of carbonization is to reduce the volatile content of the source material (a fixed carbon content of 80 per cent or higher is desirable) to convert it to a suitable form for activation (McDougall *et al*. 1982). The physical activation involves carbonization followed by gasification at higher temperature. (Lafi, 2001). The properties of the product will depend on the nature of the starting material, the conditions used for carbonization, the activation process chosen, the conditions employed in that process and the post treatment of the product. These usually lead to a very wide variety of products bearing different brand names e.g. Actibon, Acticarbon, Carboraffin and Darco (Abram, 1973).

2.6 General Uses of Activated Carbon

Nowadays, activated carbon finds wide application in many areas especially in the area of waste management. Apart from environmental pollution control, activated carbon is mainly used in industry in various liquid and gas phase adsorptions (Bansal and Goyal, 2005). Among liquid phase applications include; food processing, preparation of alcoholic beverages, decolorization of oils and fats, product purification in sugar refining, purification of chemicals (acids, amines, gylcerin, glycol, etc.), enzyme purification, decaffeination of coffee, gold recovery, refining of liquid fuels,

purification in electroplating operations, purification in the clothing, textile, personal care, cosmetics, and pharmaceutical industries, and applications in the chemical and petrochemical industries. Gas phase applications include recovery of organic solvents, removal of sulfur-containing toxic components from exhaust gases and recovery of sulfur, biogas purification, and use in gas masks, among others. Activated carbon is also used in medical and veterinary applications, soil improvement, removal of pesticide residues, and nuclear and vacuum technologies (Bansal and Goyal, 2005).

2.7 Application of Activated Carbon in Environmental Pollution Studies

The use of carbon-based materials dates back to ancient times (Menendez-Diaz and Gullon 2006). However, the use of activated carbon in its current form began in the second half of the twentieth century as a consequence of the rising awareness of environmental pollution (Dabrowski, 1998). Today, activated carbon is very often utilized in the removal of various organic and inorganic species from surface water, groundwater, and wastewater.

2.7.1 Activated carbon in drinking water treatment

Adsorption by activated carbon is employed today in drinking water treatment for various purposes. An overview of historical development shows that the first application of activated carbon in the form of granulated activated carbon (GAC) was in the year 1910 in Reading, England for the purpose of dechlorination of chlorinated water (Hung *et al*., 2005). In the 1930s and 1940s, particularly in Europe, water works used high chlorine doses for the disinfection of water following the growing pollution of surface waters. Often, GAC filtration was used for dechlorination purposes. However, the dechlorination in these filters cannot be regarded as an adsorptive process since the removal of chlorine depends on a catalytic reaction taking place on the carbon surface.

However, the use of GAC for dechlorination purposes was abandoned a long time ago because of the formation of additional haloforms and other chlorine compounds within filters (Sontheimer *et al*., 1988).

The use of activated carbon in water treatment for the removal of substances responsible for taste and odour dates back to the late 1920s. The undesirable taste and odour in drinking water was mainly attributed to the presence of chlorophenols formed in water as a result of the chlorination of phenols at the disinfection stage (Sontheimer, 1988). Powdered Activated Carbon (PAC) was used for the control of taste and odour in drinking water for the first time in the USA in 1929–1931 (Sontheimer, 1988). The first GAC filters were installed in Germany in 1929 and in the USA in 1930 for taste and odour removal. By 1932, about 400 water treatment works in the USA were adding PAC to their water to improve taste and odour, and this number increased to 1200 by 1943 (Sontheimer, 1988).

2.7.2 Municipal wastewater treatment

The first full-scale advanced (tertiary) wastewater treatment plant incorporating GAC was put into operation in 1965 in South Lake Tahoe, California (Hendricks, 2006). The The purpose in employing GAC was to reuse the effluent of municipal wastewater treatment plants for purposes such as industrial cooling water and irrigation of parks. Physicochemical treatment options involving PAC adsorption were also tested in lieu of biological treatment. The idea was that primary settling was followed by coagulation and PAC adsorption, settling and perhaps filtration. However, secondary treatment could not be replaced with a merely physicochemical process because of cost (Hendricks, 2006). Today, GAC filtration or PAC-assisted membrane operation are

mainly conducted as a tertiary treatment step to remove dissolved and refractory organic matter from secondary sewage effluent.

2.7.3. Industrial wastewater treatment

Activated carbon adsorption is most commonly applied in industrial wastewater treatment to meet stringent regulations for discharge into receiving waters. In industrial wastewater treatment, activated carbon adsorption can be utilized as a separate unit process. It may be placed after various physicochemical treatment steps such as coagulation/clarification, filtration, and dissolved air flotation (Hendricks, 2006). Another alternative is to use activated carbon adsorption prior to biological treatment to remove compounds which might be toxic to a biological system. However, the most widely adopted procedure is to place activated carbon adsorption as a tertiary or advanced treatment step subsequent to biological treatment for removal of refractory organics (Hendricks, 2006). To some extent this procedure may also be effective in the removal of inorganics (Sontheimer, 1988). Nowadays, activated carbon finds wide application in the treatment of wastewaters generated from industries such as food, textile, chemical, pharmaceutical, pesticides and herbicides production, coke plant, munitions factories, petroleum refineries and storage installations, organic pigments and dyes, mineral processing plants, insecticides, pesticides, resins, detergents, explosives, and dyestuffs (Sontheimer, 1988). It is also employed in the treatment of sanitary and hazardous landfill leachates (Hendricks, 2006).

2.7.4. Hospital wastewater treatment

In the past, treatment of hospital wastewater was primarily concerned with the preservation of public health and esthetic concepts such as the elimination of visible signs of pollution and the maintenance of oxygen levels for sustenance of marine life in

receiving waters (John, 1998). In the last decade, two new concepts have been developed. The first is that water is becoming scarce so that it may be necessary to use water more than once and secondly is that natural waters should be maintained in a condition of purity so that the overall impact of water use on the environment is minimized (John, 1998). This new concept is achieved through the advanced waste treatment process which consists of coagulation step with alum followed by filtration then adsorption on activated carbon and lastly disinfection with chlorine (John, 1998). Out of the conventional techniques employed to treat hospital wastewater, adsorption technique is the most effective and efficient (Hajira and Muhammed, 2008). The groups of organics that are generally amenable to adsorption onto activated carbon include pesticides, herbicides, aromatic solvents, polynuclear aromatics, chlorinated aromatics, phenolics, chlorinated solvents, high-molecular-weight (HMW) aliphatic acids and aromatic acids, HMW amines and aromatic amines, fuels, esters, ethers, alcohols, surfactants, and soluble organic dyes Hendricks (2006). Compounds having low molecular weight (LMW) and high polarity, such as LMW amines, nitrosamines, glycols, and certain ethers, are not amenable to adsorption Hendricks (2006).

The adsorption of metal ions from wastewater was investigated using pecan shell granular carbon activated by acid stream (Bansode 2003). The result shows that acid stream activated pecan shell based granulated activated carbon (GAC) are effective metal ion adsorbents and can potentially replace typical coal-based GACs in the treatment of metal contaminated waste water. The effectiveness was found to depend on the activating agent and also differs with metal ions. Activated carbon derived from coconut tree sawdust was reportedly used to remove Cr (VI) from wastewater (Selvi 2001). Activated carbon developed from a rapidly renewable bio-source was used for the removal of cadmium (II) and nickel (II) from dilute wastewater (Bass *et al.*, 2002).

Sandhya and Tonni (2003) conducted a study on the Cr(VI) removal from wastewater using coconut shell charcoal and commercial activated carbon modified with oxidizing agents and reported that that the use of chemically modified CSC for Cr(VI) removal appears to be technically feasible, eco-friendly, and economically attractive for the treatment of Cr-contaminated wastewater.

2.8 Activated Carbon Adsorption

Adsorption is force of physical attraction between the surface of a porous solid and a component molecule being removed from the bulk phase. The most fundamental property of adsorbate-adsorbent interaction is the adsorption equilibrium (Cheremisinoff and Ellerbusch, 1978).). The equilibrium at a given temperature is usually presented under the form of adsorption isotherms, which are useful for selecting the most appropriate adsorbent and also for predicting the performance of adsorption system.

A physical-chemical process that involves the mass transfer of a solute (adsorbate) from the fluid phase to the adsorbent surface till the thermodynamic equilibrium of the adsorbate concentrations is attained with no further net-adsorption is a general expression for adsorption. It involves the interphase accumulation or concentration of substances at a surface or interface between any two phases such as liquid-liquid, gas-solid, or liquid-solid interfaces (Cheremisinoff and Ellerbusch, 1978). The material being concentrated or adsorbed is the adsorbate and the adsorbing phase is termed adsorbent.

2.9 Theory of adsorption

Adsorption is the formation of a layer of gas, liquid or solid on the surface of a solid or less frequently of a liquid (Daintith, 2000). Adsorption occurs at solid-solid, gas-solid,

solid-liquid, liquid-solid, liquid-liquid, liquid-gas interfaces (Cheremisinoff and Ellebusch, 1978).

2.9.1 Types of adsorption

There are two main types of adsorption, these are physisorption and chemisorptions.

***Physisorption*:** This is an interaction between adsorbate and adsorbent in which non-specific forces of attraction such as dispersion or dipole is involved and the binding energy of the adsorbate is less than 20kJ/mol Adamson (1960) and Atkins (2003). These forces are non specific since they do not depend on any property of either the adsorbate or the adsorbent (Parfitt and Sing, 1976). It occurs in minutes and the process is reversible (Atkins, 2003). Multilayers are easily formed at higher pressure/concentration in physisorption due to small heat of adsorption.

***Chemisorption*:** This is a type of adsorption in which some degree of specific chemical interaction between the adsorbate and adsorbent is involved in the energy of adsorption may be quite large comparable to those of chemical bond formation. Typically, the enthalpy values are in the region of 200KJ/mol. The enthalpy of adsorption depends on the extent of surface coverage, mainly because the adsorbate particles interact. If the particles repel each other, the adsorption becomes less exothermic as coverage increases. If the adsorbate particles attract one another, then they tend to cluster together in islands, and growth occurs at the borders. The distance between the surface and the closest adsorbate atom is also typically shorter for chemisorption than for physisorption. At low temperature chemisorption may be so slow that for practical purposes only physisorption is observed, whereas chemisorption predominates at high temperature

(Adamson, 1960). On a general note, monolayer is formed in chemisorption due to the short-range chemical forces between the adsorbate and adsorbent (Atkins, 2003).

2.9.2 Extent of adsorption

The extent of surface coverage is normally expressed as the fractional coverage, θ. It represents the extent of adsorption, Equation 2.4.

$$\theta = \frac{\text{No.of adsorption sites occupied}}{\text{No.of adsorption sites available}} \qquad 2.4$$

2.9.3 Adsorption equilibria and the adsorption isotherm

The adsorption isotherm is a functional expression for the variation of adsorption with concentration of adsorbate in bulk solution at constant temperature (Weber, 1973). Generally, in adsorption a time is attained when a dynamic equilibrium will be established in the adsorption process. The distribution of solutes between the adsorbate and the adsorbent is a measure of the position of the equilibrium and depend on: Concentration and nature of the competing solutes and nature of the solution.

2.9.4 Types of adsorption isotherms

The different heat of adsorption obtained from a given adsorbate-adsorbent interaction gives rise to isotherms of different shapes which are highly dependent on the nature of the adsorbent surface (Parfitt and Sing, 1976). If the solid is mesoporous, capillary condensation takes place in the middle and upper part of the isotherm, whereas if the solid is microporous, microporous filling occur at the low pressure (Parfitt and Sing, 1976). An indication of the nature of the adsorption process is gained by inspection of

the isotherm shape. All adsorption isotherms fit into one of the five (5) types shown in Figure 1 based on the BET classification

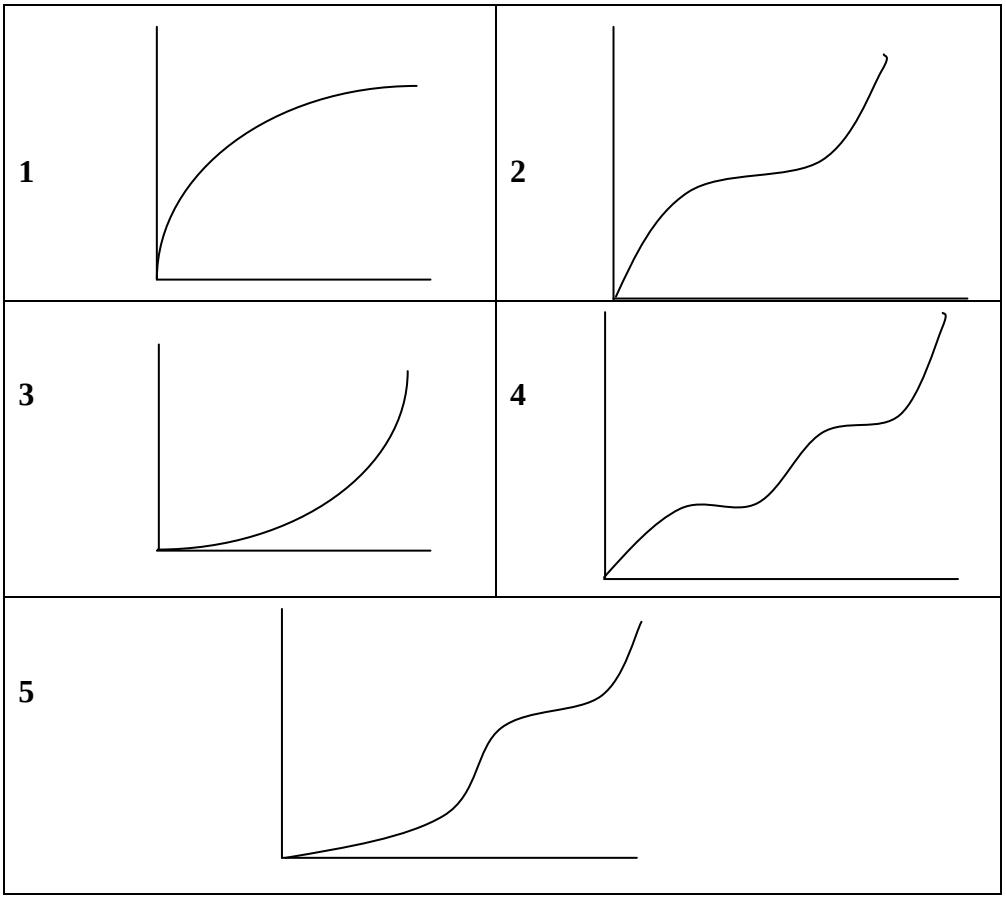


Figure 2. 1: BET classification of the different types of adsorption isotherm

Type 1; is encountered when adsorption is limited to monolayer as observed in chemisorption. The asymptotic approach to a limiting quantity indicates that all of the surface sites are occupied. Physisorption that produces the Type 1 isotherm indicates that the pores are microporous and that the exposed surfaces reside almost exclusively within the micropores which once filled with adsorbates, leave little or no external surface for additional adsorption.

Type 2; is most frequently encountered when adsorption occurred on nonporous adsorbent or adsorbent with pore diameter larger than micropores. The inflection point

usually occurs near the completion of the first adsorbed monolayer and with increasing relative pressure, second and higher layers are completed until at saturation the number of adsorbed layers becomes infinite.

Type 3; isotherms are characterized principally by heat of adsorption that are less than adsorbate heat of liquefaction. Thus, as adsorption proceeds interaction with an adsorbed layer is greater than the interaction with adsorbent surface.

Type 4; occurs on porous adsorbents possessing pores in the range of 15-1000 Angstroms. The slope increases at elevated pressures, indicating an increased uptake of adsorbate as pores are being filled.

Type 5; result from adsorbate adsorbent interaction potential similar to the type 3. However, Type 5 is also associated with pores in the range as those of Type 4 isotherm.

Generally, Type 1, 4 and 5 are associated with porosity, while Type 1 usually corresponds to micro porosity, Type 4 and 5 are associated with pores ranging from about fifteen to several hundred angstroms. Each of these types is observed in practice but by far the most common are types are Type 1, 2 and 4 (Thomas and Crittenden, 1998).

An inherent property of Type 1 isotherm is that adsorption is limited to the completion of a single monolayer of adsorbate at adsorbent surface. Type 1 isotherms are observed for the adsorption of gases on micro porous solids whose pore sizes are not much lagers than the molecular diameter of the adsorbate. Similarly, Type 3 isotherms, which are continuously convex with respect to the partial pressure axis, show a steady increase in adsorption capacity with increasing relative pressure. Type 4 isotherms are similar to Type 2 isotherms except that adsorption terminates near to a relative pressure of unity (Thomas and Crittenden, 1998).

Five different models are used to fit single component isotherms, some of those models have been originally proposed for the treatment of gas mixtures; however, their application to liquid mixtures is supported by theoretical and practical reasons (Jaroniec and Madey, 1988). They can be classified into:

Simple isotherm models for homogeneous surfaces without lateral interactions, like Langmuir equation (Langmuir, 1918) and Jovanovic equation (Jovanovic, 1969) as presented in Equations 2.5 and 2.6; Isotherm models for heterogeneous surfaces without lateral interactions, like Freundlich equation (Freundlich, 1906); Other empirical isotherm models, like Redlich-Peterson equation (Redlich and Peterson, 1959) and Khan Equation (Khan *et al.,* 1997) are presented in Equations 2.7, 2.8 and 2.9 respectively.

Model	**Equation**	
Langmuir	$q = (q_{max}KC)/ (1+KC)$	2.5
Jovanovich	$q = q_{max} (1-e^{-(KC)})$	2.6
Freundlich	$q = K(C)^{\gamma}$	2.7
Redlich-Peterson	$q = (aKC)/(1+K(C)^{\gamma})$	2.8
Khan	$q = (aKC)/(1+KC)^{\gamma}$	2.9

Where:

q is the amount of adsorbed compound at equilibrium per unit amount of adsorbent,

$\mathbf{q_{max}}$ is the monolayer capacity,

C is the concentration of adsorbate in aqueous phase at equilibrium,

γ, **K** and **a** are the model parameters.

2.9.5 Langmuir adsorption isotherm:

In 1918, Langmuir described adsorbate-adsorbent system in which the extent of adsorbate coverage is limited to monolayer at or before a relative pressure of unity is reached. Although the theory is more appropriate for the description of chemisorption, it is adopted for a number of systems where the coverage is low. The following assumptions were made in deriving the Langmuir equation:

l. Adsorption cannot proceed beyond monolayer coverage

ll. Each adsorption site is equivalent in terms of energy of adsorption and uniform i.e. the surface is perfectly flat on a microscopic scale.

lll. There are no interactions between adjacent adsorbate molecules

The Langmuir isotherm is represented mathematically in Equation 2.10

$$C_s/X_m = 1/bQ_o + C_s/Q_o \qquad 2.10$$

X_m = Amount of adsorbate adsorbed per unit weight of carbon

Q_o = Constant relating to monolayer adsorption capacity

b = Langmuir constant or adsorption coefficient

C_s = Equilibrium concentration of the adsorbent in solution

A plot of C_s/X_m against C_s gives a straight line with a slope of $1/Q_o$ and an intercept of $1/bQ_o$ **.**

2.9.6 Freundlich adsorption isotherm

The Freundlich adsorption isotherm is a special case for heterogeneous surface and is usually used to model adsorption from solution. The Freundlich equation as presented in Equation 2.11.

$$X_m = K_f C^{1/n} \quad 2.11$$

Where:

X_m = Amount of adsorbate adsorbed per unit weight of carbon

K_f = Constant measuring adsorption capacity

C = Equilibrium concentration of the adsorbent in solution

n= Constant related to adsorption efficiency and energy of adsorption

The Freundlich equation is basically empirical but is often useful as a means for data description. This is because the equation is adequate to describe non-linear adsorption in a narrow range of adsorbate concentration**.** It describes the adsorption processes on surface adsorption sites that are energetically heterogeneous. The simplified mathematical equation of the Freundlich equation is presented i9n Equation 2.12.

$$\log X_m = \log K_f + 1/n \log C \quad 2.12$$

A plot of log X_m against logC gives a straight line with a slope 1/n and an intercept of log K_f. The K_f value increases with the total adsorption capacity of the adsorbent to bind the adsorbate. The numerical value of n is a useful index of the adsorption capacity or efficiency and is related to the energy of adsorption intensity. The amount adsorbed is presented in Equaton 2.13.

$$(C_o-C_e)V/W \quad 2.13$$

Where C_o and C_e are the initial and equilibrium concentrations (M), respectively of the adsorbate, while V is the volume (ml), and W is the weight (g) of the adsorbate.

The adsorption isotherm is useful for predicting the capacity that an activated carbon has for adsorbing adsorbate (Weber, 1973).

2.9.7 Factors affecting adsorption

In general, the factors that influence the adsorptive behavior of activated carbon from aqueous solution are:

(i) The nature of the activated carbon and its particle size distribution:

The nature of the adsorbate is particularly important in dictating the degree of adsorption that can actually occur. As a rule, braed- chain compounds are more sorbable than straight – chain compounds (Weber, 1973). The type and location of the substituent functional group affects absorbability, and molecules low in polarity and solubility tend to be preferentially adsorbed. Unless physical blockage of the carbon pores actually occurs, large molecules are more sorbable than small molecules of similar chemical nature (Weber, 1973).

(ii) pH of the solution:

Carbon generally has a low affinity for ions, particularly those with a high charge-to surface ratio. pH affect ionicity as evaluated in the study of Yankassa sheep wool, it is observed that the efficiency of the wool matrix reduces with increase in pH (Kagbu *et al.,* 2001).

(iii) Temperature:

Adsorption reactions are generally exothermic and high temperature usually slow or decrease the adsorption process. Adsorption generally decreases with increasing temperature (Gauntlett and Packman, 1973). Kagbu *et al.,* 2001 evaluated Yankassa sheep wool as an adsorptive matrix for bleaching textile effluents and found that increase in temperature of the effluent resulted in substantial decrease in its colour.

2.10 Adsorption Process

There are different adsorption processes, the major once include; Fixed-bed adsorption; Expanded-bed adsorption; Moving-bed adsorption and Fluidized-bed adsorption. The down flow fixed-bed adsorption is the most common type of adsorption column for wastewater treatment. This is because the down flow fixed-bed also acts as depth filters for particles that can be contained in wastewater (Wentz, 1995). The fixed-bed can be in series or parallel.

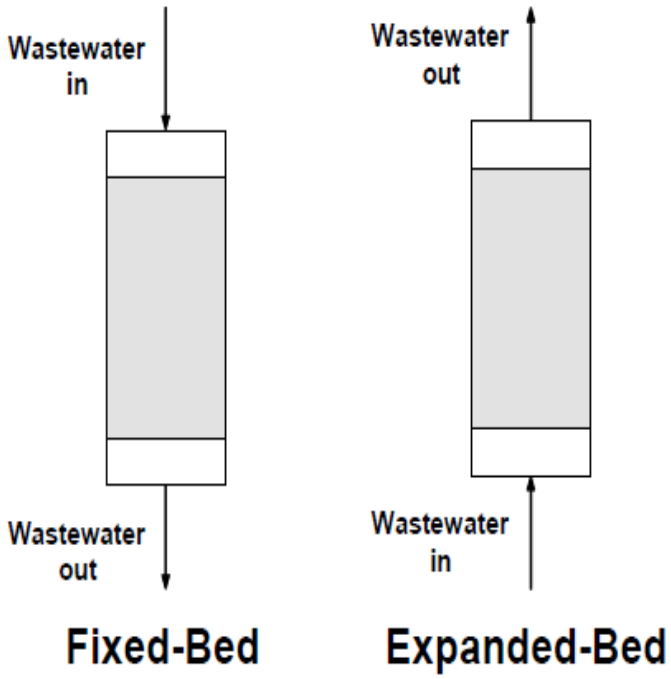


Figure 2. 2: Fixed and Expanded Adsorption bed

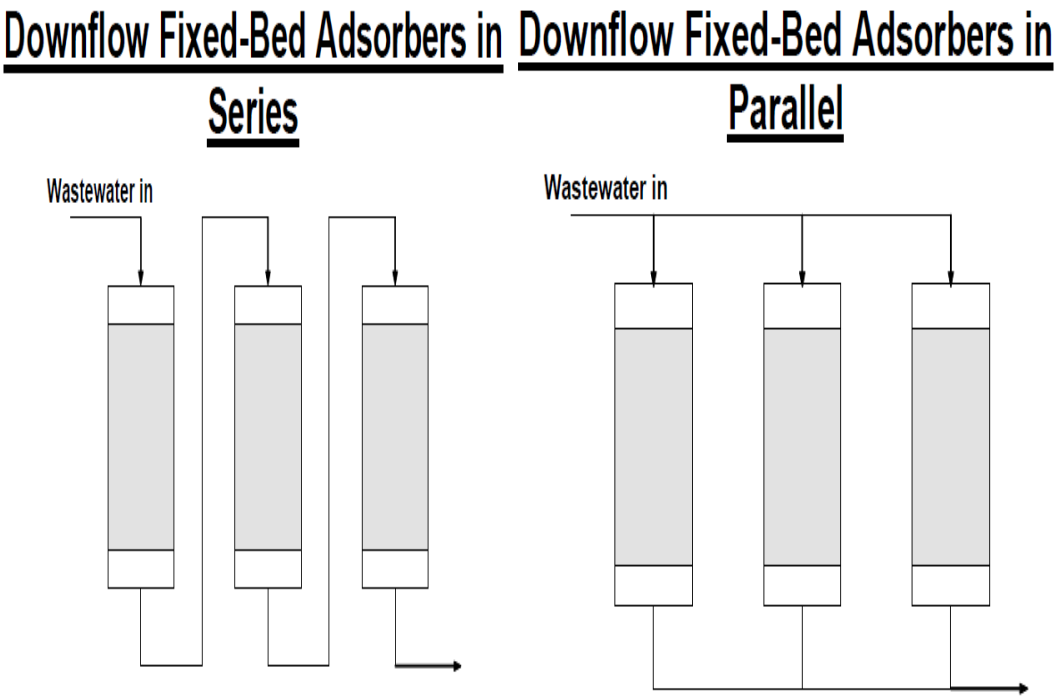


Figure 2. 3: Comparism between fixed-bed adsorbers in series and parallel

The most important design factors in fixed-bed adsorption systems includes: Particle size; Diameter of column; Flow rate of incoming wastewater; Height of adsorption bed; Pressure drop and Time required achieving breakthrough (Wentz, 1995).

As the wastewater moves through a fixed-bed of adsorbent, the pollutant to be adsorbed will move from the wastewater to the adsorbent bed (Wentz, 1995). Several steps are involved in the overall adsorption process of a single molecule of pollution;

Mass transfer step: Mass transfer from the bulk of the wastewater to the surface of the adsorbent through the boundary layer around the particle.

Diffusion step: Internal diffusion through a pore

Adsorption step: Adsorption onto the surface of the adsorbent. In fixed bed adsorption, at any given time the bed can be divided into 3 approximate zones i.e., saturated zone (containing carbon nearly saturated with the pollutants), followed by the adsorption zone (were adsorption actually takes place) and then the last zone in which the

adsorbent contains little or no adsorbed pollutant (Wentz, 1995). The size and location of the three zones within the bed change with time.

2.11 Modeling of Column Study Results: Bohart–Adams Model

Bohart–Adams model based on the surface reaction theory (Goel *et al.,* 2005; Malkoc *et al.,* 2006) and it assumes that equilibrium is not instantaneous; therefore, the rate of the sorption is proportional to the fraction of sorption capacity still remaining on the sorbent (Liao *et al.,* 2004; Aksu and Gönen, (2004)). According to the Bohart–Adams model, Equation 2.14 is use to predict the performance of continuous adsorption columns:

$$t = N_oX/C_ov + ln\,[(C_t/C_o)] \times 1/C_ok \qquad 2.14$$

where, t is the time to break point (min); Co the influent concentration (mg/l); C_b the concentration at break through (mg/l); N_o the Bohart-Adams adsorptive capacity or saturation concentration of the adsorbent (mg/L); X the bed depth of column (m); v the linear flow rate (ml/sec); K is the rate or mass transfer coefficient (ml/ (mg min)). A straight line was attained for this system by plotting X against t, which gives the value of K and N_o from the slope and intercept of the line respectively. The Bohart-Adams equation can be simplified and rewritten as in Equation 2.15 where the parameters a and b are expatiated in Equations 2.16 and 2.17 respectively.

$$t = aX + b \qquad 2.15$$

Where

$$a = N_o/C_ov \qquad 2.16$$

$$b = In\,(C_t/C_o) \times 1/C_ok \qquad 2.17$$

The breakthrough capacity $Q_{0.5}$ (at 50% or C_t/C_o = 0.5) expressed in mg of adsorbate adsorbed per gram of adsorbent was calculated using Equation 2.18.

$$Breakatrough\ capacity, Q_{0.5} = \frac{metal\ adsorbed\ on\ adsorbent\ bed\ (mg)}{mass\ of\ adsorbent\ in\ bed\ (g)} \qquad 2.18$$

$$= \frac{breakthrough\ time\ (at\ 50\%) \times flow\ rate \times feed\ concentration}{mass\ of\ adsorbent\ in\ bed}$$

2.12 The Pseudo-Second Order Rate Kinetic Model

The pseudo-second order model when applied on the adsorption capacity, it predicts the behaviour over the whole range of studies supporting the validity, and is in agreement with chemisorption being the rate-controlling step (Ho and McKay, 1998). Based on equilibrium adsorption, the linearized pseudo-second-order kinetic equation is expressed in Equation 2.19.

$$\frac{t}{q_t} = \frac{1}{h} + \frac{t}{q_e} \qquad 2.19$$

Where q_t (mg/g) is the amount of adsorbate retained at time, *t* (min).

The slope and intercept from the plots of t/q_t versus *t* is used to calculate the value of the adsorption capacity of the activated carbons q_e, the pseudo-second-order rate constant k_2, (g/mg min), the initial adsorption rate constant *h* (mg/g min), and the coefficient of determination R^2. The constants k_2 and *h* were calculated respectively from the intercept and slope of the linear plots obtained. The straight lines in the plots prove a good agreement of experimental data with the second-order kinetic model. According to (Ho and Mckay, 1995), if the plot is linear, then the adsorption process may be described as chemisorption.

2.13 The Weber-Morris Intraparticle Diffusion Model

Intraparticle diffusion is a transport process involving movement of species from the bulk of the solution to the solid phase (Uzunova *et al.*, 2013). The structure of the solid and its interaction with the diffusion substance influences the rate of transport. Adsorbents may be in the form of porous barriers and solute movement by diffusion from one fluid body to the other by virtue of concentration gradient (Shrihari, 2005; Shrihari and Das, 2009). The possibility that the diffusion mechanism might be the rate limiting stage in regard to the entire process was evaluated by the linear dependence on the Weber-Morris Intraparticle Diffusion Model (WMIDM) (Weber and Morris, 1963) as presented in Equation 2.20.

$$q_e = k_{id}t^{1/2} + C_i \qquad 2.2$$

A plot of the amount of adsorbate sorbed, q_e (g/g) versus the square root of the time t, gives the rate constant k_{id} (gg^{-1} $min^{-1/2}$) which is the intraparticle diffusion rate coefficient as the slope of the plot and C_i (g/g) is the intraparticle diffusion coefficient as the intercept of the line accounting the bonding effect between the activating agent and the carbon. Larger k_{id} values indicate better adsorption which is related to improved bonding between adsorbate and adsorbent particles (Aksu and Gowen, 2004) and may simply be due to the fact that higher adsorbate concentration adds to a greater driving force for diffusion of adsorbate molecules into the pores (Sunil and Arti, 2010). According to Itodo *et al.*, (2009), the adsorption mechanism assumes intraparticle diffusion if the following conditions are met:

(i) High R^2 values to ascertain applicability;

(ii) Straight line which passes through the origin for the plot area q_t vs. $t^{1/2}$;

(iii) Intercept $C_i < 0$.

CHAPTER THREE

3.0 MATERIALS AND METHODS

3.1 Materials

Distilled water used in the experiments was produced at the Physical Chemistry Laboratory of the Department off Chemistry, Ahmadu Bello University, Zaria. All reagents used were of analytical grade and no further purification was carried out before use.

3.2 Sample Collection

3.2.1 Neem sample collection

Neem husks and seed cakes were collected from the National Research Institute for Chemical Technology (NARICT), Zaria, Nigeria.

3.2.2 Wastewater sample collection

Wastewater samples were collected using water sampler at different locations and depths of the treatment plant from the Abuja University Teaching Hospital, Gwagwalada. A composite of these collected samples was made and used for the study.

Samples for physiochemical and microbial analysis were collected in a clean sterile rubber container. Samples for the oxygen parameters were collected in 500ml bottles with stoppers, one millimeter each of Winkler's solutions A and B were added to samples on site to fix the oxygen. The samples were transported to the laboratory where analysis was commenced immediately within five hours of collection at the multi-user research laboratory of Ahmadu Bello University, Zaria.

3.2.3 Description of wastewater sampling area

The study area was University of Abuja Teaching Hospital wastewater Treatment plant located in University of Abuja Teaching Hospital, Gwagwalada Abuja, at Latitude 8°57' N and Logitude 7°03' E as presented in Figure 3.1. The hospital environment consists of several departments/units and each department/unit in the hospital has waste management chambers which are all channelled to the central waste management plant. The waste management plant has about 24 outlets. Twelve of the outlets were randomly selected as points were the wastewater samples were collected.

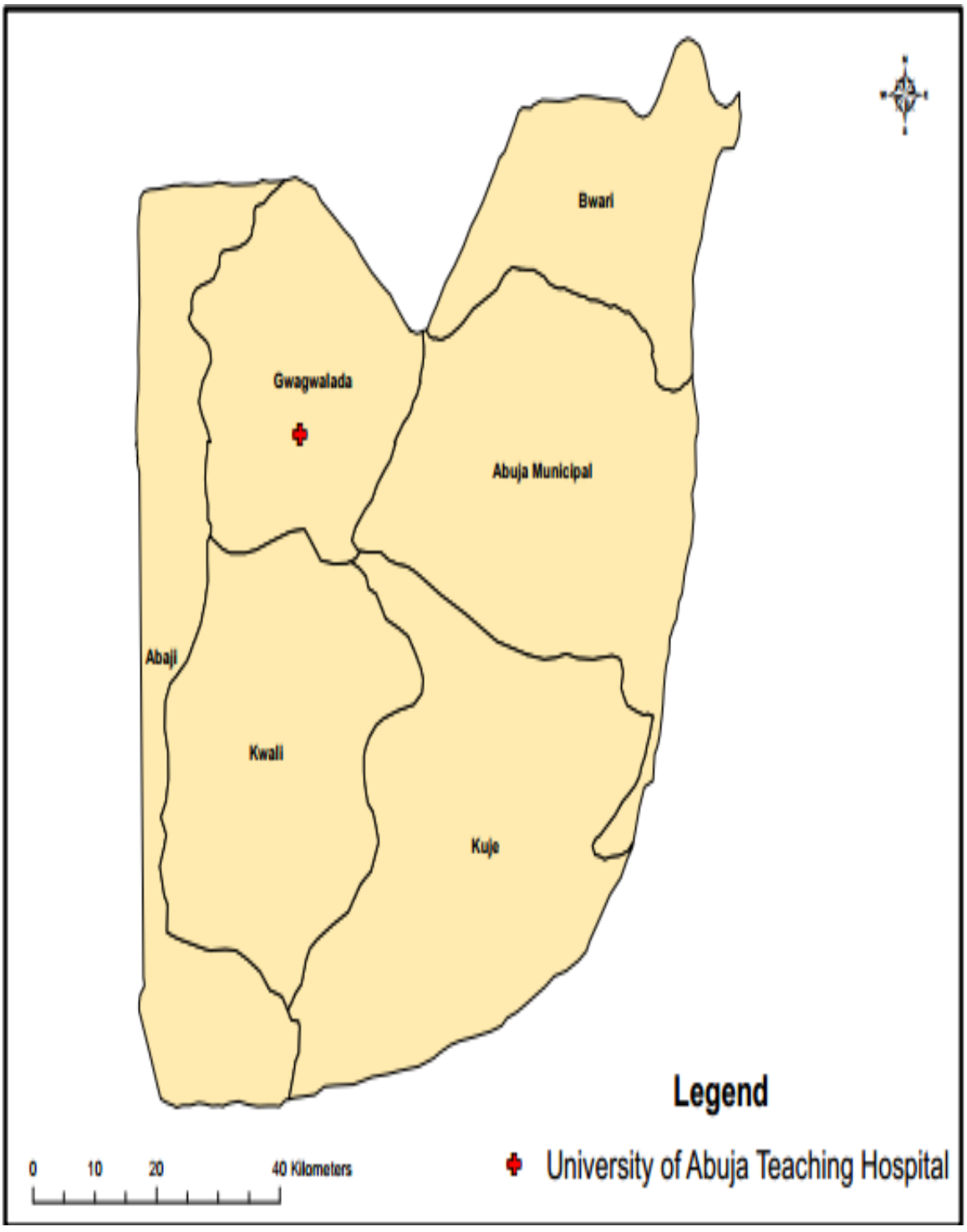


Figure 3. 1: Map of Abuja indicating the location of University of Abuja Teaching hospital

3.3 Neem Sample Preparation (Itodo *et al.,* 2009)

The Neem husk and seed cake collected were sun-dried for three days to remove moisture according to Itodo *et al.,* 2009. The sun-dried samples were properly washed under running tap to remove dust and water-soluble impurities. The samples were allowed to drain off excess water accumulated during washing and dried in an oven for another 12 hours after which they were introduced into a thermostatic laboratory oven set at 105 ^{o}C for 24 hours. The dried samples were gently crushed using a ceramic laboratory mortar and pestle followed by sieving with a <400 µm aperture sieve. The less than 400 µm samples were stored in airtight containers for further use.

3.4 Carbonization of Neem samples (Gimba *et al.,* 2004)

The prepared neem husks and seed cakes were carbonized at 400 ^{o}C in a muffle furnace using the methods described by Gimba *et al.* (2004). Prior to carbonization, the minimum carbonization temperatures for the neem husks and cake sample were determined using the method of Guzel and Uzun (2002). Two grams of the Neem samples were weighed into two separate, clean crucibles of known weight and heated for 15 minutes at 200 ^{o}C. The experiment was repeated at varying temperature of 250 ^{o}C, 300 ^{o}C, 350, 450 ^{o}C and 500 ^{o}C. A graph of weight loss versus temperature was plotted. The least temperature to completely carbonize the sample was chosen as the minimum carbonization temperature. Exactly 50 g of the Neem husks and seed cakes were individually placed in large sized ceramic crucibles and carbonized in the furnace. The carbonized samples were allowed to cool in desiccators prior to activation.

3.5 Chemical Activation of the Carbon (Abechi , 2011)

Chemical activation of the carbonized samples was done using $ZnCl_2$ and H_3PO_4 as activating agents. Prior to activation, the optimum activation temperatures for the carbonized neem husks and cake sample were determined using the method of Guzel and Uzun (2002). Two grams of the carbonized neem samples were weighed into two separate, clean crucibles of known weight. The two samples were impregnated with the activating agents ($ZnCl_2$ and H_3PO_4) at room temperature. This was heated gradually for 2 hours and then temperature elevated and heated for 2 hours at 450 ^oC. The process was repeated two times and the average was taken. This activated carbon samples were then allowed to cool in a desiccator prior to washing severally with hot distilled water. The washed samples were oven dried at 105 ^oC for 6 hours to constant weight. This was then sieved into different particle sizes with a sieve made of brass frame and steel mesh with an aperture of 400 µm, 425 µm, 500 µm and 600 µm. The fine sieved samples were stored in a clean airtight container and stored for characterization. The process was repeated at different temperatures of 500, 550 600 and 650^oC. Adsorption studies were carried out using the batch process with methylene blue as adsorbate to determine the optimum activation temperature.

3.6 Physico-chemical Characterization of Raw and Modified Neem Samples

The following physico-chemical tests were carried out to characterize the raw neem husk and seed cake and the corresponding activated carbon from neem husk and seed cake; Moisture and dry matter content, ash content, volatile matter content, fixed carbon and bulk density.

3.6.1 Moisture and dry matter content (Ekpete and Horsefall, 2011)

Thermal drying at 105℃ in an air circulation oven to constant weight, which is the most common technique, was employed. Two clean crucibles were washed and rinsed with distilled water, dried in an oven at 105 ℃ and cooled in a desiccator. The weights of the crucibles were recorded. One gram each of the sieved sample (raw neem husk and neem cake) was weighed into the dried crucibles and then placed in an air circulated oven at 105 ℃ and dried to constant weight after 8 hours. This process was repeated and the weighted average was used to determine the percentage air-dry moisture from loss in weight was calculated using Equation 3.1 and dry matter was calculated using Equation 3.2.

Moisture (%) = [Loss in weight on drying (g)/Initial sample weight (g)]*100 3.1

Dry Matter (%) = 100 – moisture (%) 3.2

3.6.2 Ash content (Aloko and Adebayo, 1997)

The ash is the inorganic residue left after the organic matter has been burnt off. The ash content was determined by the method employed by Aloko and Adebayo (1997). Porcelain crucibles were washed and oven dried at 105 ℃ for an hour, and cooled to room temperature in a desiccator after which they were weighed and their weights recorded (W_c). Exactly 2 g (W_o) each of the prepared samples were placed in the preweighed crucibles. The crucibles containing the sample were transferred to a muffle furnace and the temperature was allowed to rise slowly to 500 ℃ for one hour after which the crucibles and their content were transferred to a desiccator and allowed to cool. The crucibles and their contents were reweighed and the new weight was recorded (W_f). The percentage ash content was calculated using the Equation 3.3.

$$A_c\ (\%) = (W_f - W_c/W_o) \times 100 \qquad 3.3$$

where;

A_c is the percentage ash content of the materials.

3.6.3 Volatile matter content (Aloko and Adebayo, 1997)

The volatile contents were determined using the methods employed by Aloko and Adebayo (1997). Where 2g of each of the dried samples were heated for 10 minutes in a partially closed preweighed porcelain crucible in a preheated muffle furnace set at 300 ^{o}C. The crucible and its content were retrieved and cooled in a dessicator. The difference in weight was recorded and the volatile matter content calculated usng Equation 3.4.

$$V_c\ (\%) = [(W_o - W_f)/W_o \times 100] \qquad 3.4$$

where V_c is the percentage volatile matter content of the samples; W_o is the initial weight of the dry sample; W_f is the final weight of the sample after cooling.

3.6.4 Fixed carbon content

The fixed carbon content was determined by using the value of volatile content and ash content obtained in section 3.62 and 3.63 in Equation 3.5.

$$F_c\ (\%) = [100 - V_c - A_e] \qquad 3.5$$

where V_c and A_c are the percentage volatile content and Ash contents respectively.

3.6.5 Density and bulk density (Ekpete and Horsefall, 2011)

The Bulk densities of the raw and modified samples were measured using a modification of the method of bulk density calculation employed by Ekpete and Horsefall (2011). Empty measuring cylinders (10 ml and 20 ml) were weighed and the weight recorded (M_c). The samples were dried again at 105 ^oC to constant weigh. The samples were introduced into the cylinder without the introduction of water because the materials are swellable in water. The samples in the cylinder were compacted by gently tapping the cylinder continuously. The depressions were covered by adding more of the samples till the cylinders were filled to the 10 ml and 20 ml volumetric marks. The gentle tapping and refilling were repeated till no more depressions were observed. The samples and the cylinders were reweighed and the new weight was recorded (M_f). The process was repeated and the weighted average was used to calculate the bulk density using Equation 3.6.

$$B_D\ (g/dm^3) = [(M_f - M_c)/\text{Volume of cylinder}] \qquad 3.6$$

Where B_D is the bulk density, M_f and M_c are the final and initial weight of the cylinders respectively. The mean of the bulk densities from the two cylinders was calculated and used as the average bulk densities of the samples.

3.7 Structural and Morphological Characterization

The following analytical techniques were carried out to investigate the structure and morphology of the raw samples and their corresponding activated carbon samples.

3.7.1 Brunauer Emmet Teller (BET) surface area

The Brunauer–Emett–Teller (BET) surface area was measured from N_2 sorption isotherm at 77 K using a Micrometrics Tristar II. The samples were degassed under flowing nitrogen at 250 °C for 4 hours using the Smart Prep™ 065. The degassing unit removes adsorbed contaminants from the surface and pores of a sample in preparation for analysis. The sample tube in the analysis port was again degassed before the Dewar containing liquid nitrogen was automatically elevated upwards to submerge the sample tube. A predetermined pressure of nitrogen was bled into the manifold above the analysis port. The sample analysis port valve was then opened, exposing the sample to nitrogen. The quantity of adsorbed nitrogen was determined by the difference in the recorded pressure.

The sample analysis port was then closed and the manifold filled with a slightly higher pressure of nitrogen before re-exposure to the sample followed by calculation of the next value. Repeat of the process led to the generation of an isotherm, the surface area of the sample was then calculated from the isotherm using the Brunauer–Emett–Teller (BET) equation and N_2 cross-sectional area of $0.162 nm^2$. The analysis was done in the School of Chemistry and Chemical Engineering Queens University, Belfast, United Kingdom. Equation 3.7 represents the BET equation.

$$\frac{P_e}{(P_o - P_e)V_{ads}} = \frac{1}{CV_m} + \frac{(C-1)}{CV_m} * \frac{P_e}{P_o} \qquad 3.7$$

where P_e is the equilibrium pressure (after sample is exposed to N_2 in manifold); P_o the saturation pressure; V_{ads} the volume of nitrogen adsorbed; V_m the volume of nitrogen monolayer and C is constant that measures the surface area of the adsorbent.

3.7.2 Fourier Transform Infrared Spectroscopy (FTIR) analysis

The FT-IR spectra of the raw and modified neem samples were recorded on a Shimatzu (FTIR-8400) Fourier Transform Infrared Spectrometer at the National Research Institute for Chemical Technology (NARICT), Zaria, Nigeria. The sample was mixed with Potassium bromide (KBr) and then ground to a homogeneous blend and compressed to give a small transparent disc of 13 mm diameter. The disc containing the sample was then placed in the infrared spectrometer and the spectrum of the samples was collected. There were 20 scans collected for each measurement over the spectral range of 4000-400 cm^{-1} with a resolution of 4 cm^{-1}. All spectra were presented without baseline correction or normalization.

3.7.3 Scanning Electron Microscopy (SEM) analysis

The morphology of the activated carbon samples was analysed by SEM analysis. Minimal preparation included acquisition of the sample and placing the sample on a clean carbon strap that was attached on the sample holder, which fit into the SEM chamber and some accommodation to prevent charge build-up and the sample from making a contact with the detector. SEM was viewed using Quanta Scanning Electron Microscope FEI Quanta 250 at the School of Chemistry and Chemical Engineering Queens University, Belfast, United Kingdom.

3.7.4 Thermal Gravimetric Analysis (TGA)

Thermal characterization of the activated carbon samples was performed using Mettler-Toledo TGA/DSC I STARMettler-2012) instrument with heating rate of 20 ºC/min in nitrogen (N_2) atmosphere and carried out at the School of Chemistry and Chemical Engineering, Queens University, Belfast, UK. Thermal Analysis (TGA and DSC)

detects the inter-atomic and inter-/intra- molecular interactions as related to an imposed external change in temperature. The samples were placed in the specimen holder and the temperature of the furnace was raised to 500 °C, the initial weight was set to read 100%, then heating program was initiated. The gas environment was preselected for thermal decomposition (inert - nitrogen gas) and an oxidative decomposition (air or oxygen). All of the samples were heated up to 500 °C. The test samples were dried under a vacuum at 120 °C for 24 hours before DSC. The thermal properties were presented in thermograms.

3.8 Physico-Chemical Parameters of Wastewater

The following physico-chemical parameters of the wastewater were investigated before and after treatment with the activated carbon.

3.8.1 pH (APHA, 1998)

The pH was measured accurately as described by APHA (1998) in the laboratory using a HANNA hand held digital pH meter. The pH meter was calibrated using HACH 1997 buffers of pH 4.0, 7.0 and 10.0. The wastewater samples were transferred into 100 ml beaker and the pH meter was placed in the wastewater. The pH meter was allowed to stabilize before the results were recorded.

3.8.2 Turbidity Test (APHA, 1998)

A turbidity meter (2100N Model) was used to measure turbidity of the Hospital wastewater sample with reference to the manufacturer's instruction manual. The unit for turbidity is Nephelometric Turbidity Units (NTU).

3.8.3 Conductivity (AOAC, 1998)

Conductivity was measured in the laboratory with the use of a conductivity meter. The conductivity meter was calibrated with distilled water prior to analysis. About 60 ml of the wastewater sample was transferred into 100 ml beaker. The probe of the conductivity meter was placed into the wastewater in the beaker and allowed to stabilize for about 3 minutes after which the conductivity of the raw and treated wastewater samples was recorded.

3.8.4 Biological Oxygen Demand (BOD) (Ademoroti, 1996)

The biological oxygen demand of the wastewater was determined by diluting equal volumes of wastewater specimen with a known volume of distilled water which has been thoroughly shaken to ensure oxygen saturation. After this, an oxygen meter was used to determine the concentration of oxygen within one of the vials. The remaining vial was then sealed and placed in darkness and tested five days later. BOD was then determined by subtracting the second meter reading from the first. The dissolved oxygen content was determined before and after 5 days of incubation using Equation 3.8.

$$BOD5 = DO \text{ (after 5 days incubation)} - DO \text{ (1st day)} \quad 3.8$$

3.8.5 Chemical Oxygen Demand (COD) (Ademoroti, 1996)

In the determination of the COD of the water samples, 0.4 ml of H_2SO_4 was placed in a refluxing flask. 20 ml of the samples was diluted with 20ml of distilled water. A standard solution (10 ml) of $K_2Cr_2O_7$ was then added to glass beads already heated to 600 ^oC for 1 hour. The flask was then attached to the reflux condenser and exactly 30 ml of concentrated H_2SO_4 containing Ag_2SO_4 was added through the open end of the

condenser. The resulting solution was thoroughly mixed and the resulting mixture was refluxed for 1hour, cooled and the condenser washed with 25 ml of distilled water. The mixture was diluted with 150 ml of distilled water and cooled to room temperature. Exactly 3 drops of (0.10-0.15 ml) ferroin indicator was added. The mixture was then titrated with 0.25 M $Fe(NH_4)_2(SO_4)_2$ taking as the end point the sharp colour change from blue-green to reddish brown. In the same manner a blank containing 20 ml distilled water was refluxed together with the reagent. COD was then calculated using the Equation 3.9.

$$\mathrm{COD(mg/L)} = \frac{(a-b)\times M\times 8000}{\text{Vol. of sample}} \qquad 3.9$$

where

COD=COD from potassium dichromate; a =Vol of $Fe(NH_4)_2(SO_4)_2$ used as blank;

b =Vol of $Fe(NH_4)_2(SO_4)_2$ used for sample and M= molarity of $Fe(NH_4)_2$ $(SO_4)_2$

8000 in Equation 3.9 represent the dilution multiplication factor for COD determination

3.8.6 Total Dissolved Solid (TDS) (APHA, 1998)

Exactly 20 g of the sample was filtered using a funnel and filter paper into a pre-weighed dry beaker (W_1) and the total weight recorded as W_2. The sample in the beaker was evaporated to dryness on a steam bath set at 100^{o}C. The beaker was removed from the bath after evaporation and left to cool in a desiccator prior to reweighing (W_3). The total dissolved solid was determined using Equation 3.10.

$$\%\text{Total dissolved solids(TDS)} = \frac{(W_3 - W_1)}{W_2 - W_1}\times 100 \qquad 3.10$$

W_1 = Weight of empty beaker; W_2 = Weight of beaker with sample and W_3 = Weight of beaker after drying and cooling.

3.8.7 Total Solids (TS) (APHA, 1998)

About 20 g of the sample was weighed into the prewieghed beaker (W_1) and recorded as W_2 and evaporated to dryness on a steam bath at 100 ^oC. The beaker was removed from the bath after evaporation and left to cool in a desiccator prior to reweighing (W_3). Total solid was determined using Equation 3.11.

$$\% \text{ TDS} = \frac{(w3 - w1)}{(w2 - w1)} * \ 100 \qquad 3.11$$

W_1 = Weight of empty beaker; W_2 = Weight of beaker with sample and W_3 = Weight of beaker after drying and cooling.

3.8.8 Determination of metal ions

Exactly 25 ml of 50 % HNO_3 and 20 % concentrated $HClO_4$ were added to 50 ml of each sample. The mixture was heated gently on a hot plate until solution was clear and white fumes of $HClO_4$ appeared. This was cooled and 20 ml of distilled water added. This was then be filtered and made up to 50 ml in a volumetric flask (Greenberg, 1980).

The wastewater samples were analyzed for Cd, Cr, Zn, Ni and Pb ion concentrations using the method of Ramons *et al., (*1999). The samples were filtered using Whatman 0.45 µm filter paper into clean beaker and acidified with 3 mls of 50 % HNO_3(aq) per dm^3 of water. 50 ml of the sample was measured into a beaker, 10 ml of 1:1 v/v nitric acid measured into the beaker containing the samples and placed on a water bath at 100^oC. The sample was digested for an hour, after which the process was repeated using

codes to blind analyst and to further validate the accuracy of the results. The digested samples were placed in sample bottles and tested for heavy metals using Atomic Absorption Spectrometry (AAS) with the Hollow cathode lamps of Cd, Cr, Zn, Ni and Pb respectively. The average results from the AAS for both the raw and treated samples were recorded and correlated. The analysis was done in the Department of Soil Science, Ahmadu Bello University, Zaria.

3.8.9 Nitrate, Phosphate and Sulphate

The concentrations of nitrates, phosphates and chlorides in the raw and treated wastewater samples were determined digitally by the use of water analyser/ multiparameter logging spectrophotometer (HANNA multiparameter HI83200). The spectrophotometer was checked for malfunctioning in anions determination by passing standard solutions of all the ions to be measured. A blank sample (deionised water) was passed between every three measurements to check for any eventual contamination or abnormal response of the equipment.

3.8.10 Microbial Analysis and Enumeration

The microbiological analysis was carried out within 24 hours after sample collection. The microbial load in the raw and treatment wastewater were measured using spread plate technique at the Department of Microbiology, Ahmadu Bello University Zaria. Total heterotrophic bacterial and fungal counts for the raw and treated wastewater samples were enumerated. An aliquot (1 ml) of the wastewater was transferred into 9 ml of distilled water and diluted serially in ten folds up to 10^4 according to the method of Adesemoye (2006). Then, 0.1 ml aliquots of the serially diluted samples were plated in duplicate plates of molten Nutrient agar (NA) and Saboraud dextrose agar (SDA) at 45 ^oC for the isolation and enumeration of total aerobic bacteria and fungi respectively.

They were swirled to mix and colony counts were taken after incubating the plates at 37 °C for 48 hours for the bacterial count and at ambient laboratory temperature for 5 days for the fungal count. After the incubation period, bacterial colonies and pure cultures of the fungi isolates, which developed on the plates, were enumerated, multiplied by 10 and by the dilution factors, and the results expressed as the number of colony-forming units (CFU/ml) of samples.

3.9 Column Adsorption Studies

The adsorption study was conducted using a cylindrical borosilicate glass column with diameter- 2.4 cm, length- 32.2 cm, volume- about 150 ml. The column was mounted vertically and packed with 10 g of the prepared activated carbon using a dry packing technique from the top of the column and allowed to settle by gravitational force. The bottom part of the adsorbent in the column was packed with small amount of nonreactive glass wool. Distilled water was used to prevent the adsorbent from blocking the tap of the column. The schematic of the column adsorption setup is presented in Figure 3.2. The column with the adsorbent was washed with 10ml of distilled water prior to introduction of the wastewater sample to the column. Exactly 50 ml of the wastewater was transferred into the column containing activated carbon and allowed to have contact with the adsorbent for 10 minutes. The adsorbent was kept submerged throughout the runs to avoid air entrapment in the bed. After the contact time had elapsed, the tap of the column was let open and the treated water (filtrate) allowed to drain and was collected in a beaker, measured and transferred into samples bottles prior to analysis. The concentrations of the tested cations and anions were determined by measuring the amount in the treated water (via the same analyses used for the wastewater sample) and subtracting from the results of the wastewater analysis. This was repeated for each of the prepared neem carbon.

3.9.1 Column breakthrough studies

The column breakthrough study was carried out using NHH because of its low surface area relative to the other adsorbents. In the same vein, nickel ion was selected for the study due to its high concentration in the wastewater. A constant wastewater volume of 100 ml and tap flow rate of 0.133 ml/min was used while varying the bed height of NHH in the column which also affects the weight of the adsorbent as presented in Figure 3.2. The column was continuously and carefully filled with the wastewater sample, to ensure that the column did not run out of the required wastewater volume and that the column bed was not disturbed within the investigation period. The breakthrough curves for the removal of nickel ion from the hospital wastewater were analyzed using the Bohart Adams model. The breakthrough time (t_b) is defined as the time when the effluent concentration (C_t) of nickel ion reached 50% of the feed concentration (C_o). Breakthrough curve were plotted giving ratio of effluent and inlet concentrations (C_t/C_o) versus time.

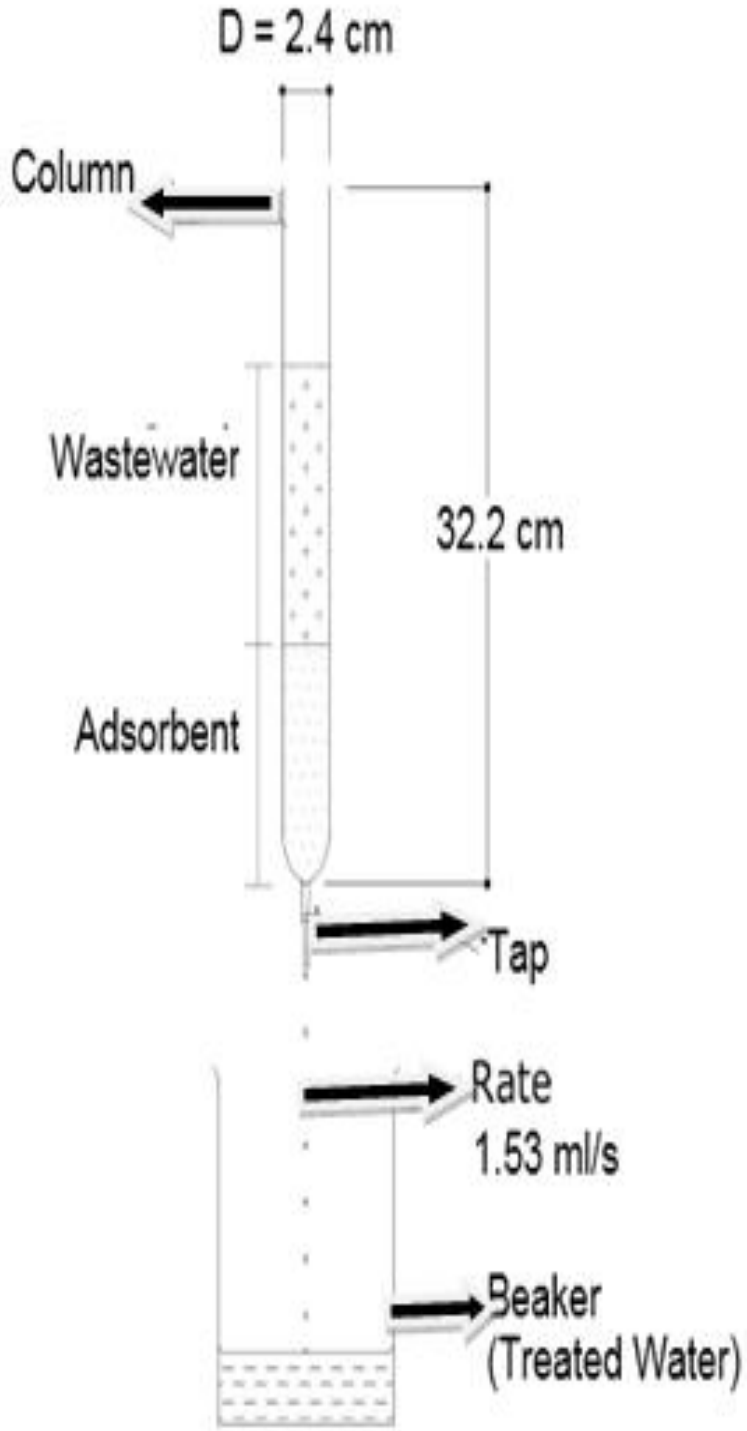


Figure 3. 2: Schematic of laboratory column adsorption filter setup

3.9.2 The effect of contact time

The effect of contact time was investigated by varying the time the wastewater had contact with the adsorbents before draining. Contact time of 10, 15, 20, 25 and 30 minutes were used. The amount of wastewater and adsorbents used were kept constant at 50 ml and 10 g respectively. This was repeated for each of the prepared neem carbon.

3.9.3 The effect of wastewater volume

The effect of wastewater volume on the treatment efficiency of the adsorbents (10g) was investigated by varying the amount of wastewater samples introduced into the column from 10, 20, 30, 40 to 50 ml. Equilibrium studies on the treatment efficiency of the adsorbents used on the tested parameter was also carried out using the data obtained by varying the wastewater volume. This was repeated for each of the prepared neem carbon.

3.9.4 Regeneration Studies

Regeneration studies were carried out by randomly selecting one of the neem activated carbons to determine its adsorption efficiency after each adsorption-desorption for five cycles. After the initial adsorption process, the activated carbon sample was washed with exactly 100 ml of hot distilled water and oven dried in an oven for an hour. After drying, the column was repacked while 50 ml of the wastewater sample was again introduced into the column and left for 30 minutes. The procedure was repeated four more times and the regeneration data were used to explain the reuse capacity for each adsorbent. The efficiency of regeneration was calculated using Equation 3.13.

$$Efficiency\ of\ regeneration = \frac{(Initial\ Conc. - Final\ Conc.)}{Initial\ Conc.} X\ 100 \qquad 3.13$$

CHAPTER FOUR

4.0 RESULTS

4.1 Physicochemical Properties of Raw Neem and the Prepared Activated Carbons

The results of the physicochemical analysis of the raw and activated carbon are presented in Table 4.1. The physicochemical parameters investigated include; the moisture content, ash content, bulk density and fixed carbon contents. Figure 4.1 and 4.2 show the efficiency of the carbonization and activation processes at various temperatures of carbonization and activation. The optimum temperatures of carbonization and activation are determined from these plots (Figure 4.1 and 4.2).

4.2 The BET Surface Area and Pore Characterization of the prepared Activated Carbon

The BET surface areas and pore sizes of the neem carbon activated with $ZnCl_2$ and H_3PO_4 are presented in Table 4.2. The results were linearly regressed using the BET equation. The coefficient of regression (R^2) for the four adsorbents were determine from the plot as shown in Figures 4.3, 4.4, 4.5 and 4.6.

Table 4. 1 Physicochemical parameters of the raw and activated neem (*Azadirachta indica*) husk and seed cake:

Parameters	**RNH**	**RNC**	**NCZ**	**NCH**	**NHZ**	**NHH**
MC (%)	4.45±0.07	8.95±0.07	3.62±0.04	3.67±0.11	3.05±0.21	3.02±0.28
DM (%)	95.5±1.41	91.05±0.92	96.38±1.27	96.23±1.27	96.95±0.83	96.98±2.82
VMC (%)	54.44±2.35	53.10±3.68	9.81±2.11	10.14±1.39	12.06±2.86	3.89±0.57
ACt (%)	11.33±1.13	6.56±3.04	18.70±0.64	18.60±2.33	18.34±2.55	20.11±2.72
FCC (%)	29.78±3.31	25.62±1.15	67.87±1.33	67.49±2.21	66.55±2.11	72.98±1.71
PS (µm)	400	400	350	350	350	350
BD (g/ml)	0.95±0.10	0.87±0.13	0.77±0.17	0.83±0.13	0.76±0.16	0.82±0.13

MC represents Moisture Contents, DM stands for Dry Matter; VMC represent Volatile Matter Content; ACt – Ash Content; FCC – Fixed Carbon Content; PS – Particle Size; and BD represents Bulk Density, RNH and RNC represent Raw Neem Husk and Raw Neem Cake respectively, NCZ and NCH represent Neem cake activated with $ZnCl_2$ and Neem cake activated with H_3PO_4 respectively; NHZ and NHH are represent Neem husk activated with $ZnCl_2$ and Neem husk activated with H_3PO_4 respectively.

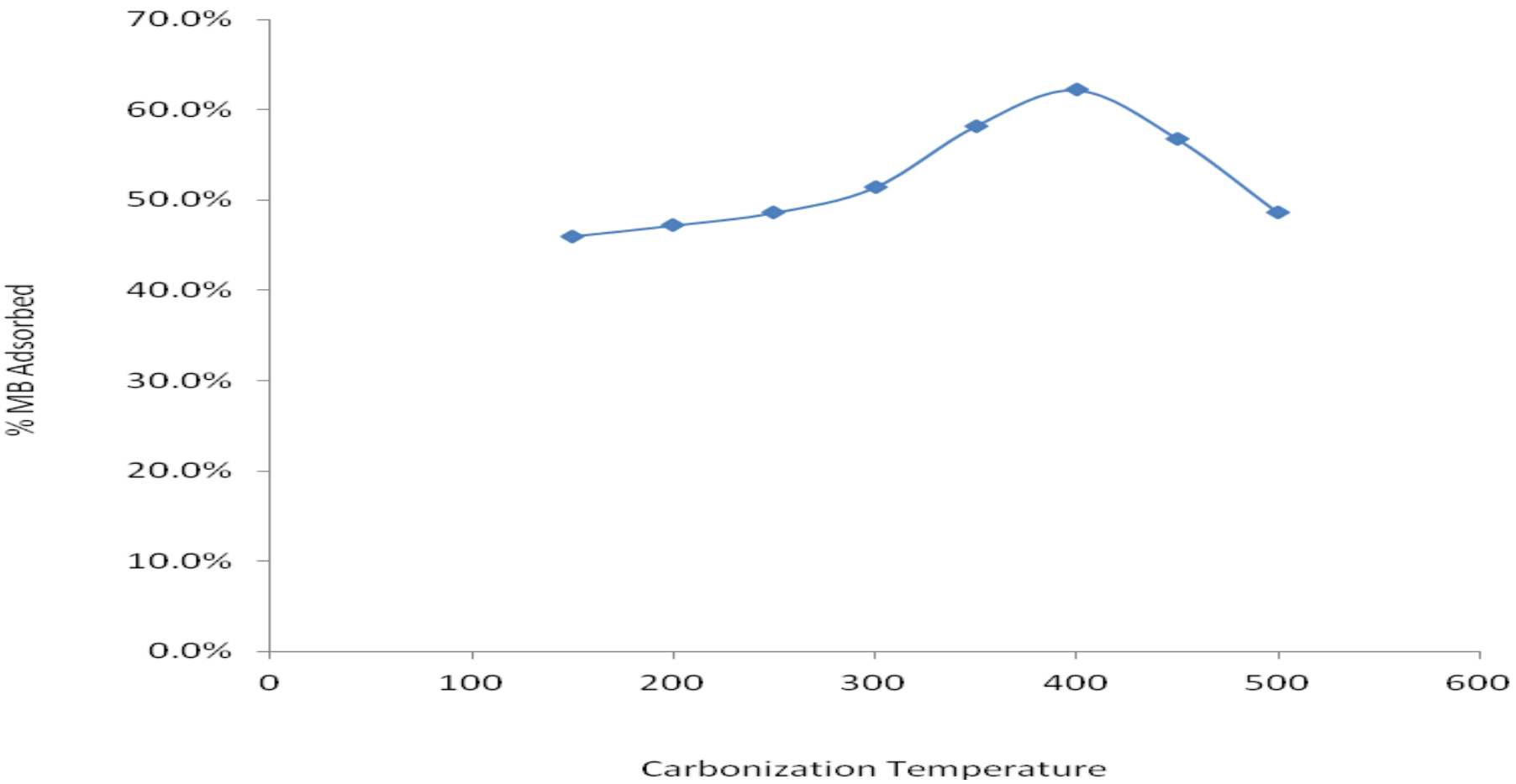


Figure 4. 1: Effect of carbonization temperature on methylene(MB) adsorption

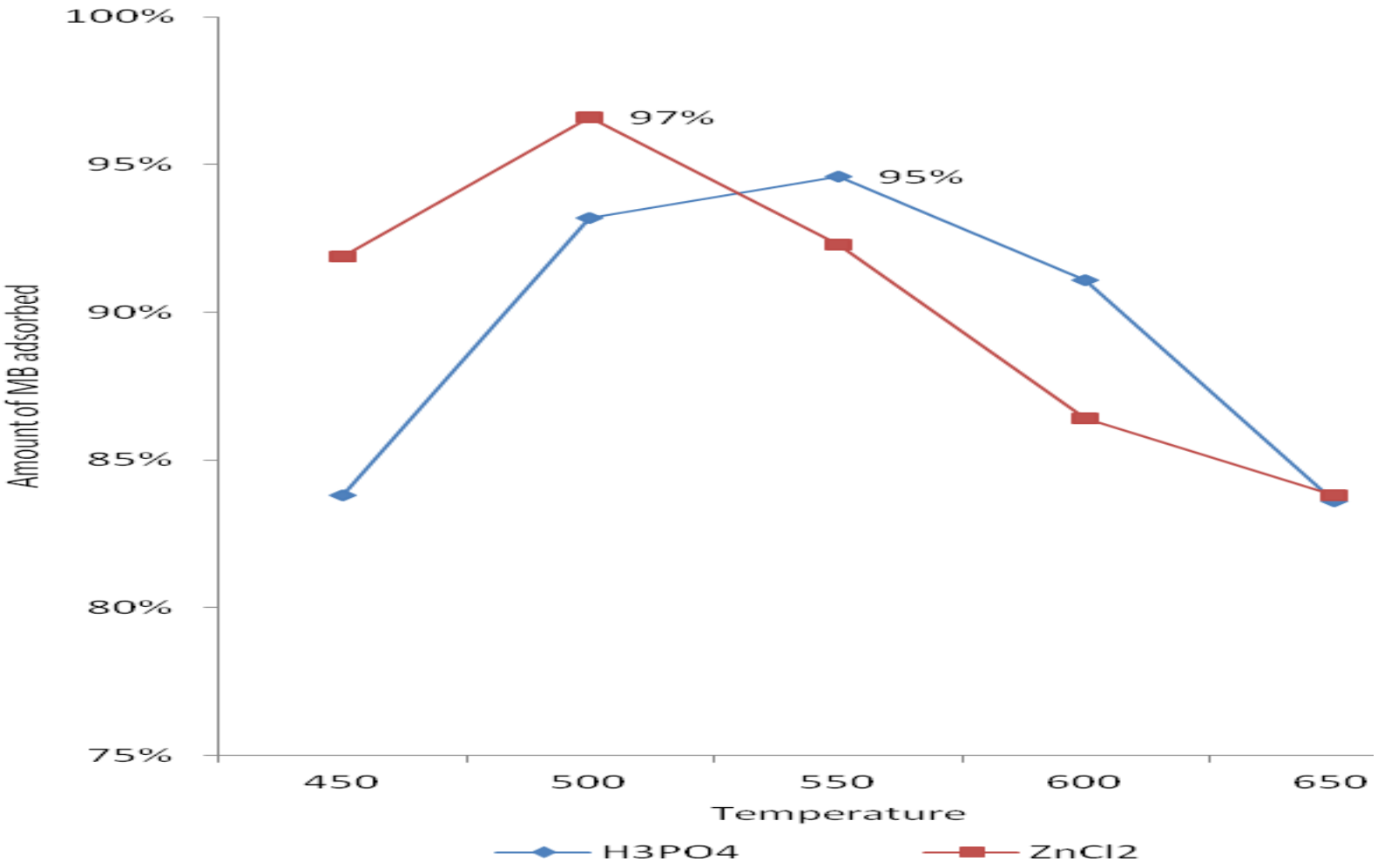


Figure 4. 2: Effect of activation temperature on methylene blue (MB) adsorption

Table 4. 2 BET Surface Area and Pore characterization of the activated carbon

	Activating Agent	**R^2**	**Type**	**Qm**	**BET_{SA} (m^2/g)**	**P_{vol} ml/g)**	**P_{Size} (Å)**
Neem	H_3PO_4	0.9969	II	53.02	230.79	0.010752	22.221
Husk	$ZnCl_2$	0.9966	II	54.80	238.56	0.009838	22.456
Neem	H_3PO_4	0.9967	IV	80.87	352.00	0.0472	34.26
Cake	$ZnCl_2$	0.9966	II	57.93	252.18	0.014657	24.155

R^2 is the coefficient of regression; *Type* represents the adsorption Isotherm type; BET_{SA} represents the Brunauar-Emmet-Teller surface area of the adsorbents; Q_m is the monolayer Quantity of gas adsorbed; P_{vol} is the pore volume of the adsorbent and P_{size} is the calculated Pore sizes of the materials.

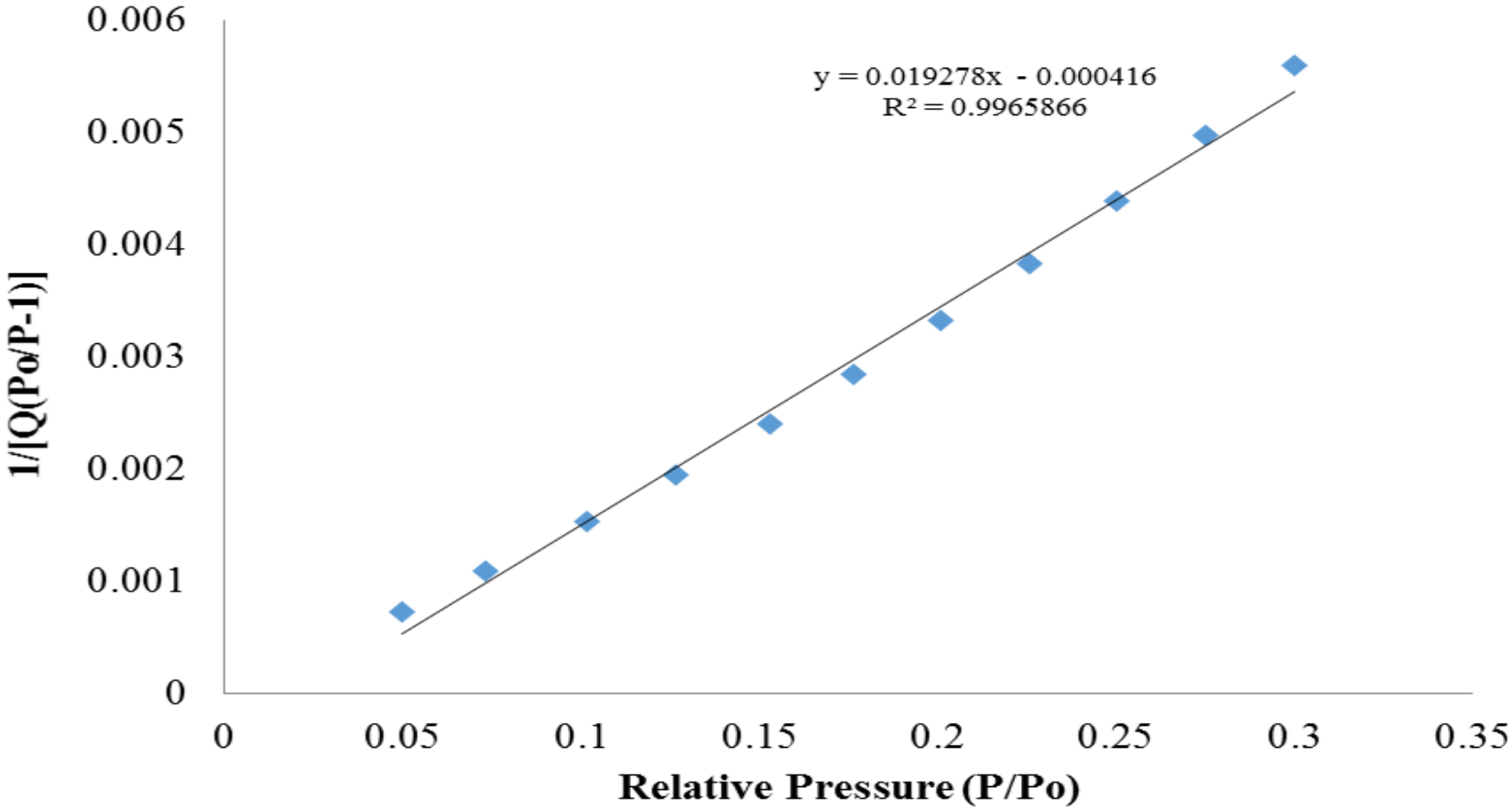


Figure 4. 3: Nitrogen adsorption isotherm plot for neem cake activated with $ZnCl_2$ (NCZ)

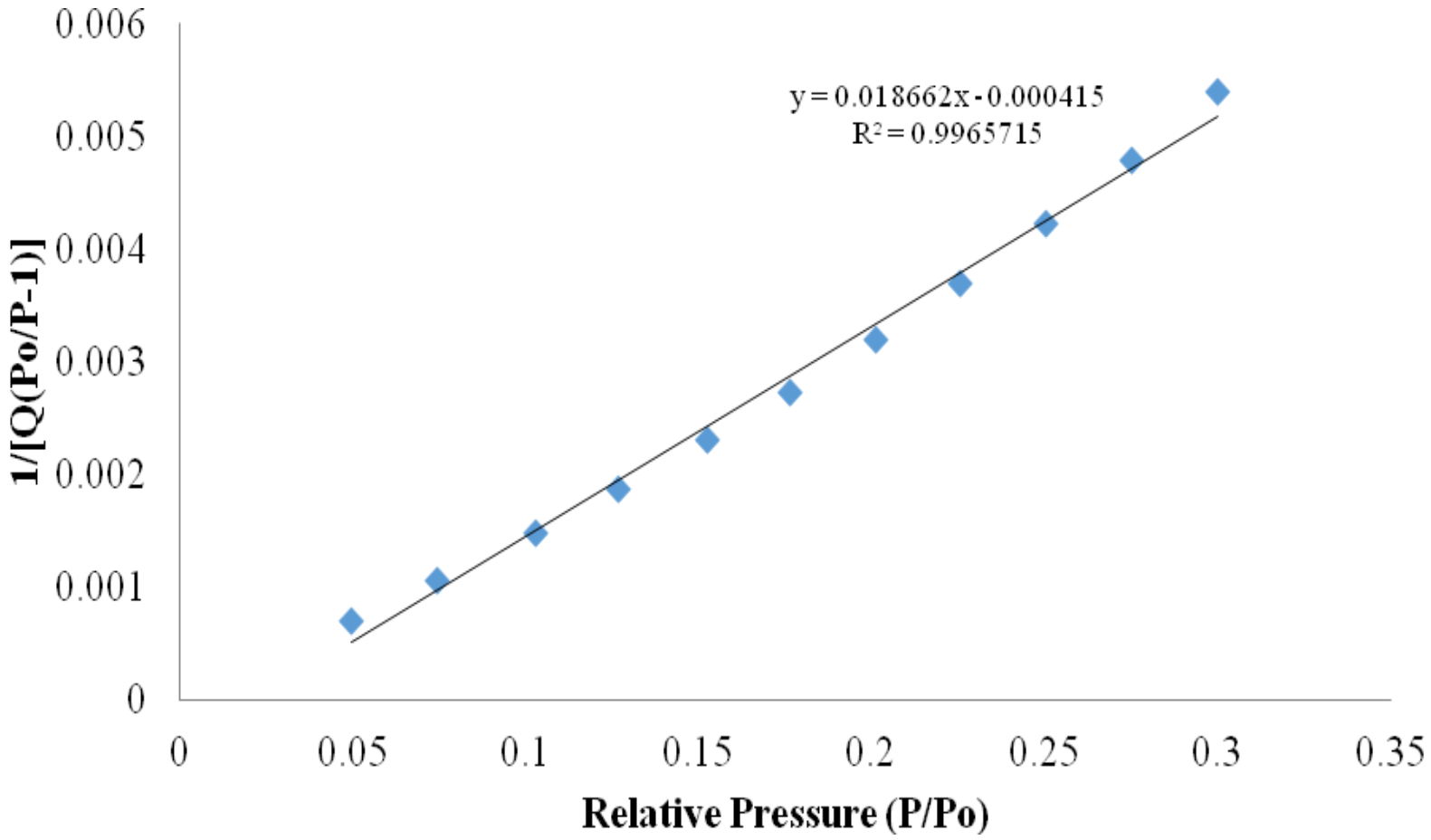


Figure 4. 4: Nitrogen adsorption isotherm plot for neem husk activated with $ZnCl_2$ (NHZ)

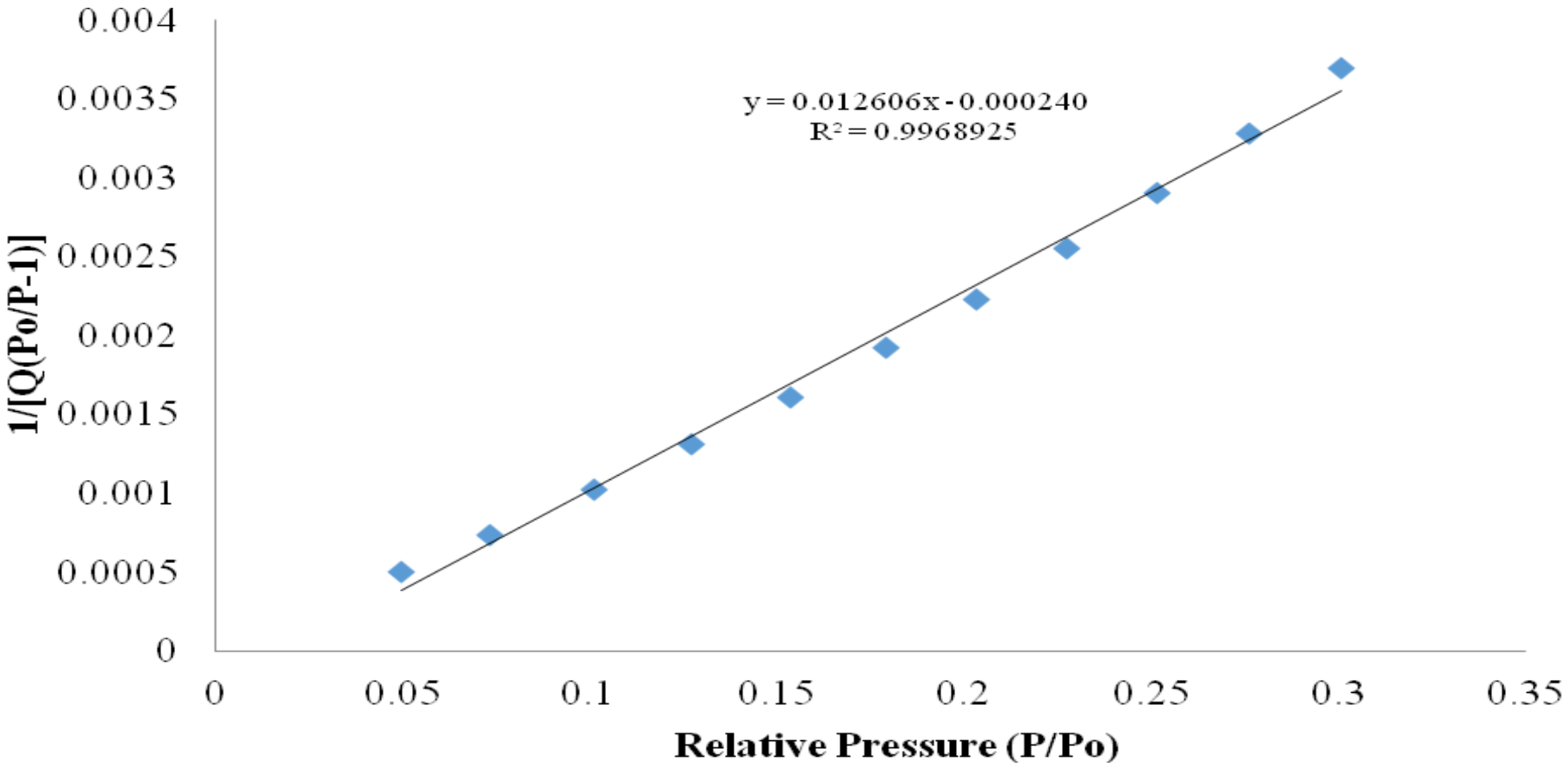


Figure 4. 5: Nitrogen adsorption isotherm plot for neem husk activated with H_3PO_4 (NHH)

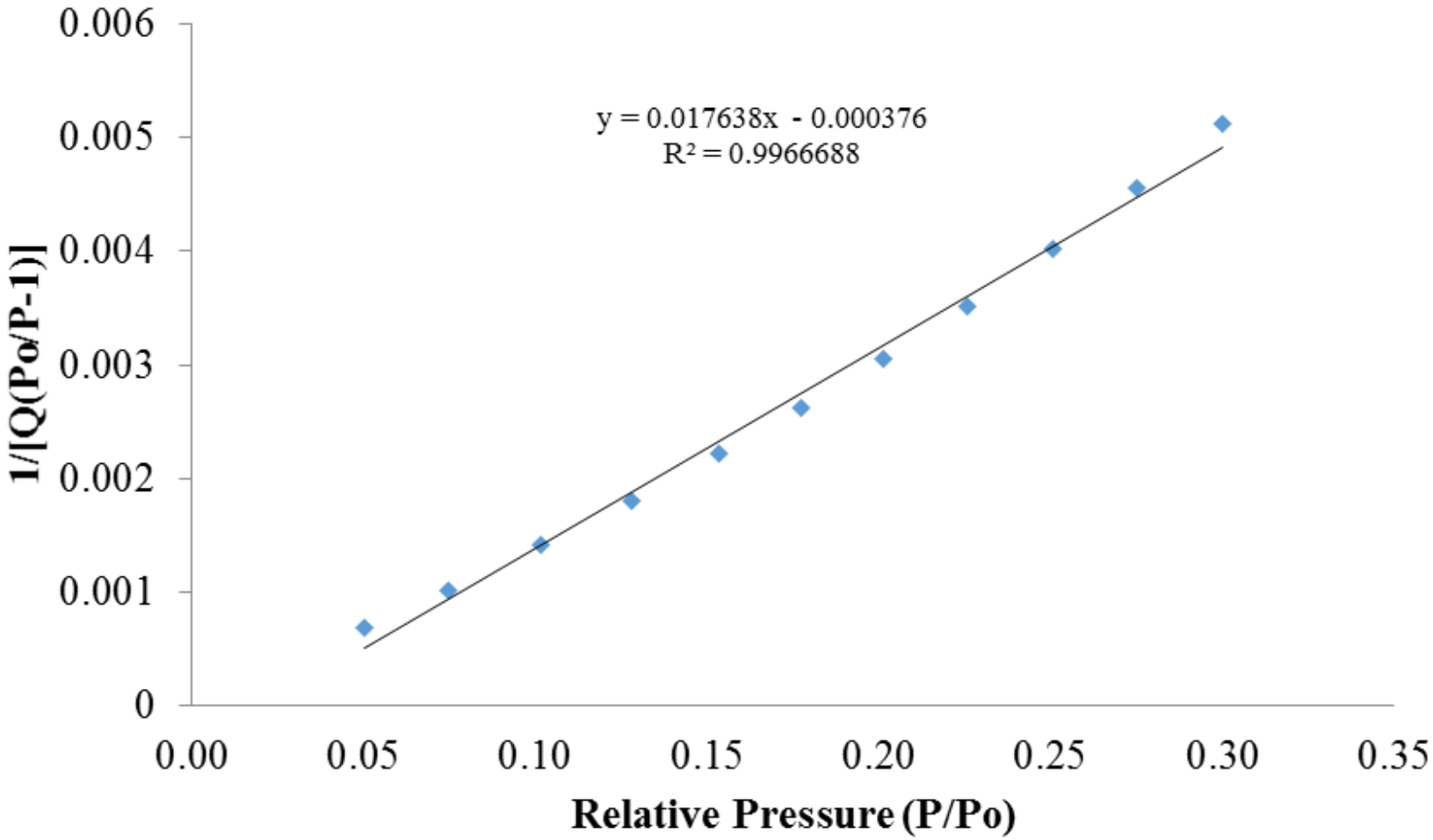


Figure 4. 6: Nitrogen adsorption isotherm plot for neem cake activated with H_3PO_4 (NCH)

4.3 Fourier Transform Infrared (FTIR) Analysis

The FTIR band positions and their assignments for the raw and activated neem carbons over the range of 400 – 4000 cm^{-1} are presented in Table 4.3. Figure 4.7 show the FTIR of the raw neem husk, the major bands were observed between 3,400 – 3,900 cm^{-1}, 2,200 – 2,400 cm^{-1}, 1,400 – 1,700 cm^{-1} and 1,000 – 1,200 cm^{-1} and less than 1,000 cm^{-1}. Figures 4.8 and 4.9 show the spectra of the activated neem husk carbons. The FTIR spectra band positions of the raw neem cake have similar band with that of the raw neem husk as presented in Figures 4.10.

4.4 Scanning Electron Microscope (SEM)

The micrographs of the transverse section of the neem activated carbons are presented in Figures 4.13 – 4.16.

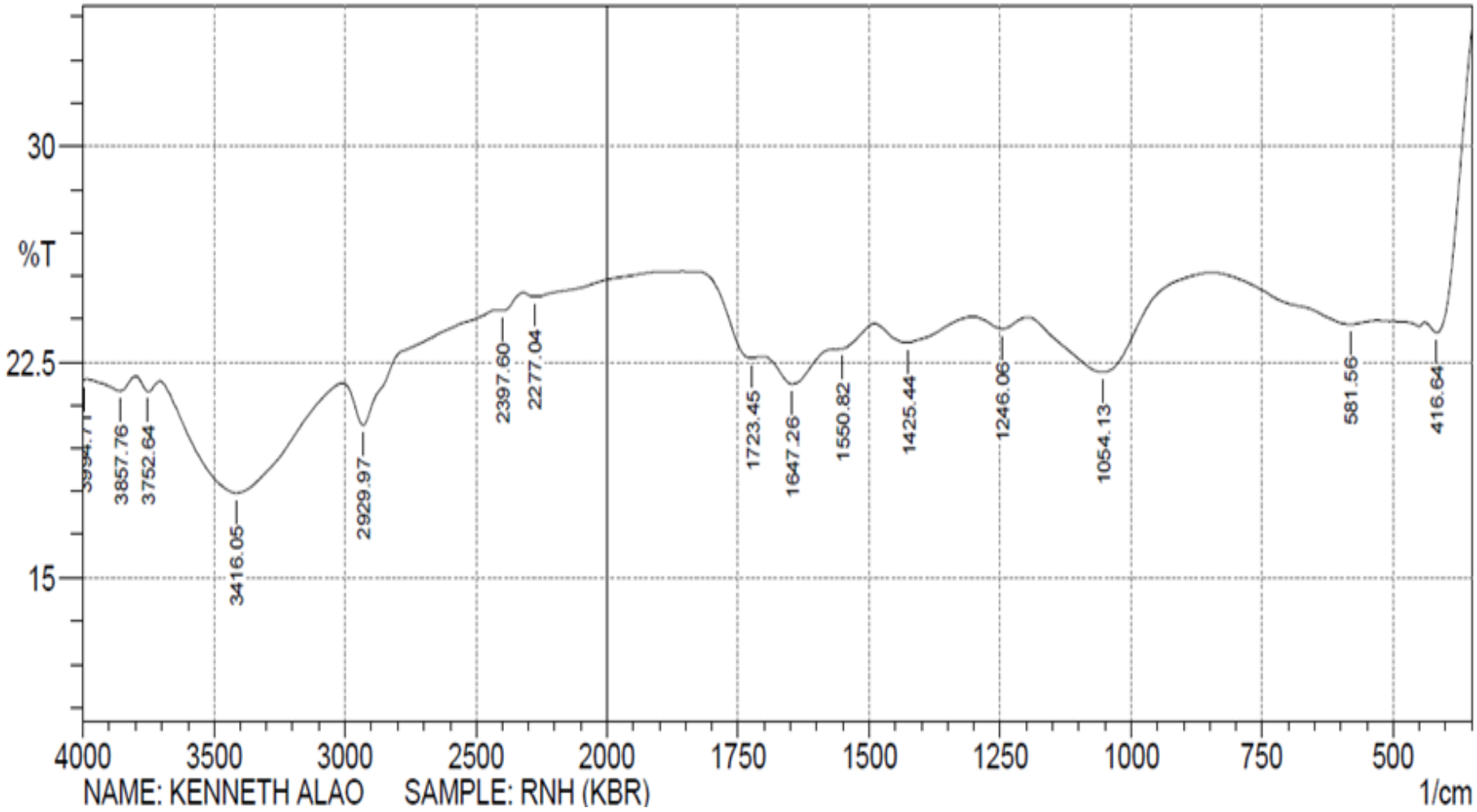


Figure 4. 7: Fourier Transform Infrared Spectroscopy of the Raw Neem Husk (RNH)

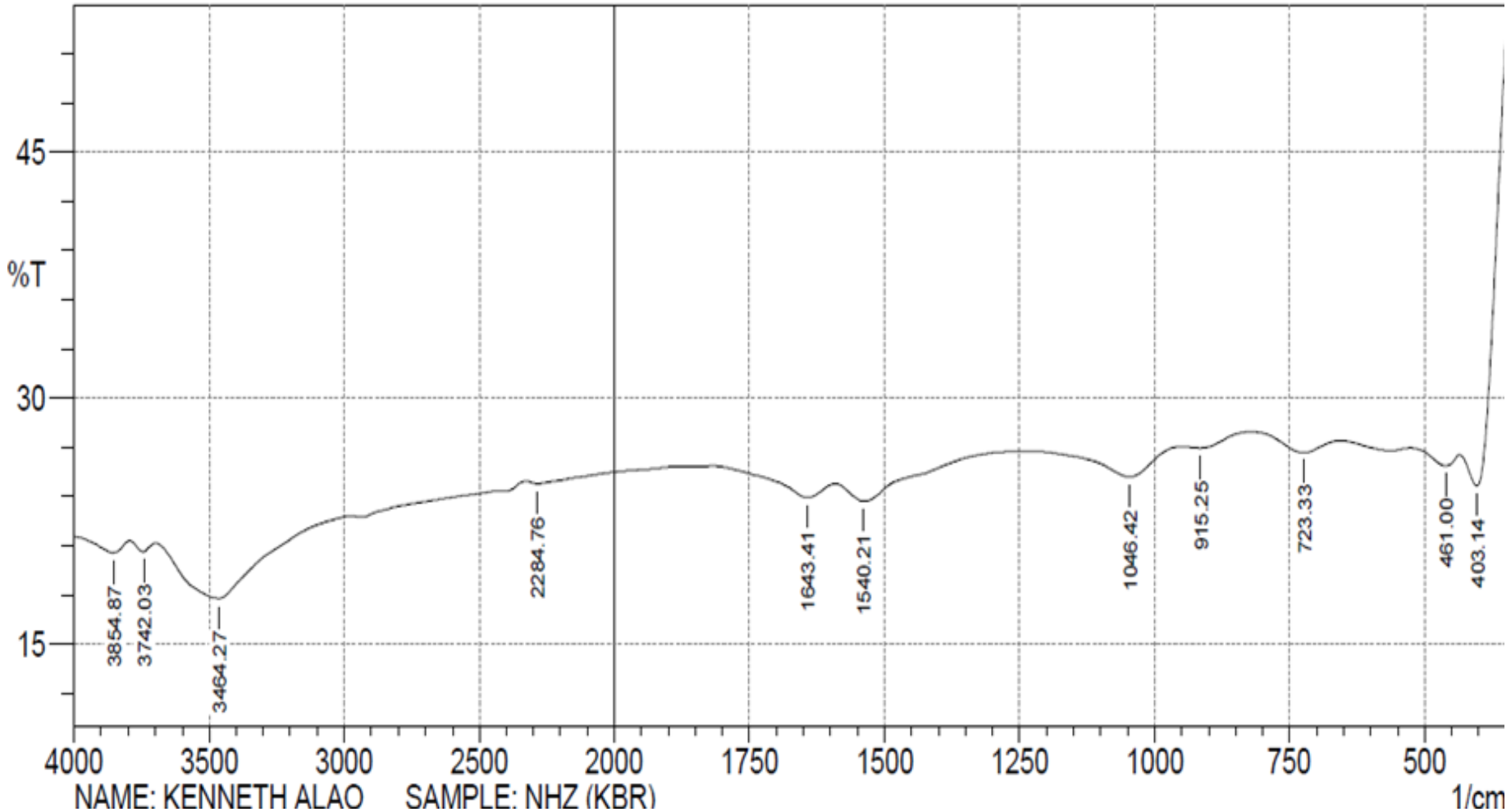


Figure 4. 8: Fourier Transform Infrared Spectroscopy of Neem Husk activated with $ZnCl_2$ (NHZ)

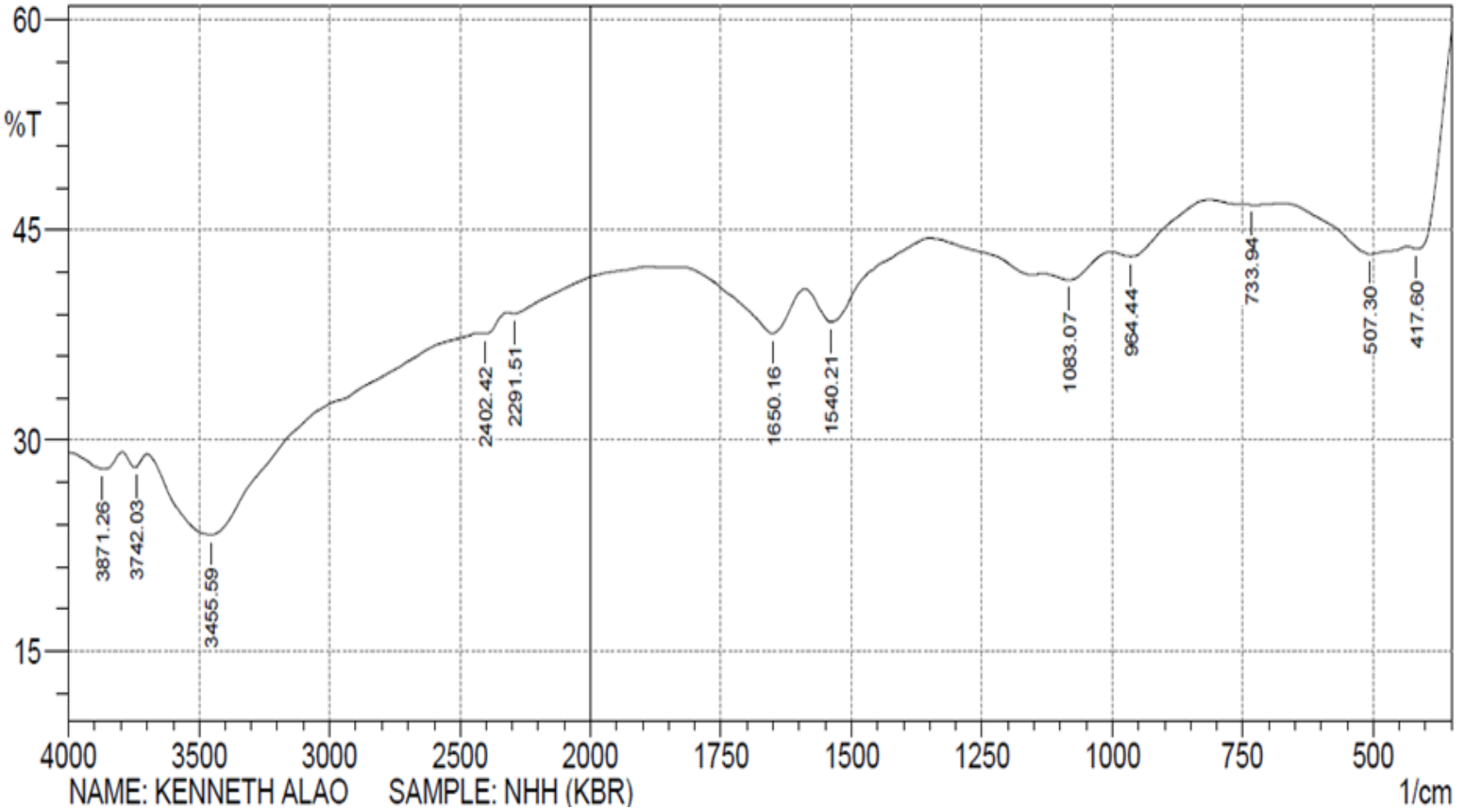


Figure 4. 9**:** Fourier Transform Infrared Spectroscopy of Neem Husk activated with H_3PO_4 (NHH)

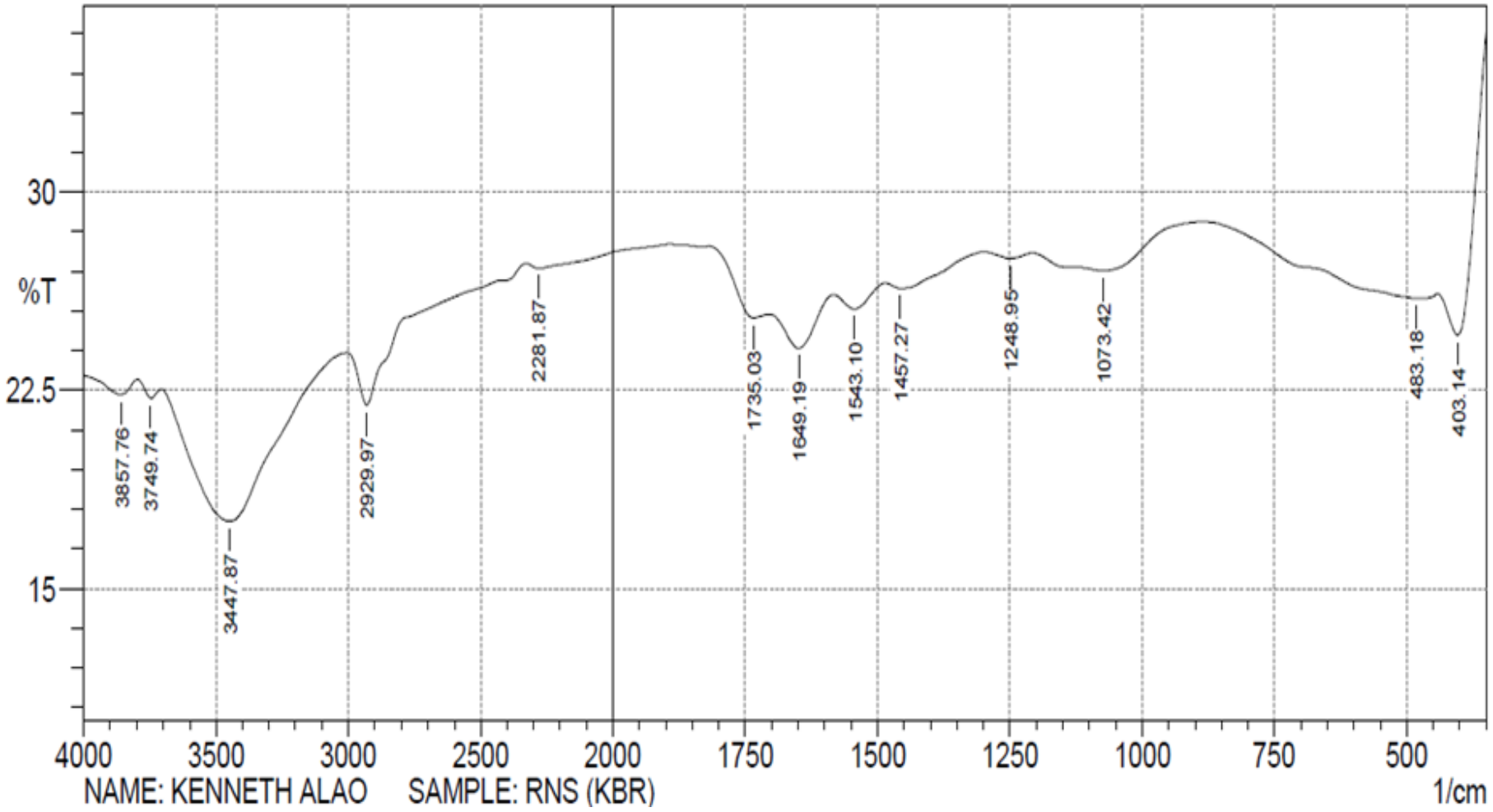


Figure 4. 10: Fourier Transform Infrared Spectroscopy of the Raw Neem Cake (RNC)

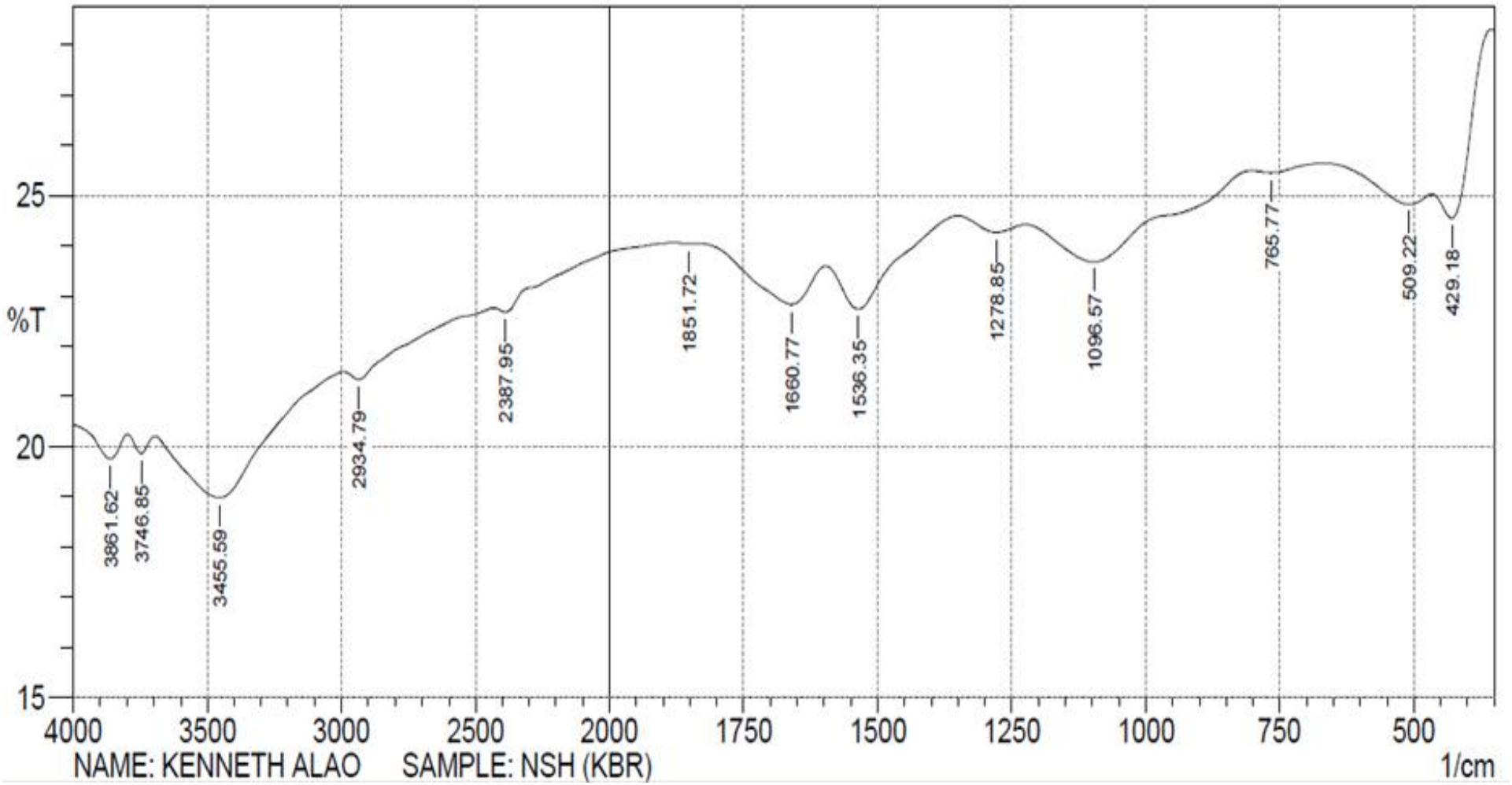


Figure 4. 11: Fourier Transform Infrared Spectroscopy of the Neem Carbon activated with H_3PO_4 (NCH)

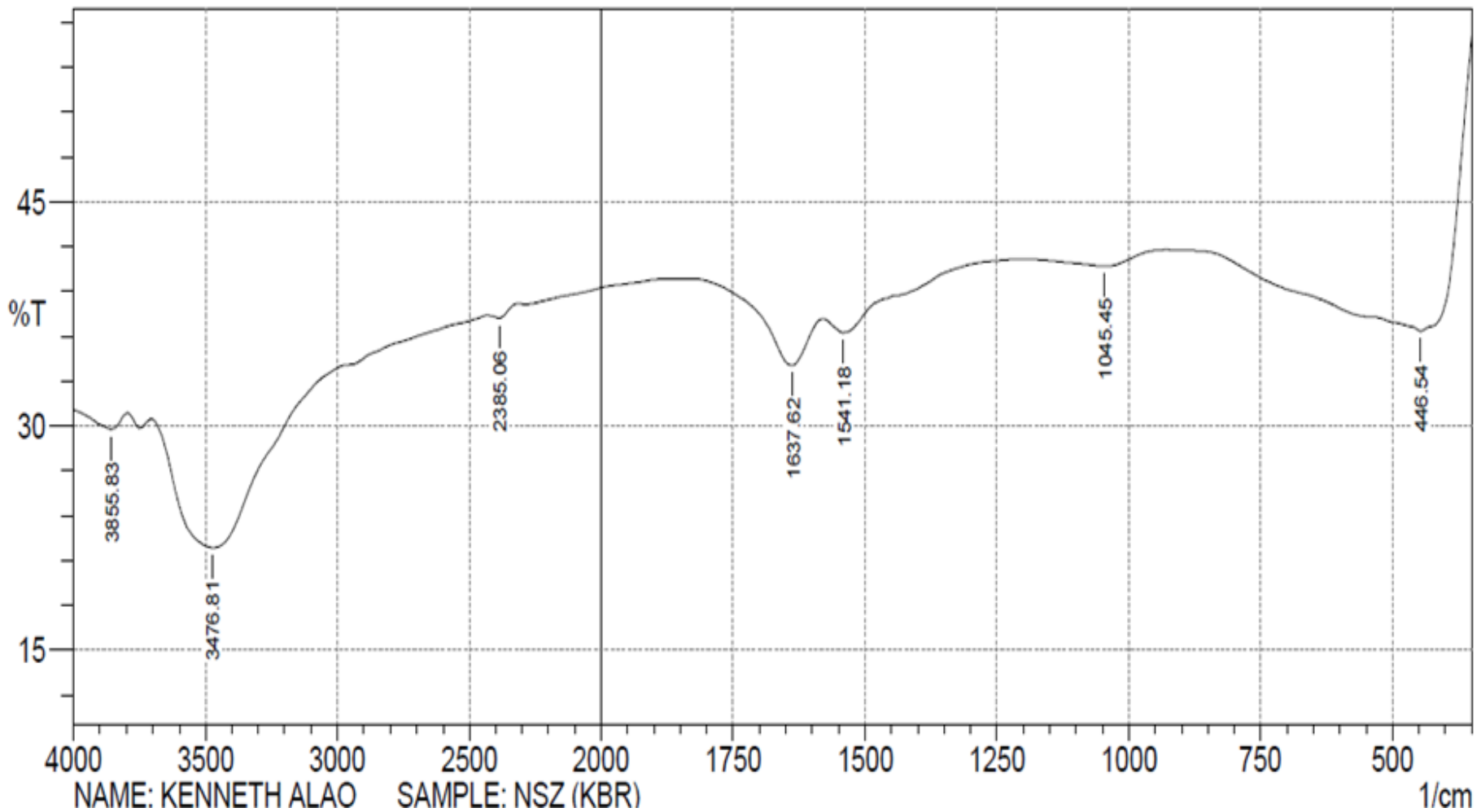


Figure 4. 12: Fourier Transform Infrared Spectroscopy of Neem Cake activated with $ZnCl_2$ (NCZ)

Table 4. 3 FTIR Table of assignment for the raw and activated neem carbon

Position (cm^{-1})	**Vibration (Raw Sample)**	**Vibration (AC Sample)**	**Inference**
547-532		M-X	Metals bound to halogens: $ZnCl_2$
914		PO_4^{3-}	Phosphates
1100-900		SiO_4	Silica/ash
1010-1000	M=N or M=O stretch*	M=O	Inorganic metal bound to Nitrogen or polysaccharides
1375	NO_2 bending		From neem oil
1480-1400	C=O stretching		Carbonate from esthers and acids in oil
1660-1620	C=C, C=O, O-H bending	C=O	Alkenes, amide bands
1745	C=O		Carboxylic acids and esters
2934-2387	C=O stretching	C=O	carbonates
3824-3440	O-H stretching	O-H stretching (Reduced)	Surface and rapped hydroxyl groups molecules.

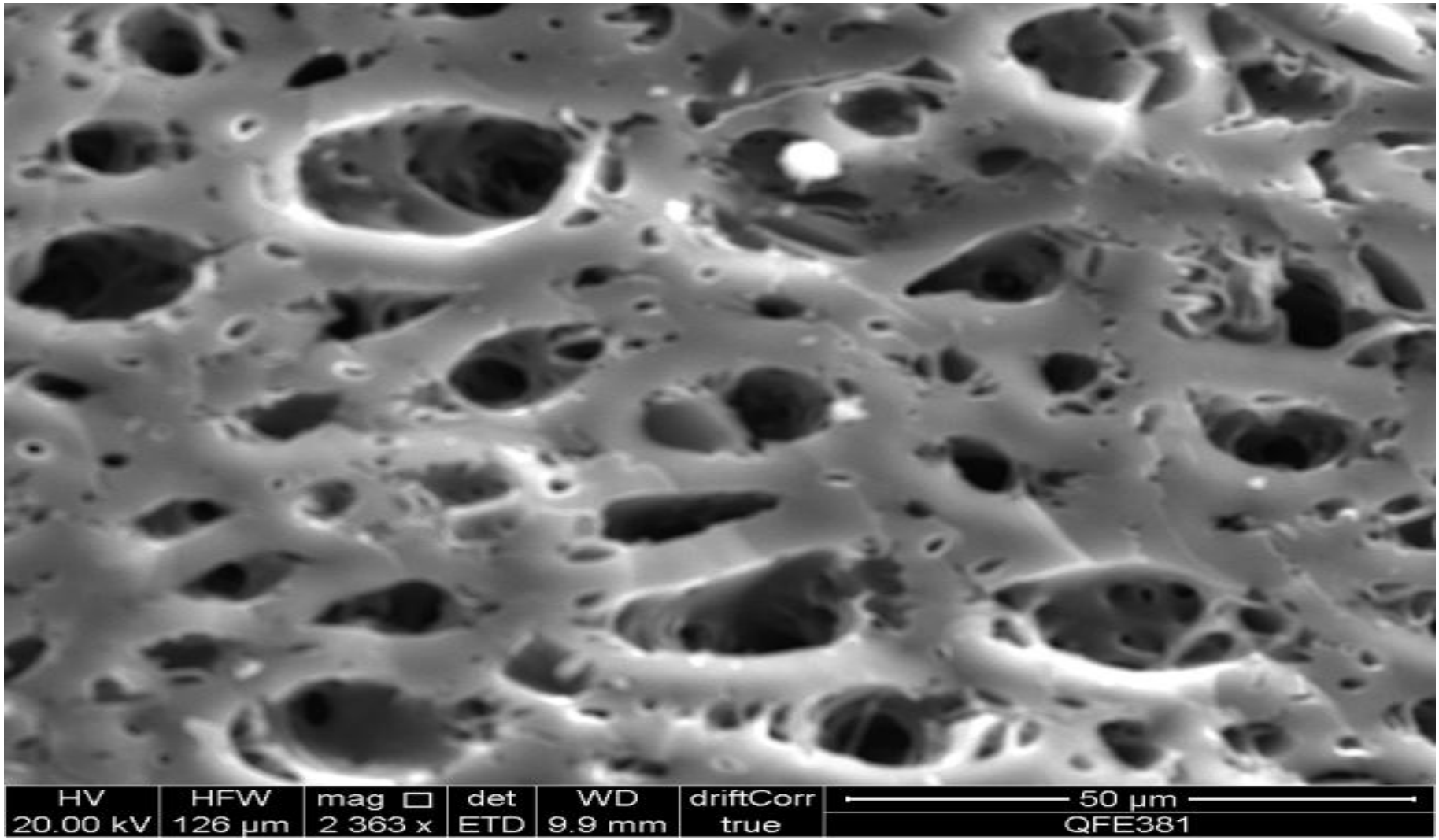


Figure 4. 13: Micrograph of the transverse section of Neem Cake activated with $ZnCl_2$ (NCZ)

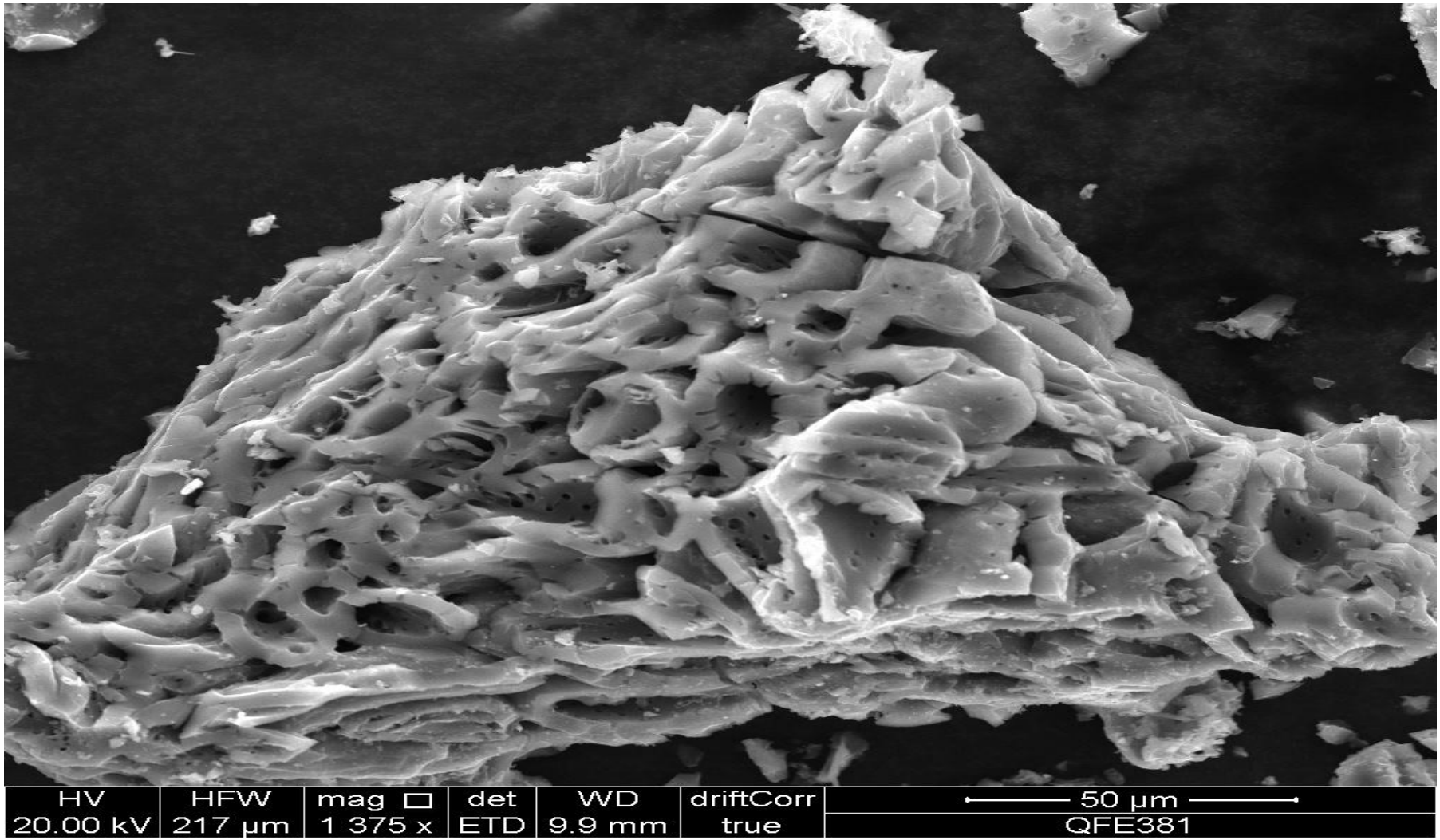


Figure 4. 14: Micrograph of the transverse section of Neem Husk activated with $ZnCl_2$ (NHZ)

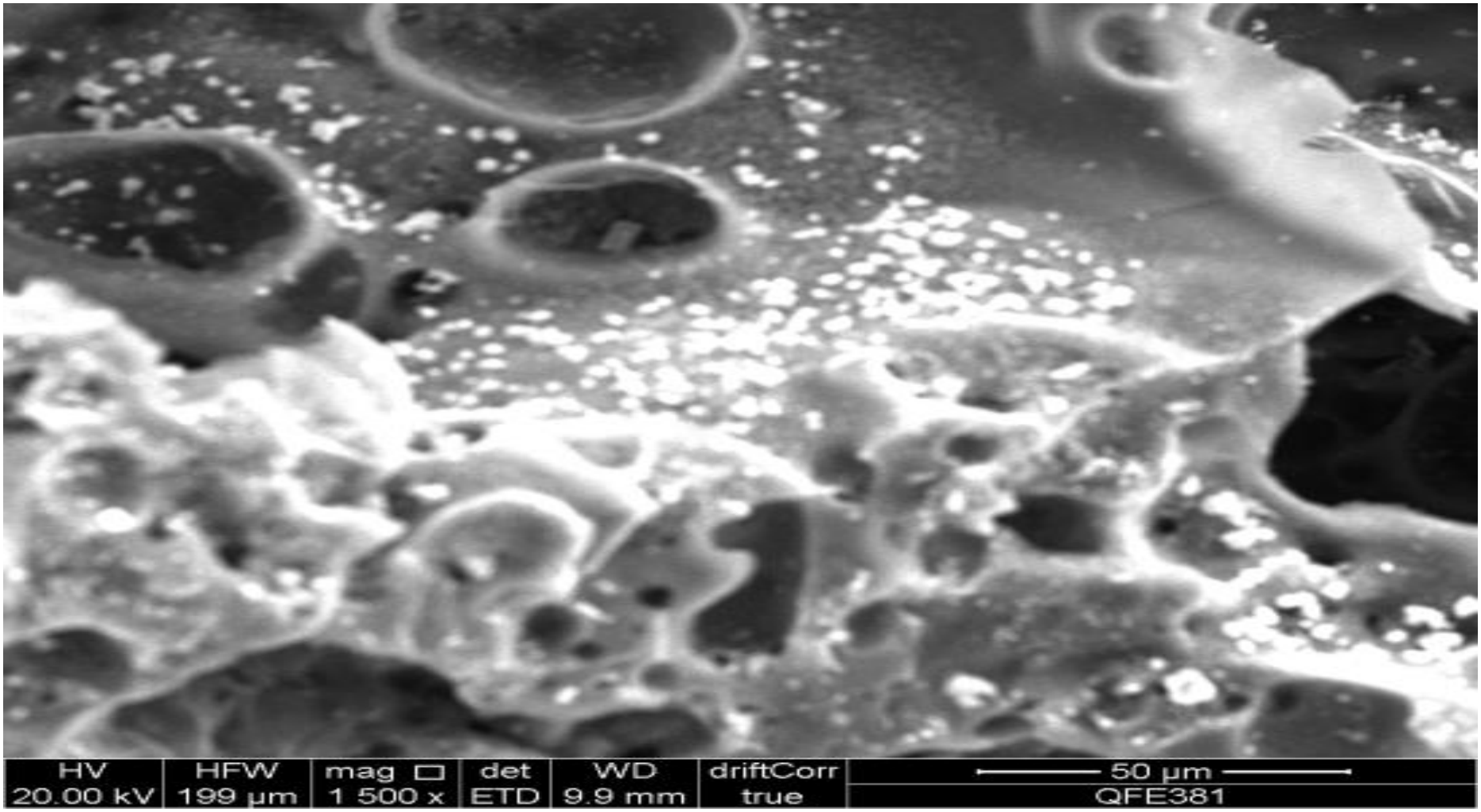


Figure 4. 15: Micrograph of the transverse section of Neem Husk activated with H_3PO_4 (NHH)

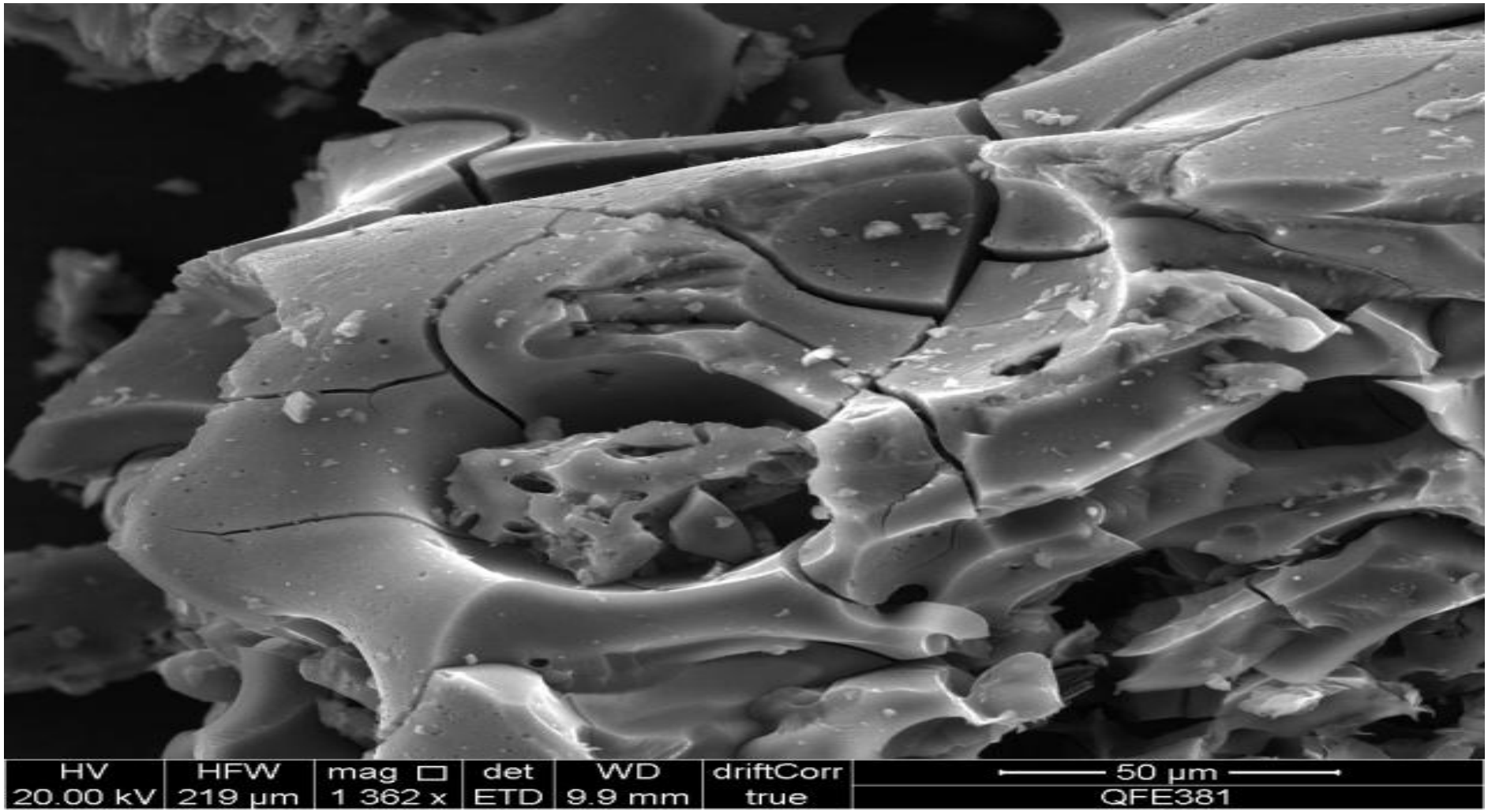


Figure 4. 16: Micrograph of the transverse section of Neem Cake activated with H_3PO_4 (NCH)

4.5 Thermal-Analytical Studies

Figures 4.17 – 4.20 present the thermograms of the activated carbons. The characterization features of the thermograms are summarized in Table 4.4. The result showed two stages; stage 1 involved mass loss between 80 – 120^{o}C while stage 2 involved mass loss at higher temperature between 350 – 500^{o}C. At lower temperature, the mass loss was within the range of 3.02 – 3.67% while the mass loss at higher temperature was within 3.89 – 12.06%.

4.6 Physicochemical Characteristics of the Hospital Wastewater Before and After Treatment

The physicochemical characteristic of the hospital wastewater before and after treatment with the neem carbon activated was investigated. The prepared neem carbons are, Neem Cake activated with $ZnCl_2$ (NCZ), Neem Cake activated with H_3PO_4 (NCH), Neem Husk activated with $ZnCl_2$ (NHZ), Neem Husk activated with H_3PO_4 (NHH). The effect of treatment of wastewater using the prepared neem carbons on biological component is presented in Figure 4.21. The effect of treatment of wastewater using the prepared neem carbons on turbidity, conductivity and pH is presented in Figure 4.22 while that of hardness and Total Dissolve Solids (TDS) is presented in Figure 4.23. The chemical characterization of the wastewater on nitrates, phosphate and chloride ions are presented in Figure 4.24 while characterization of the heavy metals (Cadmium, Chromium, Zinc, Nickel and Lead) is presented in Figure 4.25. The bacterial and fungal count of the wastewater after treatment with the neem carbons is presented in Figure 4.26.

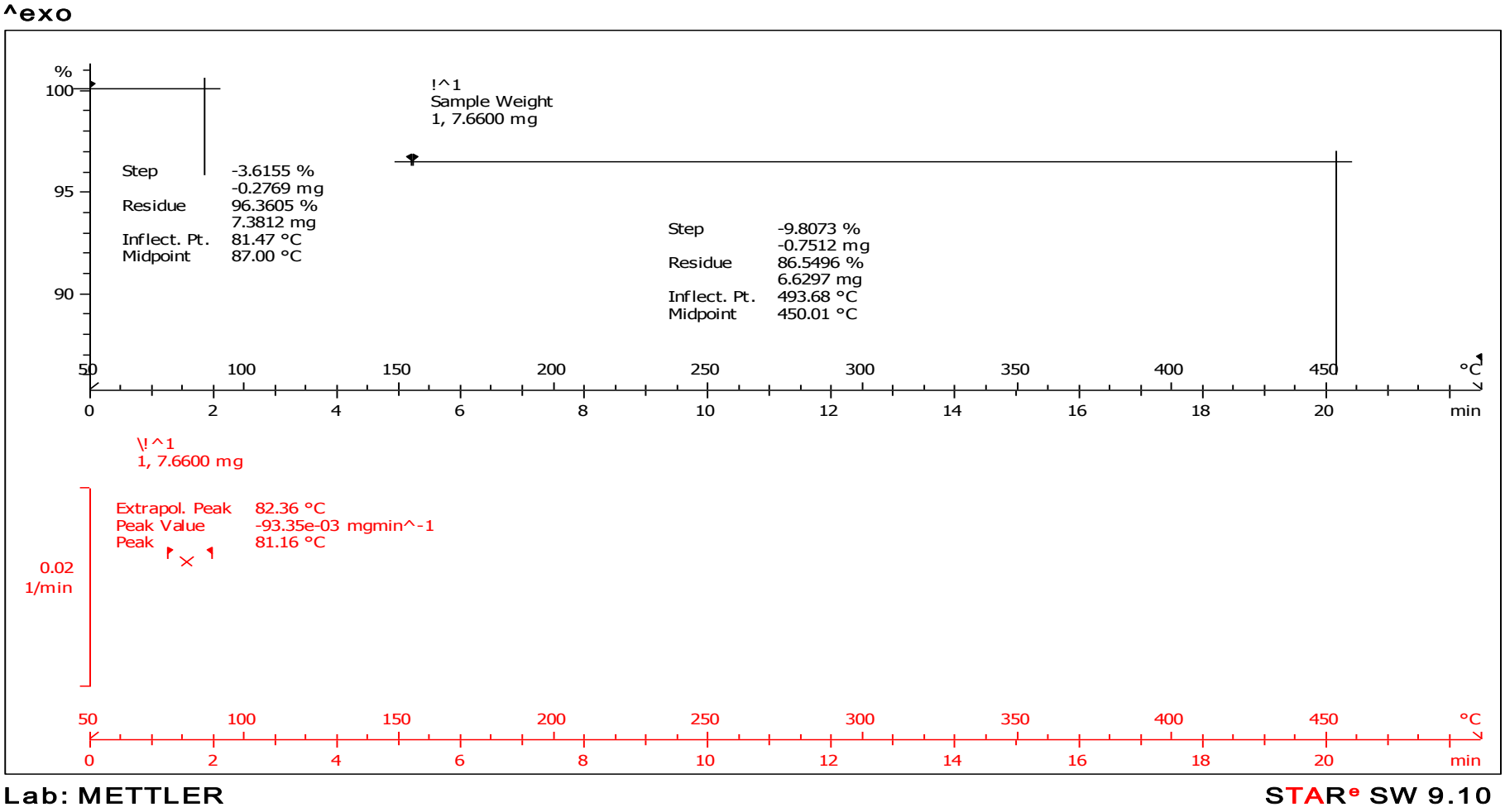


Figure 4. 17: Thermogram of Neem Cake activated with $ZnCL_2$ (NCZ)

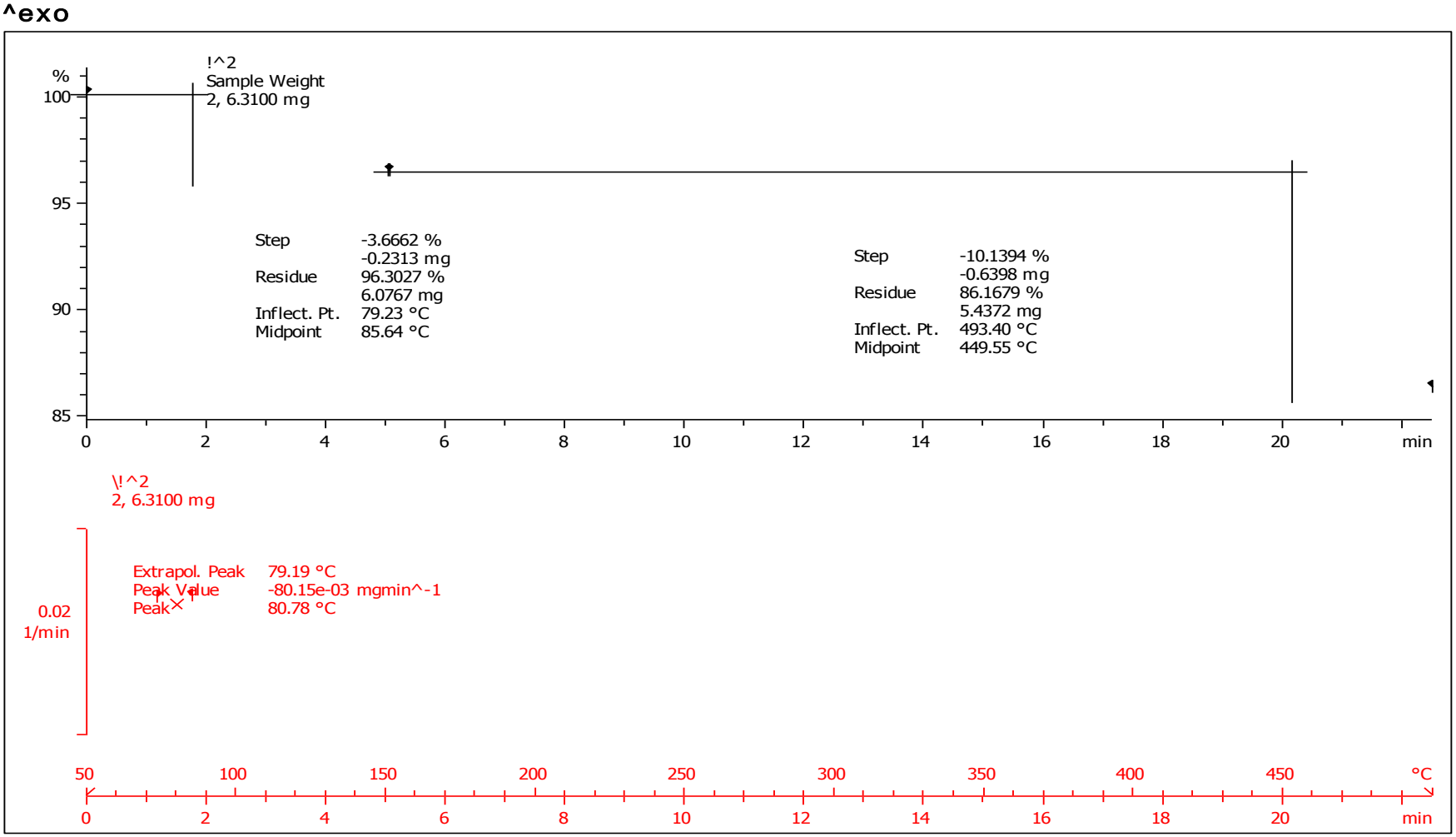


Figure 4. 18: Thermogram of Neem Cake activated with H_3PO_4 (NCH)

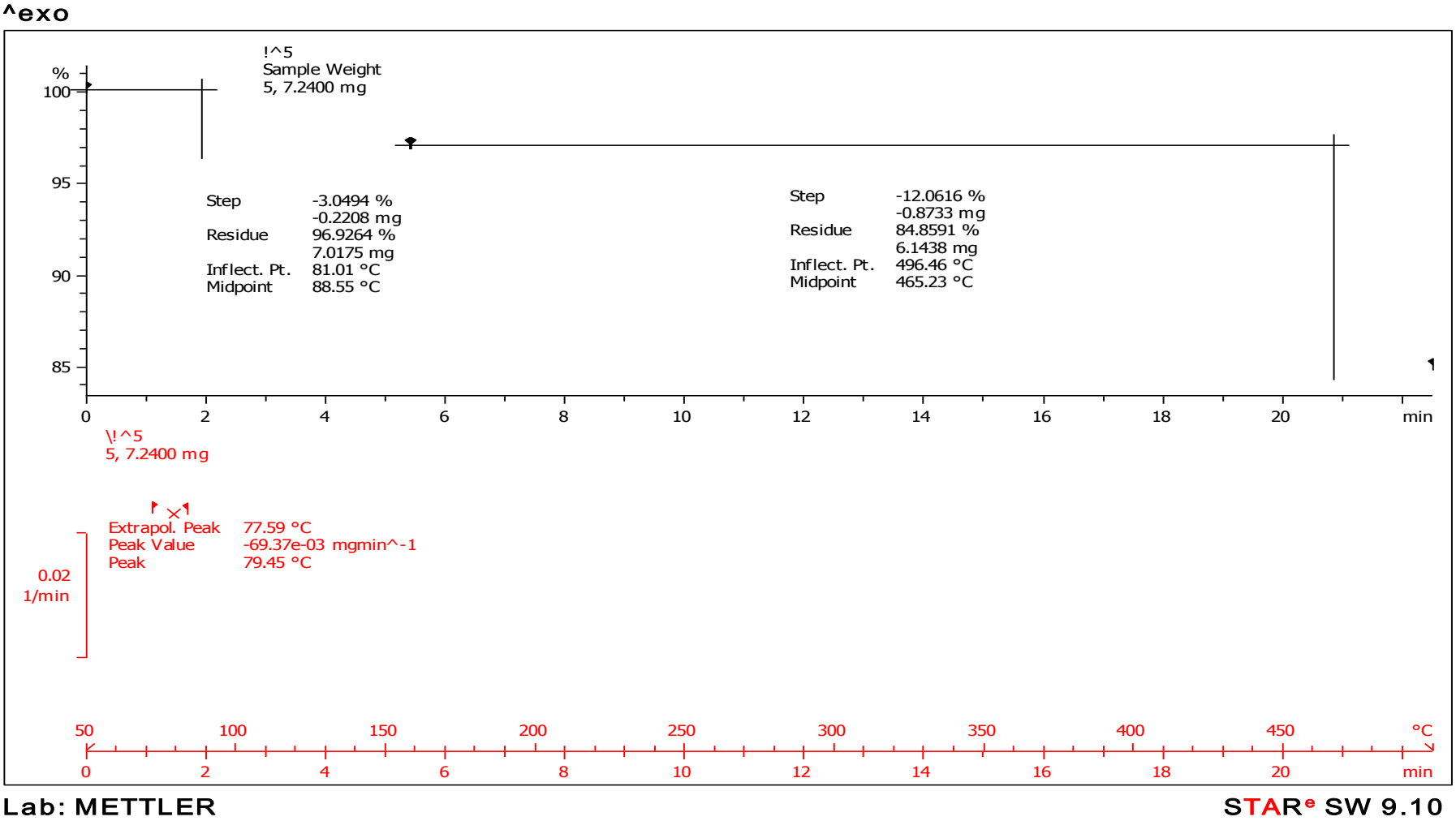


Figure 4. 19: Thermogram of Neem Husk activated with $ZnCl_2$ (NHZ)

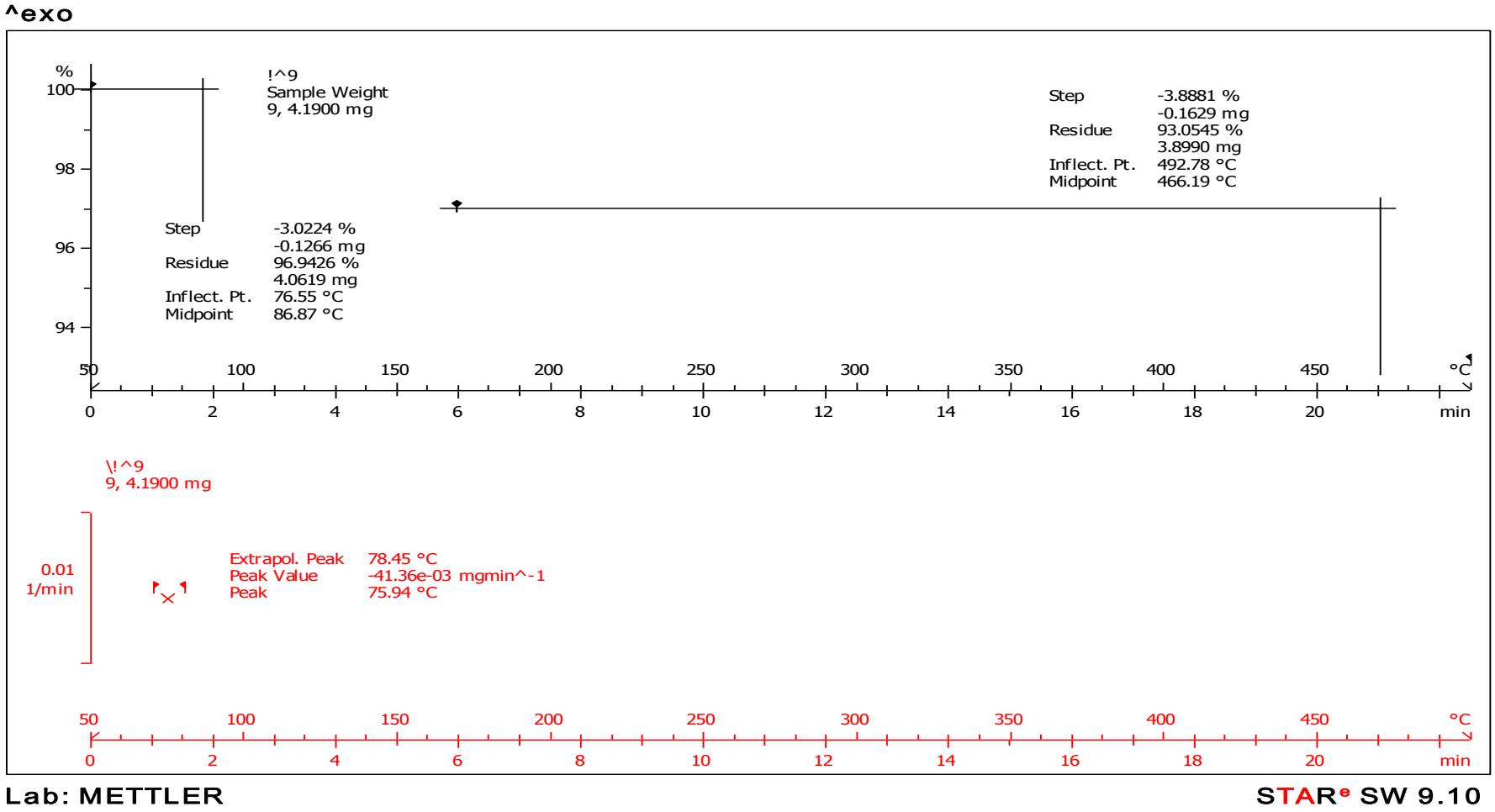


Figure 4. 20: Thermogram of Neem Husk activated with H_3PO_4 (NHH)

Table 4. 4 Thermal Gravimetric Analysis of the neem activated carbon

Sample	Stage 1 (0-350 ºC)			Stage 2 (350-500 ºC)			DTG values	
	Step (%)	Inf. Pt. (ºC)	Mid Pt. (ºC)	Step (%)	Inf. Pt. (ºC)	Mid Pt. (ºC)	Peak (ºC)	Peak Val $x10^{-3}$ (mg/min)
NCZ	3.62	81.47	87.00	9.81	493.68	450.01	81.16	-93.35
NCH	3.67	79.23	85.64	10.14	493.4	449.55	80.78	-80.15
NHZ	3.05	81.01	88.55	12.06	496.46	465.23	79.45	-69.37
NHH	3.02	76.55	86.87	3.89	492.78	466.19	75.94	-41.36

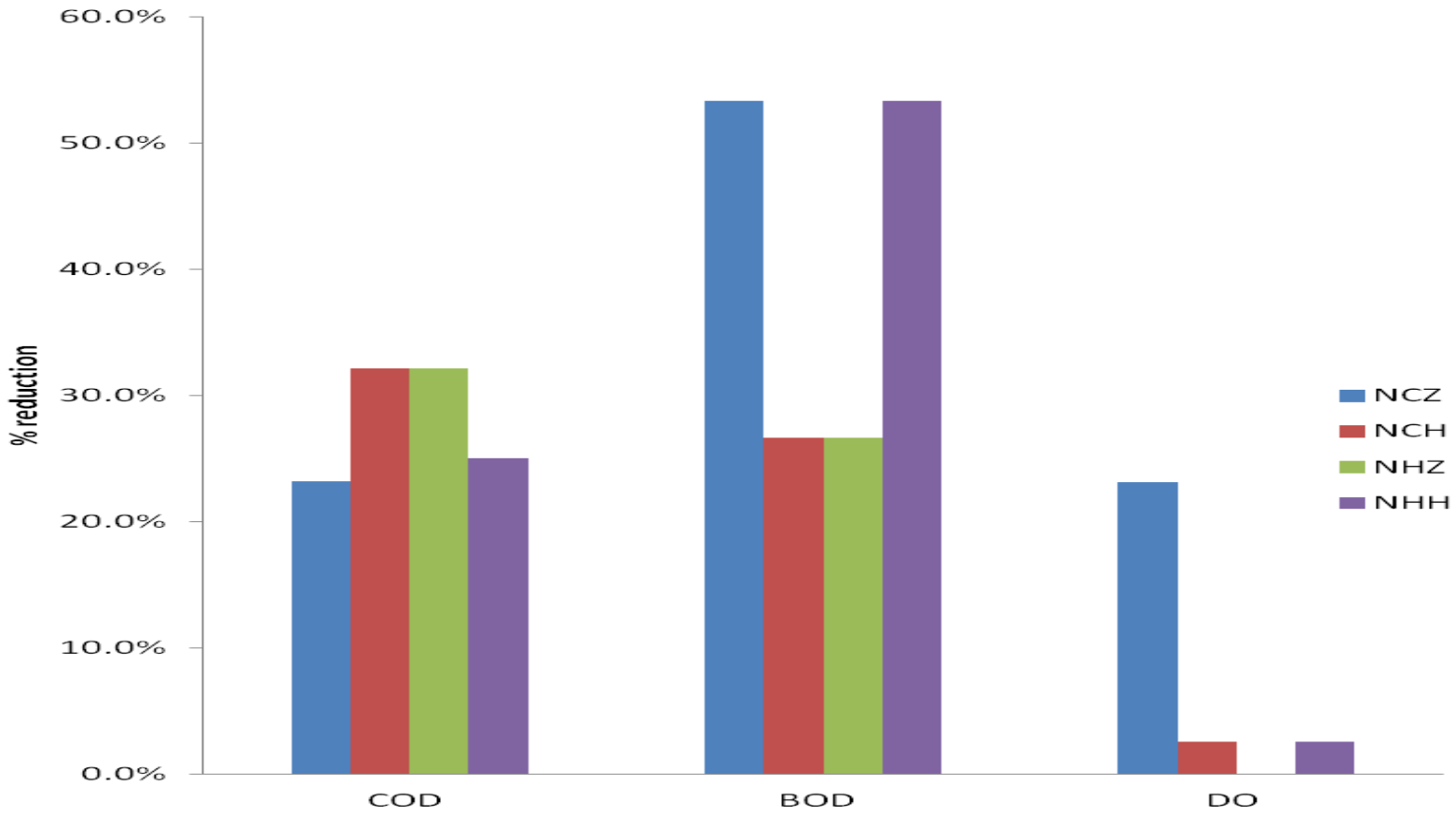


Figure 4. 21: Effect of Treatment of wastewater with prepared neem carbons on COD, BOD and DO

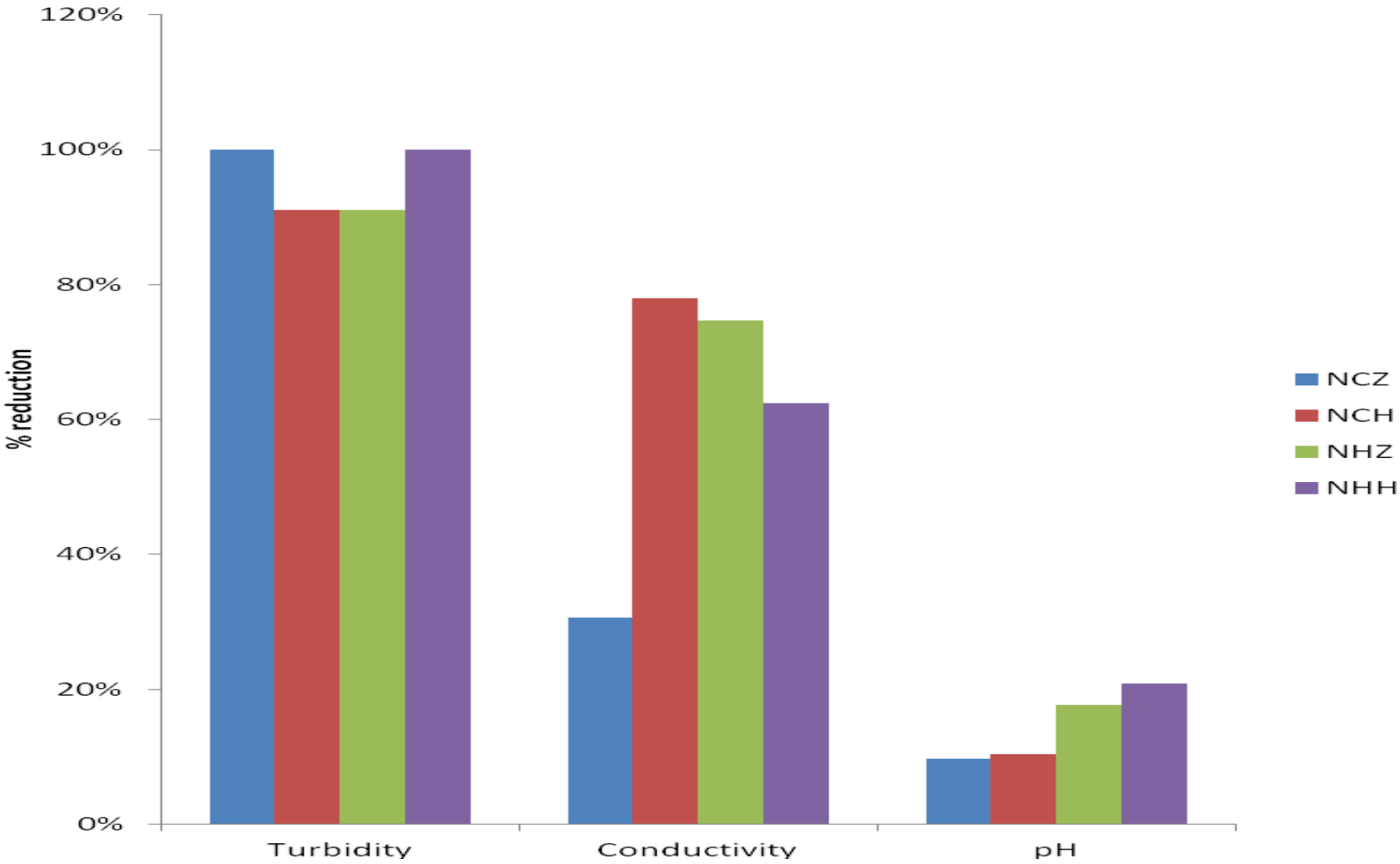


Figure 4. 22: Effect of Treatment of wastewater with prepared neem carbons on Turbidity, conductivity and pH

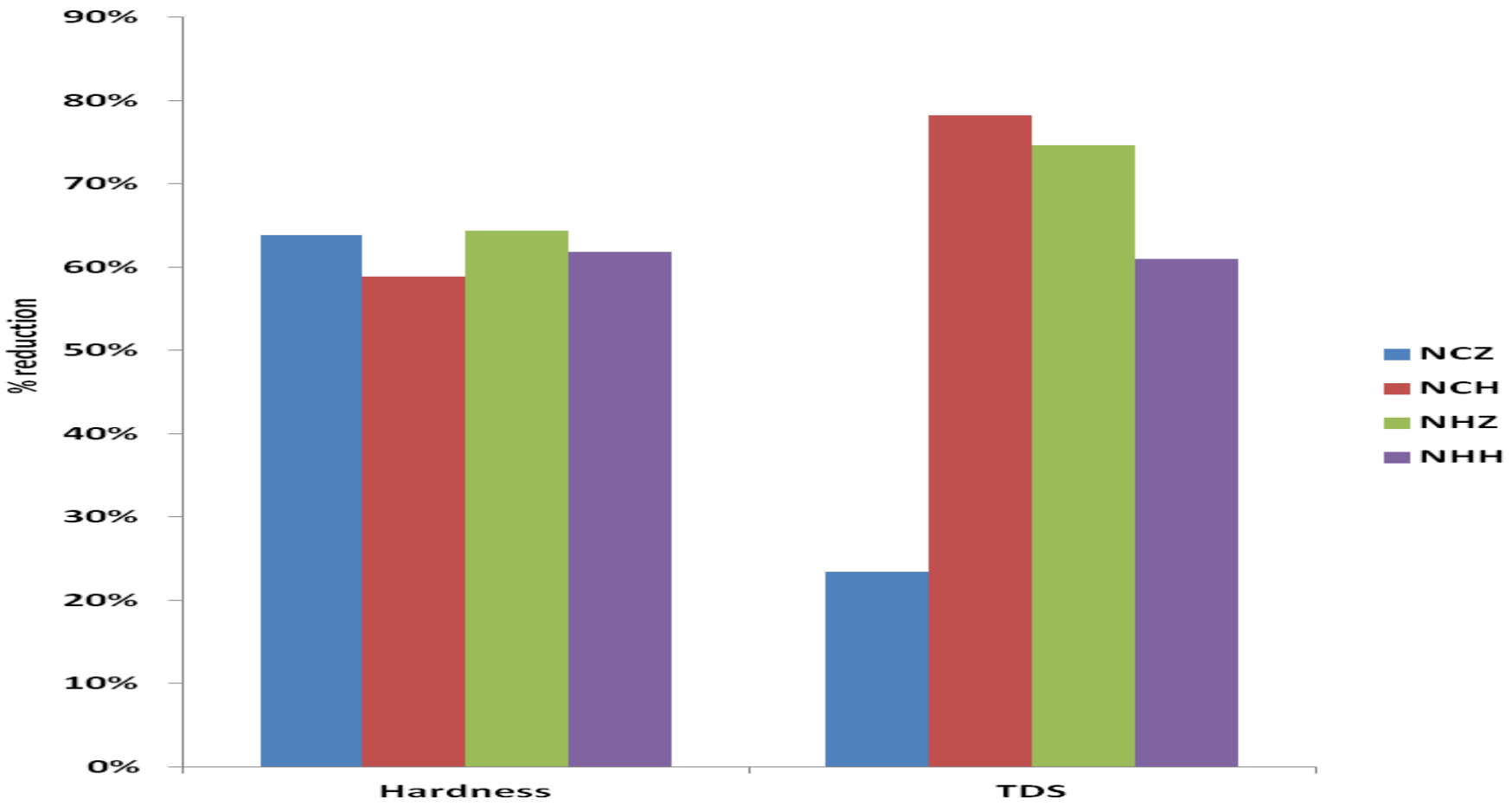


Figure 4. 23: Effect of Treatment of wastewater with prepared neem carbons on hardness and total dissolved solids

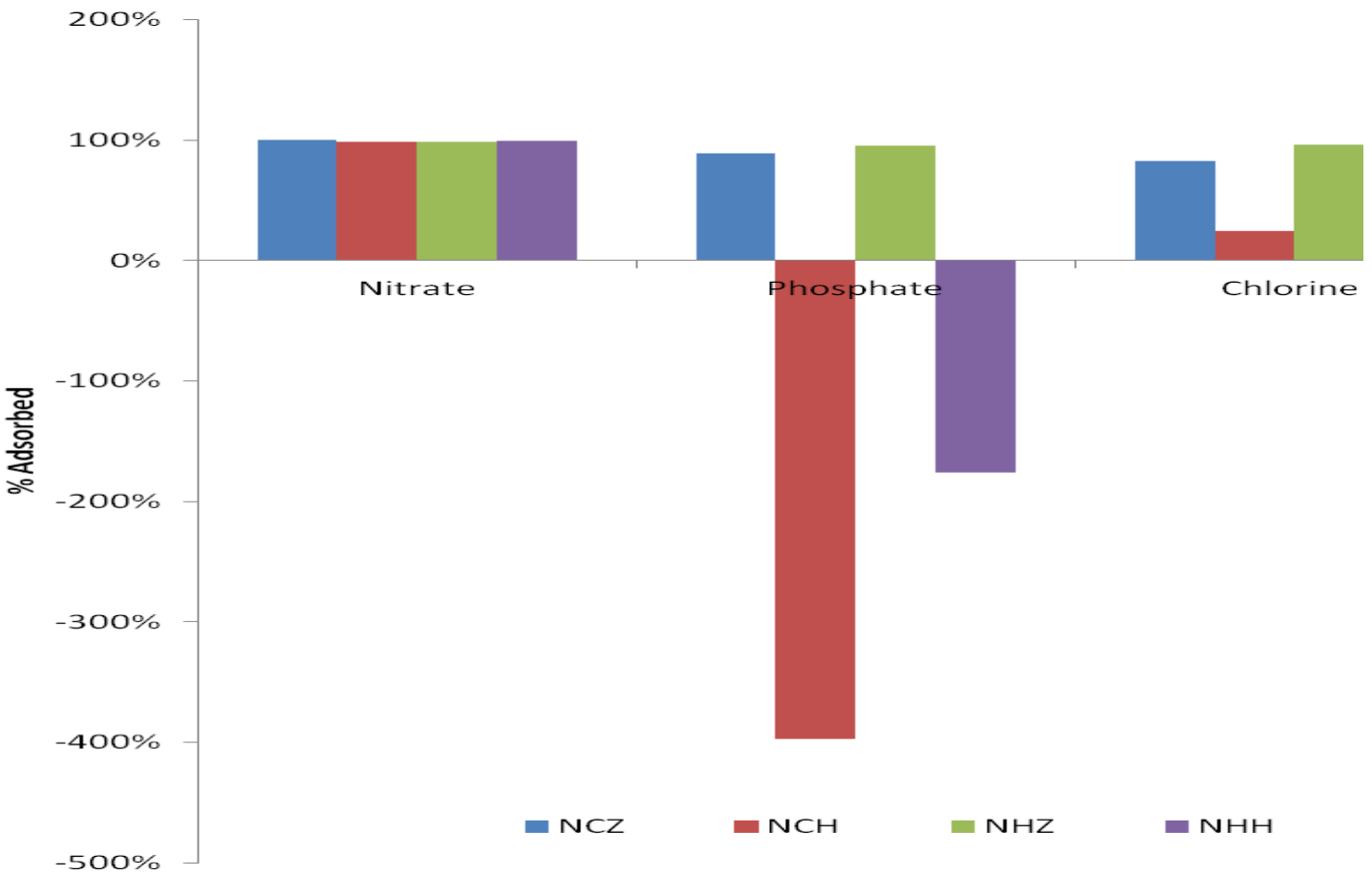


Figure 4. 24: Effect of Treatment of wastewater with prepared neem carbons on nitrates, phosphates and chloride ions

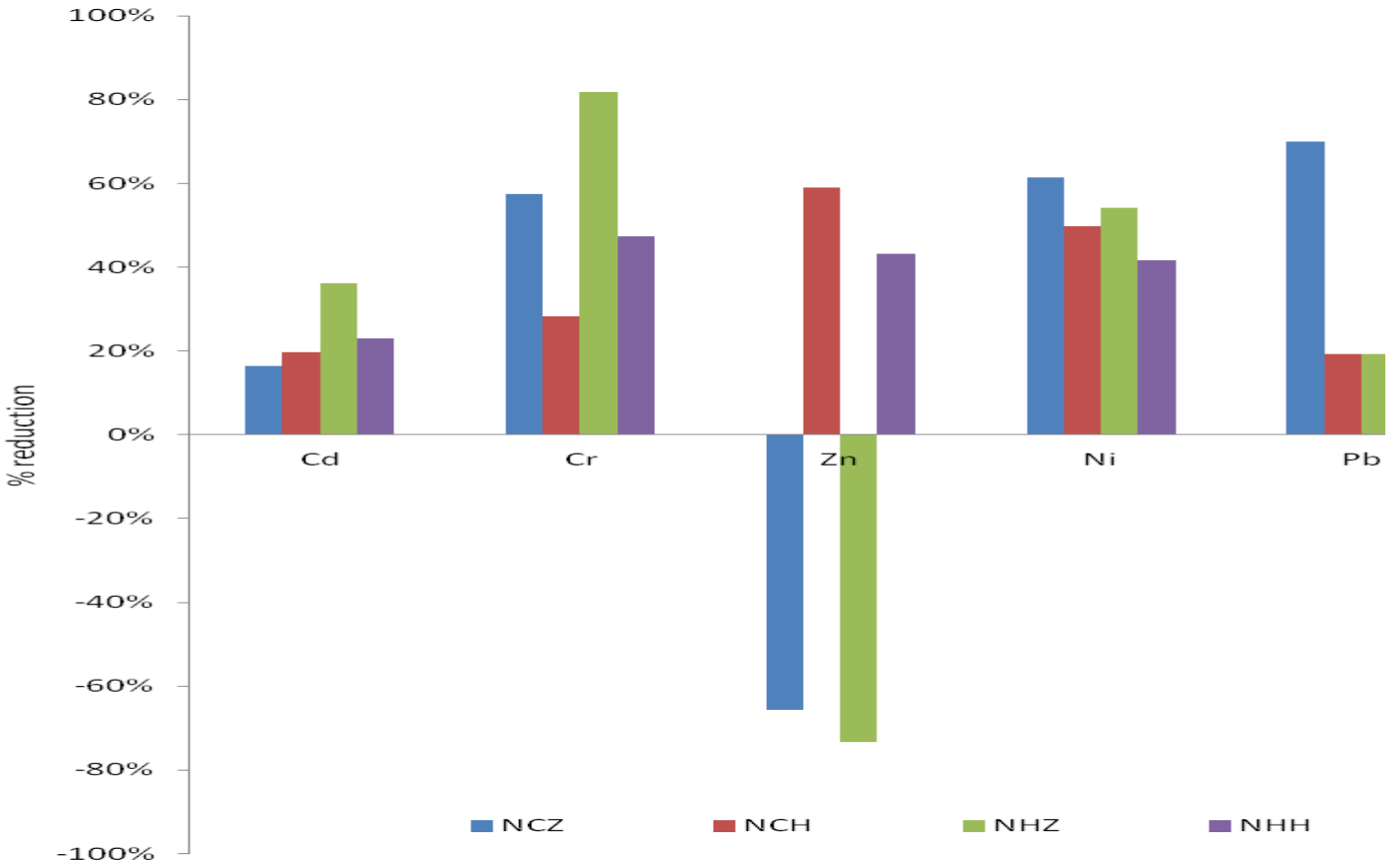


Figure 4. 25: Adsorption Capacities of sorbent for heavy metal ion

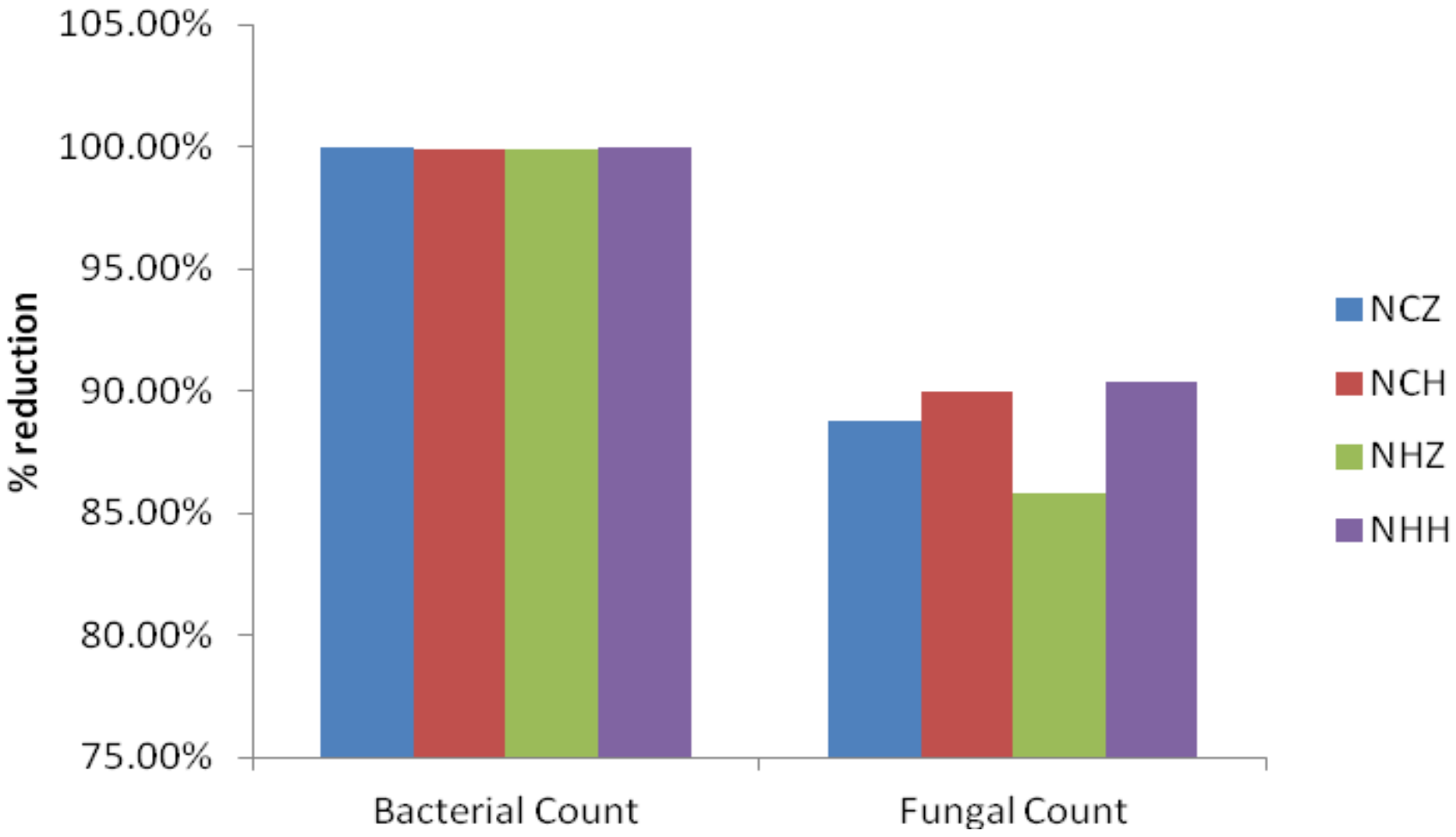


Figure 4. 26: Effect of Treatment of wastewater with prepared neem carbons on bacterial and fungal count

4.7 Kinetic Studies

Figure 4.27 presents the effect of contact time on the conductivity of the treated wastewater. Figure 4.28 shows the effect of contact time on pH of the wastewater. The effect of contact time on turbidity is presented in Figure 4.29. The effect of contact time on COD shows a sinusoidal pattern with a slide declined in COD as presented in Figure 4.30. BOD have a similar pattern with COD but the rate of decline in BOD was faster than that of COD as presented in Figure 4.31. DO also have similar pattern with COD and had the most effective contact time at 25 minutes as shown in Figure 4.32. The effect of contact time on the hardness of the treated wastewater is presented in Figure 4.34. Figures 4.35 – 4.42 present the effect of contact time on nitrates, phosphates, chloride ions and the heavy metals. The effect of contact time on bacterial and fungal load is presented in Figure 4.43 and 4.44.

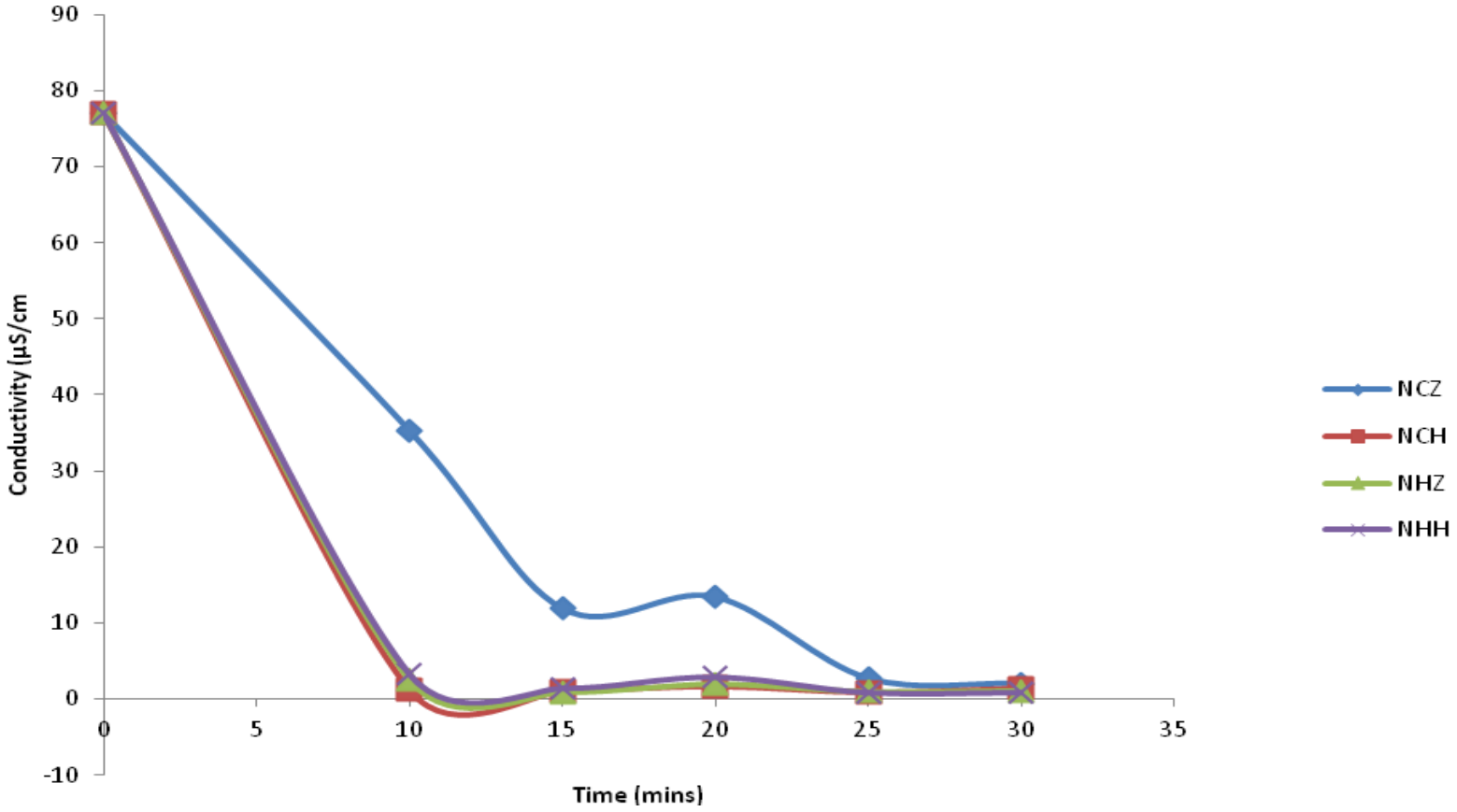


Figure 4. 27: The effect of contact time on conductivity of treated water

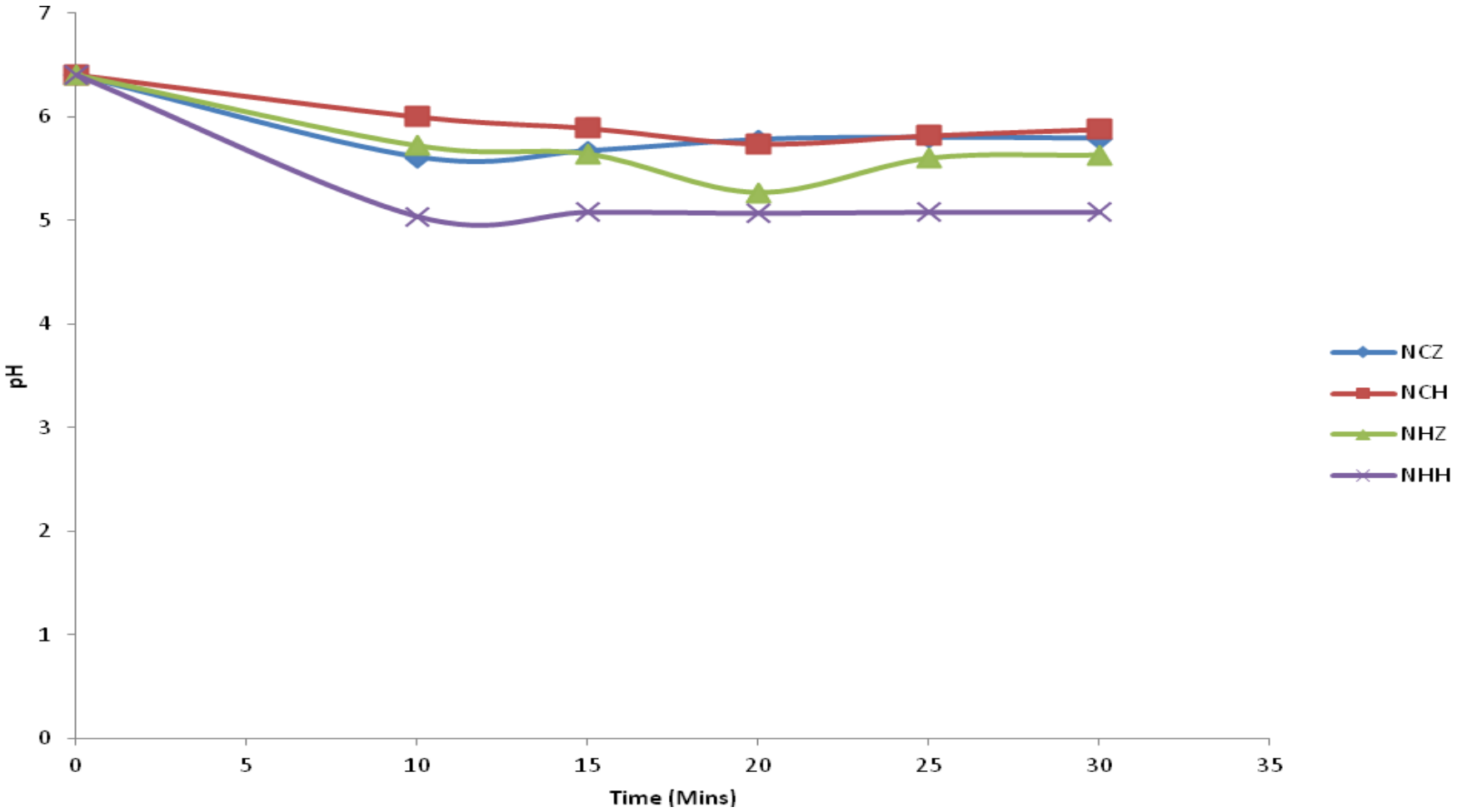


Figure 4. 28: The effect of contact time on pH of treated water

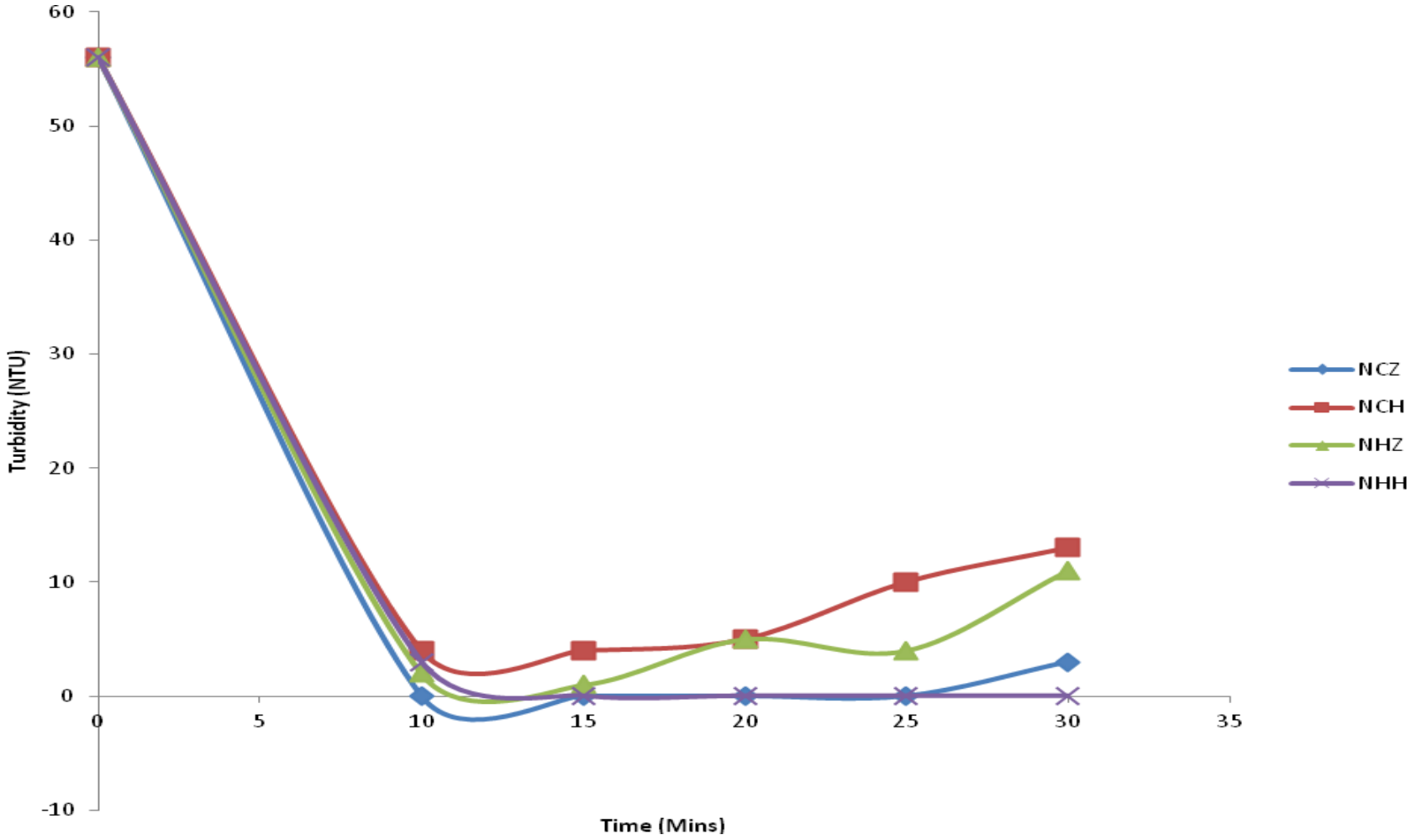


Figure 4. 29: The effect of contact time on turbidity of treated water

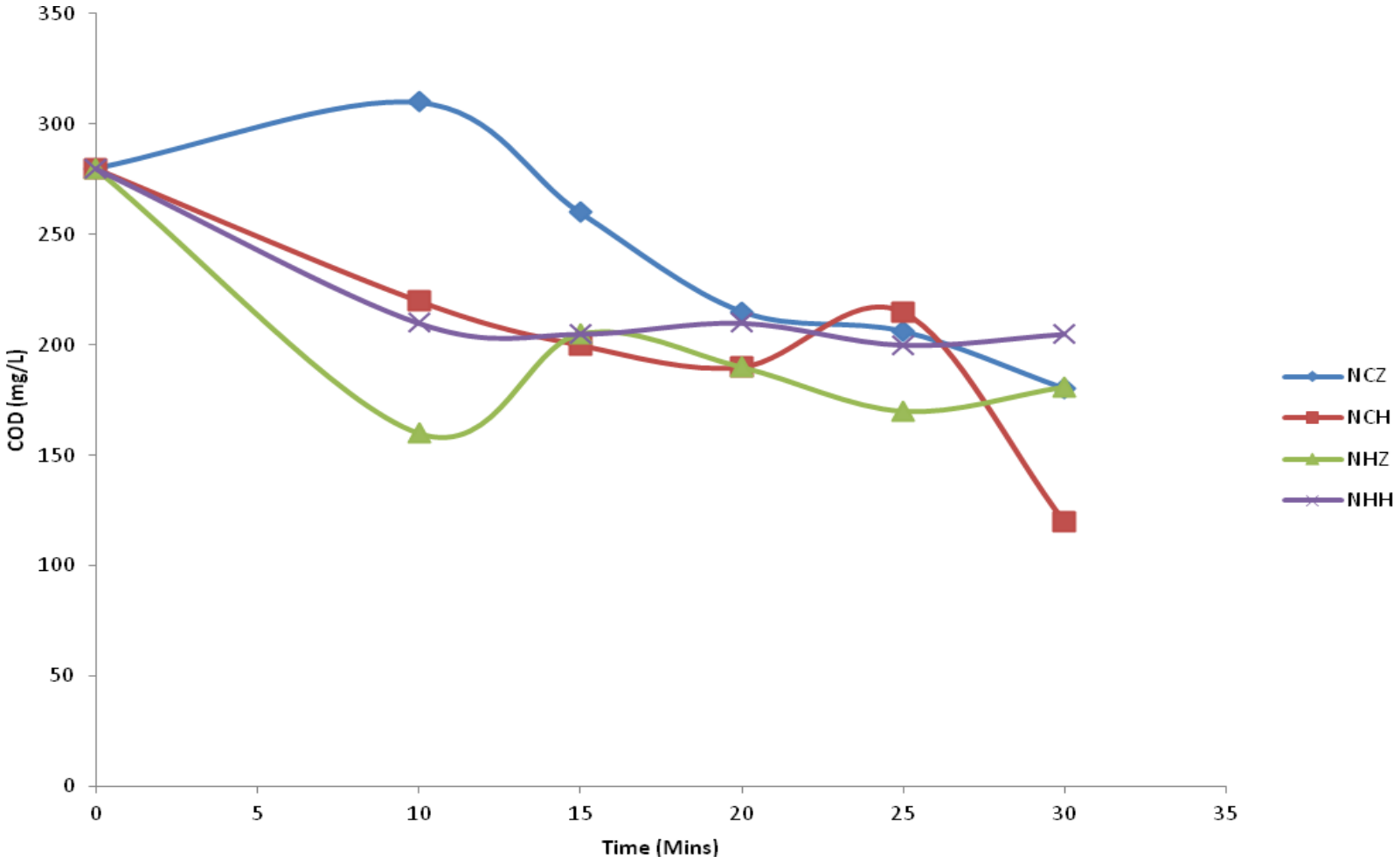


Figure 4. 30: The effect of contact time on COD of treated water

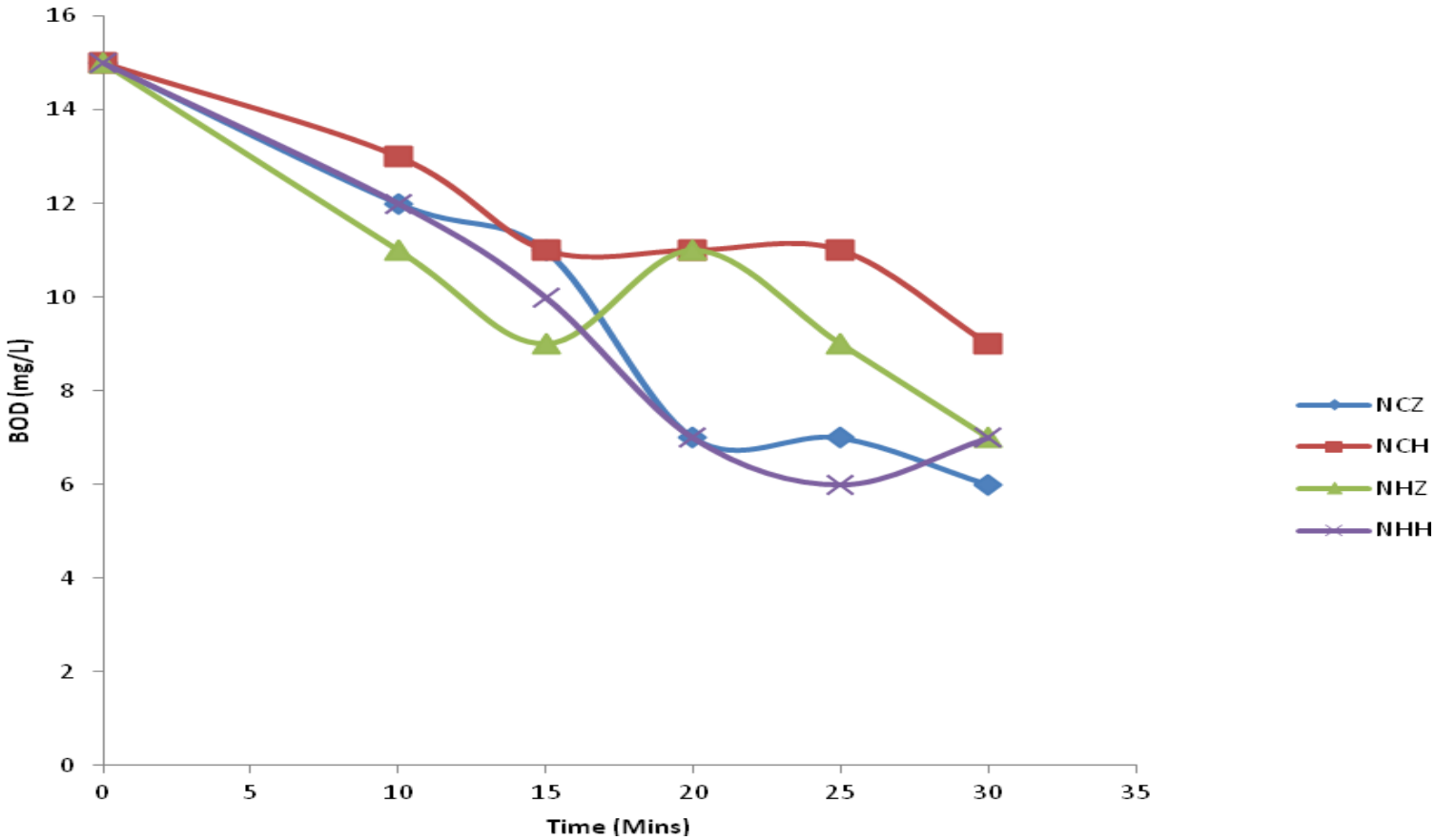


Figure 4. 31: The effect of contact time on BOD of treated water

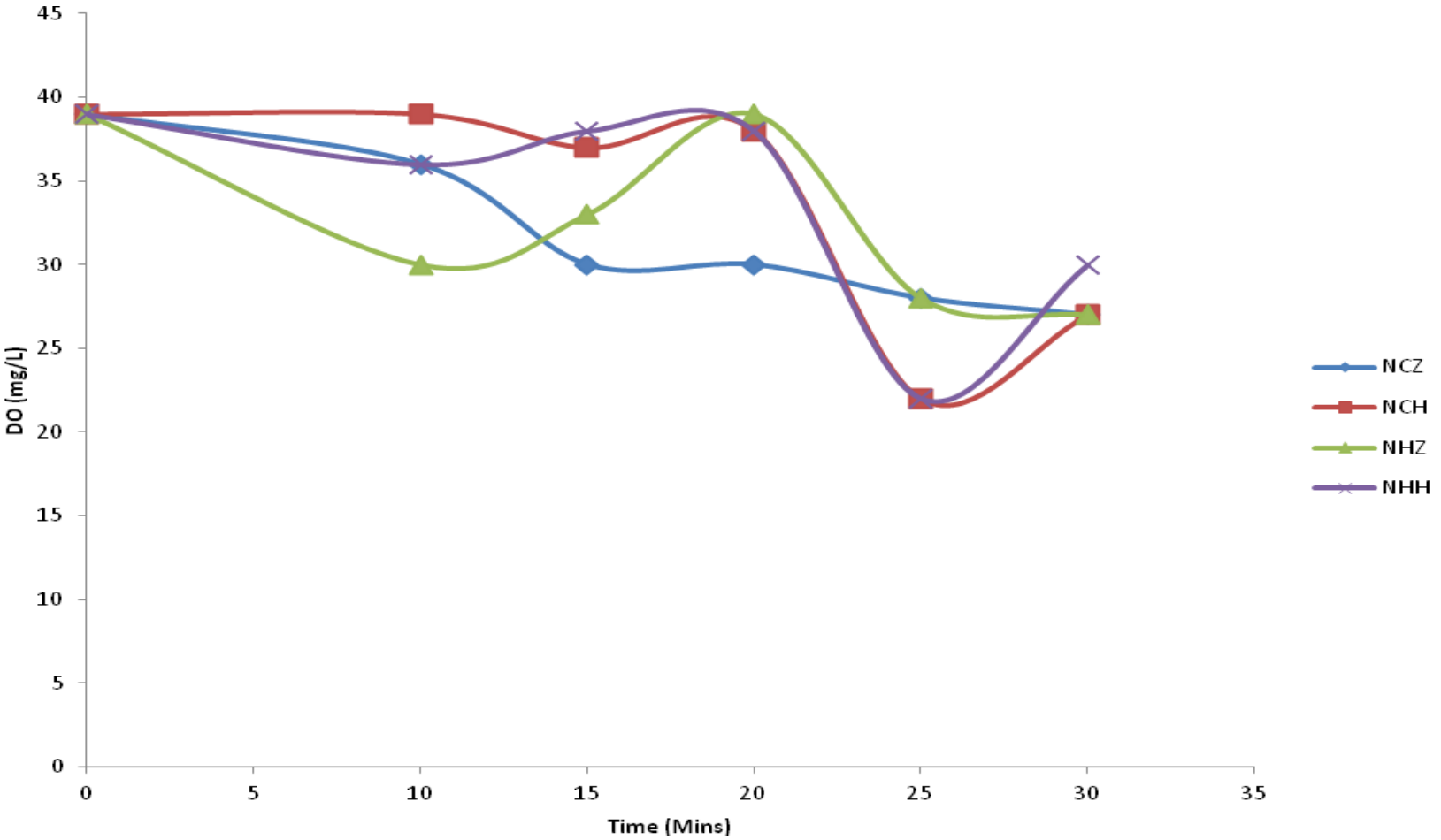


Figure 4. 32: The effect of contact time on DO of treated water

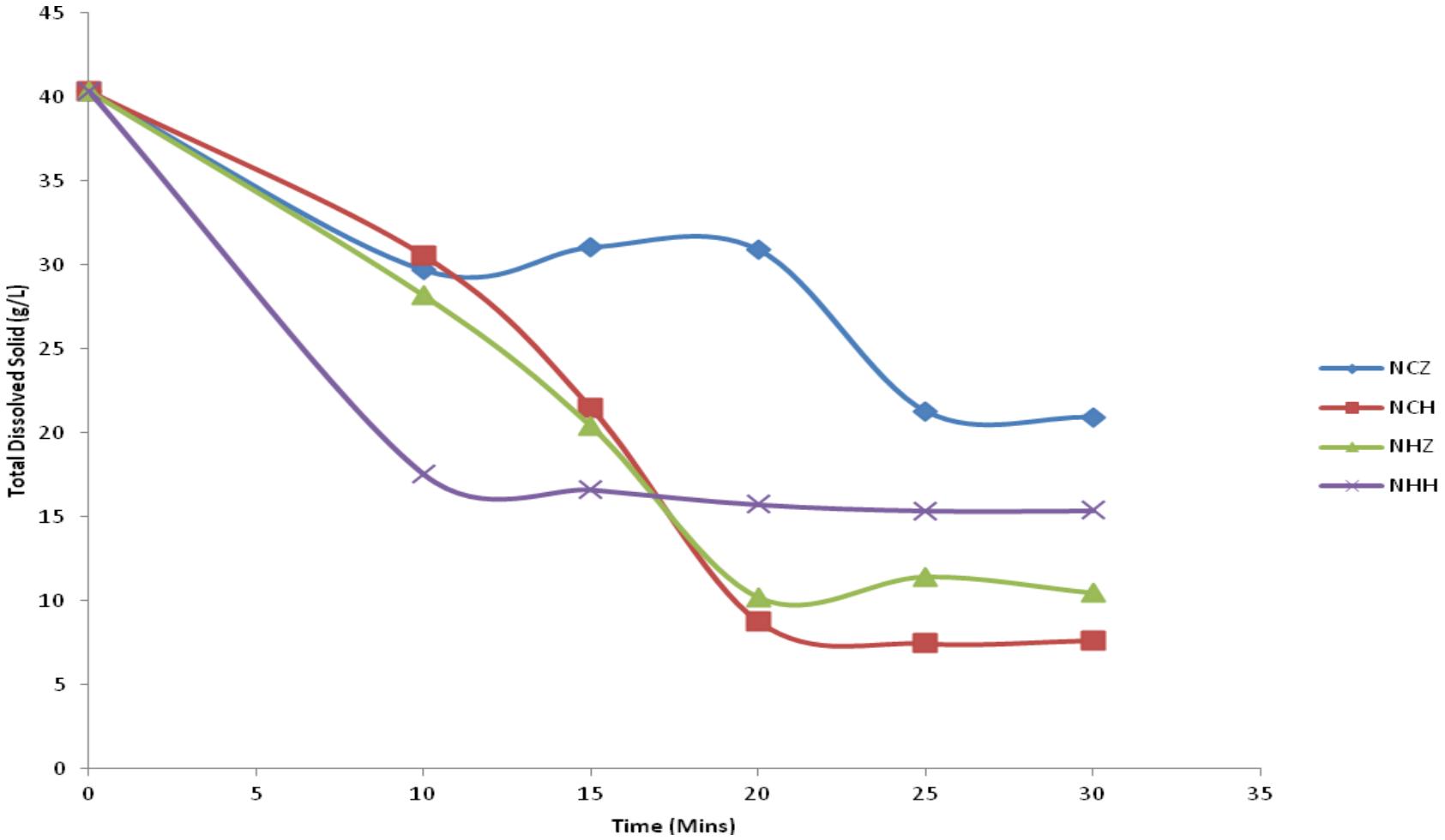


Figure 4. 33: The effect of contact time on TDS of treated water

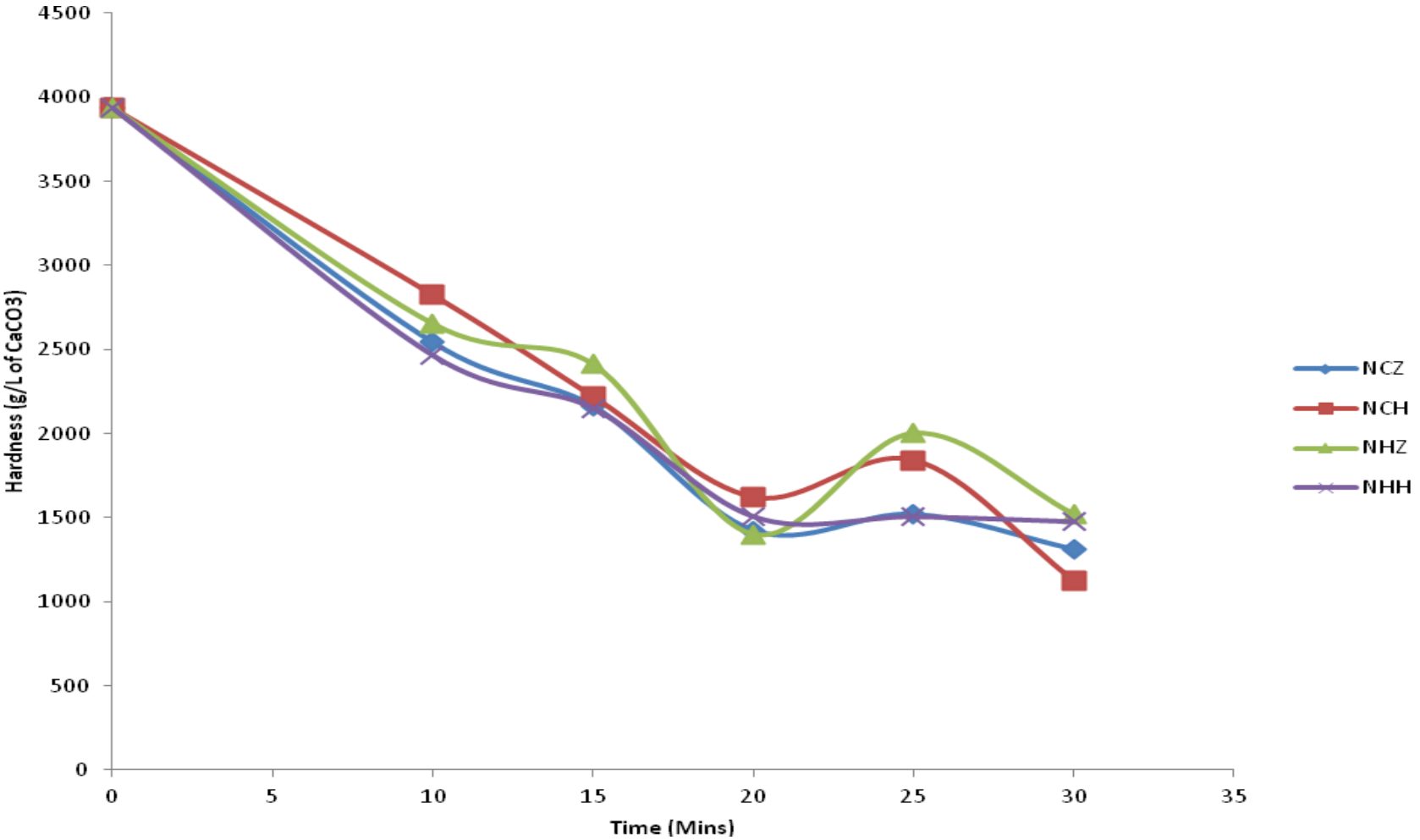


Figure 4. 34: The effect of contact time on hardness of treated water

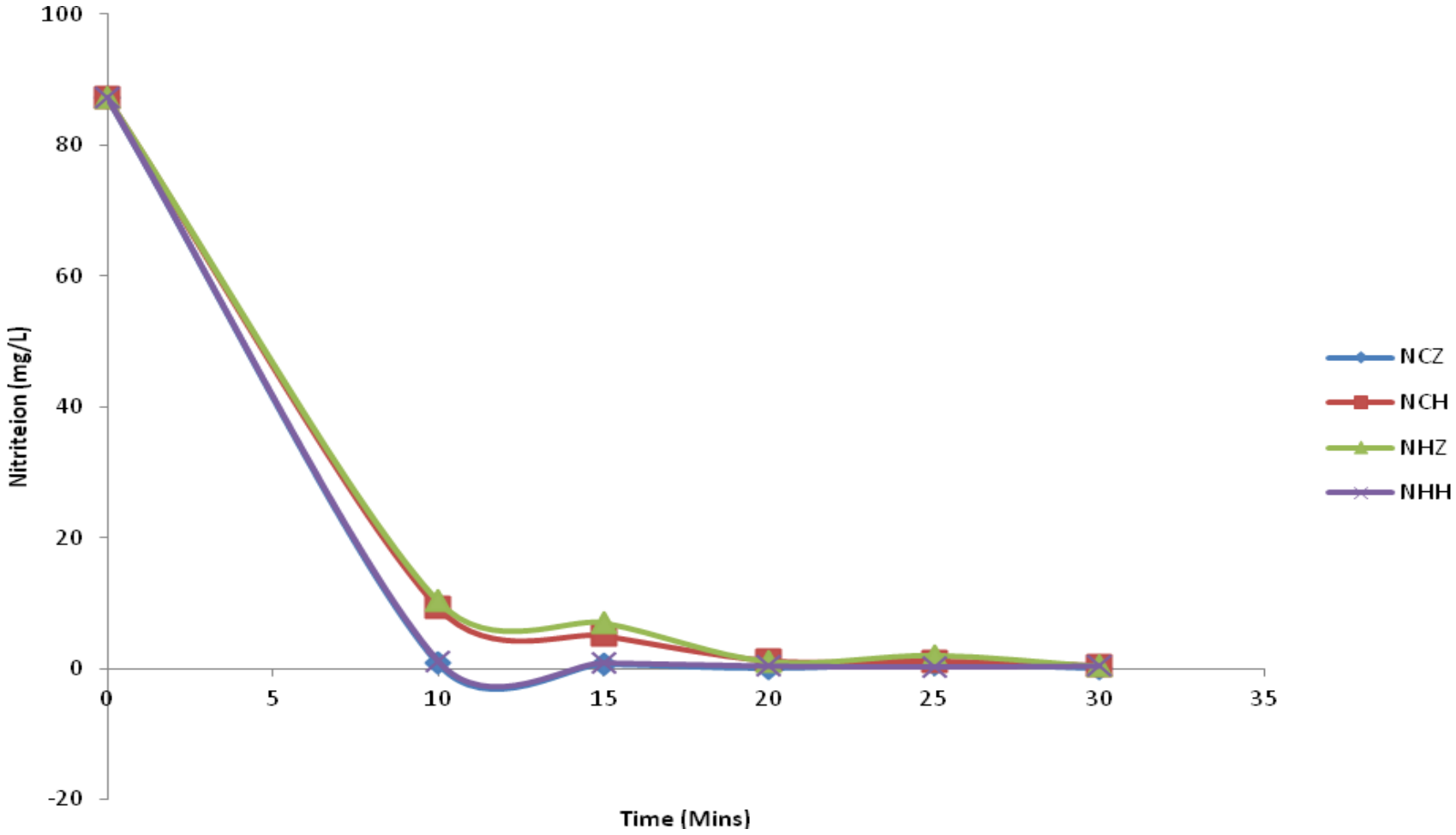


Figure 4. 35: The effect of contact time on nitrate concentration of treated water

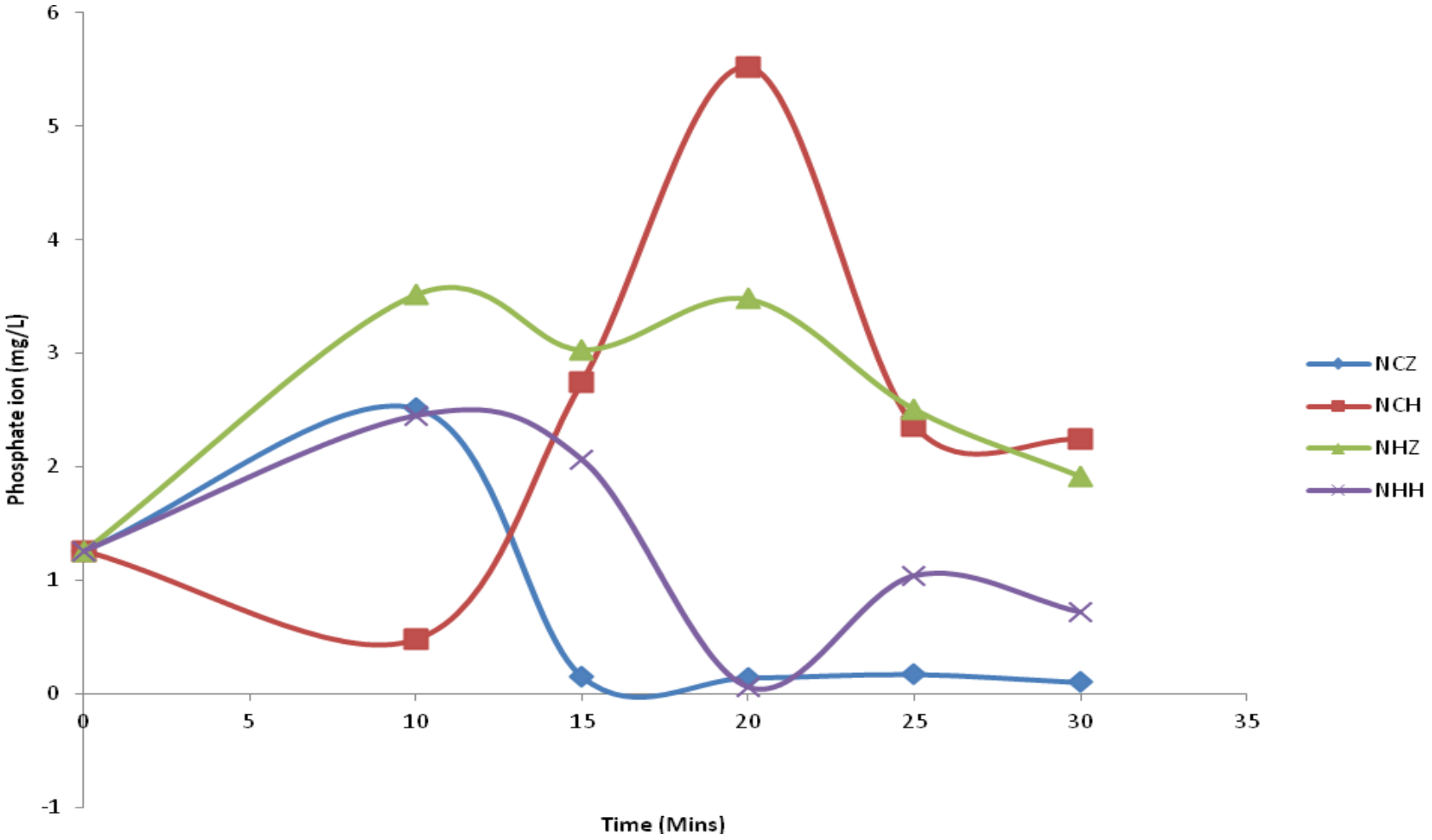


Figure 4. 36: Effect of contact time on phosphate concentration of treated water

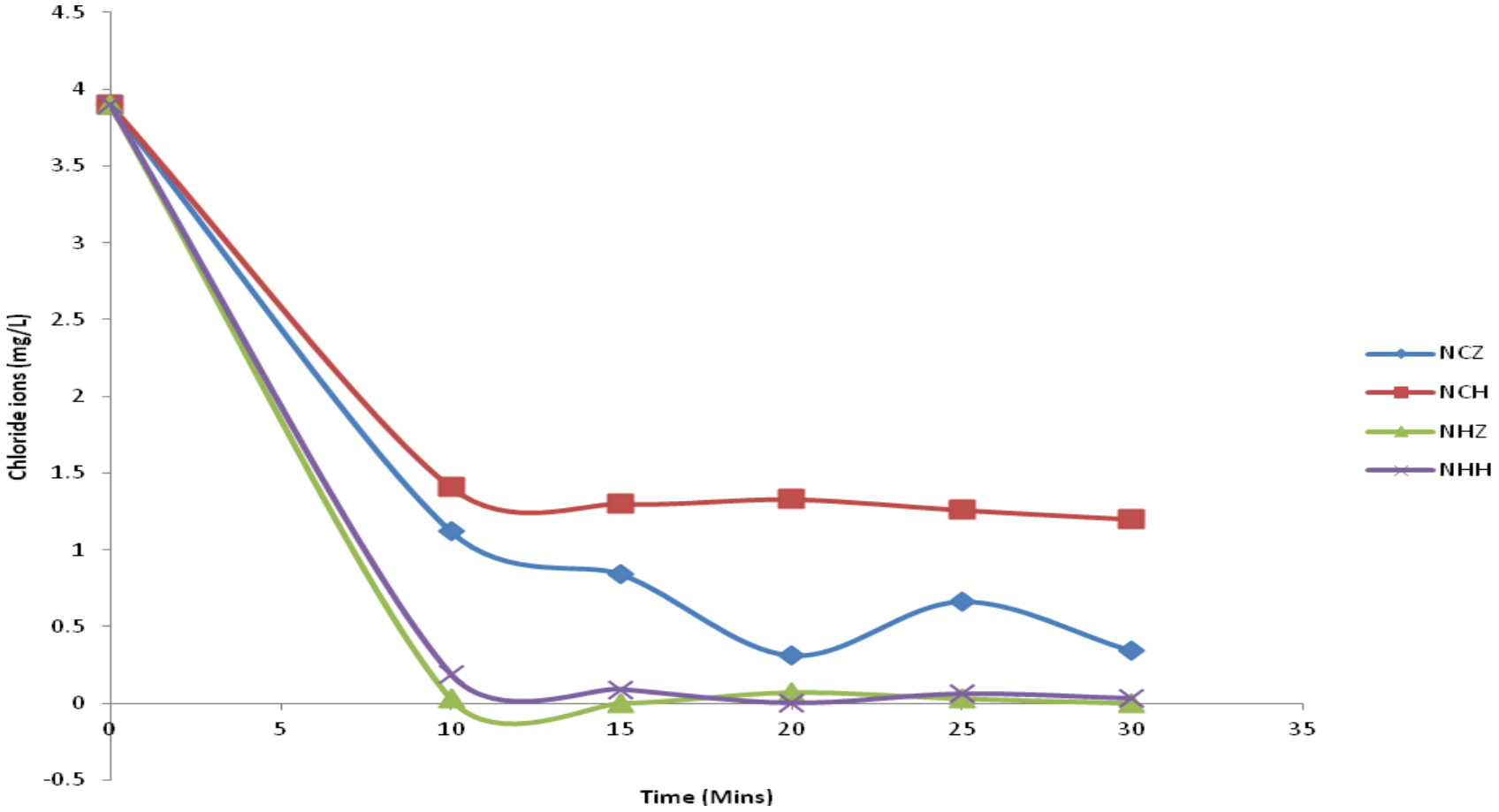


Figure 4. 37: Effect of contact time on chloride concentration of treated water

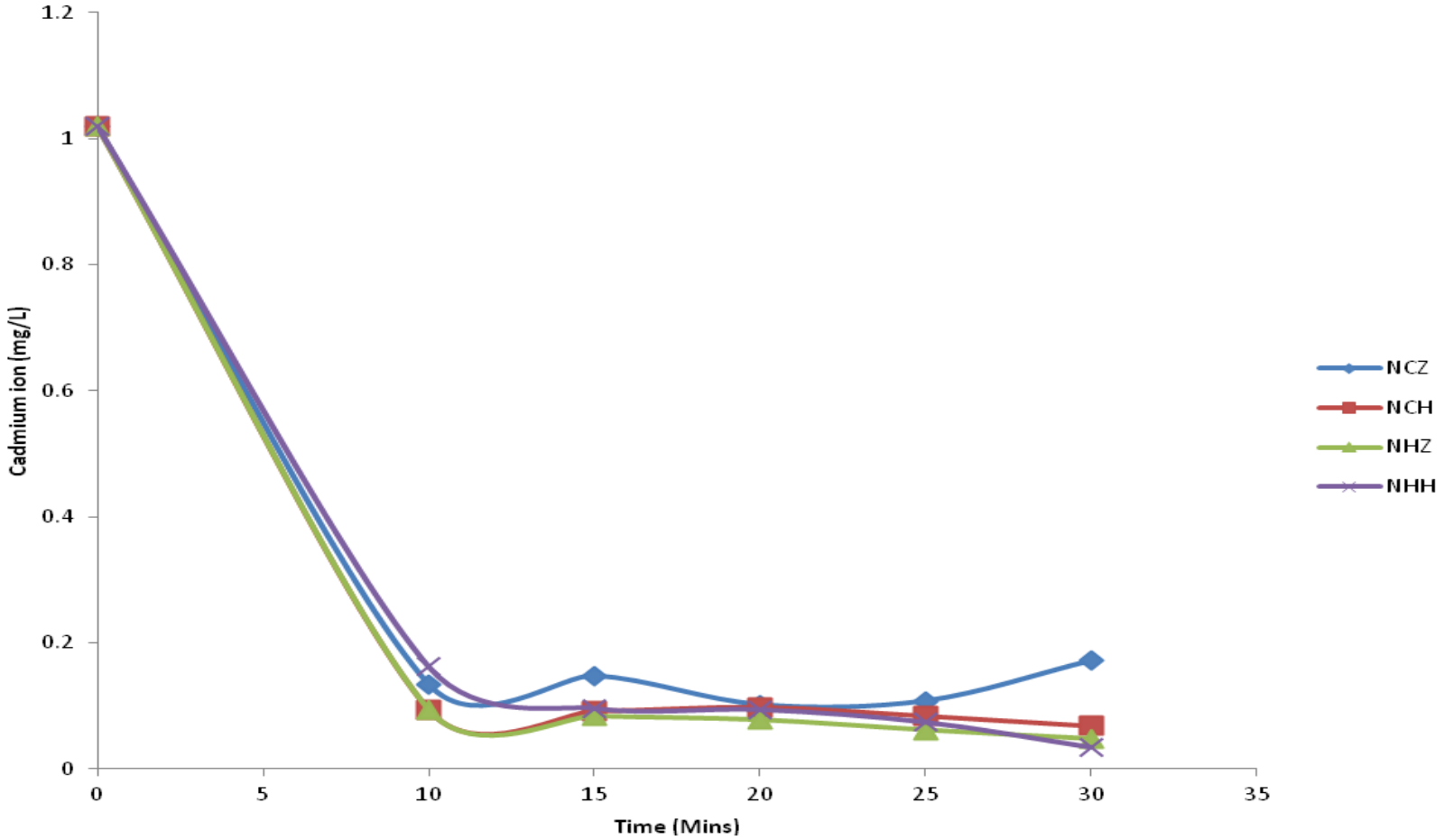


Figure 4. 38: Effect of contact time on cadmium ion of treated water

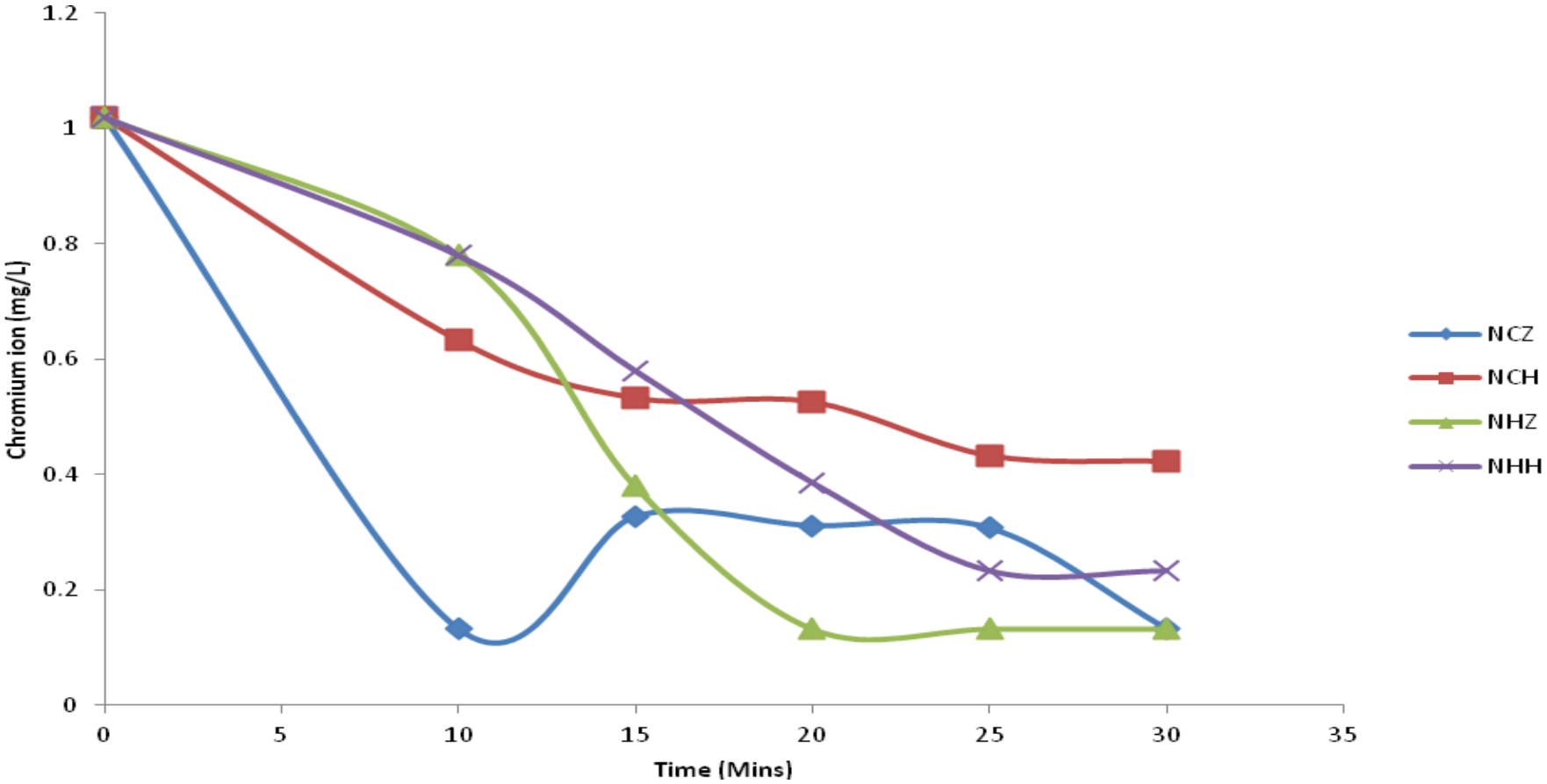


Figure 4. 39: The effect of contact time on chromium ion in treated water

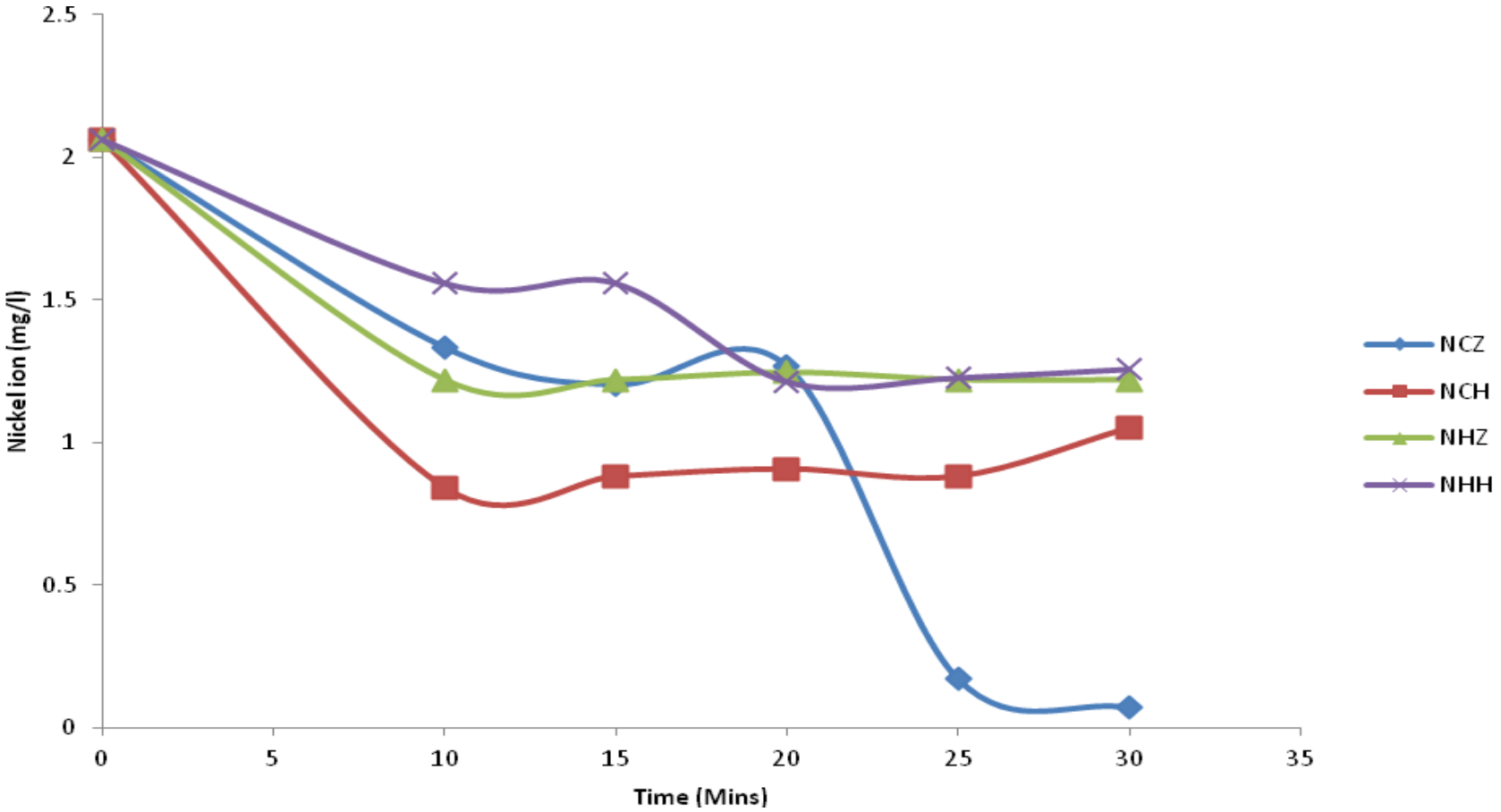


Figure 4. 40: Effect of contact time on nickel ion in treated water

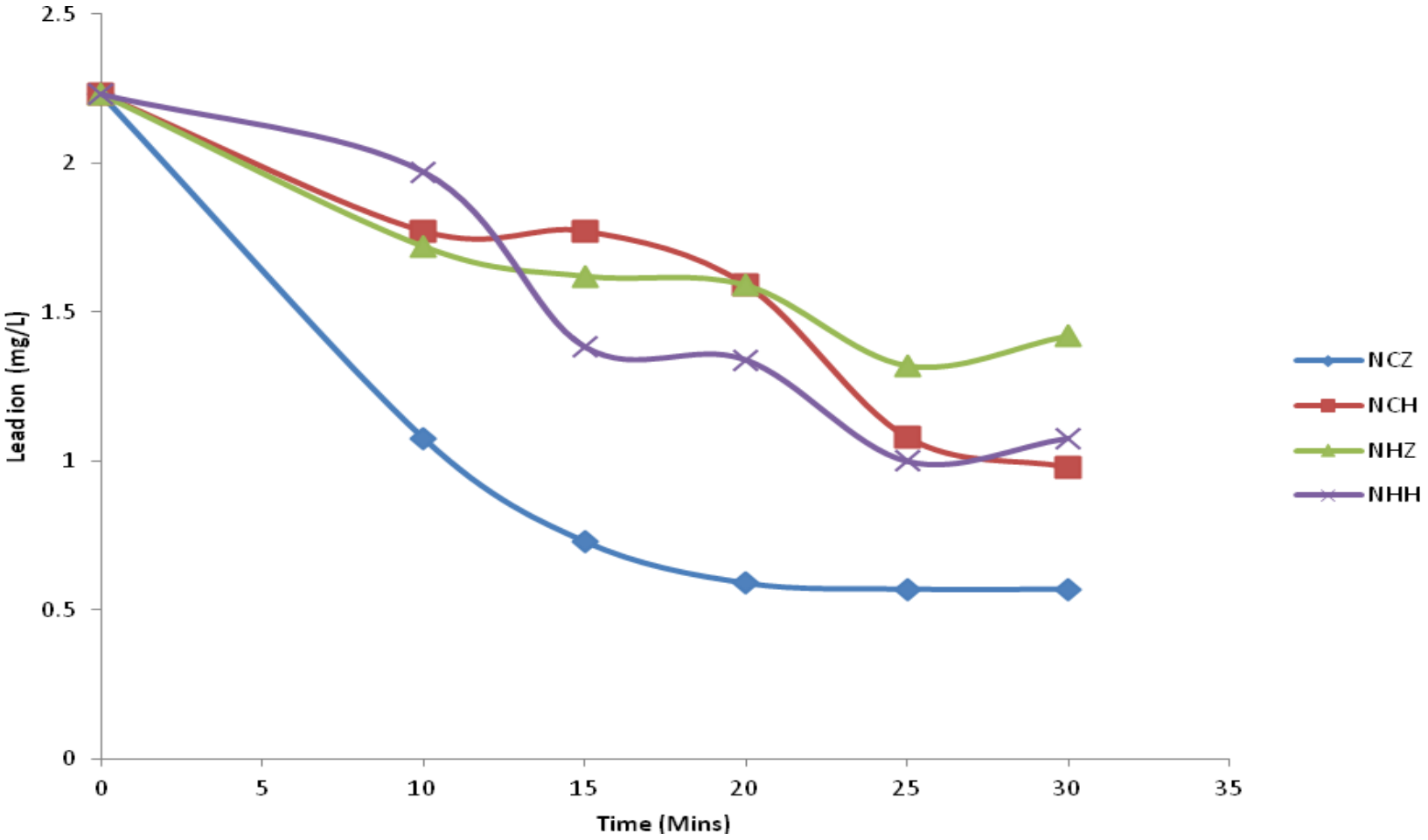


Figure 4. 41: Effect of contact time on lead ion in treated water

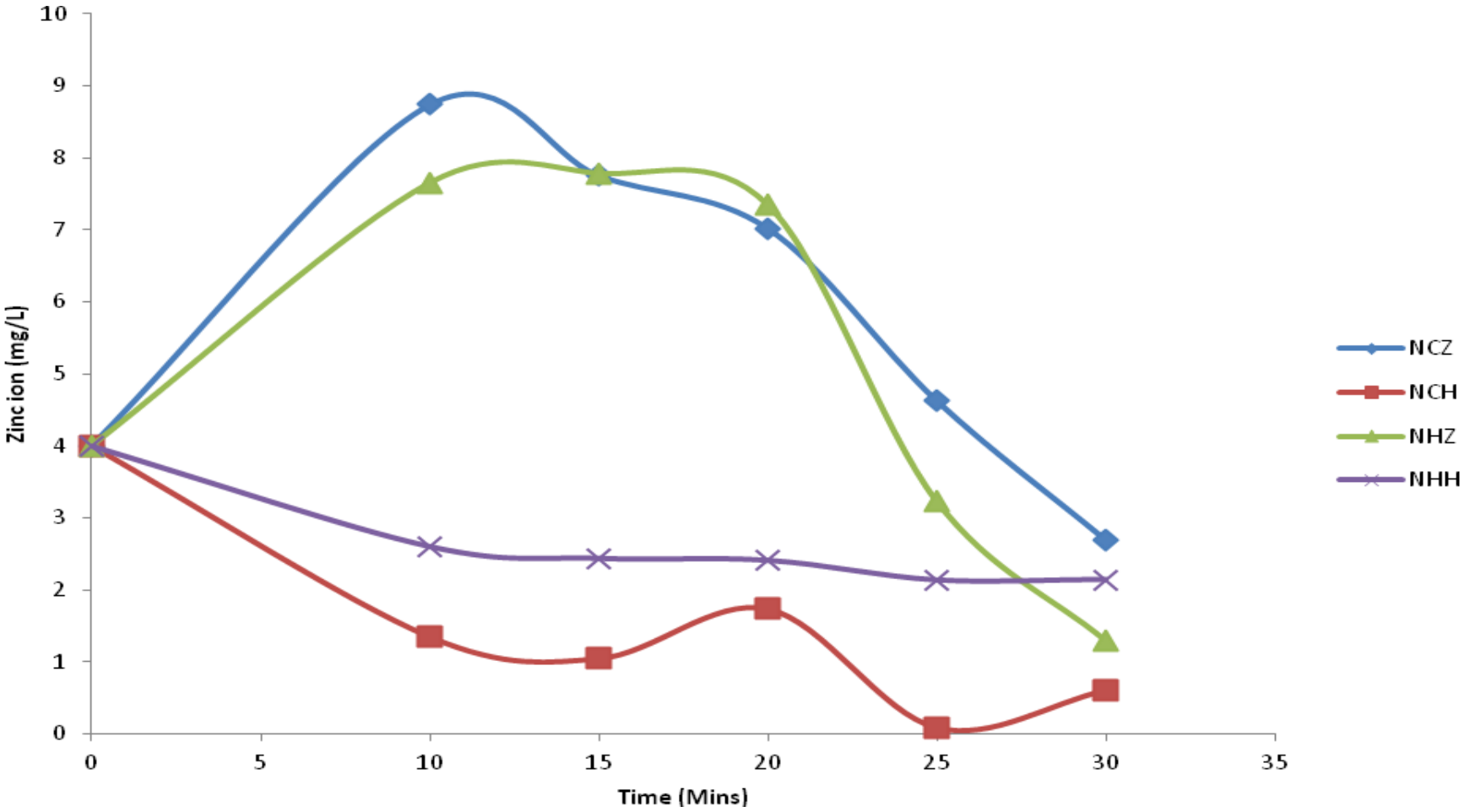


Figure 4. 42: Effect of contact time on zinc ion in treated water

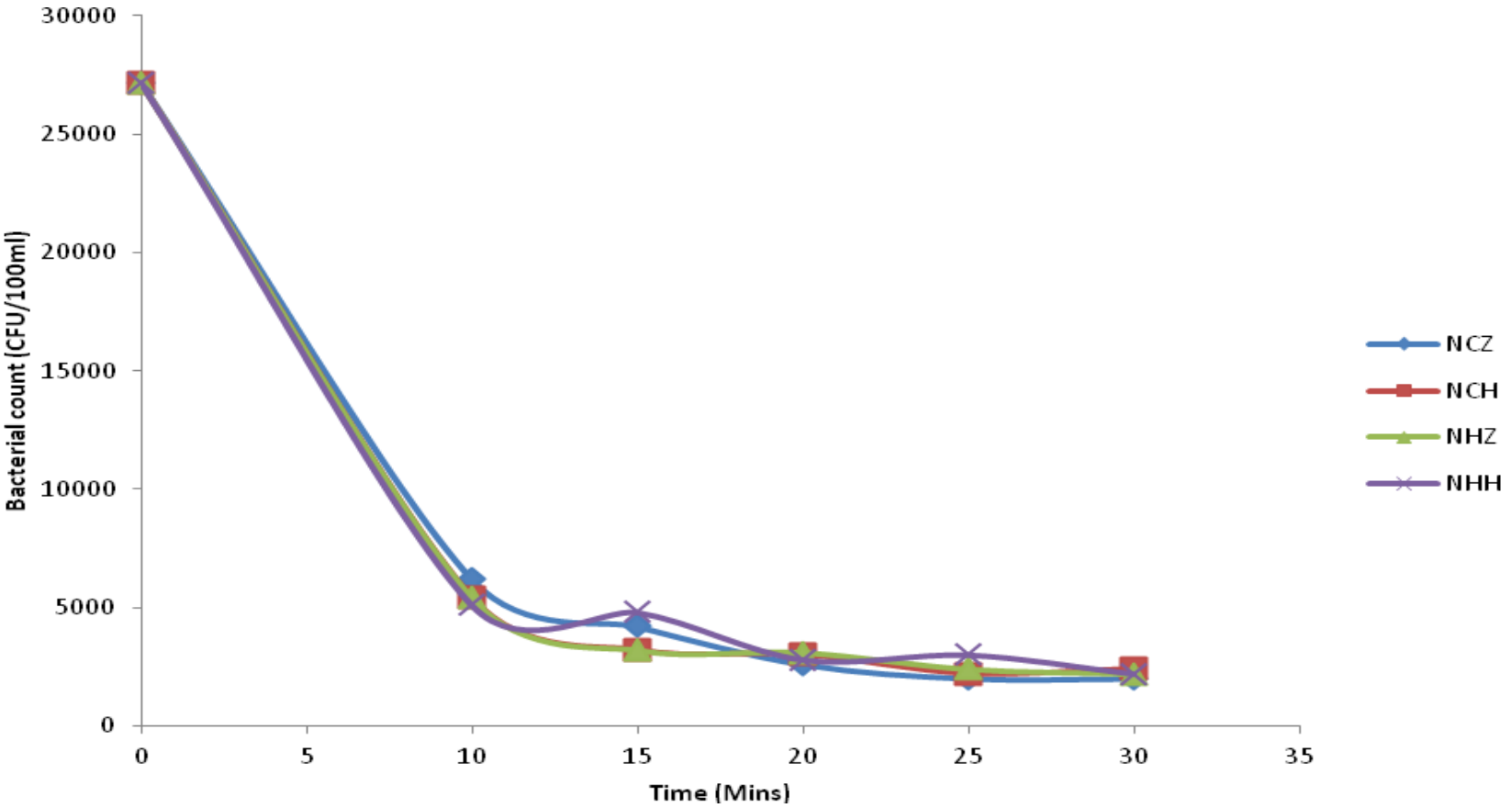


Figure 4. 43: Effect of contact time on bacterial load in treated water

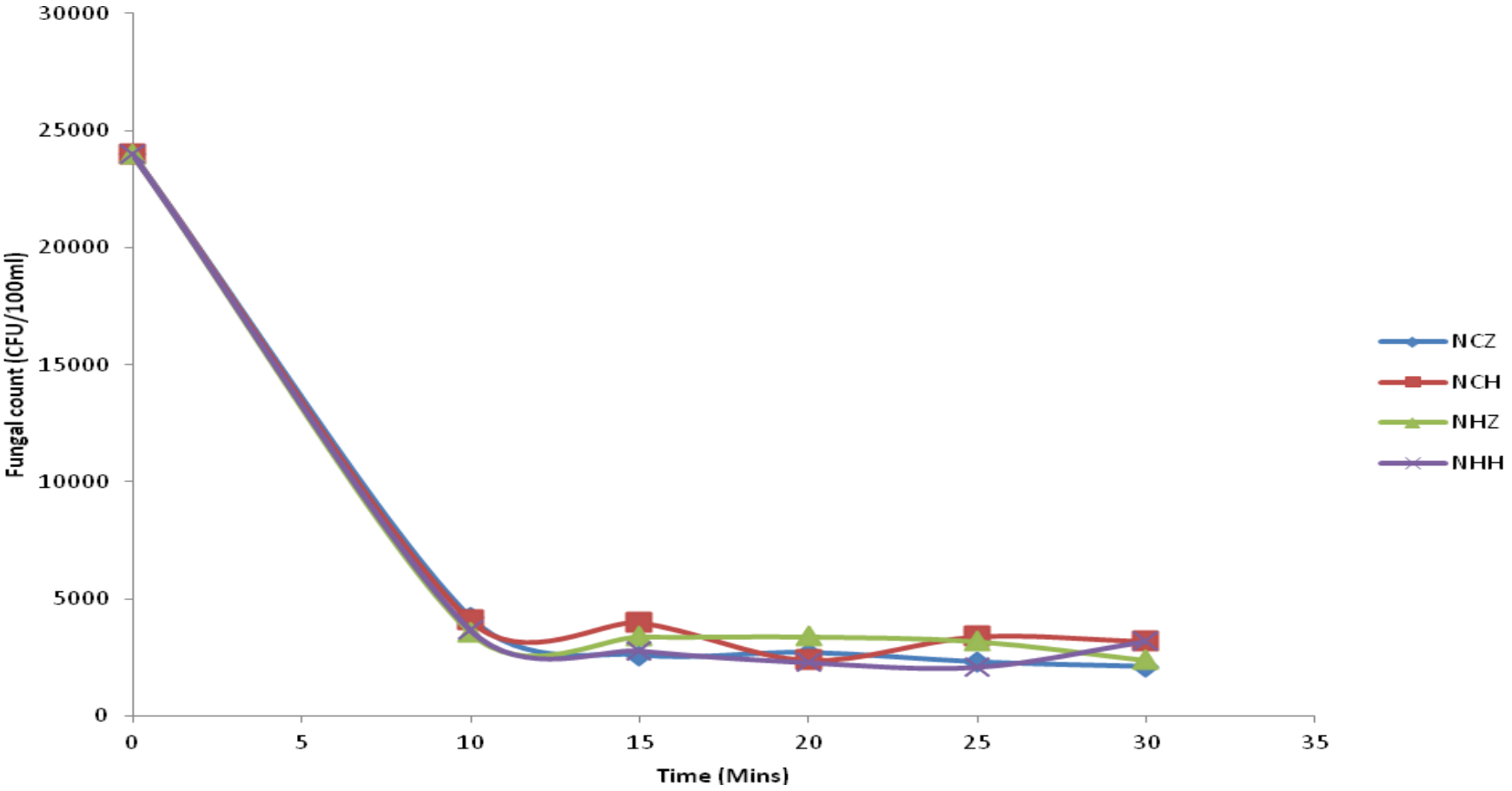


Figure 4. 44: Effect of contact time on fungal load in treated water

4.8 Pseudo-Second-Order Rate Models

The Pseudo-Second-Order Rate Kinetic Model was determined using the linearized Pseudo-Second-Order Kinetic equation. The plots of t/qt against time for the sorption of the investigated parameters are given in Figures 4.45 – 4.52. The values of the slope and the intercept were used to calculate the Pseudo-Second-Order rate constant and the adsorption capacity of the neem carbon. All the four different neem adsorbents demonstrate excellent fitness to the Pseudo-Second-Order Rate Kinetic Model with a high regression value (Table 4.5). The Pseudo-Second-Order Rate Kinetic Model for the adsorption of cadmium, chromium, zinc, nickel and lead is presented in Figures 4.48, 4.49, 4.50, 4.51 and 4.52 while the studied parameters are summarized in Table 4.5.

4.9 Weber and Morris Intraparticle Diffusion Models

The kinetic data were fed into the linearized Weber and Moris Intraparticle Diffusion (WMIDM) equation. The plot of the amount of the adsorbate q_t (g/g) against the square root of the time ($t^{1/2}$) gives a straight line. The rate constant K_{id} ($g/gmin^{-1/2}$) and the intraparticle diffusion coefficient C_i (g/g) were calculated from the slope and intercept respectively. The values of K_{id}, C_i and R^2 for the sorption of different parameters on neem carbon are summarized in Table 4.6. The WMIDM for sorption of nitrate, phosphate and chloride are presented in Figures 4.53, 4.54 and 4.55 respectively.

Figures 4.56 – 4.60 present the WMIDM for the sorption of nickel, zinc, chromium, cadmium and lead ions respectively.

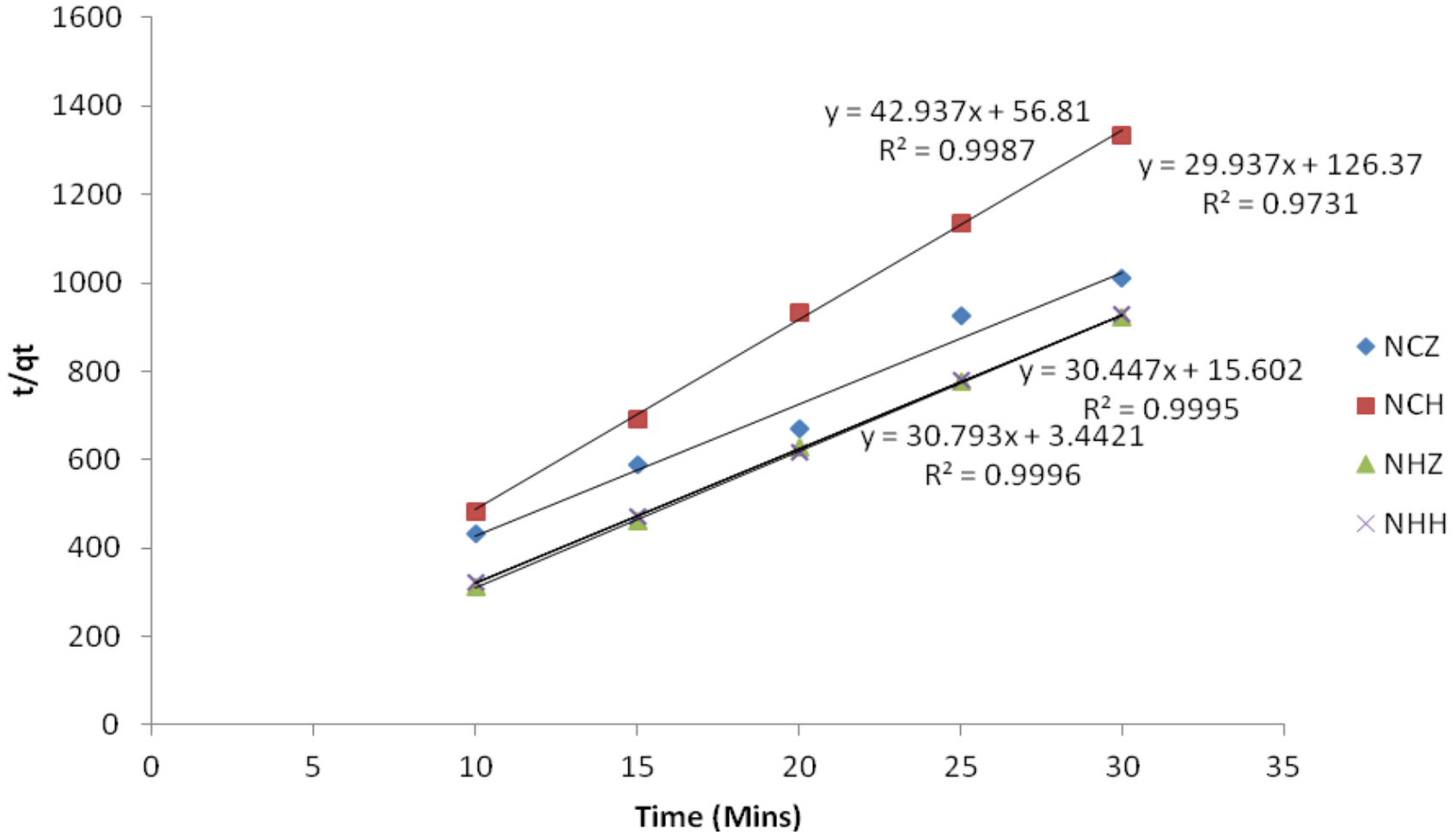


Figure 4.45: The pseudo-second order plot for chloride ions removal

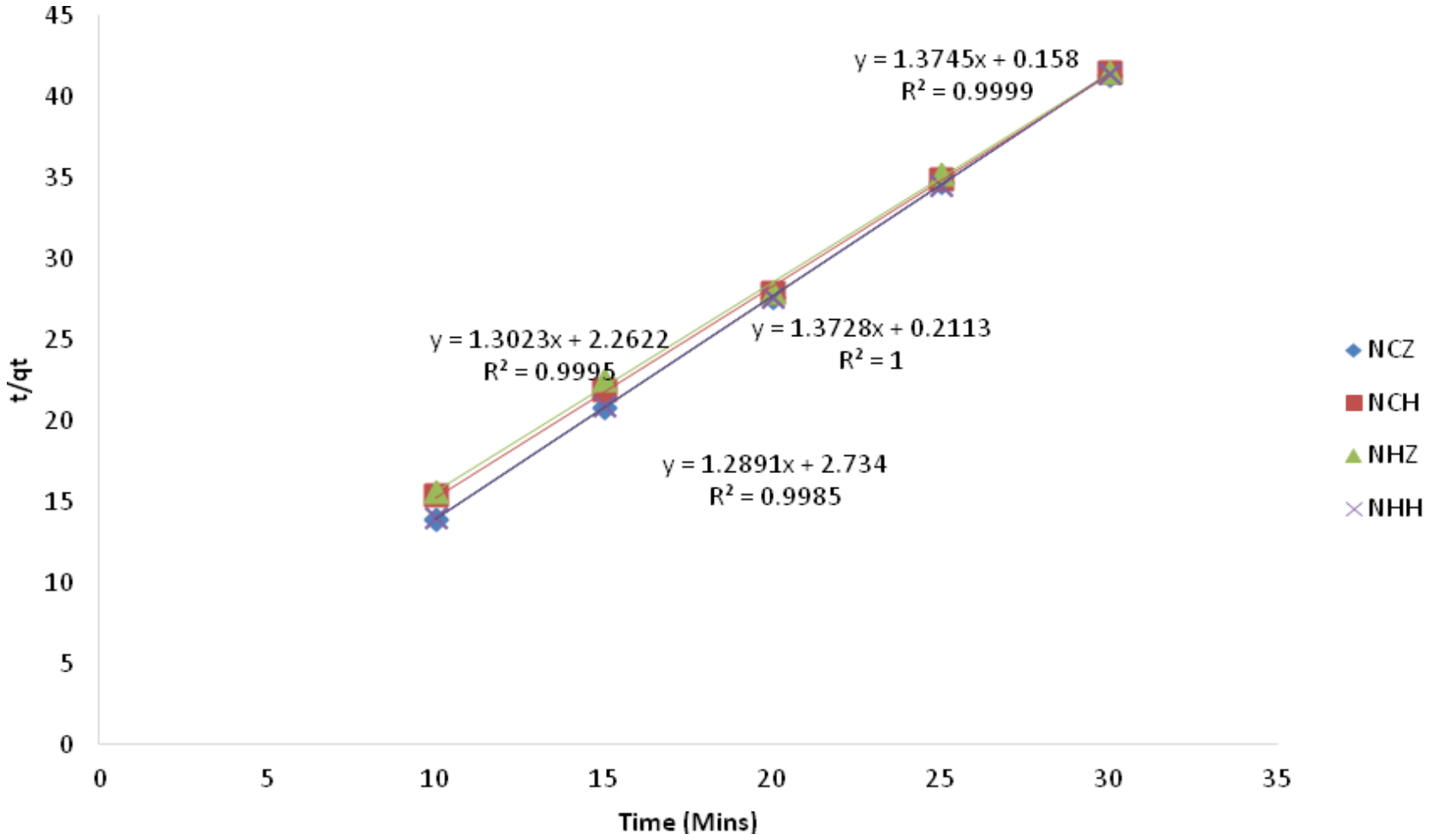


Figure 4. 46: The pseudo-second order plot for nitrate ion removal

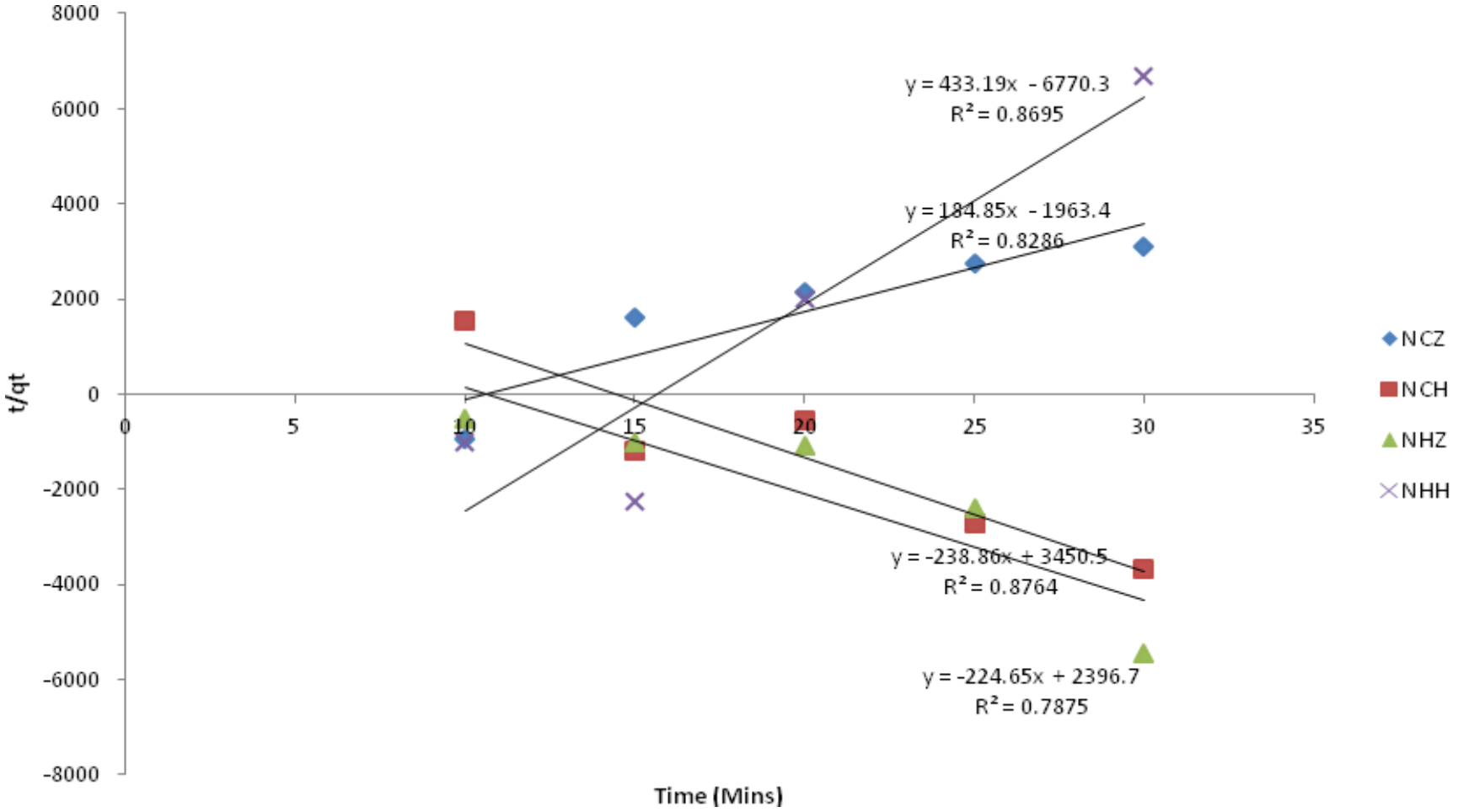


Figure 4. 47: The pseudo-second order plot for phosphate ion removal

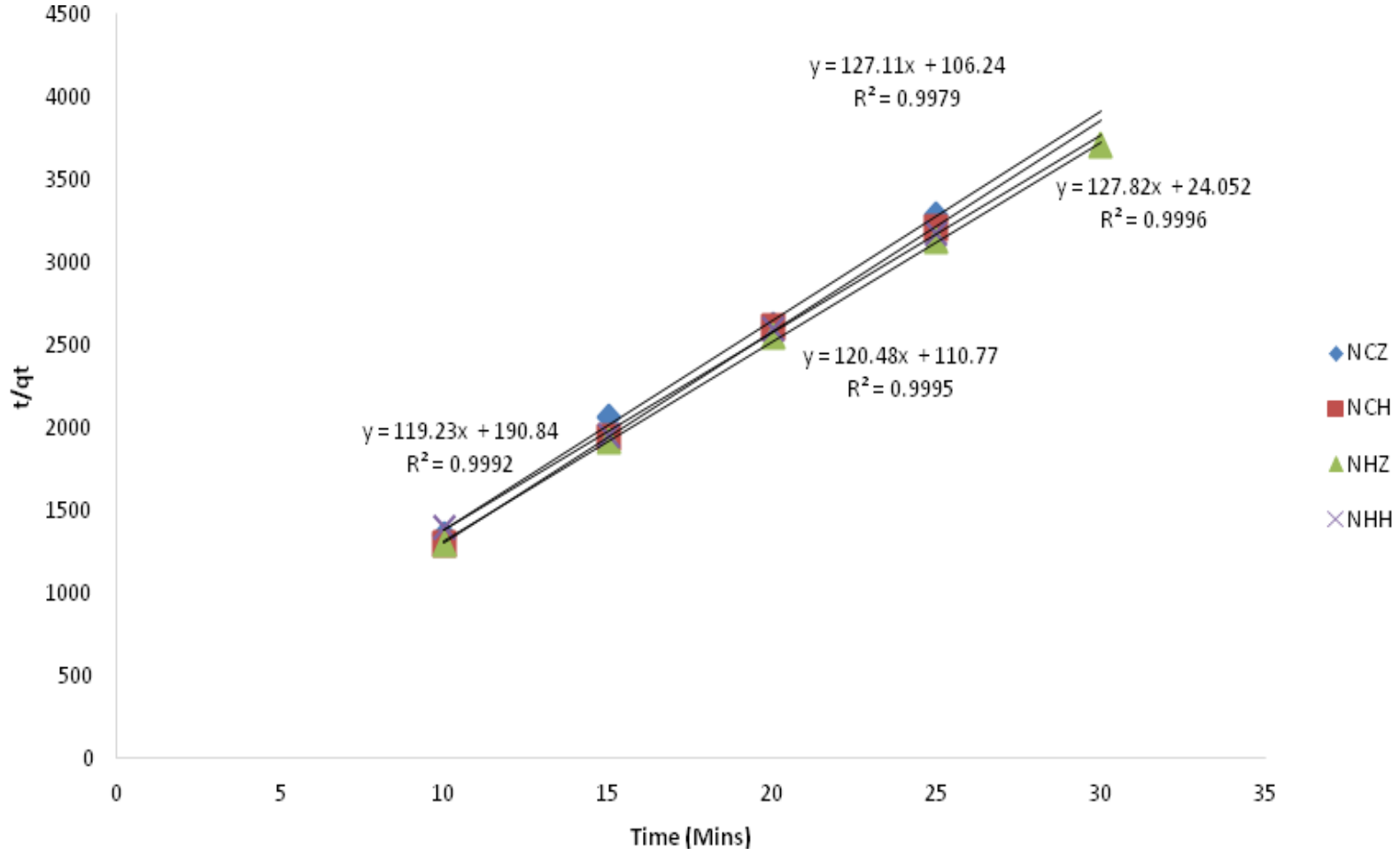


Figure 4. 48: The pseudo-second order plot for cadmium ion removal

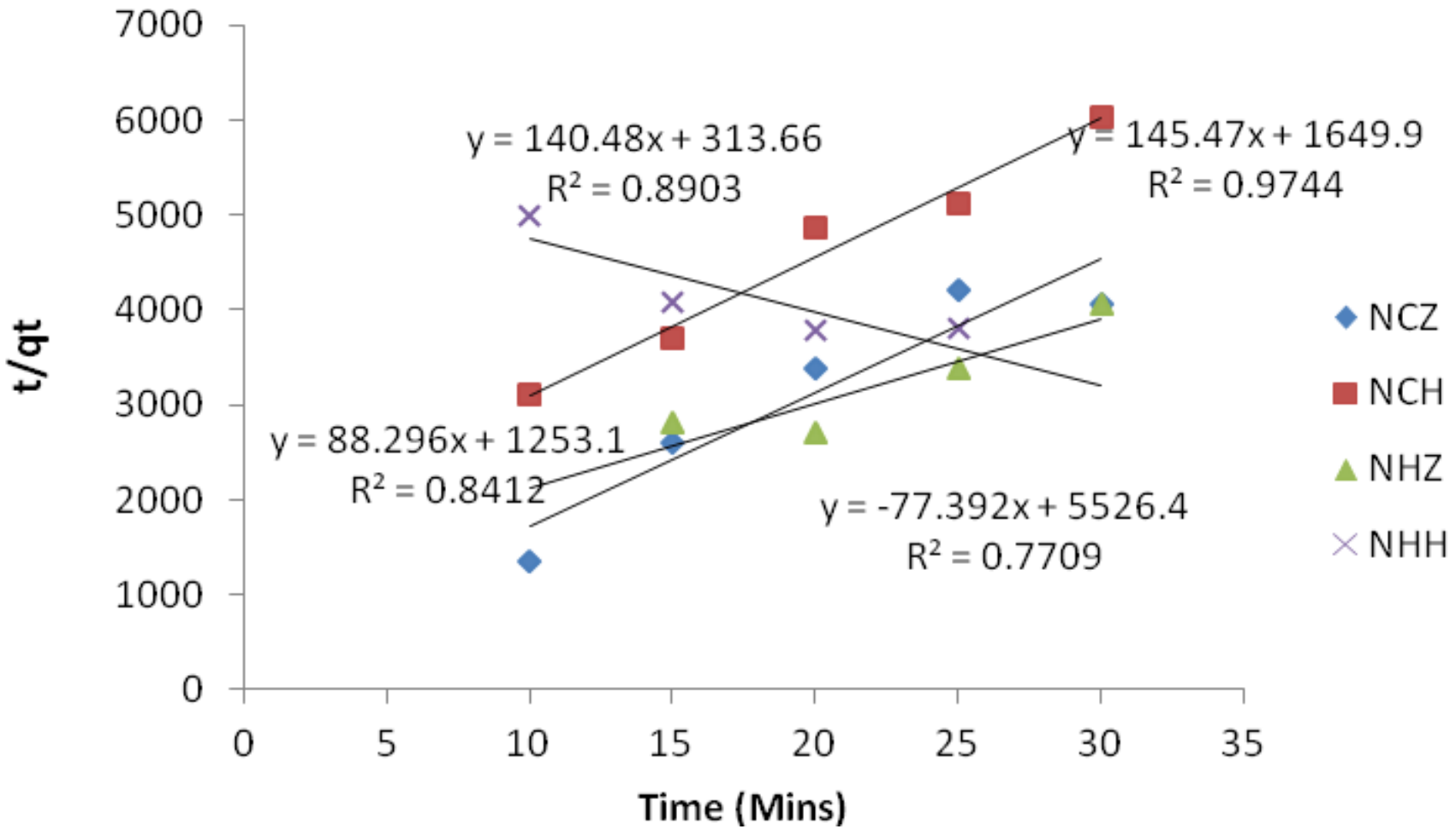


Figure 4. 49: The pseudo-second order plot for chromium ion removal

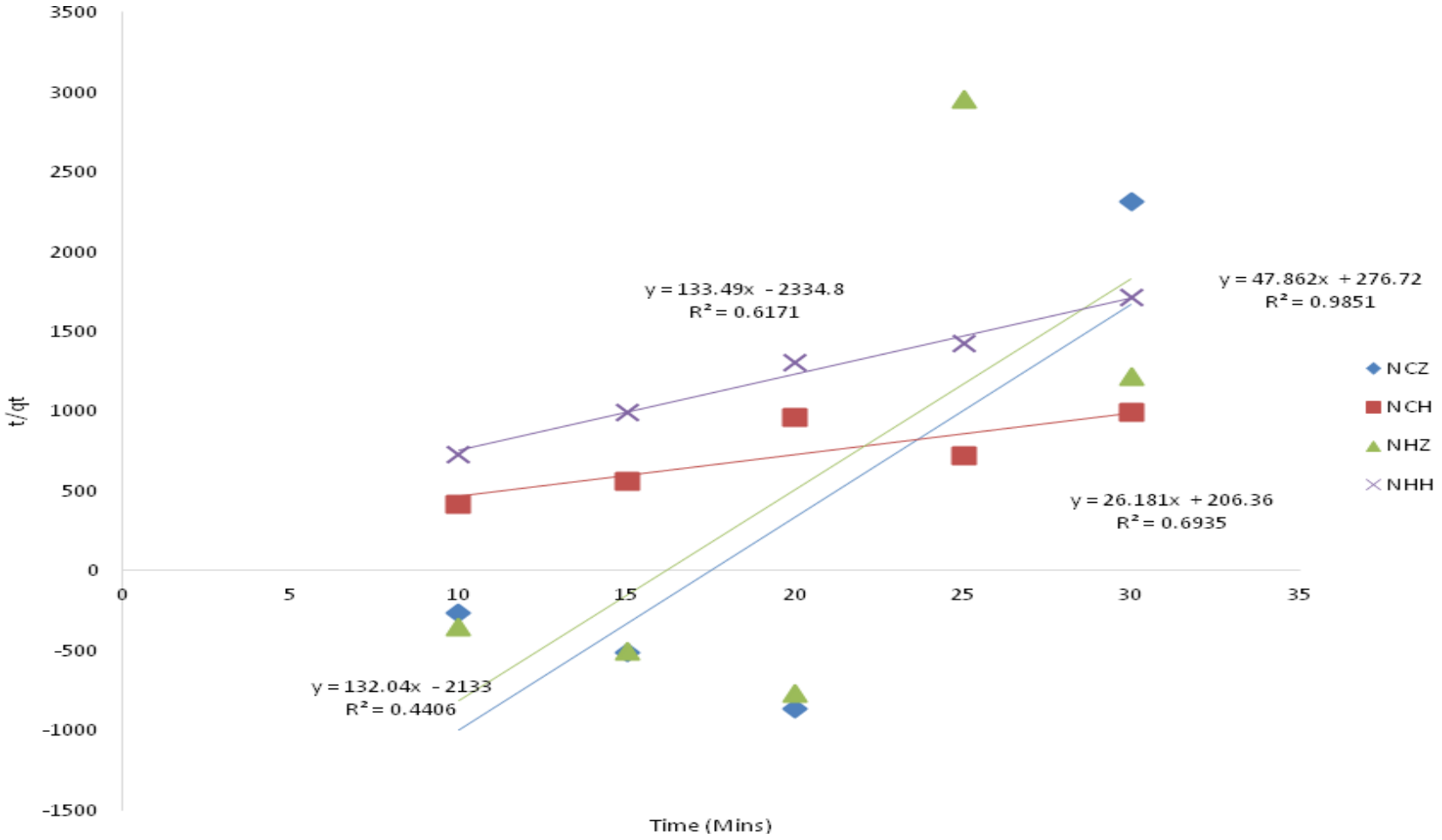


Figure 4. 50: The pseudo-second order plot for zinc ion removal

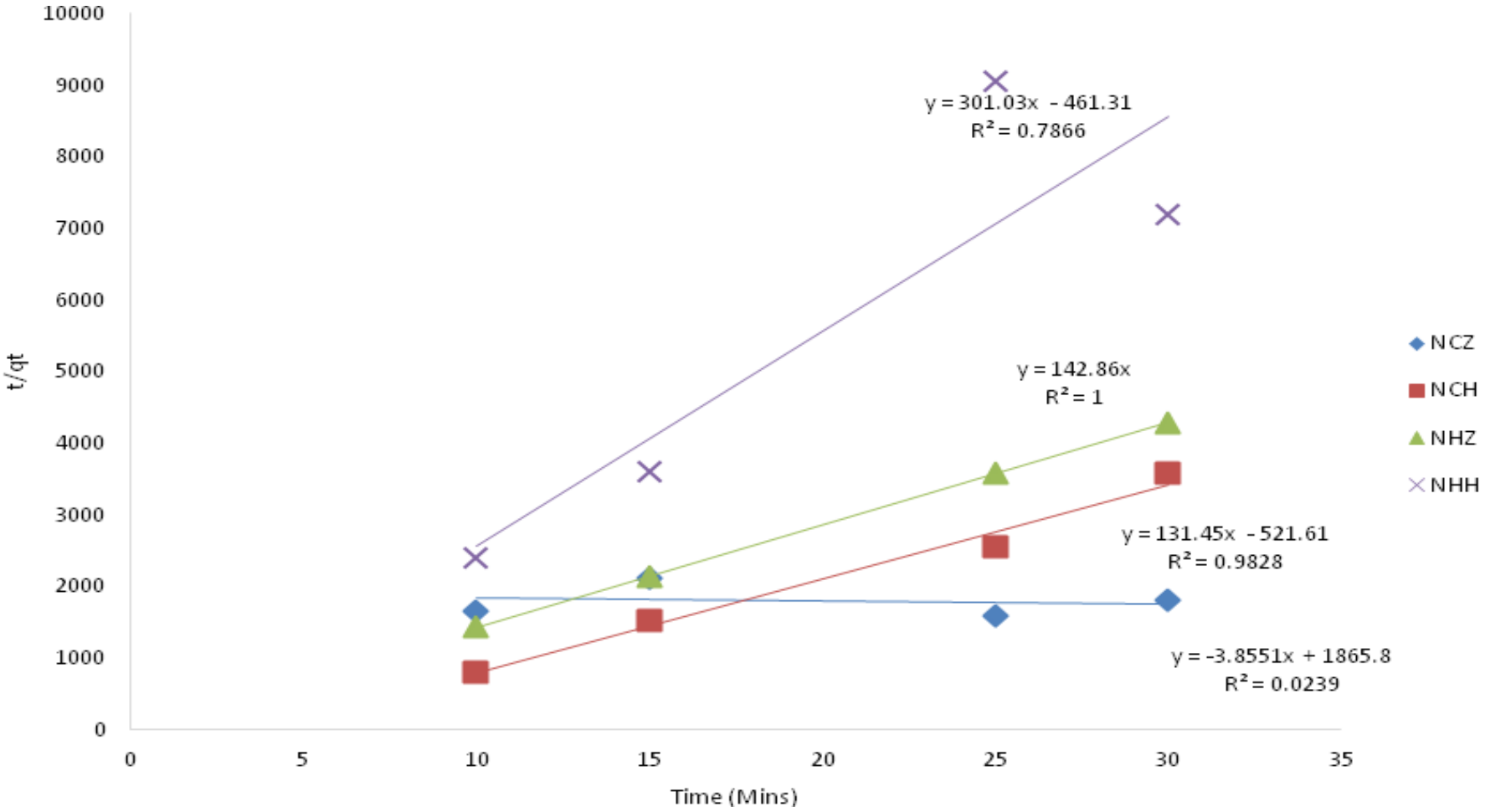


Figure 4. 51: The pseudo-second order plot for nickel ion removal

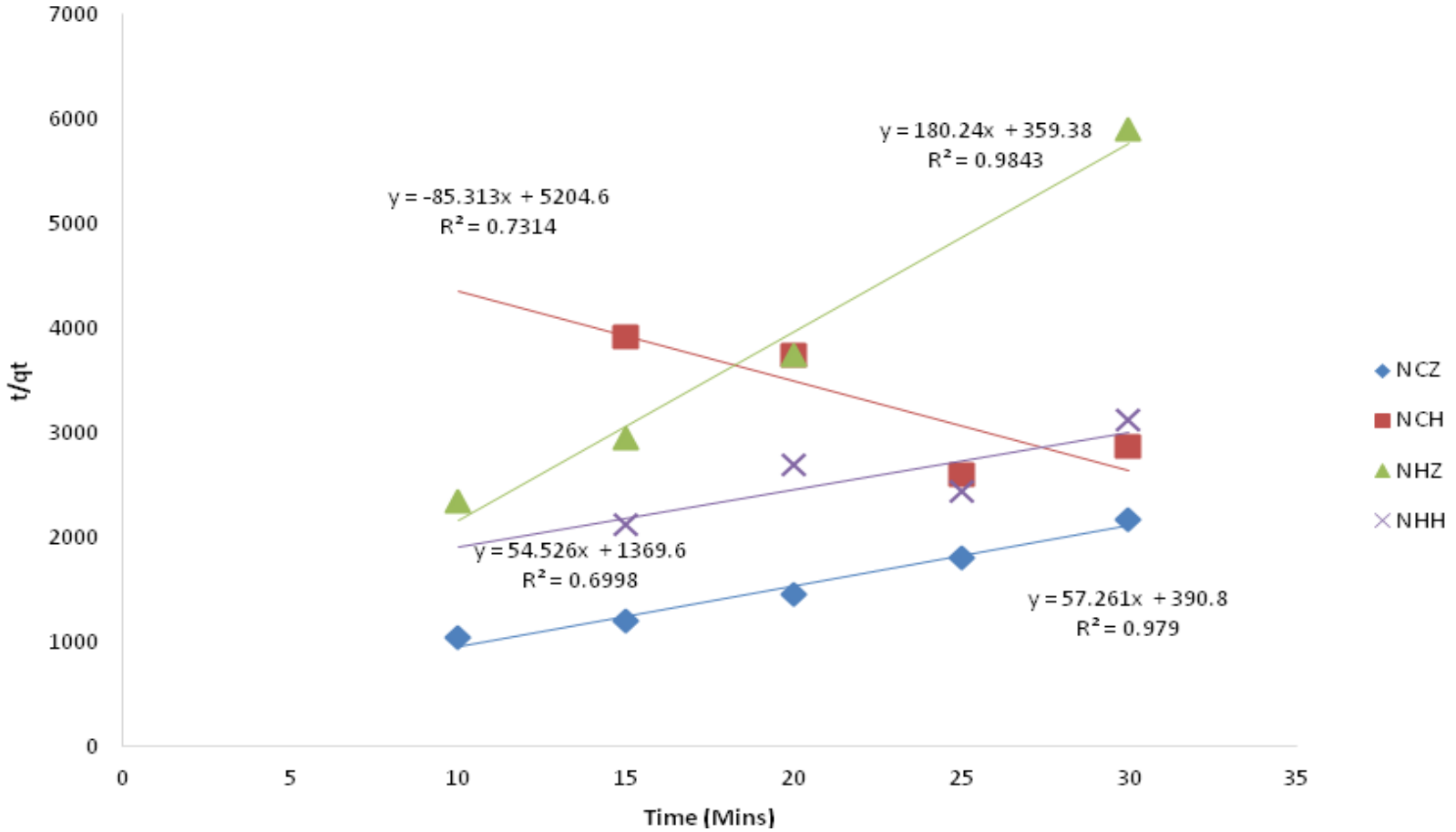


Figure 4. 52: The pseudo-second order plot for lead ion removal

Table 4. 5 The Pseudo-second-order rate equation constant for neem carbon on wastewater

	NCZ			NCH			NHZ			NHH		
	Q_e	K_2	R^2	Q_e	K_2	R^2	Q_e	K_2	R^2	Q_e	K_2	R^2
Nitrate	0.7280	11.9570	1.9999	0.7680	0.7500	1.9995	0.7760	0.6080	0.9985	0.7280	8.9190	1.0000
Phosphate	0.0050	17.4030	0.8286	0.0040	16.5350	0.8764	-0.0040	21.0570	0.7875	0.0020	44.9370	0.8695
Chloride	0.0330	7.0920	0.9730	0.0230	14.5890	0.9990	0.0330	268.1220	0.9996	0.0330	59.4170	0.9995
Cd	0.0020	48.5570	0.9979	0.0030	39.2680	0.9996	0.0080	131.0410	0.9995	0.0080	74.4910	0.9992
Cr	0.0070	62.9170	0.8903	0.0070	12.8260	0.9744	-0.0380	0.1680	0.8412	-0.0440	0.1090	0.7709
Zn	-0.0230	3.2900	0.6171	0.0380	3.3220	0.6935	0.0080	8.1740	0.4406	0.0210	8.1900	0.9851
Ni	0.2590	0.0080	0.0239	0.0080	33.1260	0.9828	0.0070	0.0000	1.000	0.0030	196.4390	0.7866
Pb	0.0170	8.3900	0.9790	-0.0640	0.0700	0.7314	0.0070	32.9250	0.9843	0.0190	0.7030	0.6998

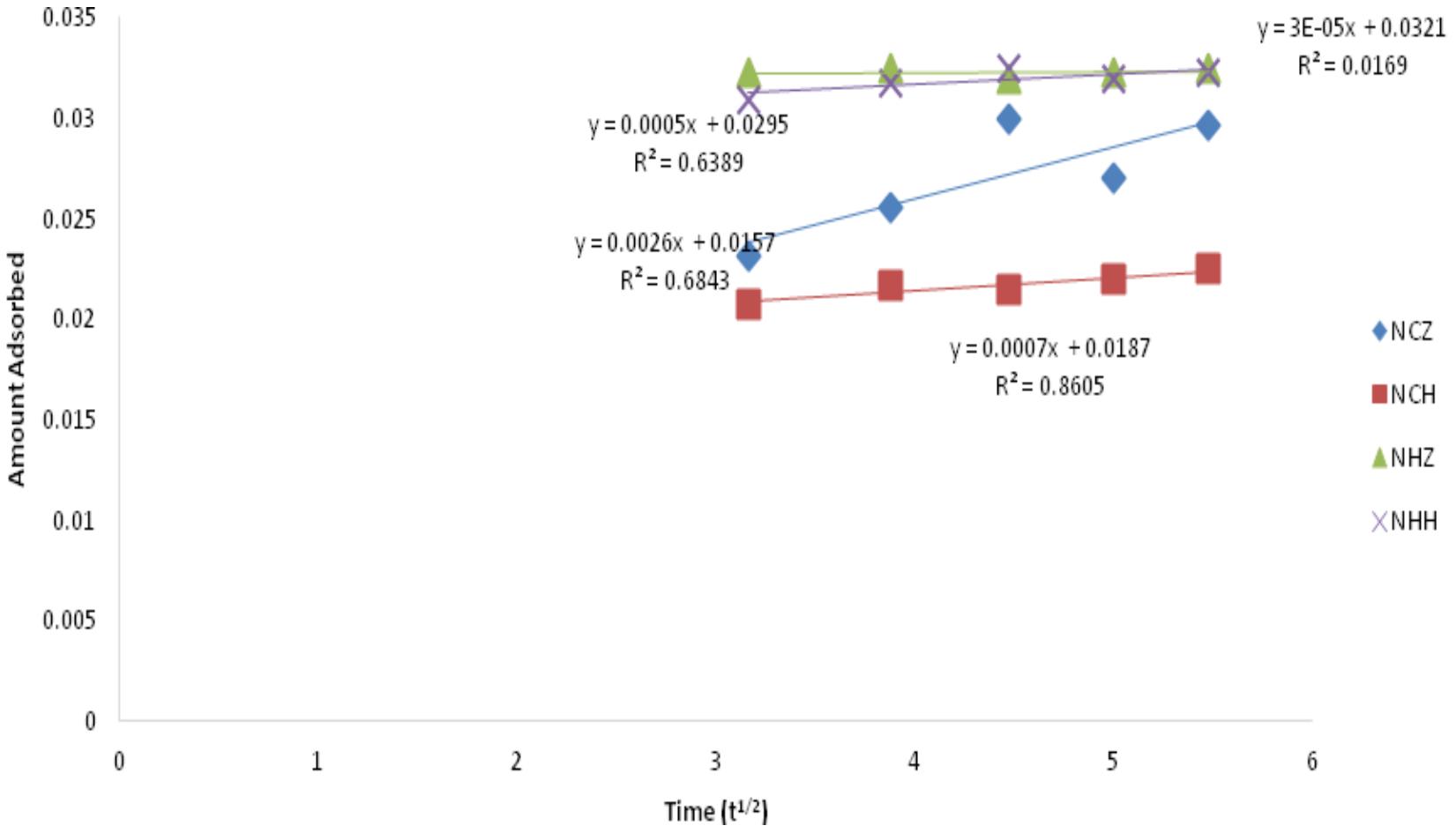


Figure 4. 53: Weber and Morris diffusion models plot for chloride ion

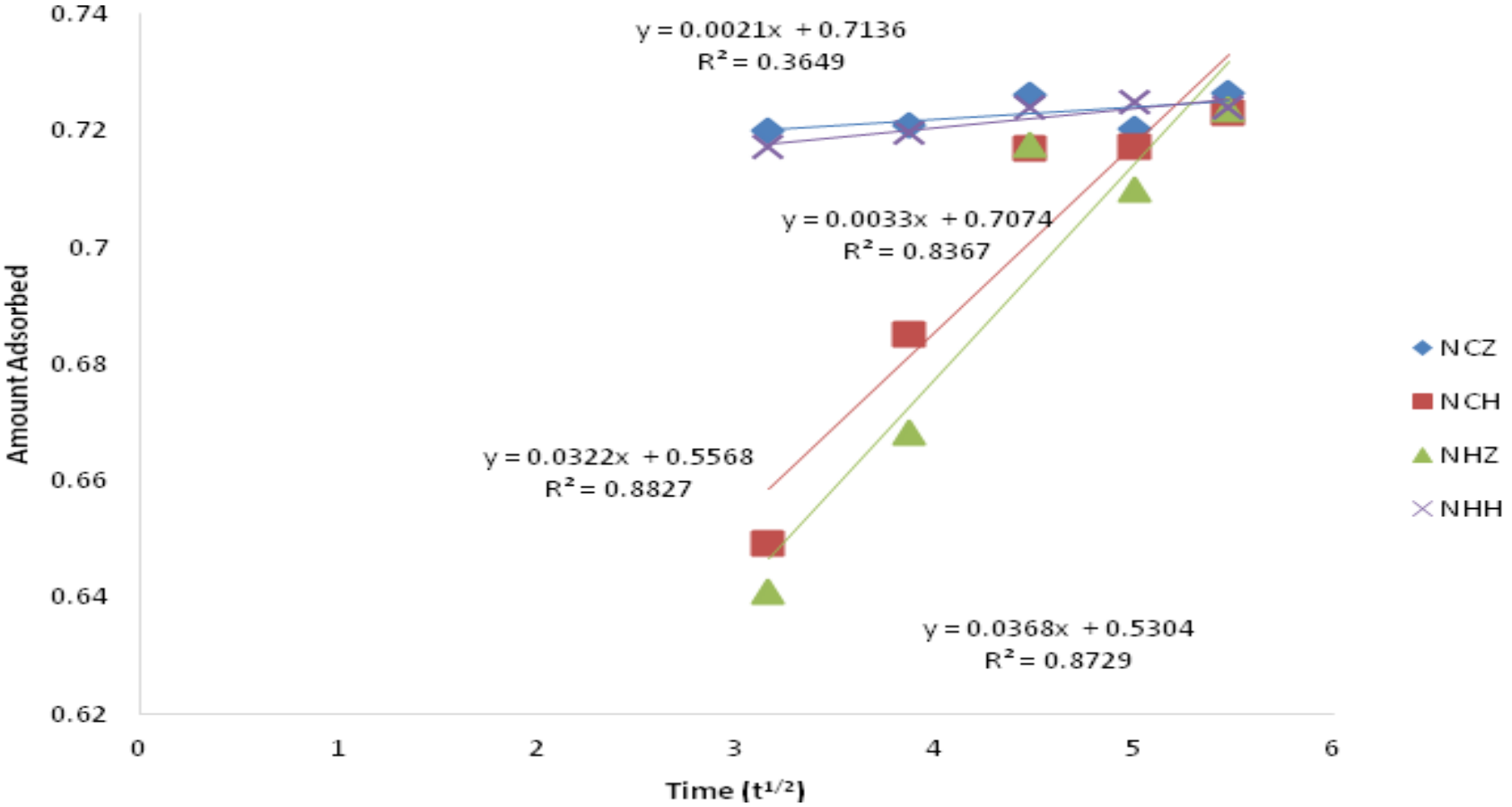


Figure 4. 54: Weber and Morris diffusion models plot for nitrates ion

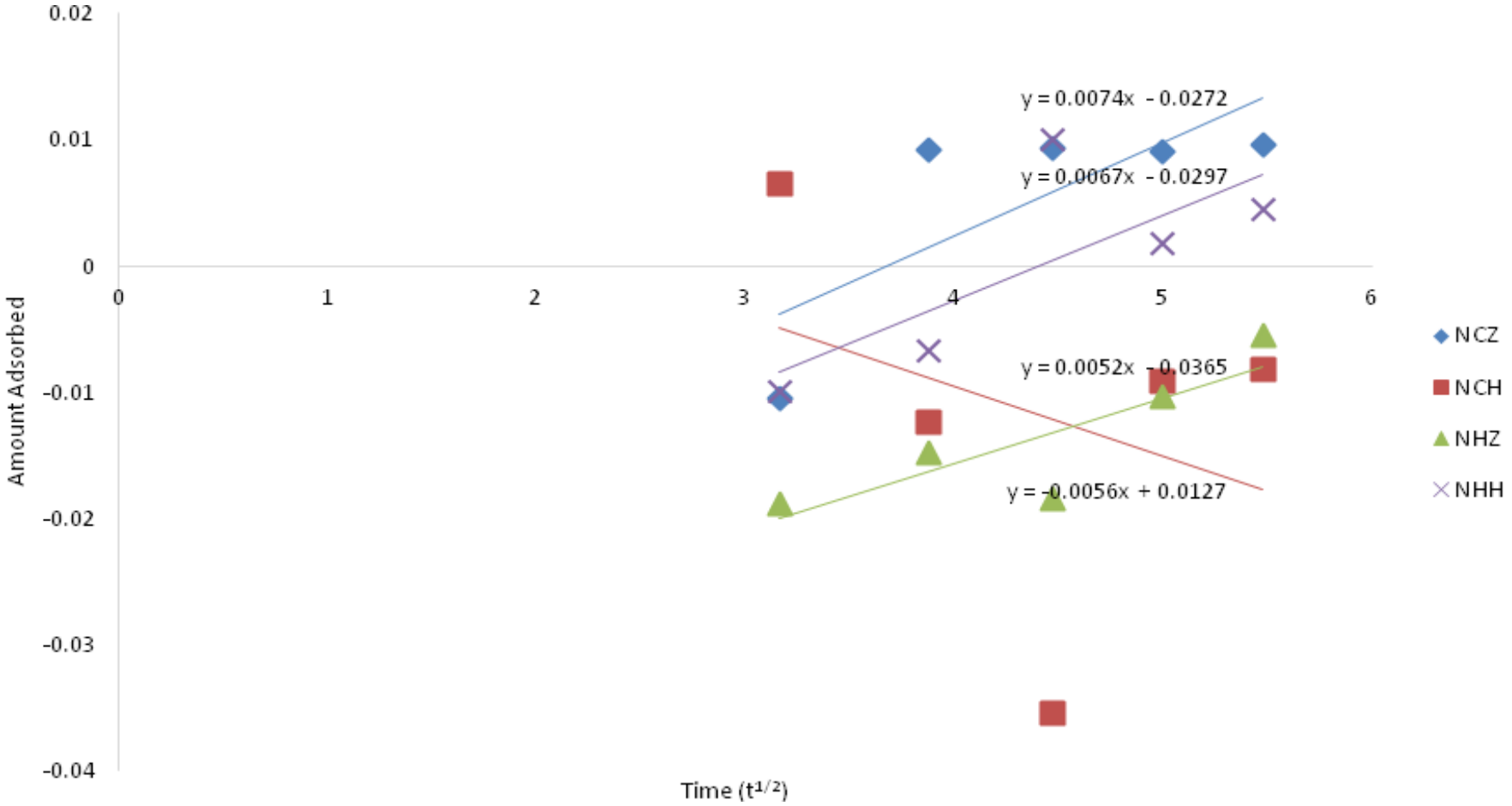


Figure 4. 55: Weber and Morris diffusion models plot for phosphates ion

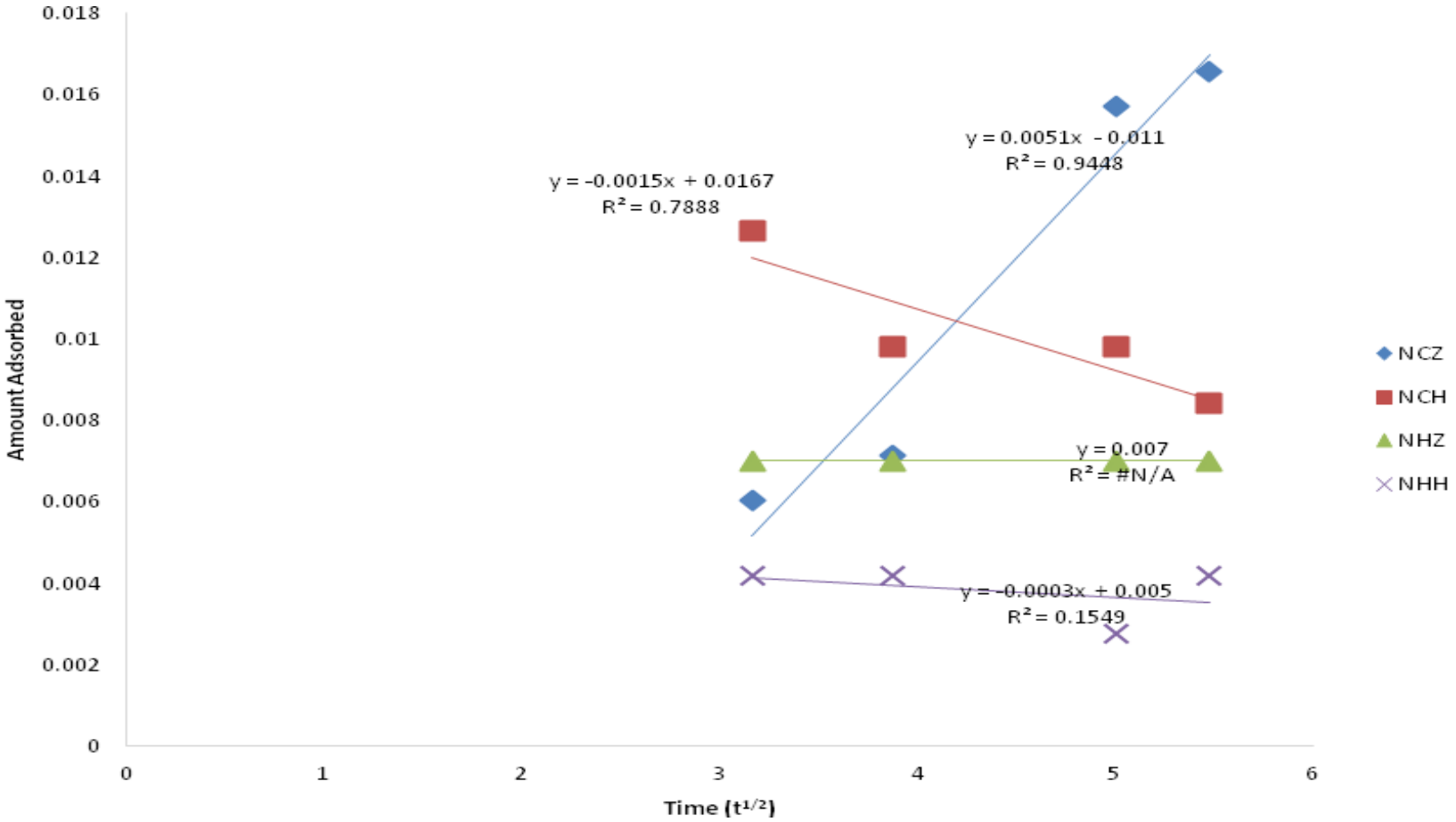


Figure 4. 56: Weber and Morris diffusion models plot for nickel ion

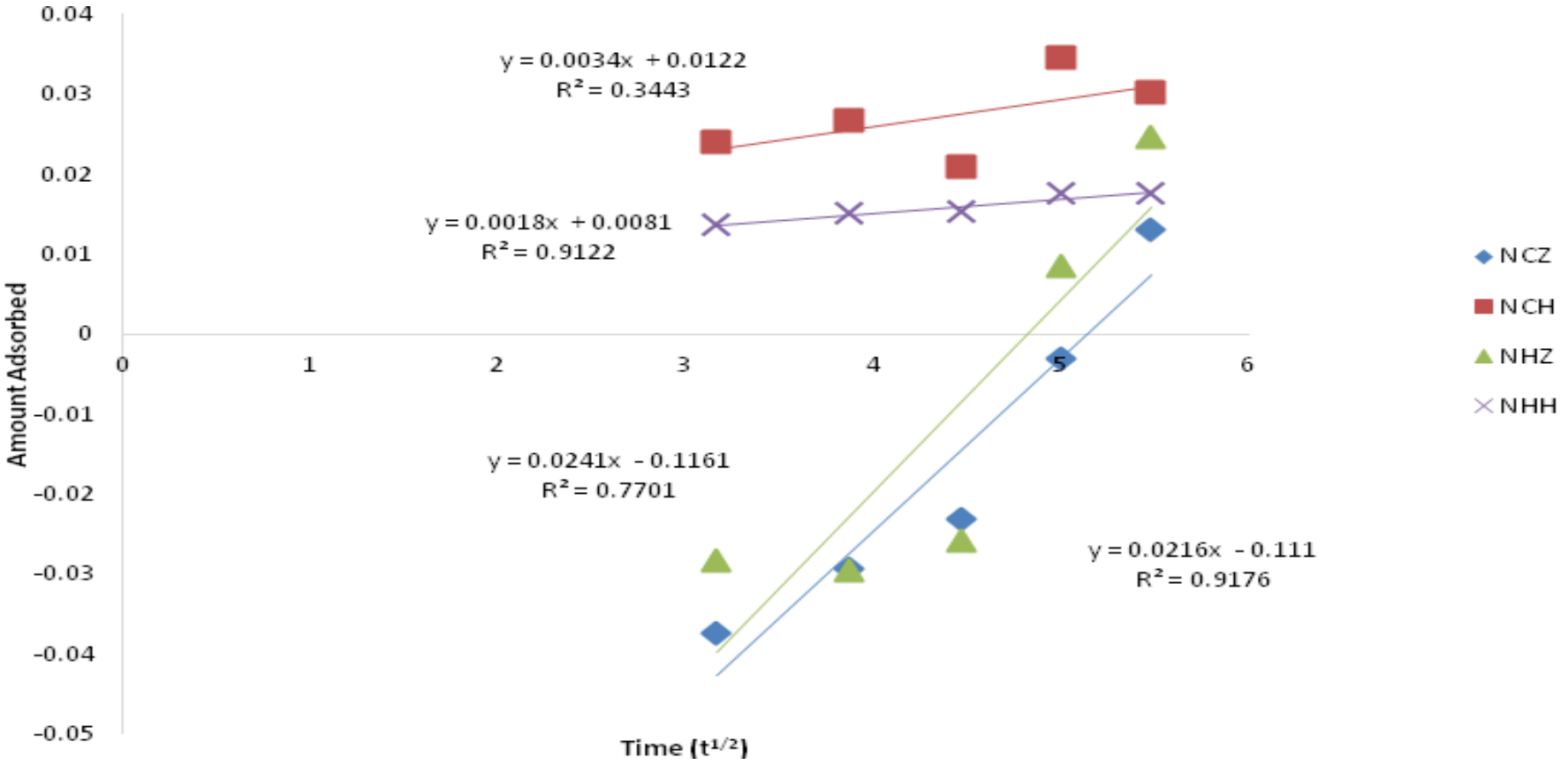


Figure 4. 57: Weber and Morris diffusion models plot for zinc ion

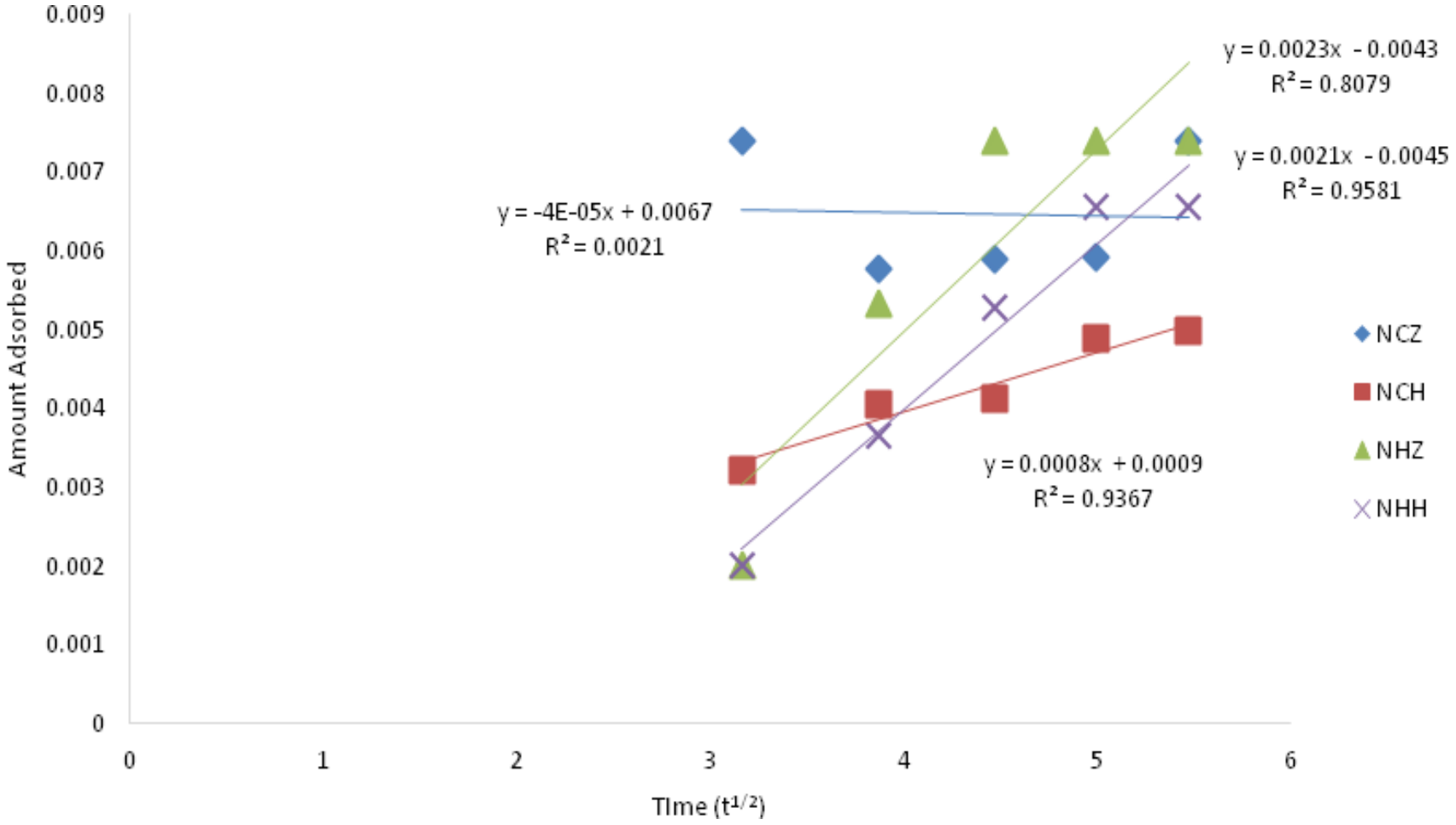


Figure 4. 58: Weber and Morris diffusion models plot for chromium ion

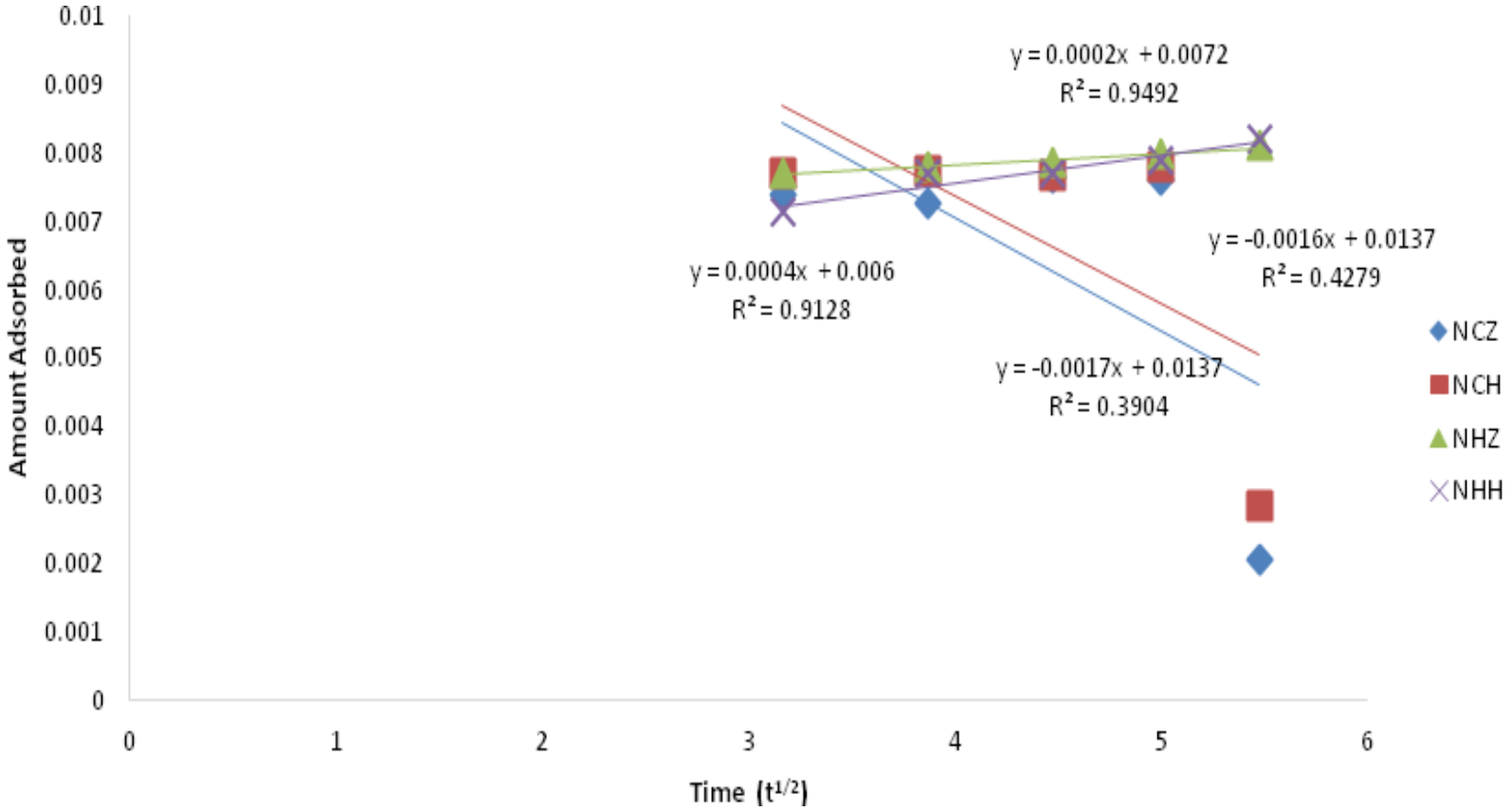


Figure 4. 59: Weber and Morris diffusion model plot for cadmium ion

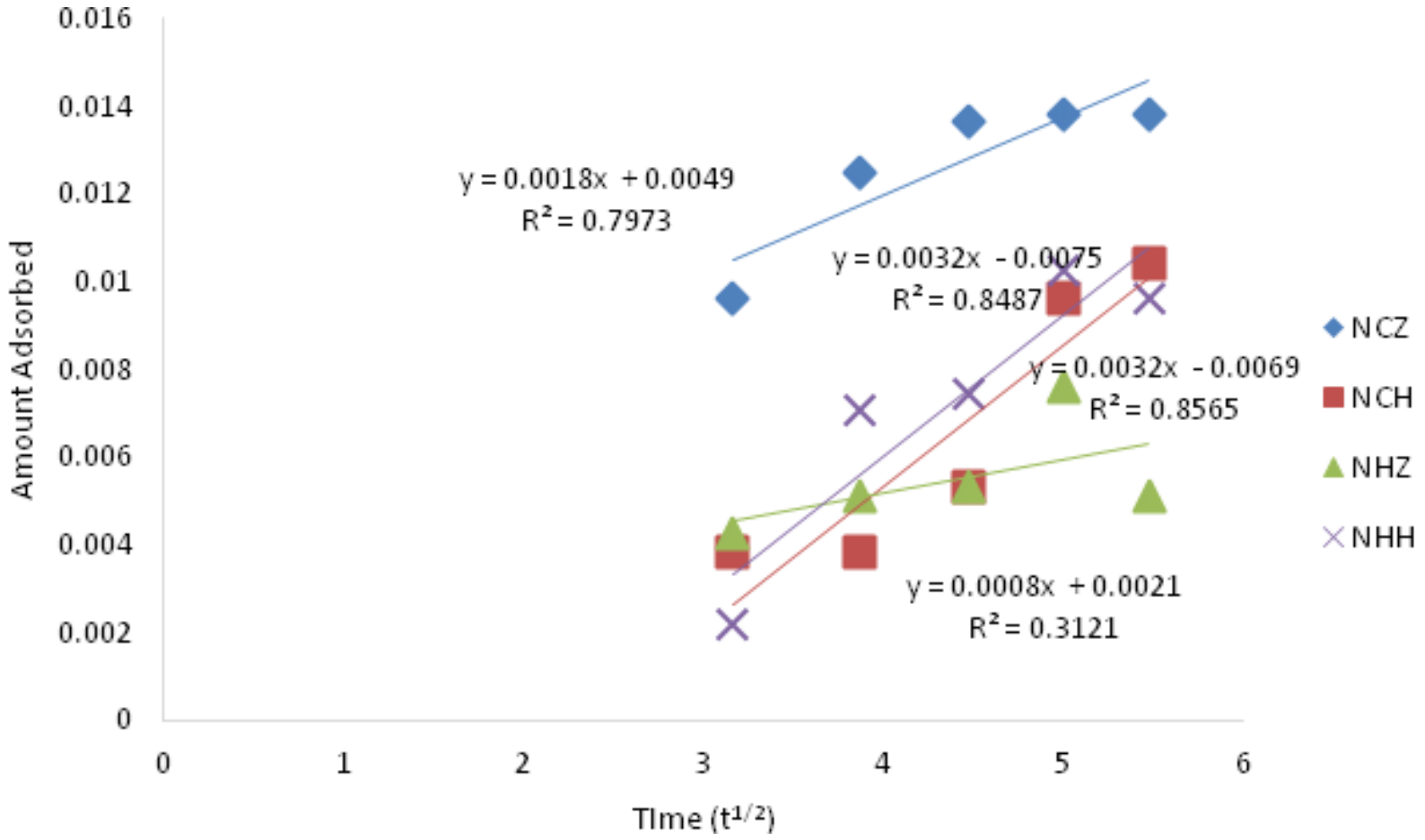


Figure 4. 60: Weber and Morris diffusion model plot for lead ion

Table 4. 6 The Weber and Morris Difussion model constants

	NCZ			NCH			NHZ			NHH		
	K_{id}	C_i	R^2	K_{id}	C_i	R^2	K_{id}	C_i	R^2	K_{id}	C_i	R^2
Nitrite	0.00	0.71	0.36	0.03	0.06	0.88	0.04	0.53	0.09	0.00	0.07	0.08
Phosphate	0.01	-0.03	0.58	-0.01	0.01	0.11	0.01	0.04	0.70	0.01	0.03	0.57
Chlorine	0.00	0.02	0.68	0.00	0.02	0.86	0.00	0.03	0.02	0.00	0.03	0.64
Cd	0.00	0.01	0.39	0.00	0.00	0.43	0.00	0.01	0.95	0.00	0.01	0.91
Cr	0.00	0.00	0.00	0.00	0.00	0.94	0.00	0.00	0.81	0.00	0.00	0.96
Zn	0.02	-0.11	0.92	0.00	0.01	0.34	0.02	-0.12	0.77	0.00	0.01	0.91
Ni	0.01	-0.11	0.94	0.00	0.02	0.79	0.00	0.01	0.00	0.00	0.01	0.02
Pb	0.01	-0.03	0.58	-0.01	0.01	0.11	0.01	0.04	0.70	0.01	0.03	0.57

4.10 Effect of initial wastewater volume on physicochemical parameters of the wastewater

The effects of the initial wastewater volume on each of the investigated are presented in Figures 4.61 – 4.78. The effect of initial volume on pH in the wastewater is presented in Figure 4.61. The most effective initial wastewater volume for the reduction of conductivity was found to be 10ml as presented in Figure 4.62. The effect of initial wastewater volume on adsorption of Total Dissolved Solid (TDS) is presented in Figure 4.63. The effect of initial wastewater volume on turbidity and hardness are presented in Figures 4.64 and 4.65 respectively.

The effect of initial wastewater volume on COD, BOD and DO are presented in Figures 4.66, 4.67 and 4.68 respectively while the effects of initial wastewater volume on chloride, nitrate and phosphate ions are presented in Figures 4.69, 4.70 and 4.71 respectively. The effects of initial wastewater on the adsorption of heavy metals (Cd, Cr, Zn, Ni and Pb) are presented in Figures 4.72, 4.73, 4.74, 4.75 and 4.76 respectively while the effects of initial wastewater on the reduction of bacterial and fungal load are presented in Figures 4.77 and 4.78.

4.11 Langmuir Adsorption Isotherm

Figures 4.80 - 4.86 show the linearized Langmuir Isotherm models for the treated wastewater. The R^2 values of the linear plot for the different parameter studied were used to ascertain the fitness of the parameter to the model. The values of the slope and intercept of the plots were used to calculate the Langmuir constants as presented in Table 4.7. Q_m represent adsorption capacity, b is Langmuir constant that relate to the energy of adsorption. The essential parameters of the Langmuir isotherms are best expressed in a dimensionless constant separated factor or equilibrium parameter (R_L).

The Langmuir adsorption model for chlorides, nitrite, and phosphate ions are presented in Figures 4.79, 4.80 and 4.81 respectively. The Langmuir adsorption model for cadmium, chromium, lead, zinc and nickel are presented in Figures 4.82, 4.83, 4.84, 4.85 and 4.86 respectively.

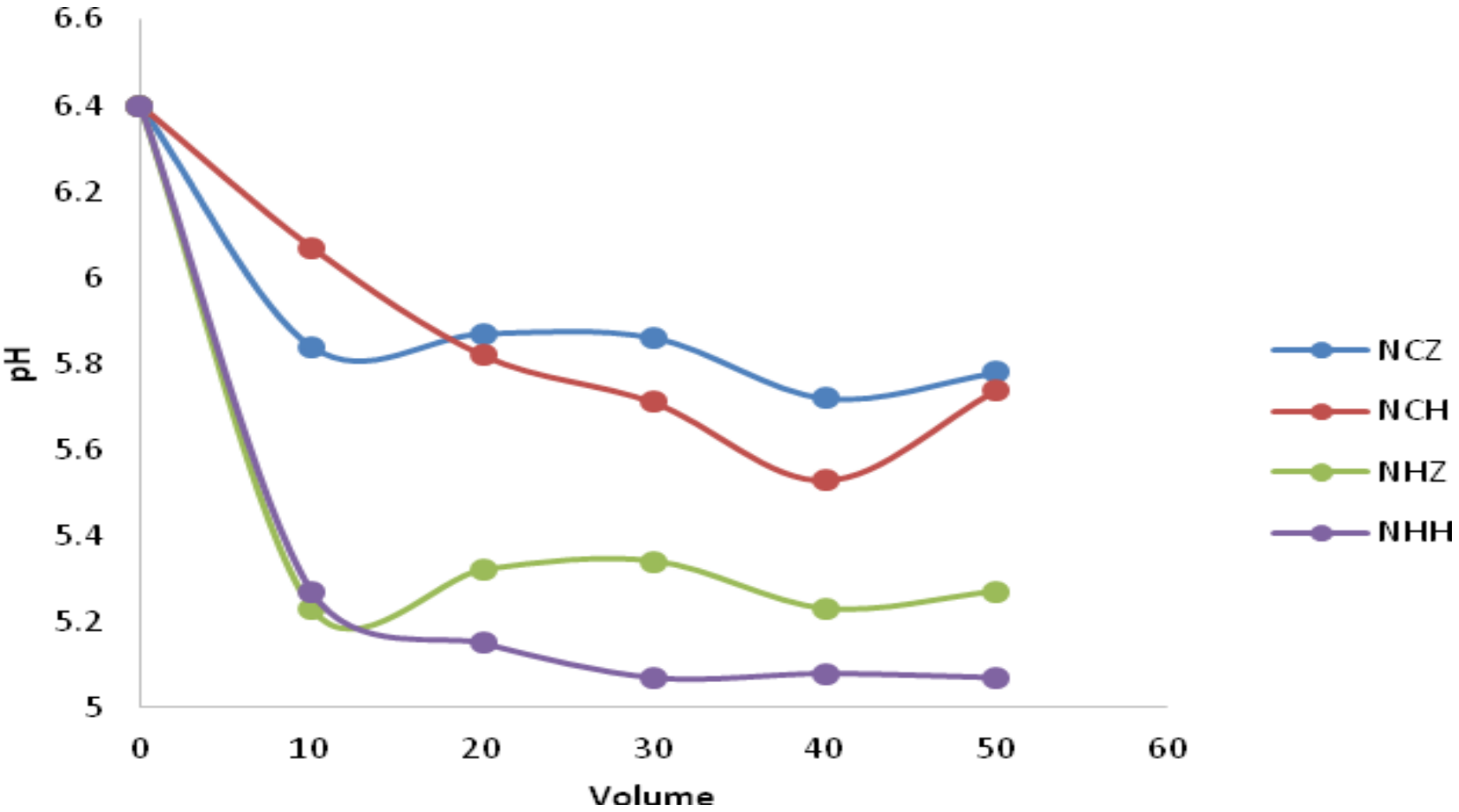


Figure 4. 61: Effect of initial volume of wastewater on pH of treated water

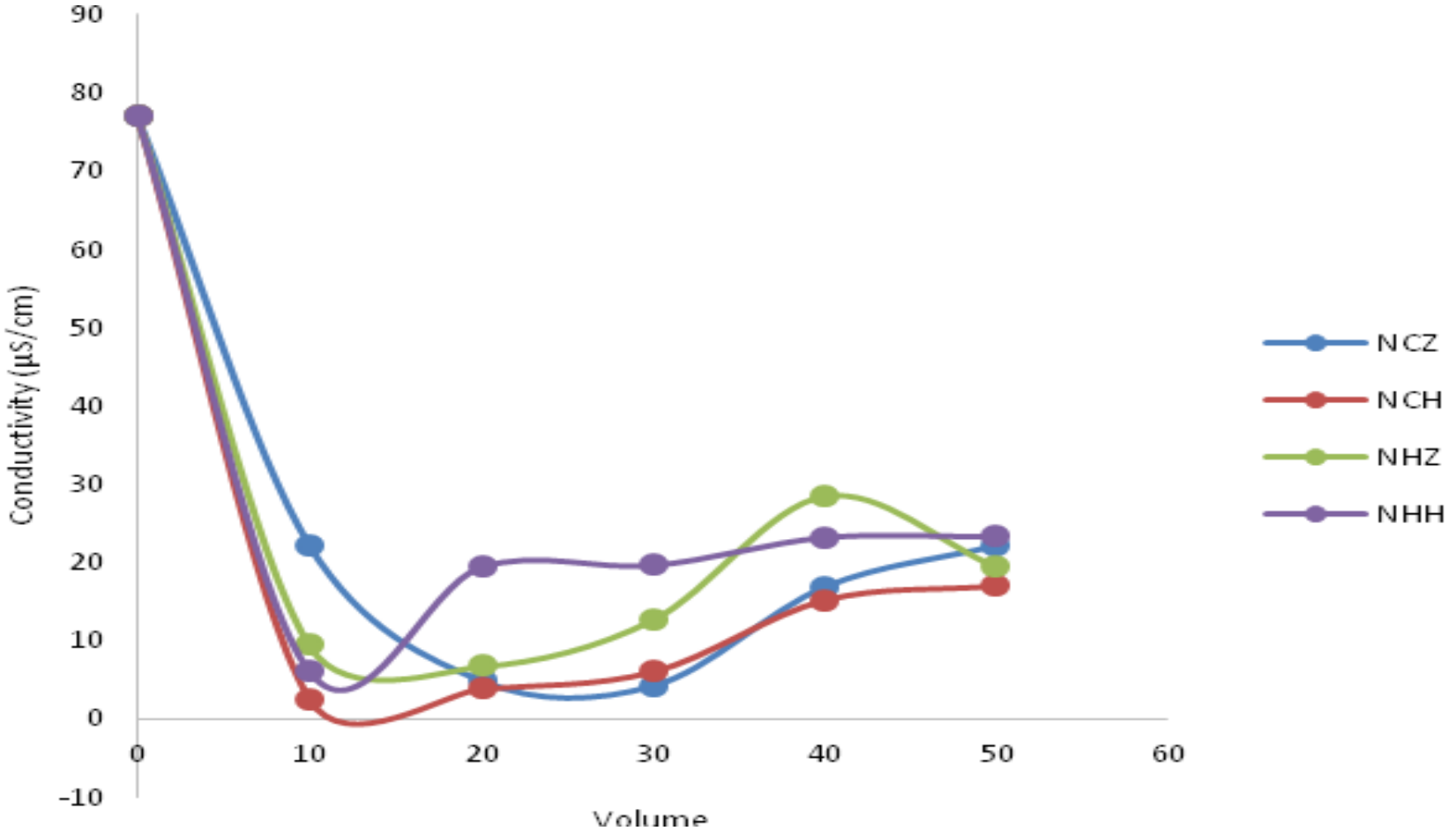


Figure 4. 62: Effect of initial volume of wastewater on conductivity of treated water

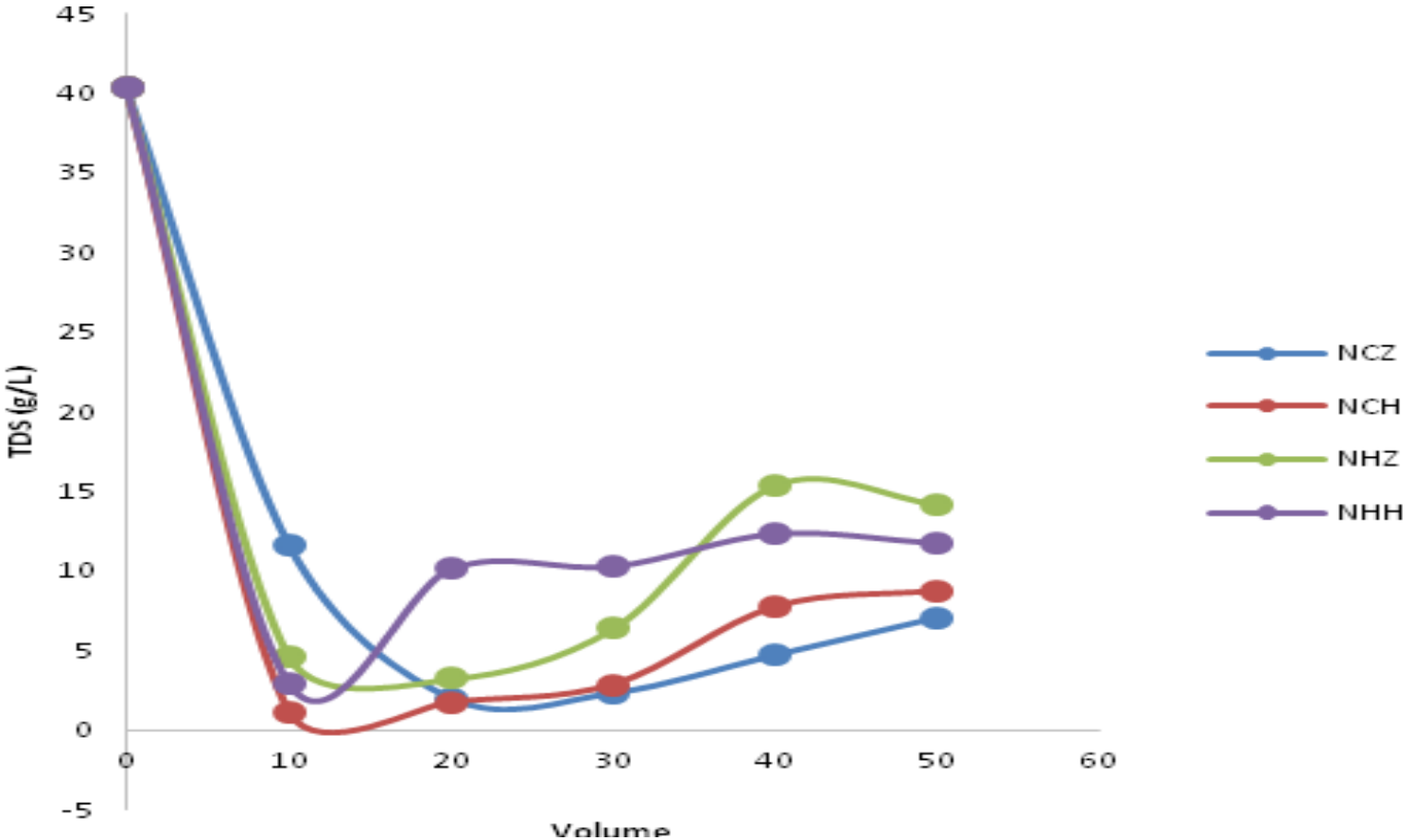


Figure 4. 63: Effect of initial volume of wastewater on TDS of treated water

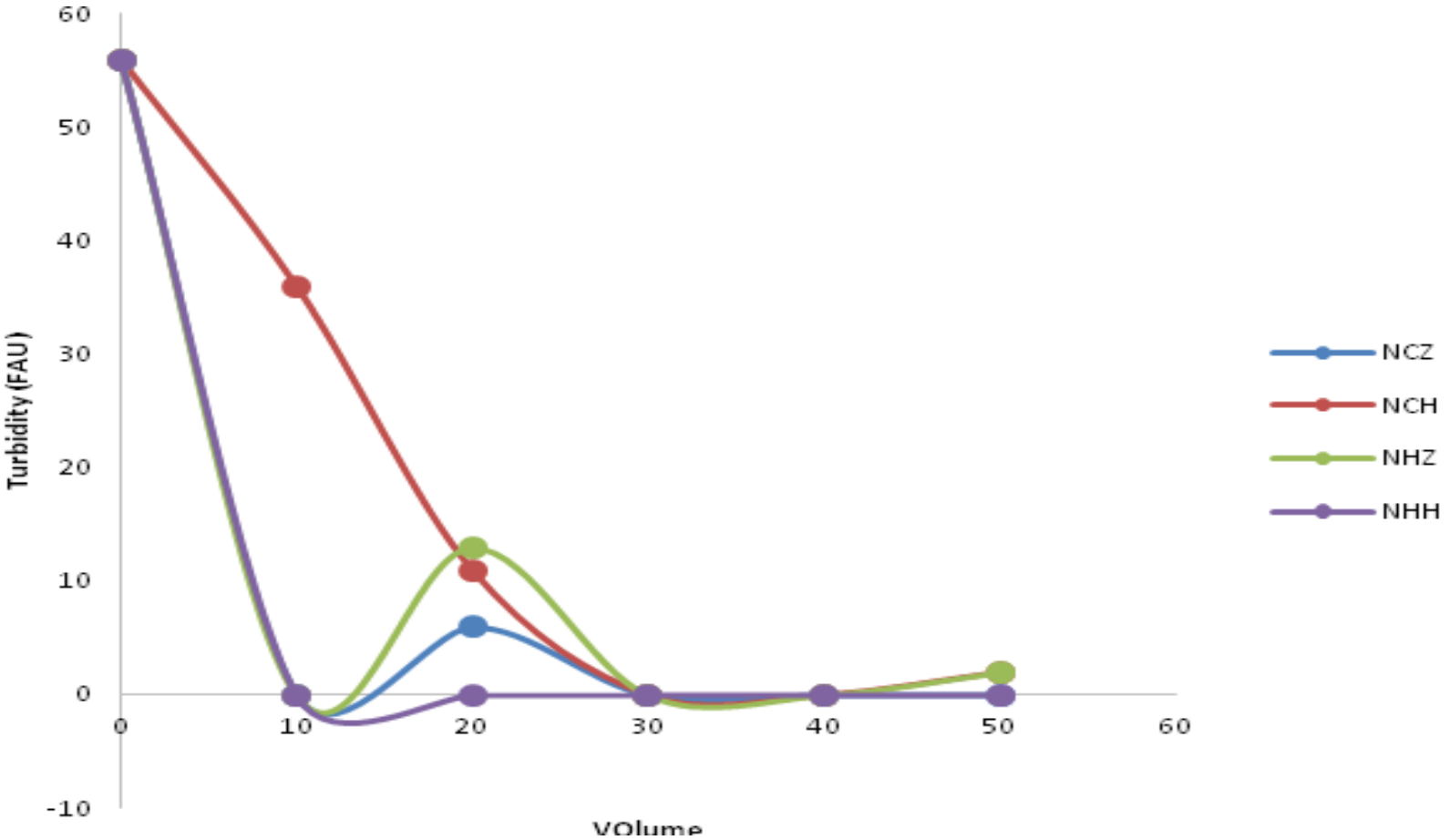


Figure 4. 64: Effect of initial volume of wastewater on turbidity of treated water

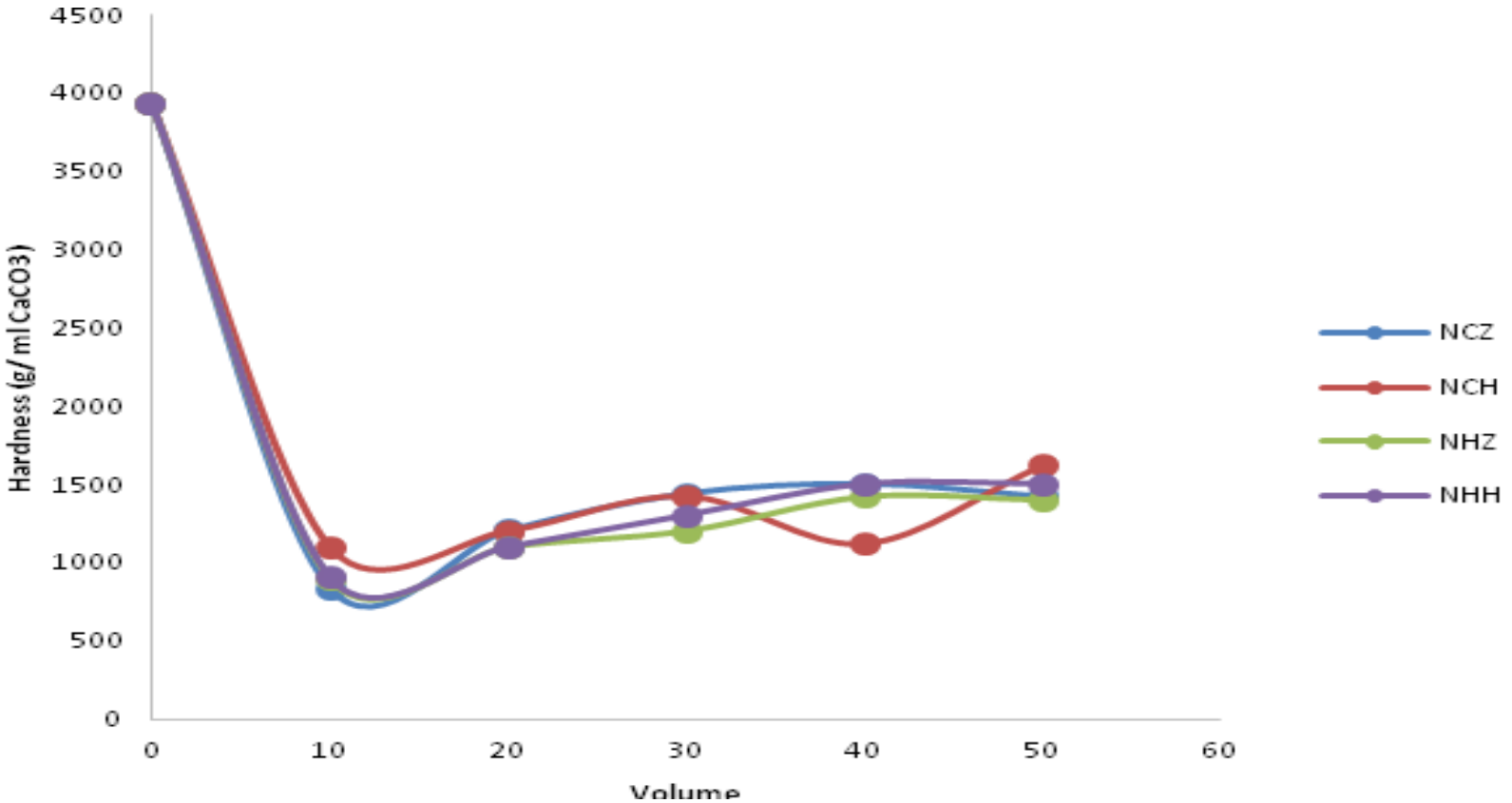


Figure 4. 65: Effect of initial volume of wastewater on hardness of treated water

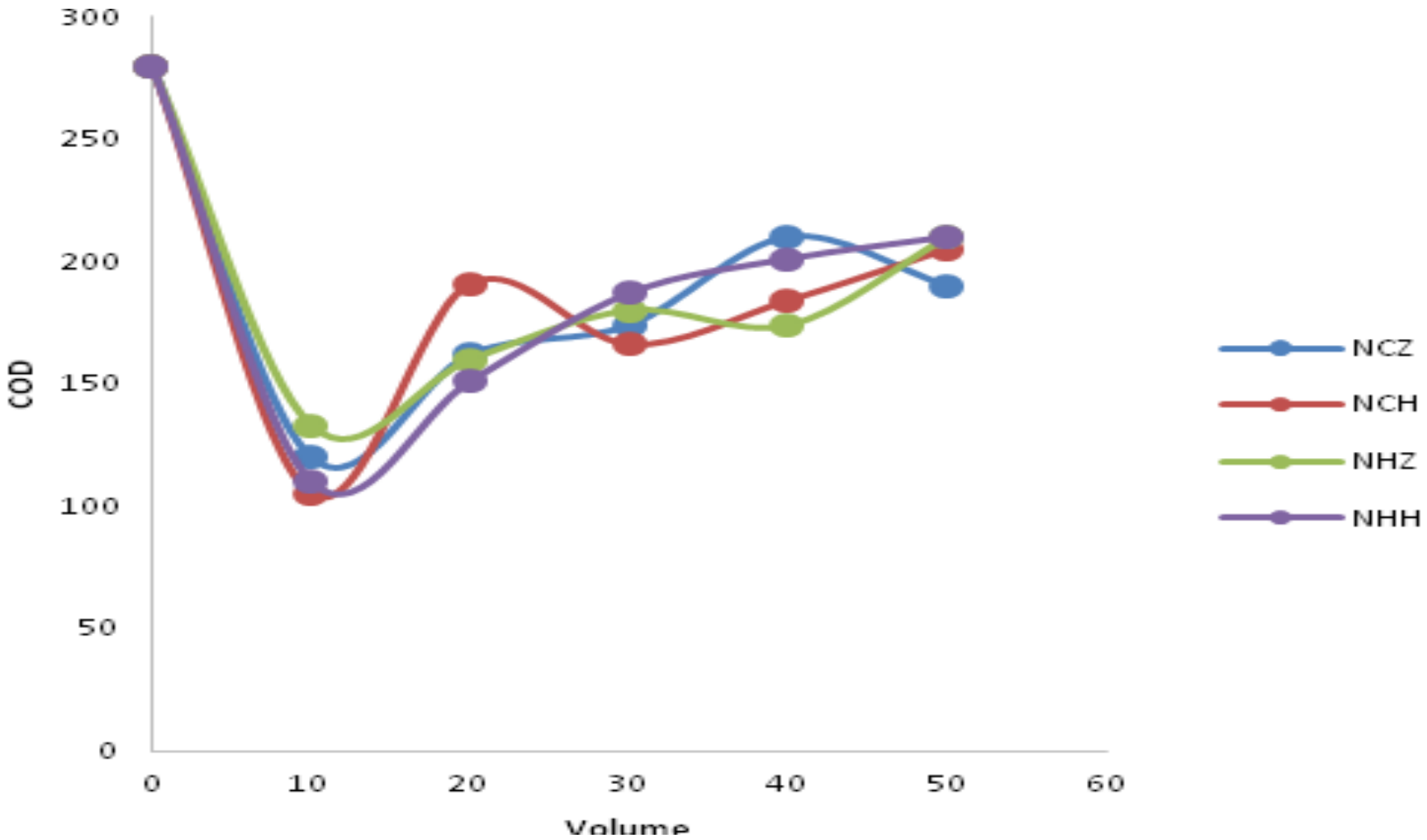


Figure 4. 66: Effect of initial volume of wastewater on COD of treated water

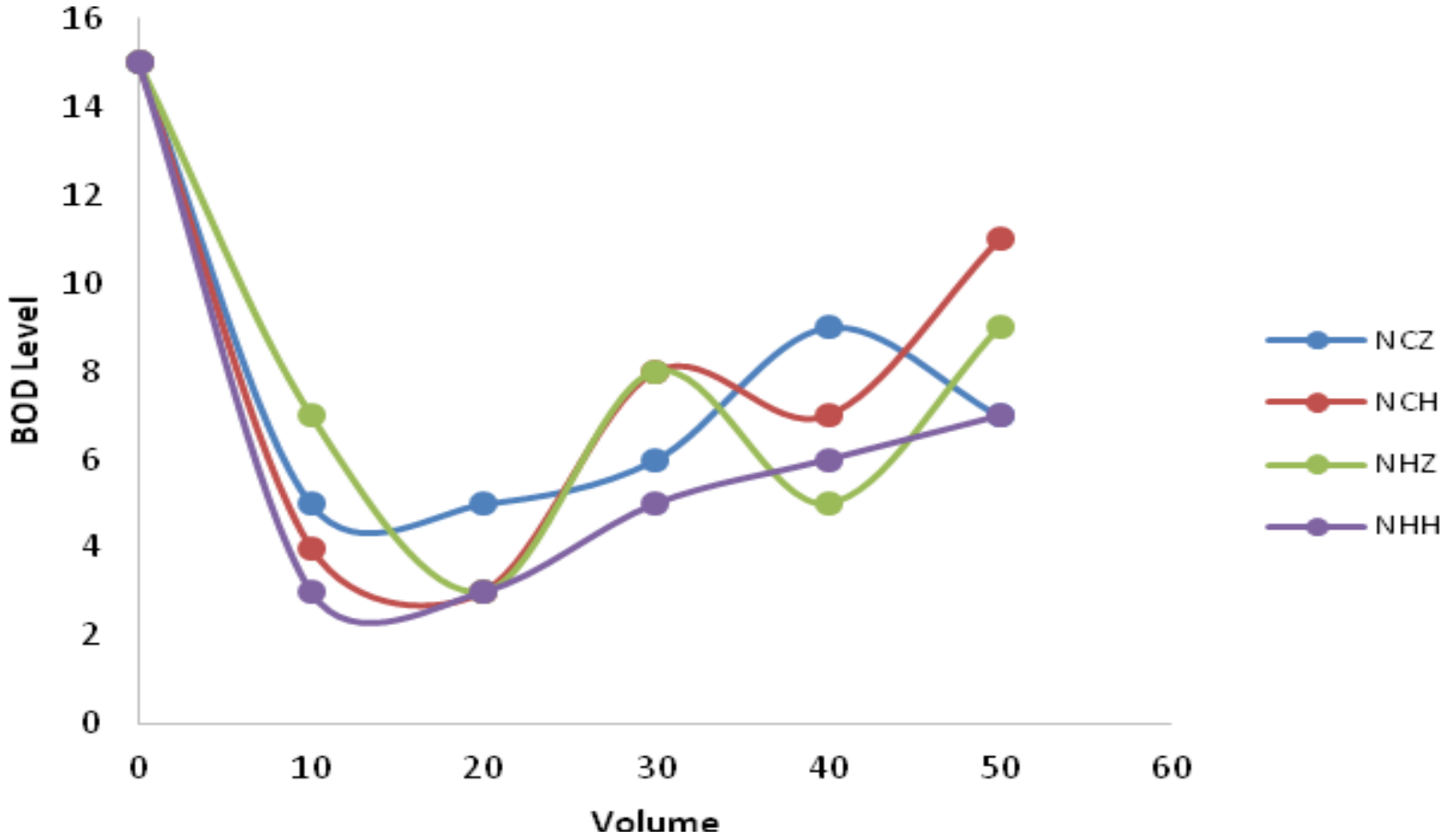


Figure 4. 67: Effect of initial volume on BOD level of treated wastewater

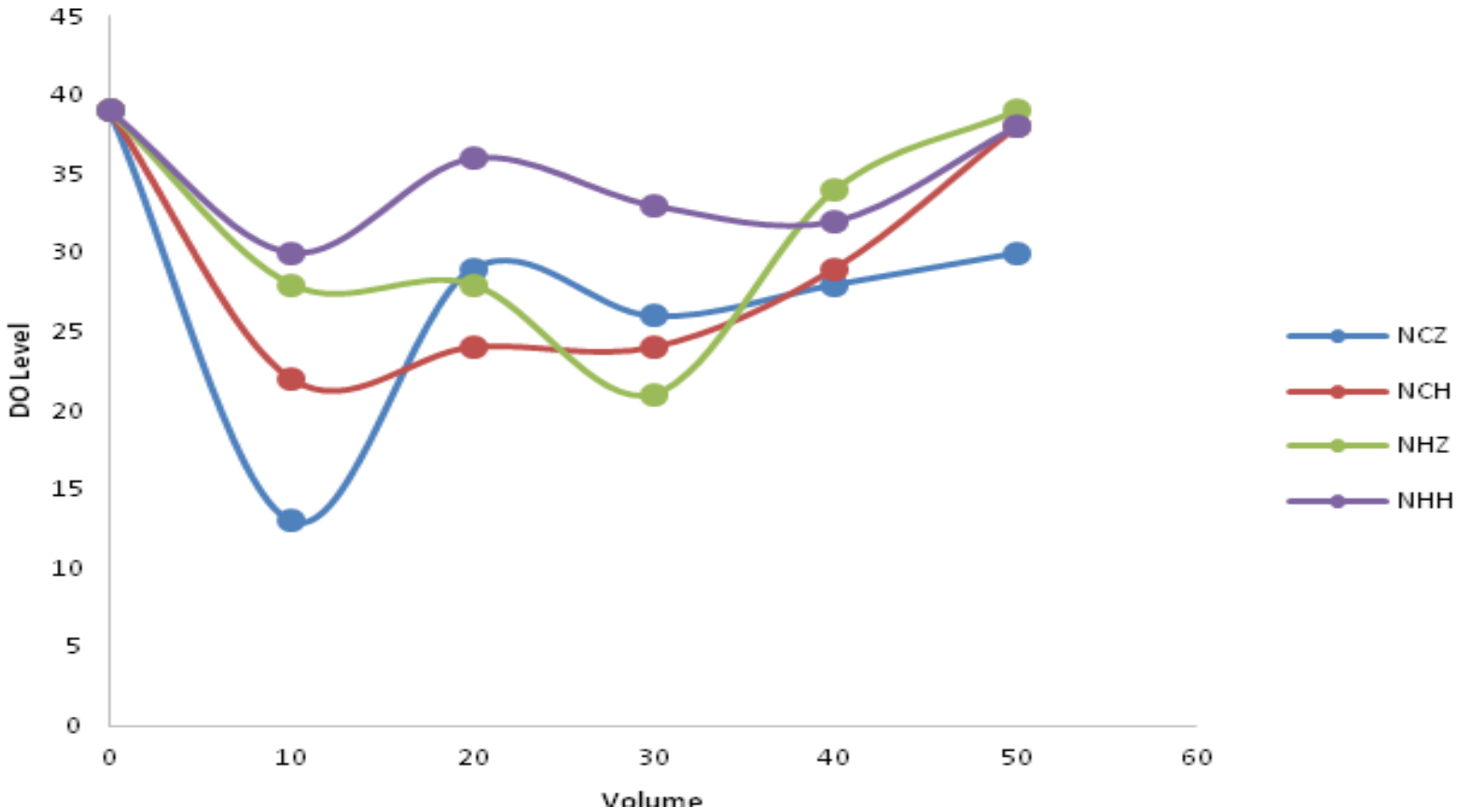


Figure 4. 68: Effect of initial volume of wastewater on DO of treated water

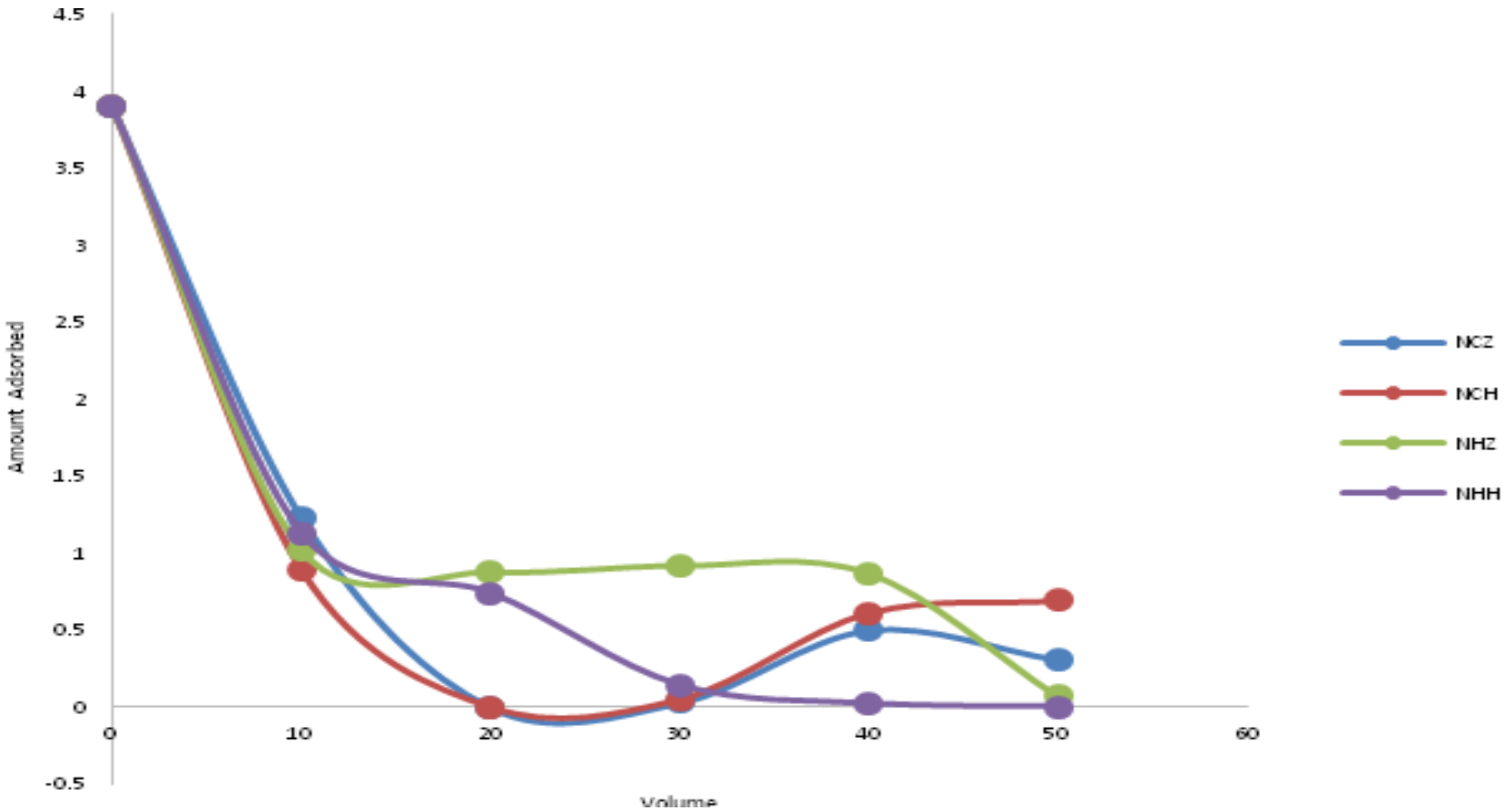


Figure 4. 69: Effect of initial volume of wastewater on chloride ion conc. of treated water

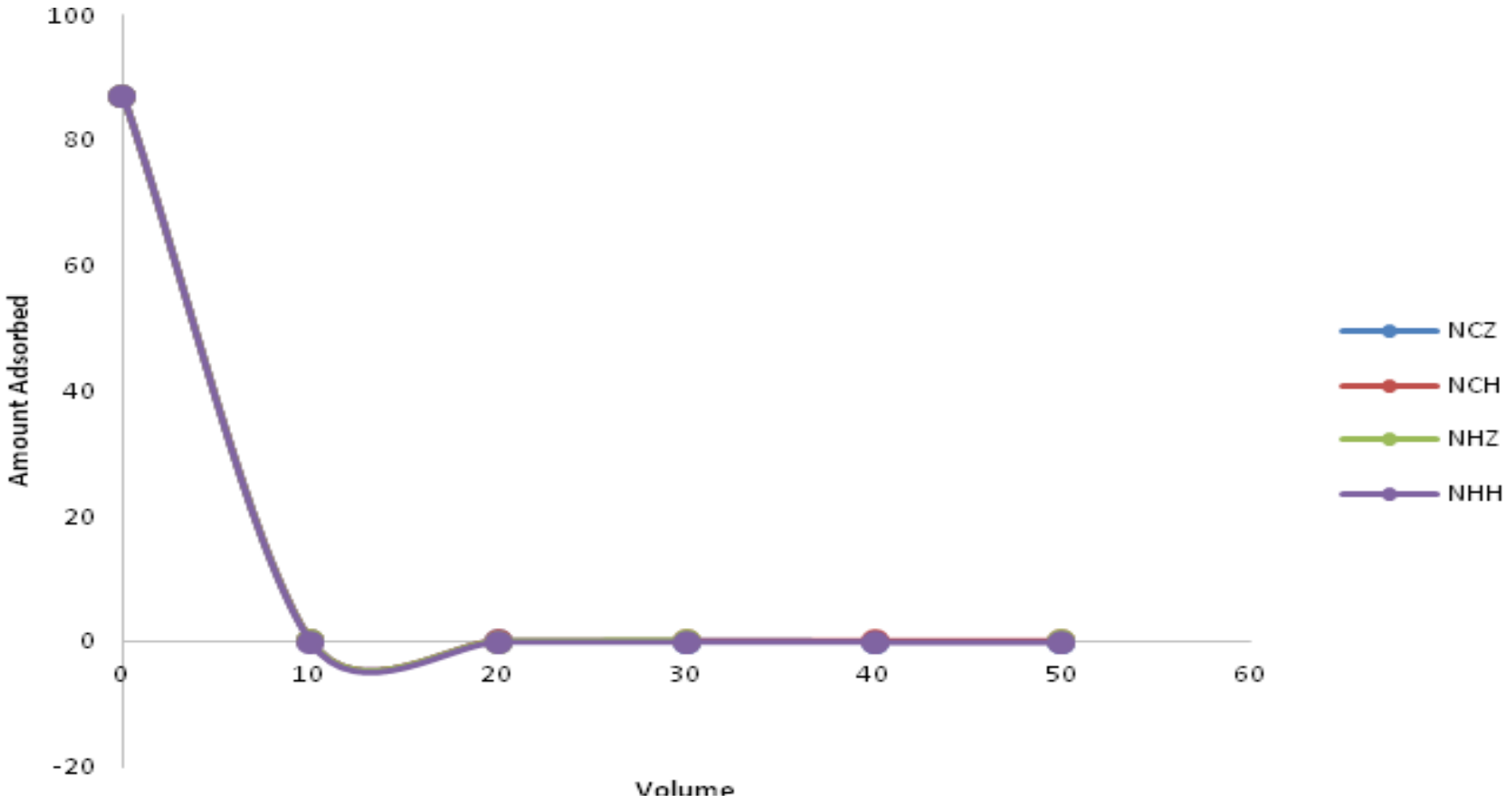


Figure 4. 70: Effect of initial volume of wastewater on nitrate ion conc. of treated water

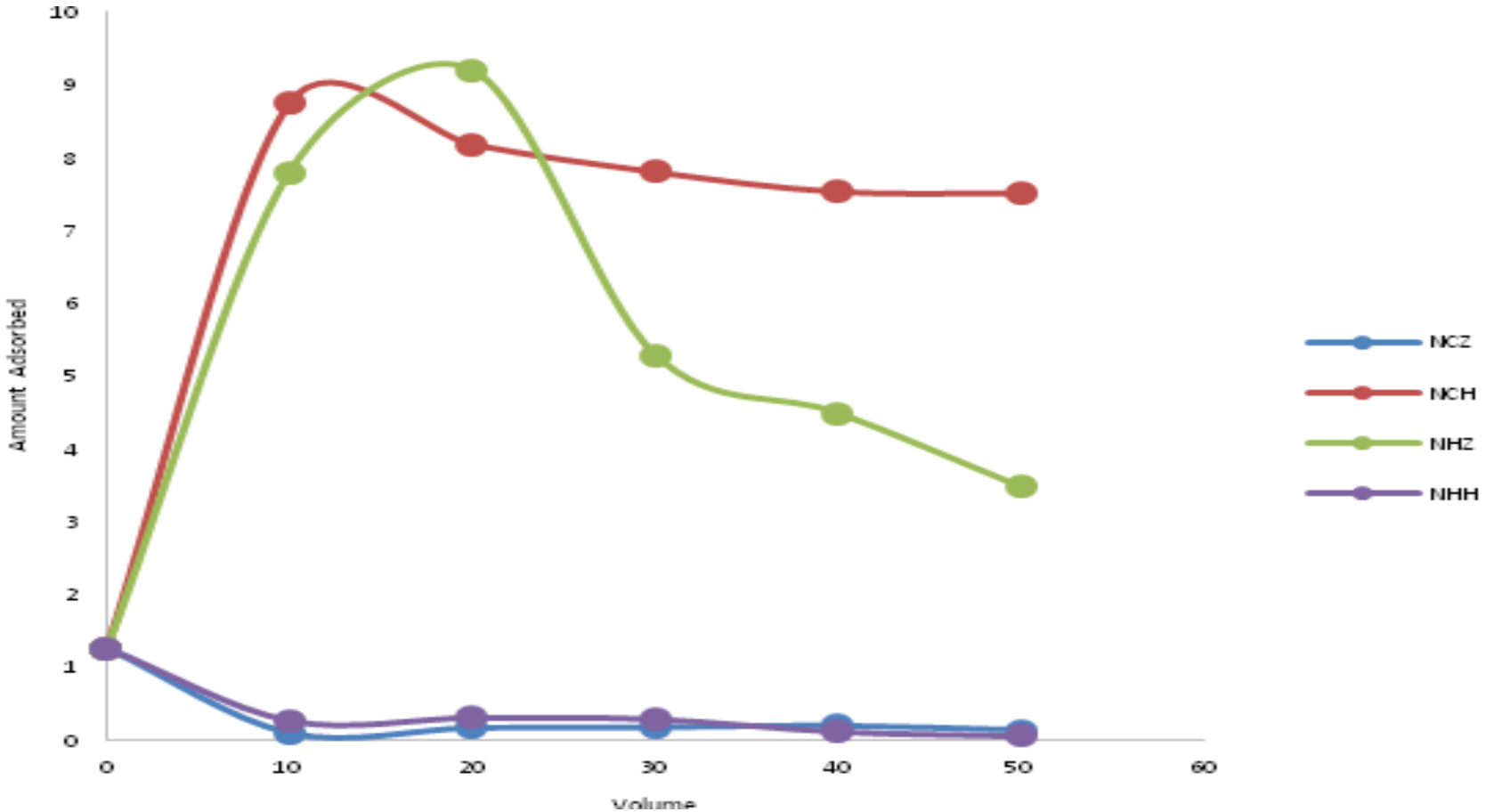


Figure 4. 71: Effect of initial volume of wastewater on phospate ion conc. of treated water

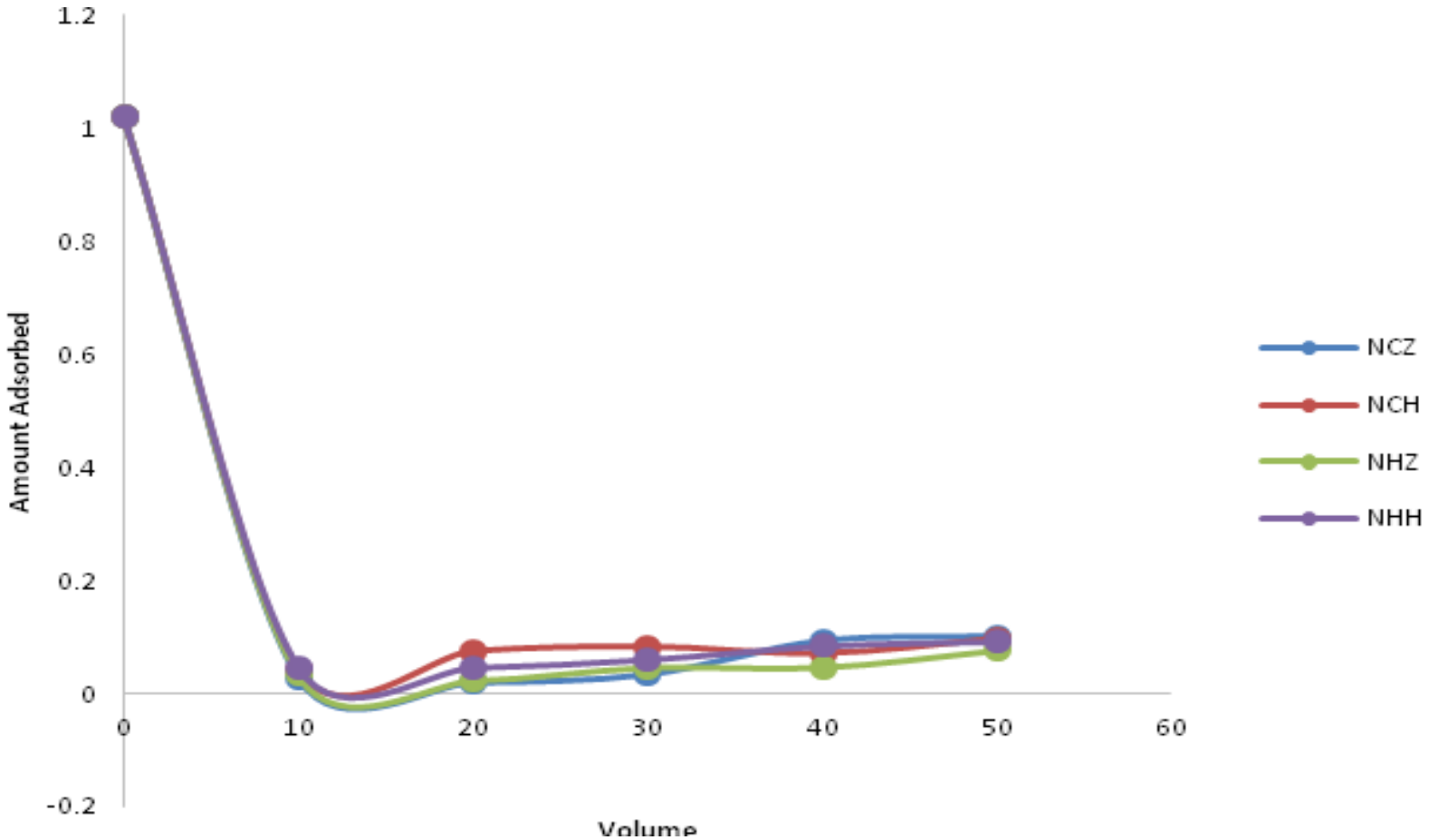


Figure 4. 72: Effect of initial volume of wastewater on cadmium ion conc. of treated water

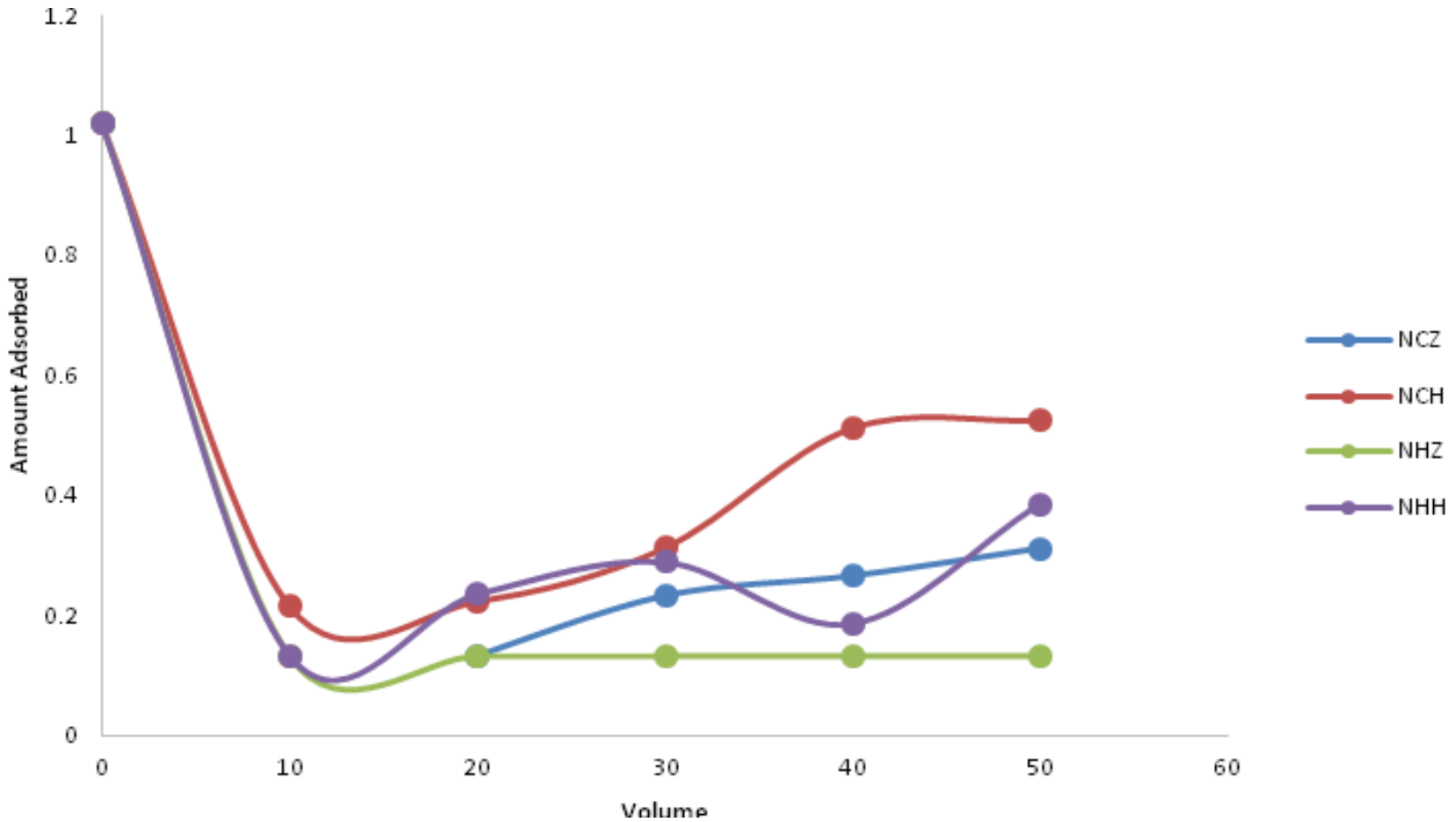


Figure 4. 73: Effect of initial volume of wastewater on chromium ion conc. of treated water

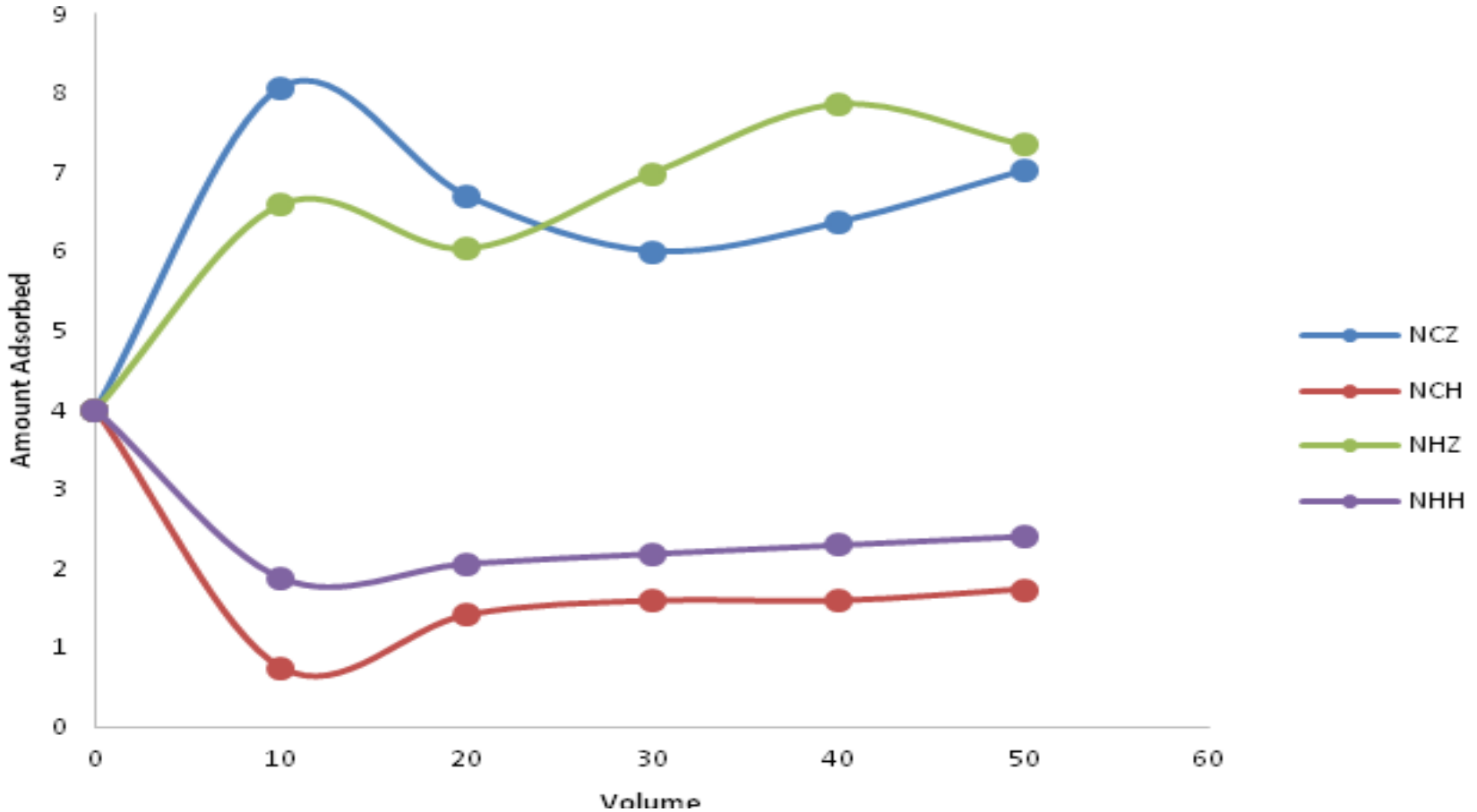


Figure 4. 74: Effect of initial volume of wastewater on zinc ion conc. of treated water

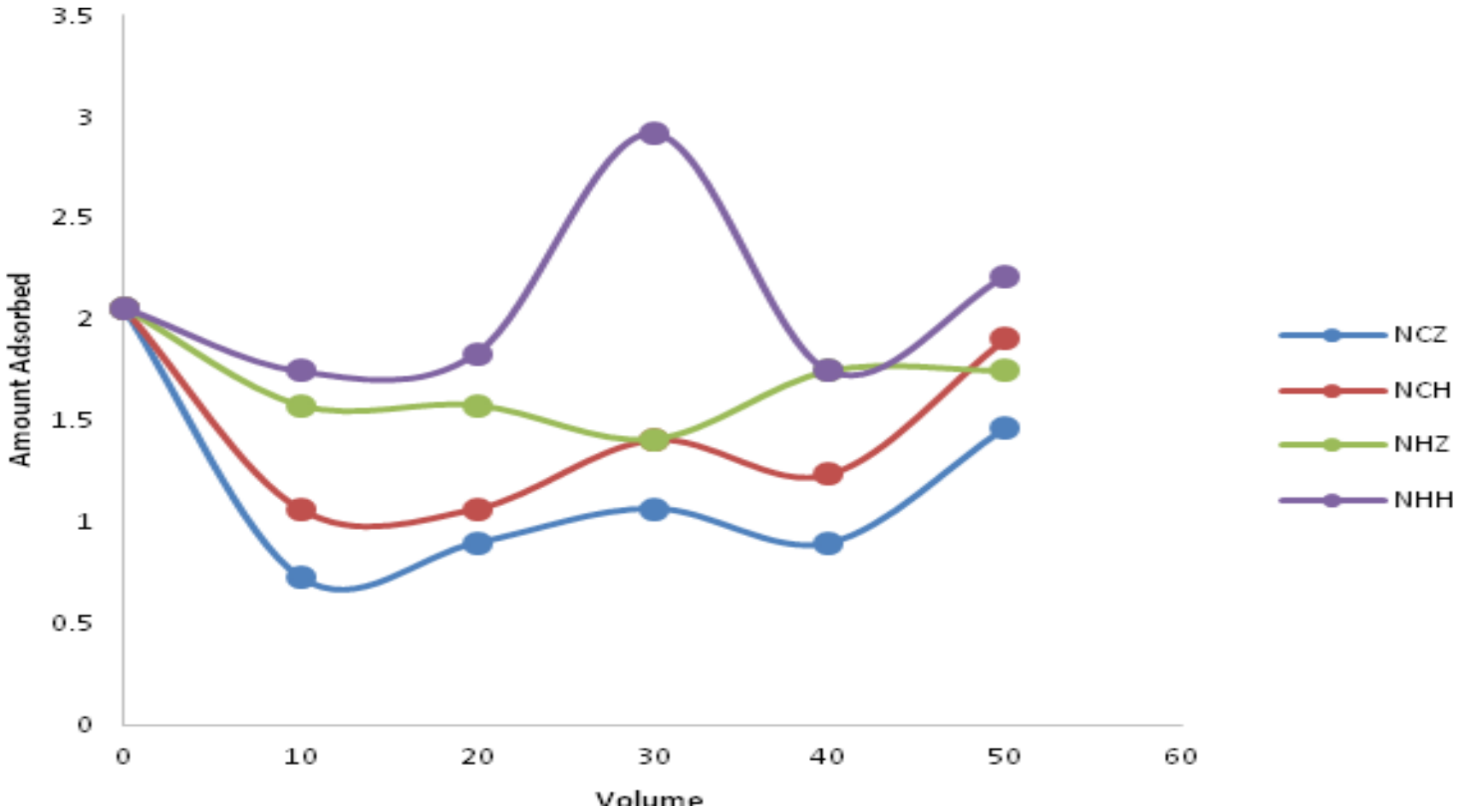


Figure 4. 75: Effect of initial volume of wastewater on nickel ion conc. of treated water

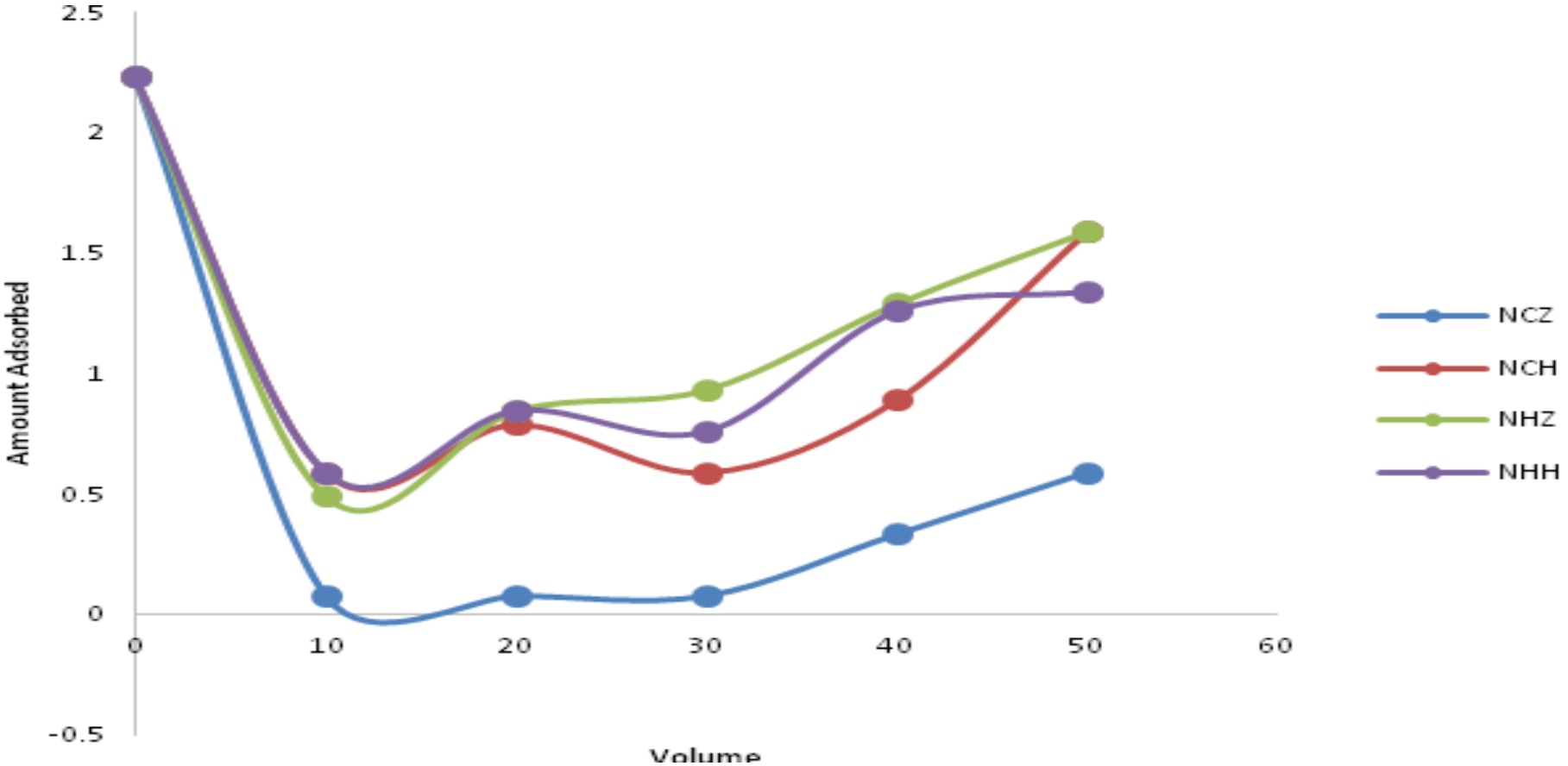


Figure 4. 76: Effect of initial volume of wastewater on lead ion conc. of treated water

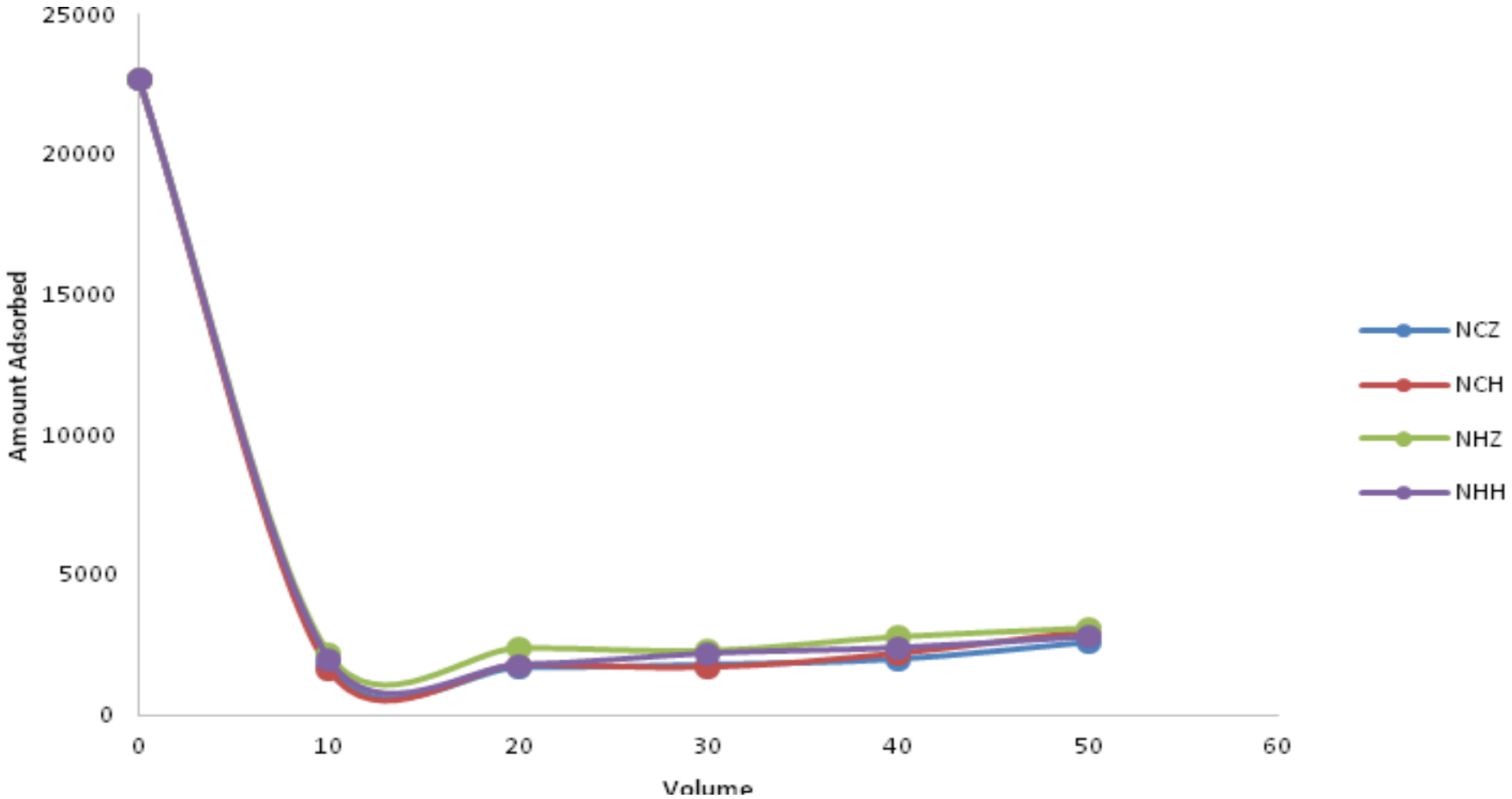


Figure 4. 77: Effect of initial volume of wastewater on bacterial load of treated water

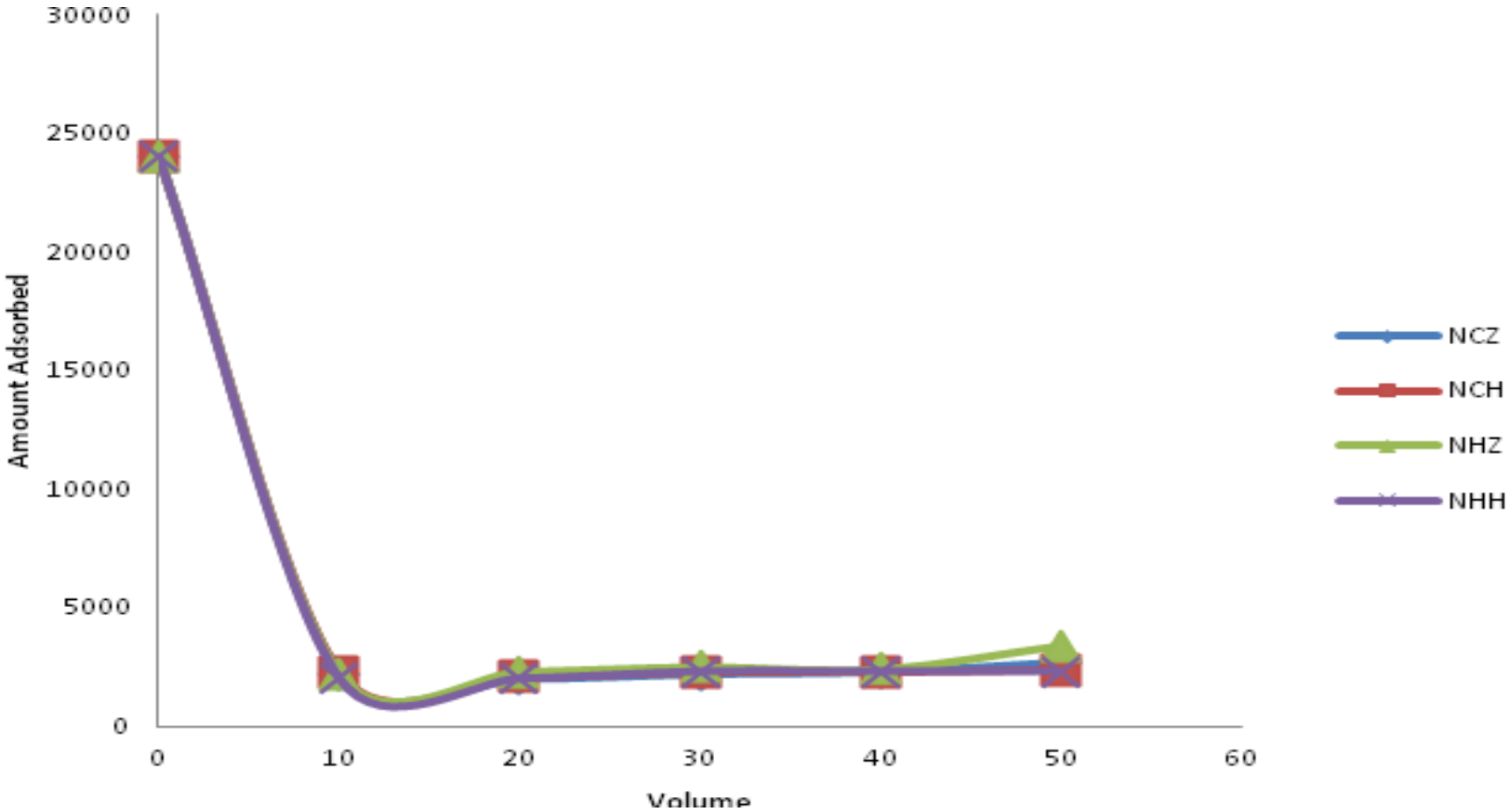


Figure 4. 78: Effect of initial volume of wastewater on fungal load of treated water

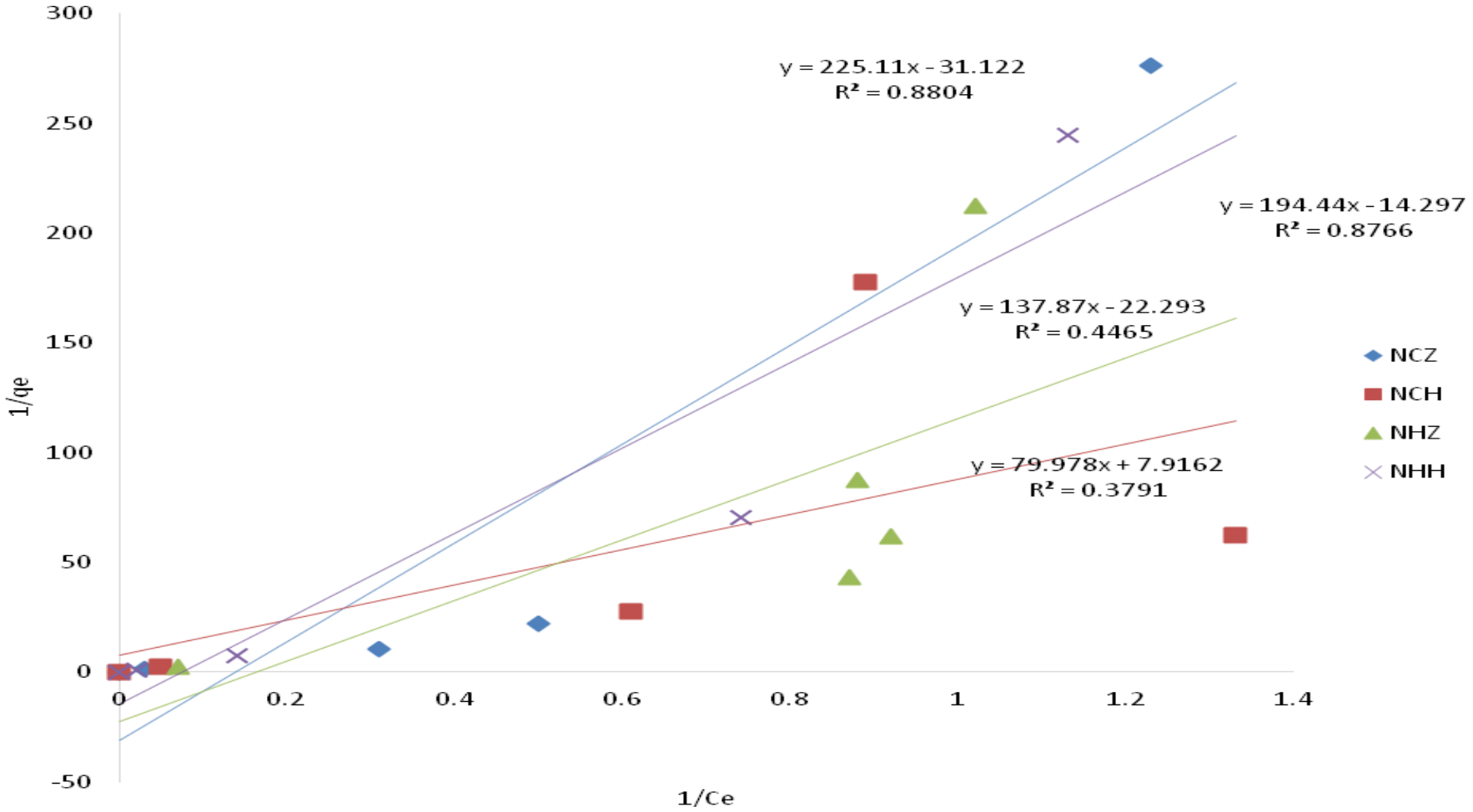


Figure 4. 79: Langmuir adsorption model for chloride ion

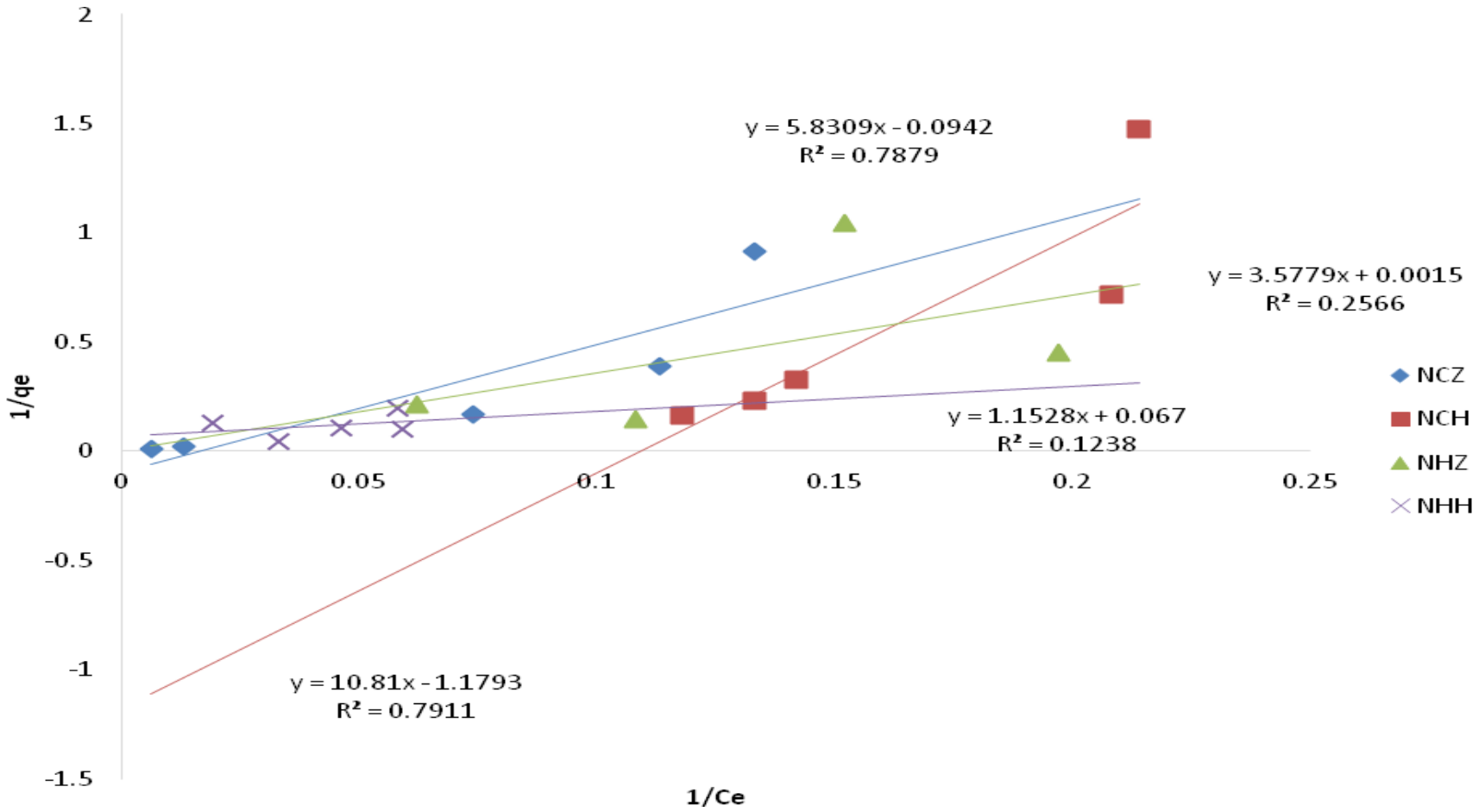


Figure 4. 80: Langmuir adsorption model for nitrate ion

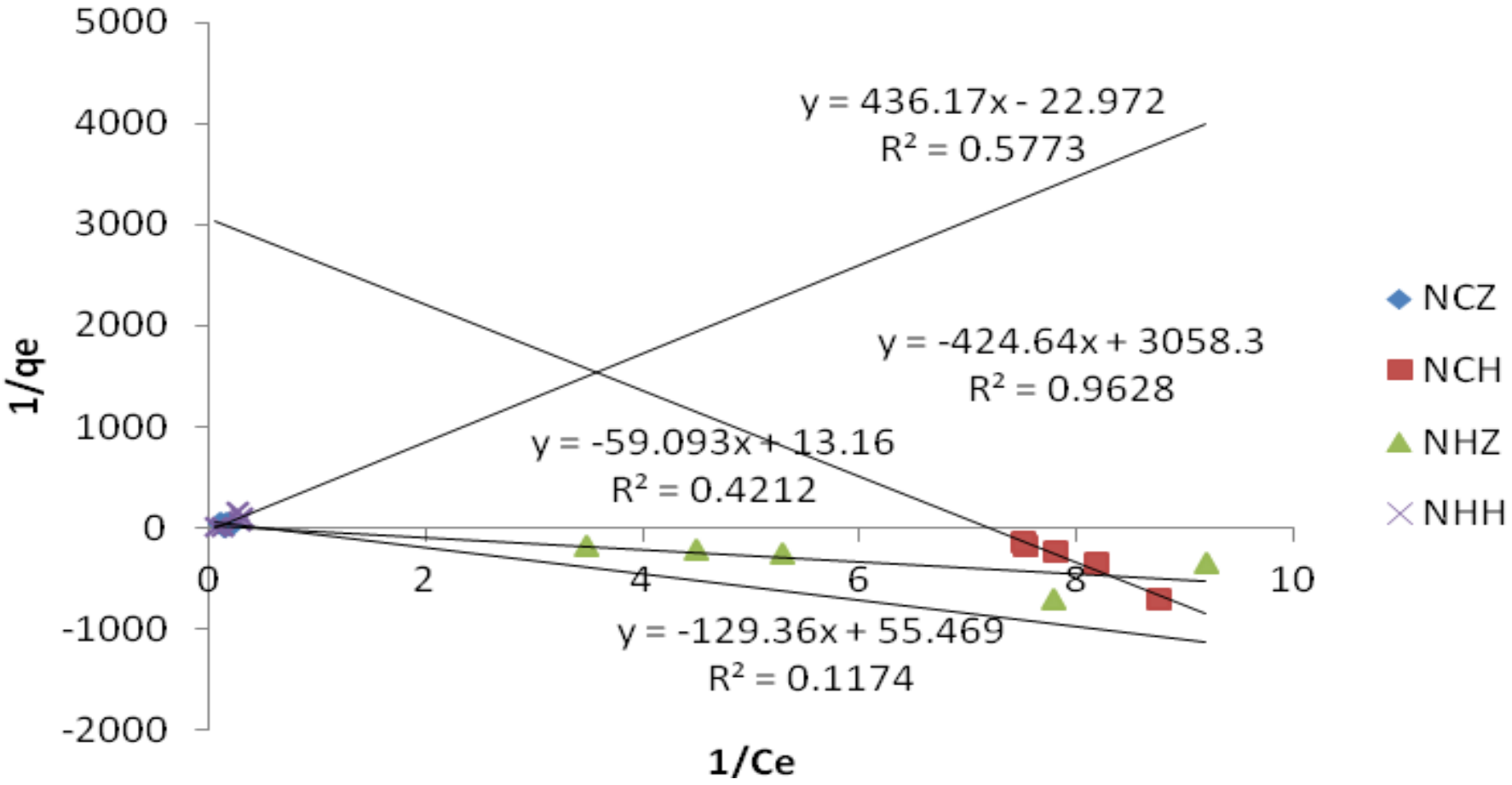


Figure 4. 81: Langmuir adsorption model for phosphate ion

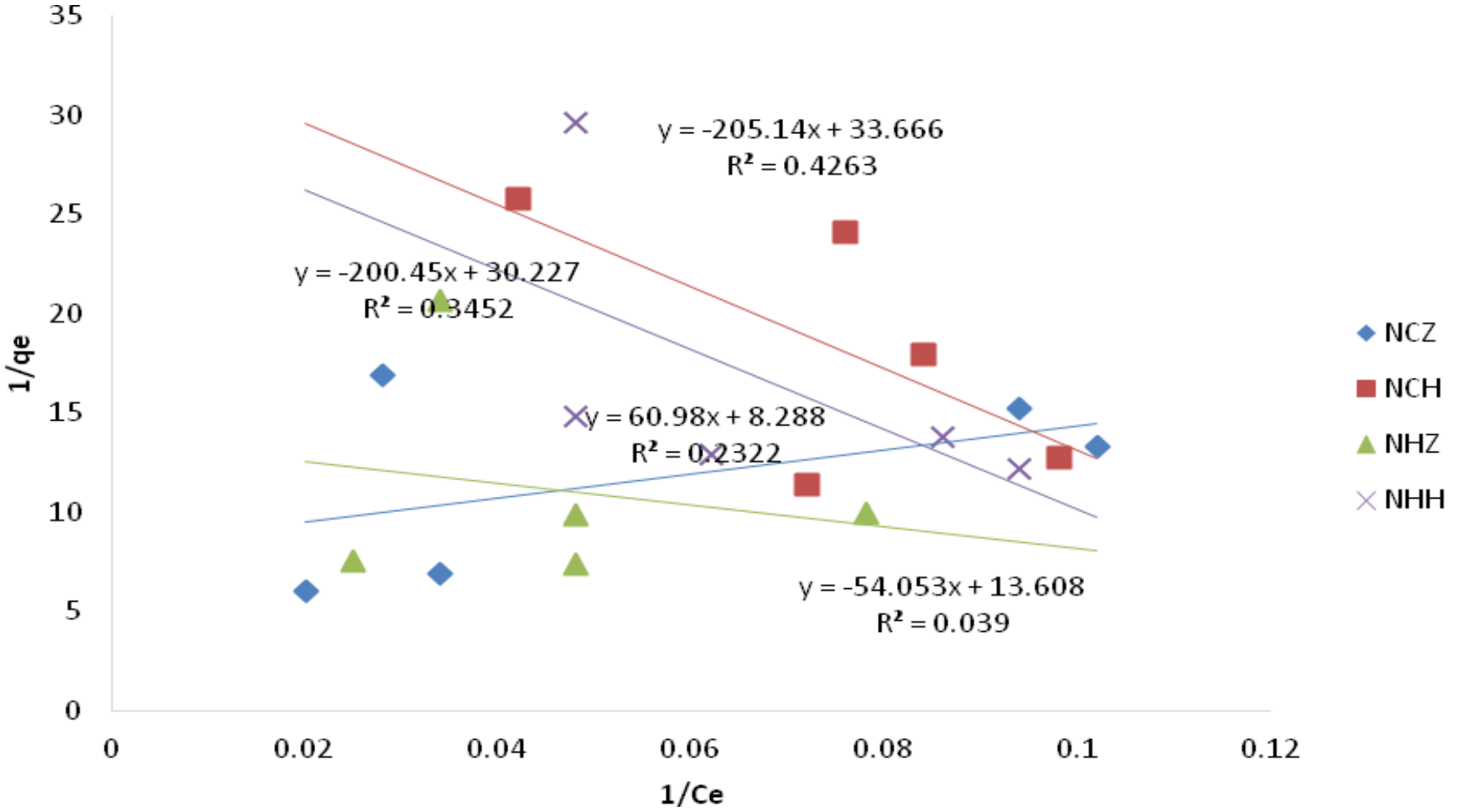


Figure 4. 82: Langmuir adsorption model for cadmium ion

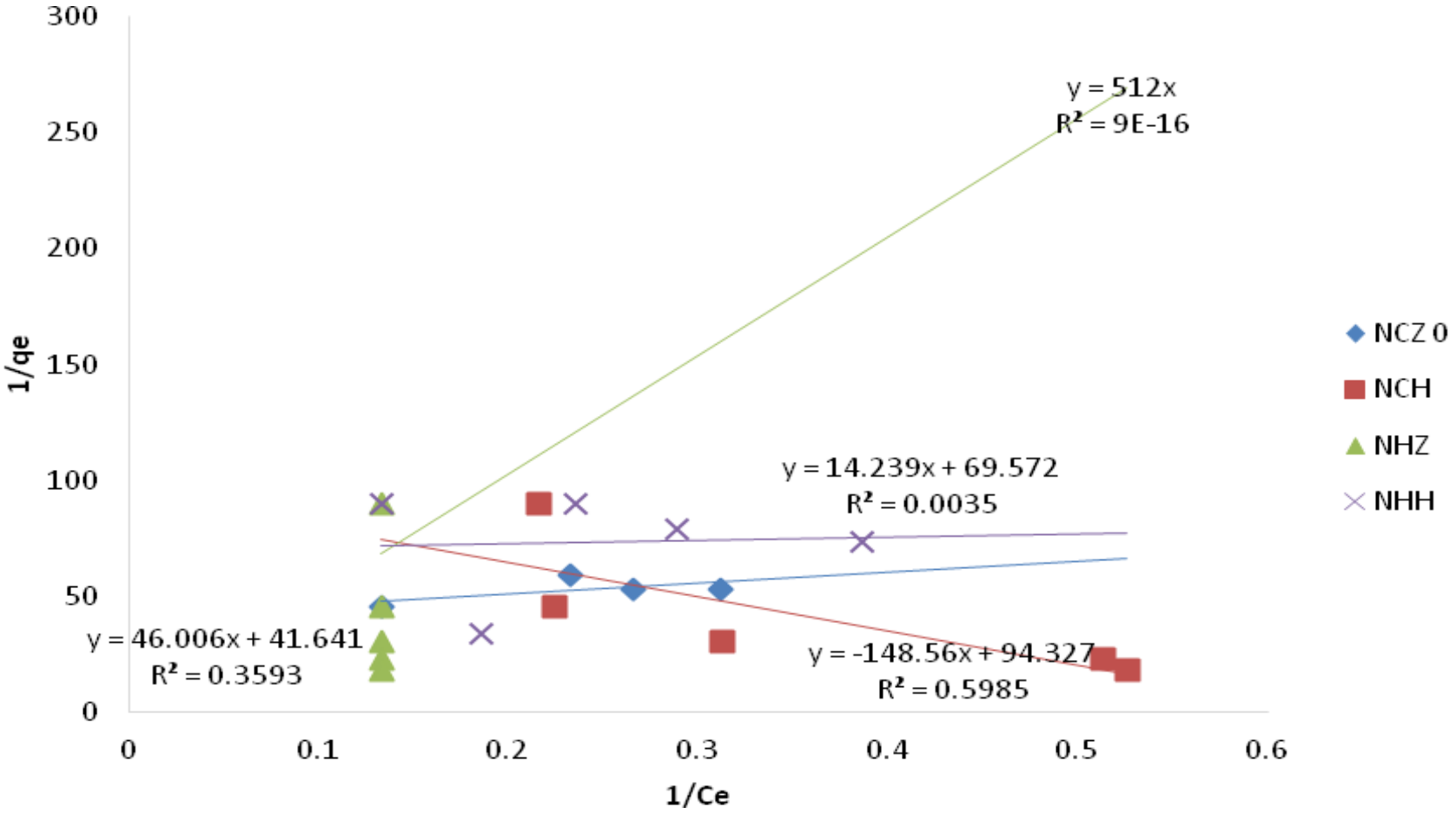


Figure 4. 83: Langmuir adsorption model for chromium ion

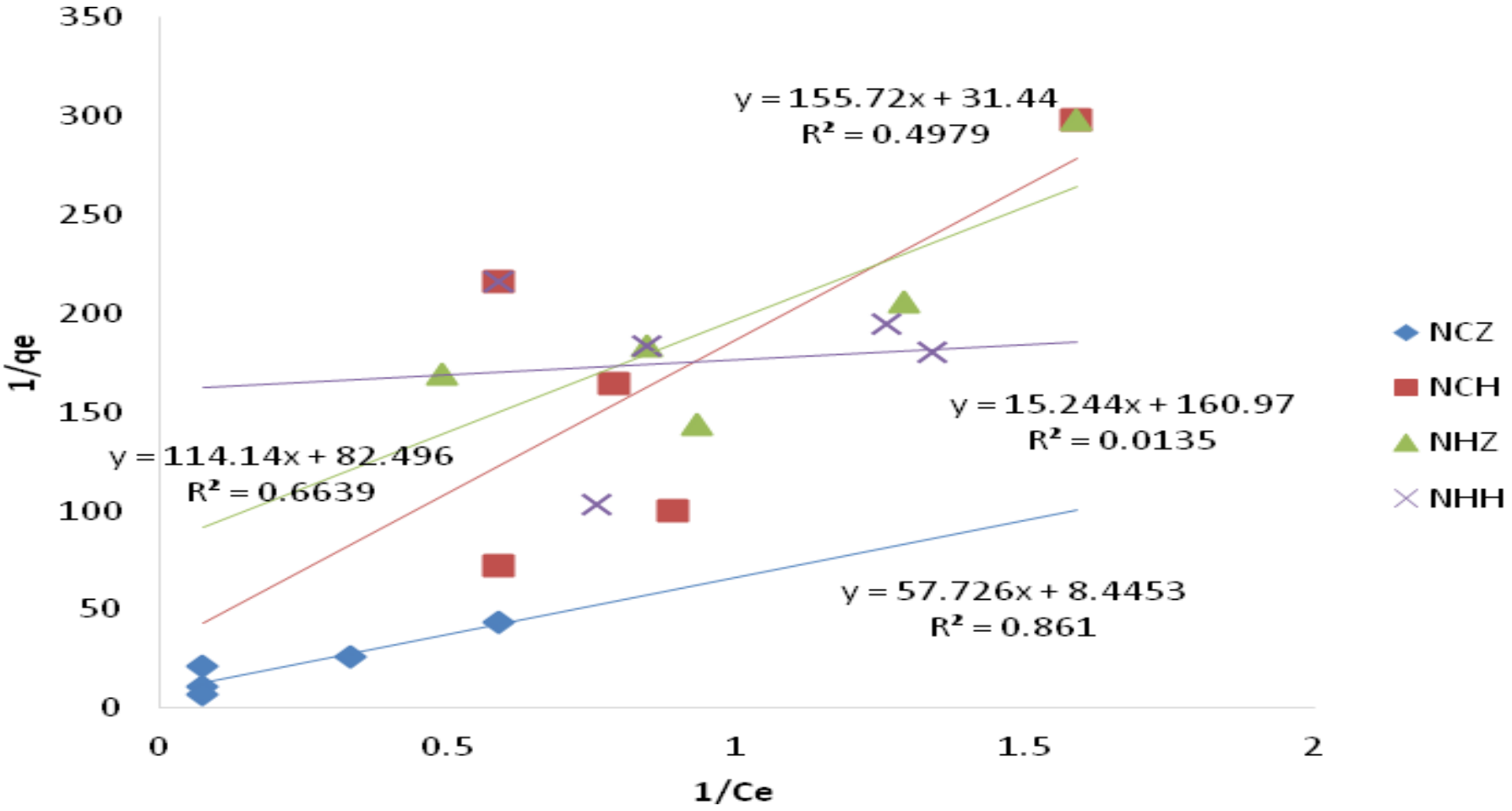


Figure 4. 84 : Langmuir adsorption model for lead ion

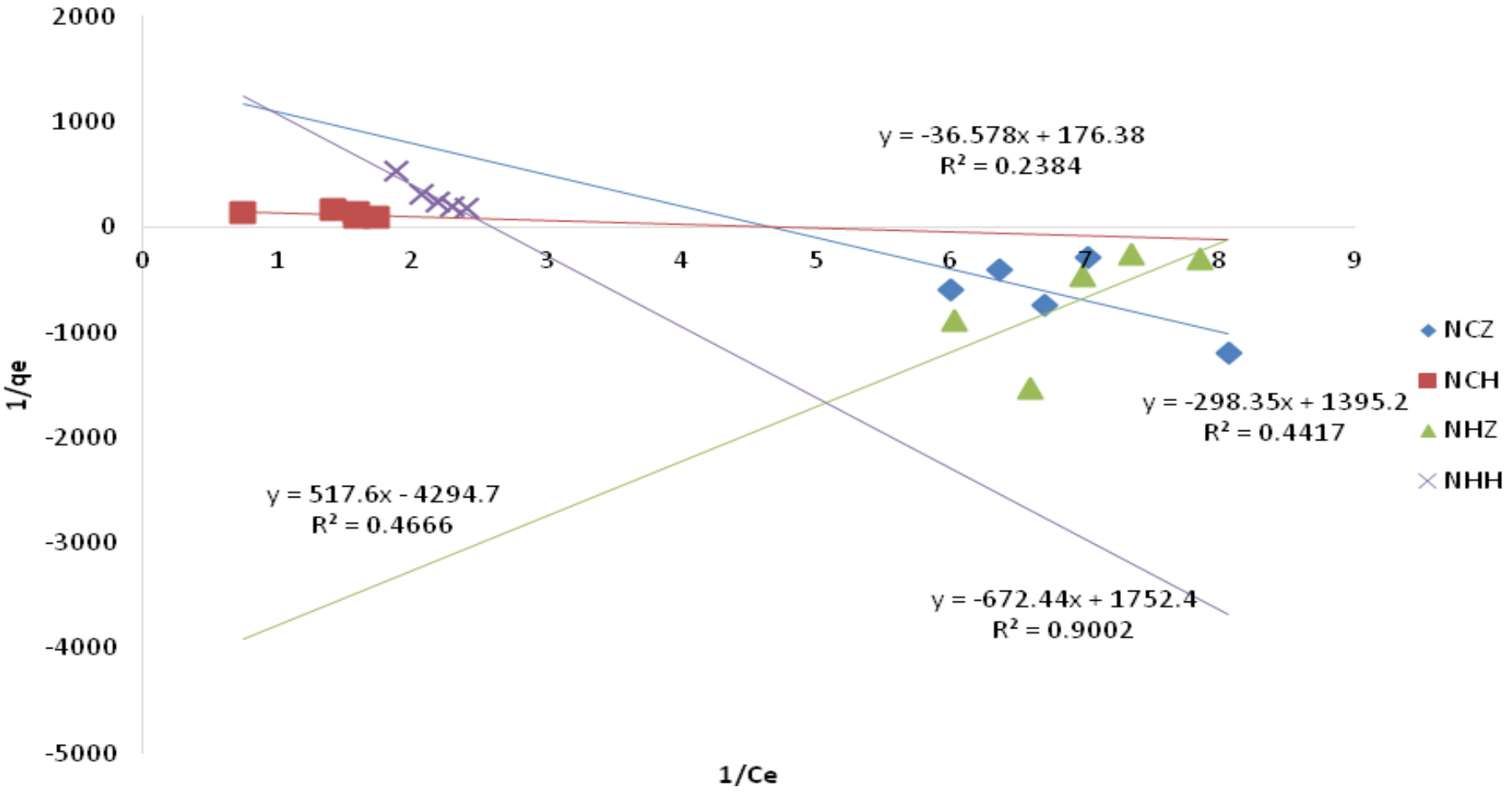


Figure 4. 85: Langmuir adsorption model for zinc ion

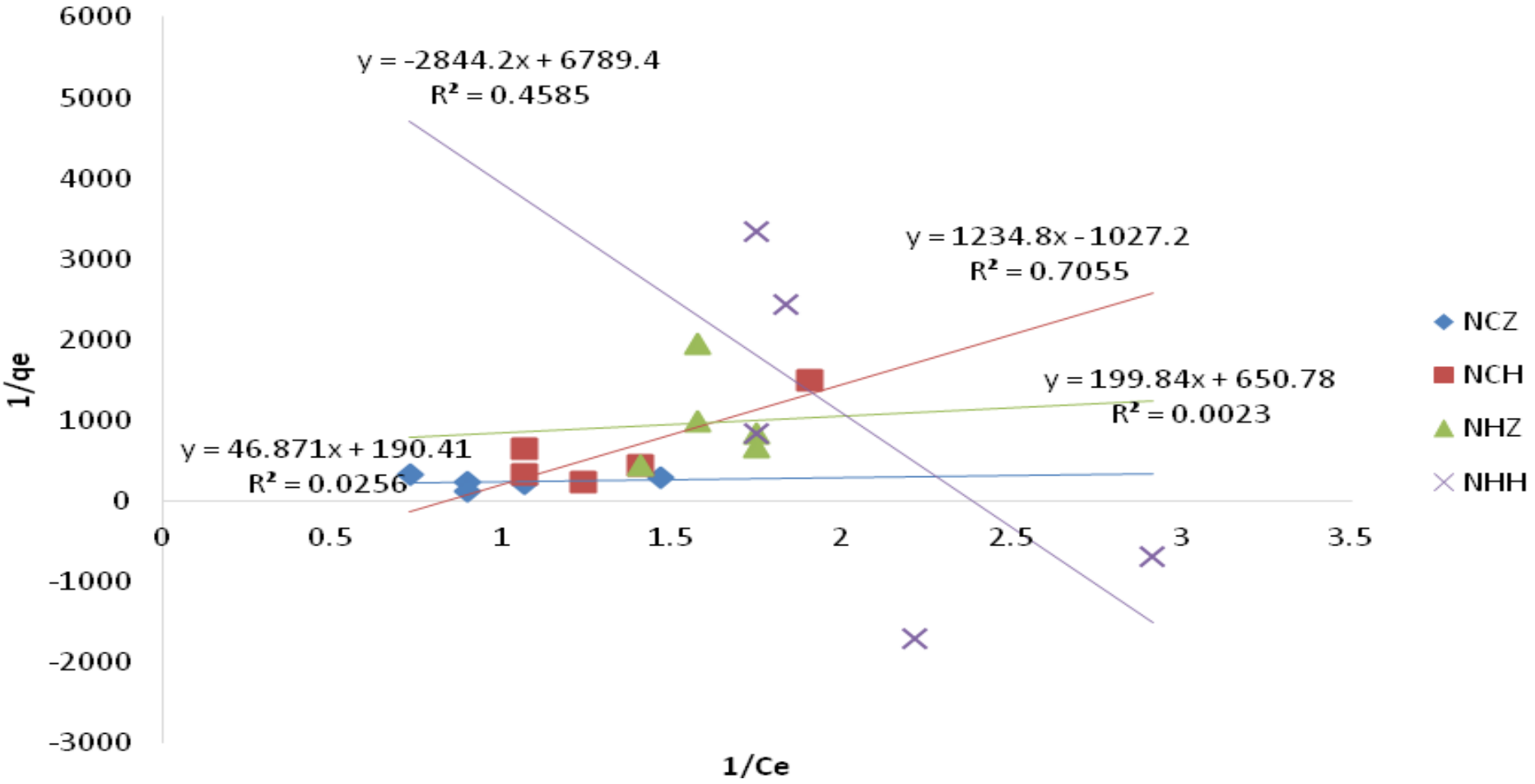


Figure 4. 86: Langmuir adsorption model for nickel ion

Table 4. 7 The Langmuir isotherm equation constants

	NCZ				**NCH**				**NHZ**				**NHH**			
	Q_{max}	*B*	*RL*	R^2	Q_{max}	*b*	*RL*	R^2	Q_{max}	*b*	*RL*	R^2	Q_{max}	*b*	*RL*	R^2
Nitrite	0.17	61.90	0.00	0.79	0.09	-9.17	0.00	0.79	0.28	1.00	0.01	0.26	0.87	17.21	0.00	0.01
Phosphate	-0.01	-2.33	-0.52	0.12	0.00	0.14	0.85	0.96	-0.02	-4.49	-0.21	0.42	0.00	18.99	0.04	0.58
Chlorine	0.00	-7.23	1.77	0.88	0.01	-10.10	2.54	0.38	0.01	6.18	0.73	0.45	0.01	13.60	0.55	0.88
Cd	0.02	7.36	0.53	0.23	0.00	-6.09	3.90	0.43	-0.02	-3.97	1.94	0.04	0.00	-6.63	5.24	0.35
Cr	0.02	1.10	0.55	0.36	-0.01	-1.57	-6.48	0.60	0.00	0.00	1.00	0.00	0.07	0.20	0.87	0.00
Zn	0.00	-0.21	10.69	0.44	-0.03	-0.21	8.27	0.24	0.00	-0.12	2.04	0.47	0.00	0.38	0.38	0.90
Ni	0.02	0.25	0.52	0.03	0.00	-1.20	-0.28	0.71	0.01	0.31	0.46	0.00	0.00	-0.42	-1.69	0.46
Pb	0.02	6.84	0.07	0.86	0.01	4.95	0.09	0.50	0.01	1.38	0.27	0.33	0.02	6.84	0.07	0.86

4.12 Freundlich Adsorption Isotherm

The linearize plot of the Freundlich Isotherm models for the treated wastewater on the prepared neem activated carbons are presented in Figures 4.87 to 4.94. The R^2 values for the different parameters studied were used to measure the extent of fitness of the parameter to the model. The values from the slope and intercept were used to calculate the Freundlich parameters presented in Table 4.8. The Freundlich parameter n represents the sorption intensity, K_F is the Freundlich constant describing the sorption capacity while R^2 is the regression coefficient. Figure 4.87, 4.88 and 4.89 present the Freundlich Isotherm model for the adsorption of chloride, nitrate and phosphate ions respectively. Figures 4.90 to 4.94 show the Freundlich models for the adsorption of chromium, zinc, cadmium, lead and nickel.

4.13: Regeneration and Reuse Studies

The effects of regeneration and reuse of the neem carbon was carried out using NHH because of its low surface area relative to the other neem adsorbents. The efficiency of regenerating and reusing NHH on the investigated parameters is presented in Table 4.9.

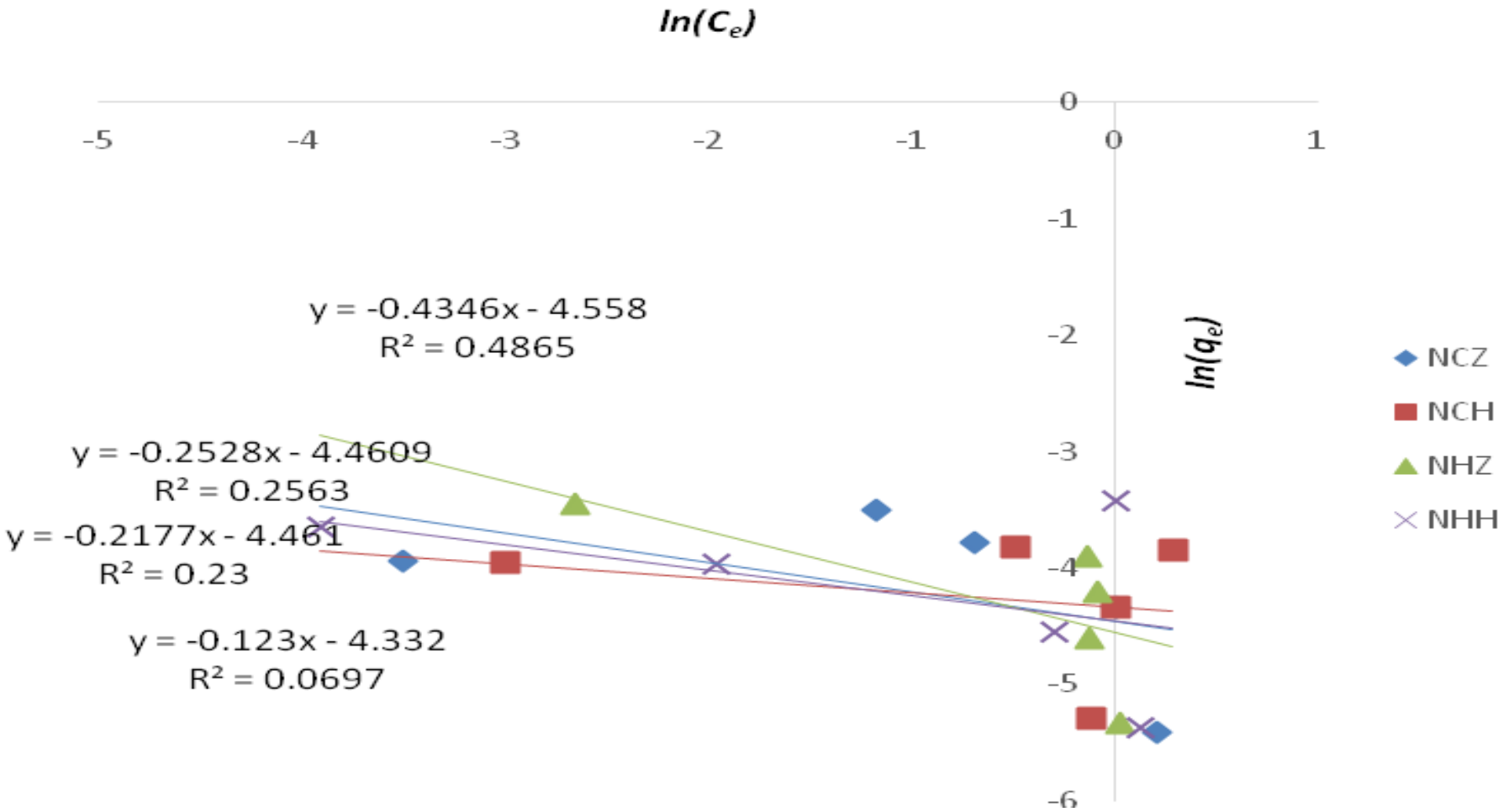


Figure 4. 87: Freundlich Isotherm models for chloride ion

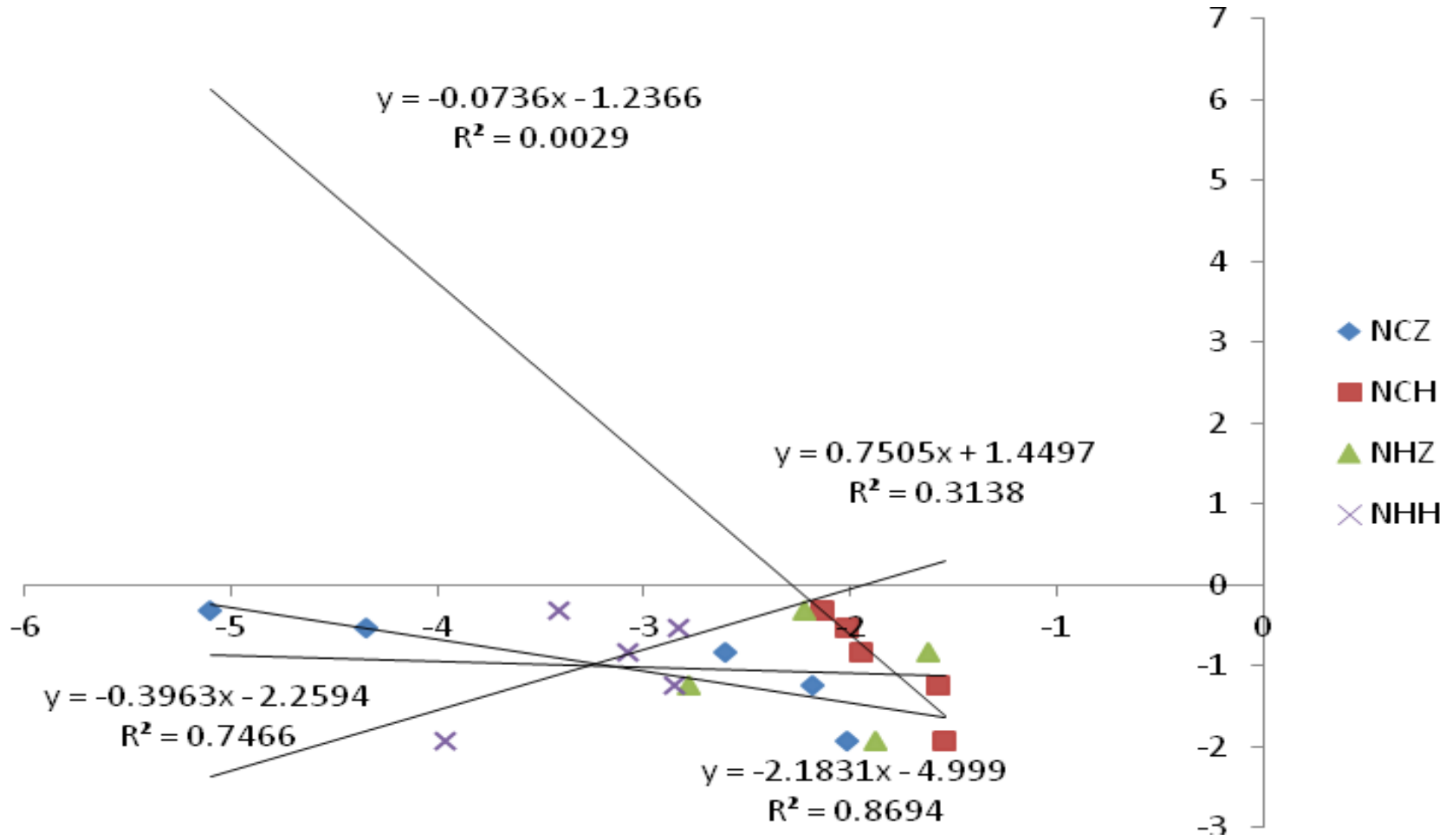


Figure 4. 88: Freundlich Isotherm models for nitrate ion

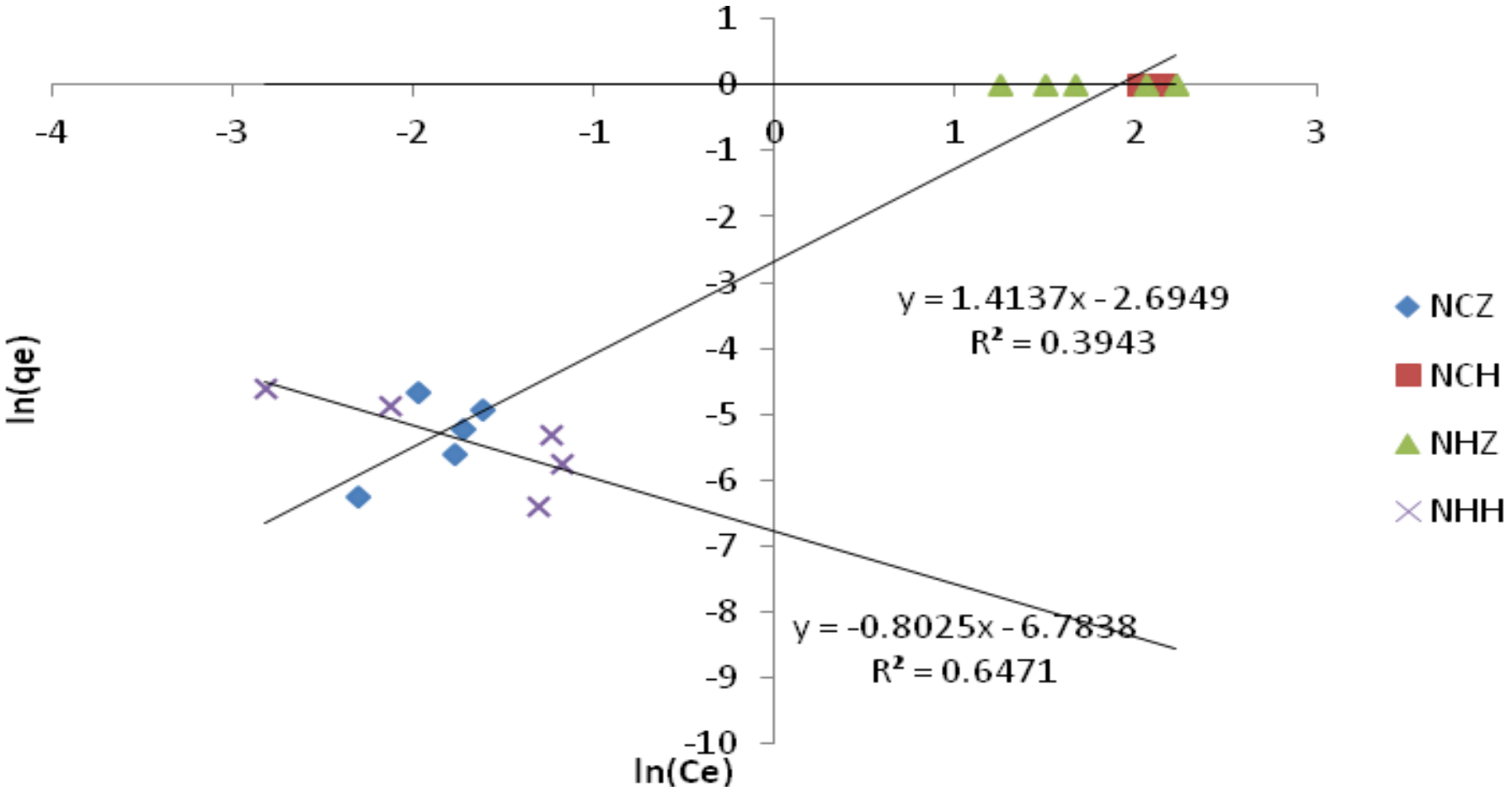


Figure 4. 89: Freundlich Isotherm models for phosphate ion

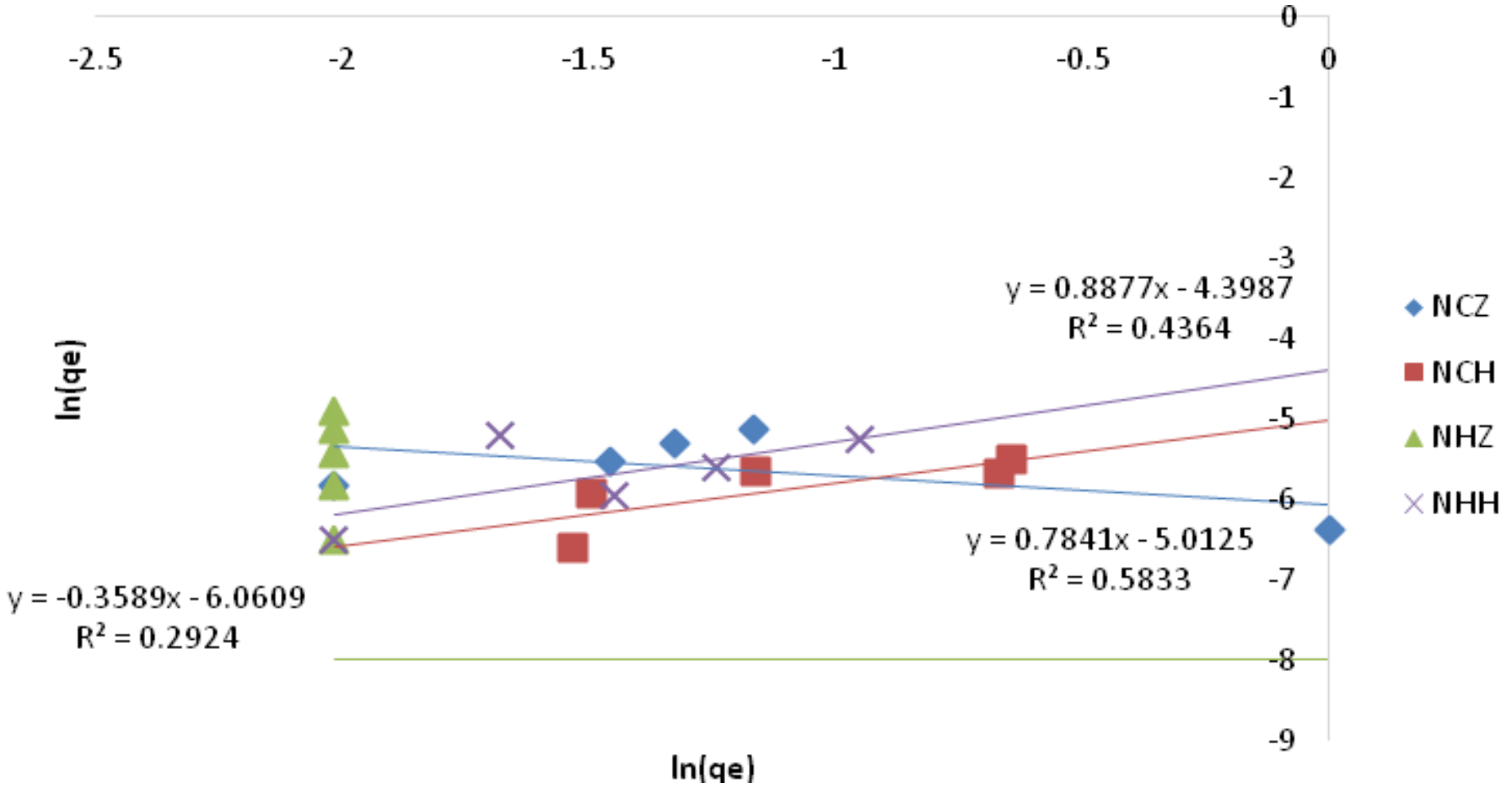


Figure 4. 90: Freundlich Isotherm models for chromium ion

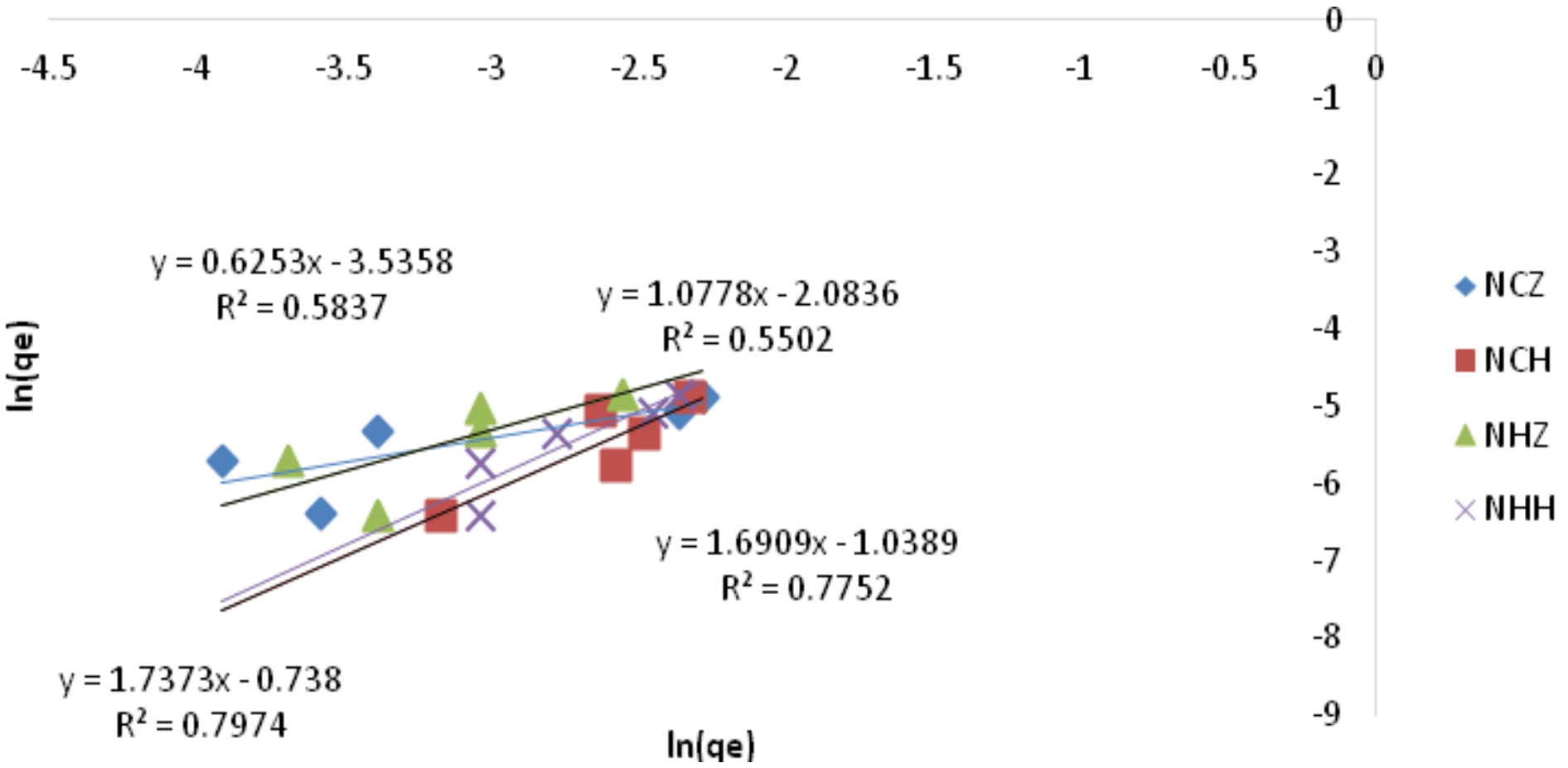


Figure 4. 91: Freundlich Isotherm models for zinc ion

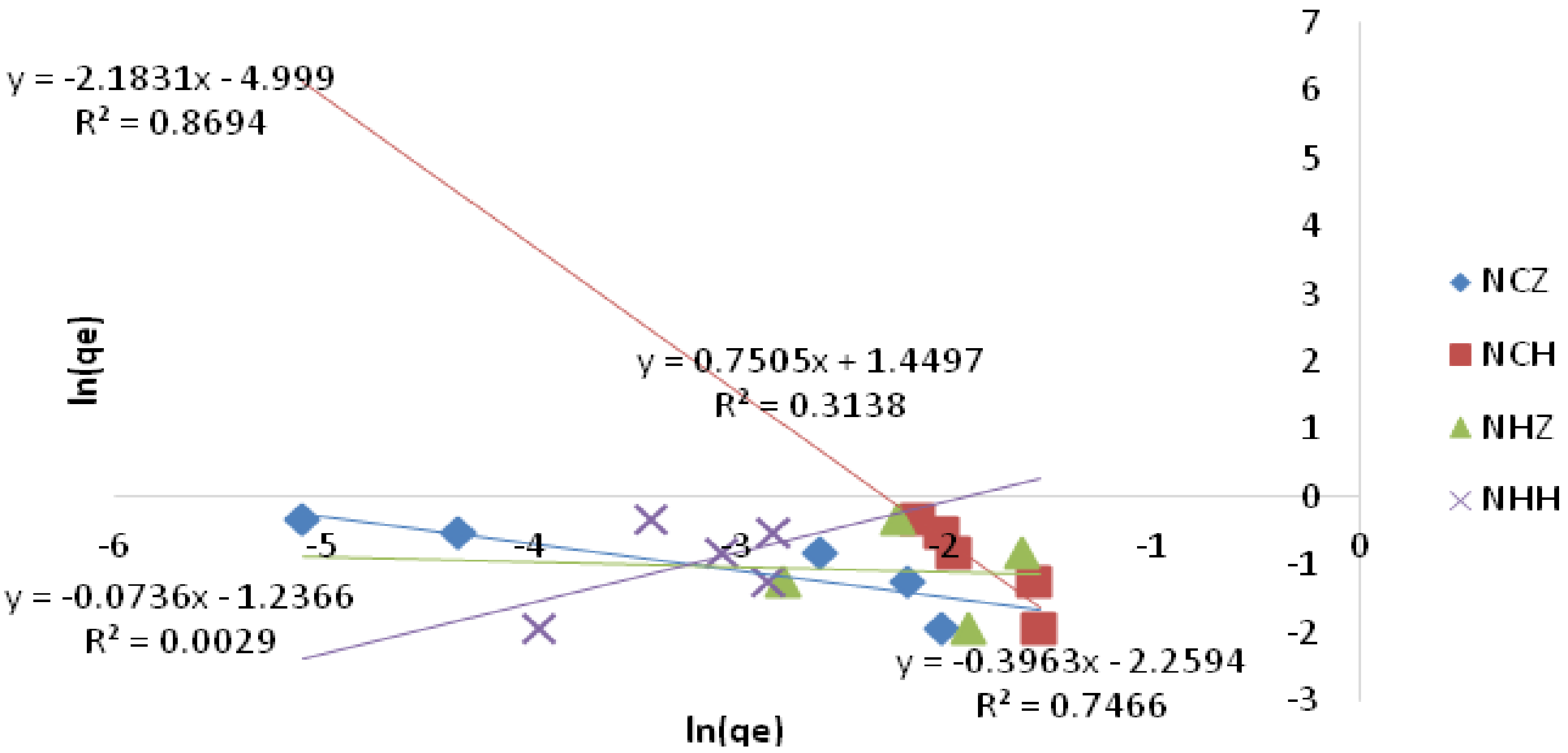


Figure 4. 92: Freundlich Isotherm models for cadmium ion

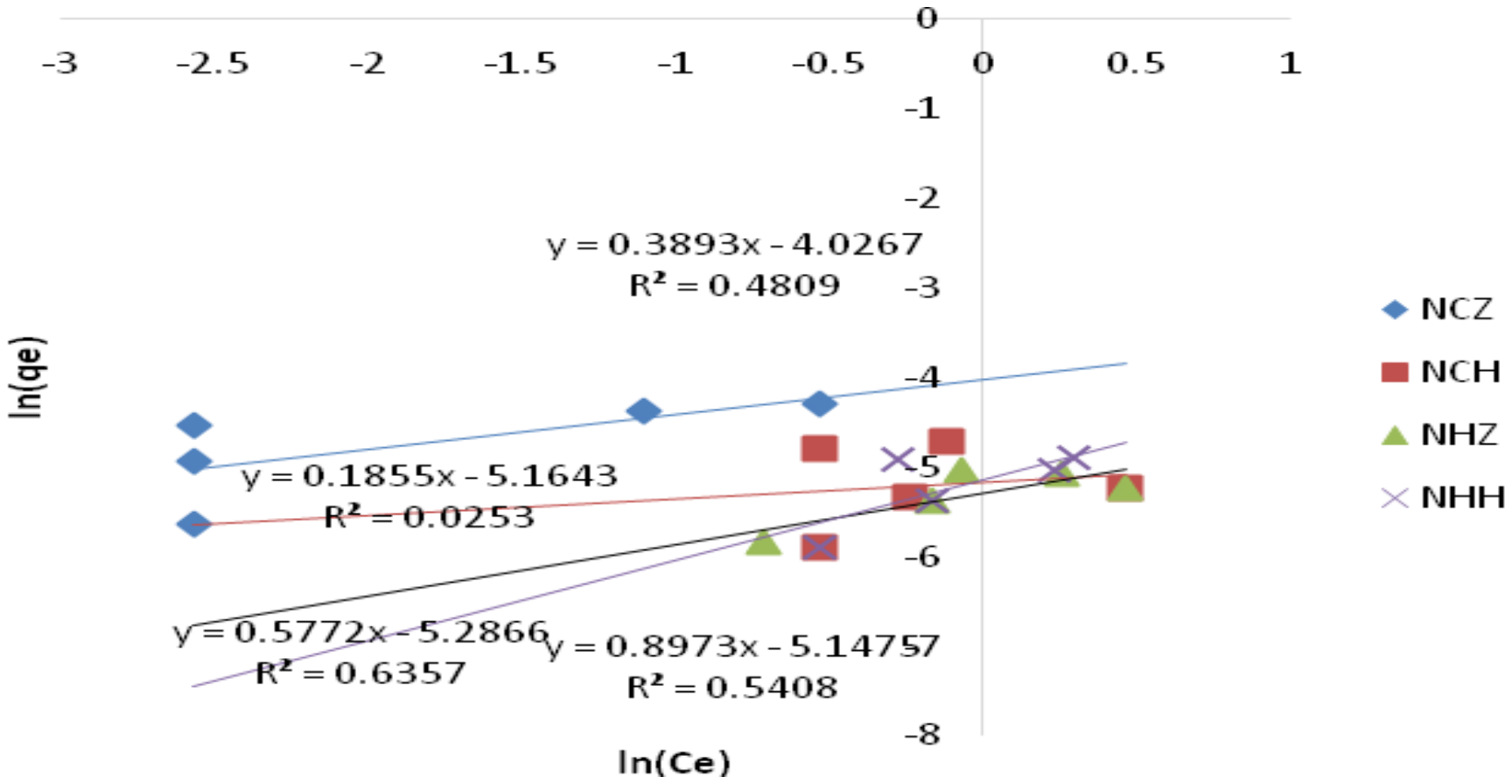


Figure 4. 93: Freundlich Isotherm models for lead ion

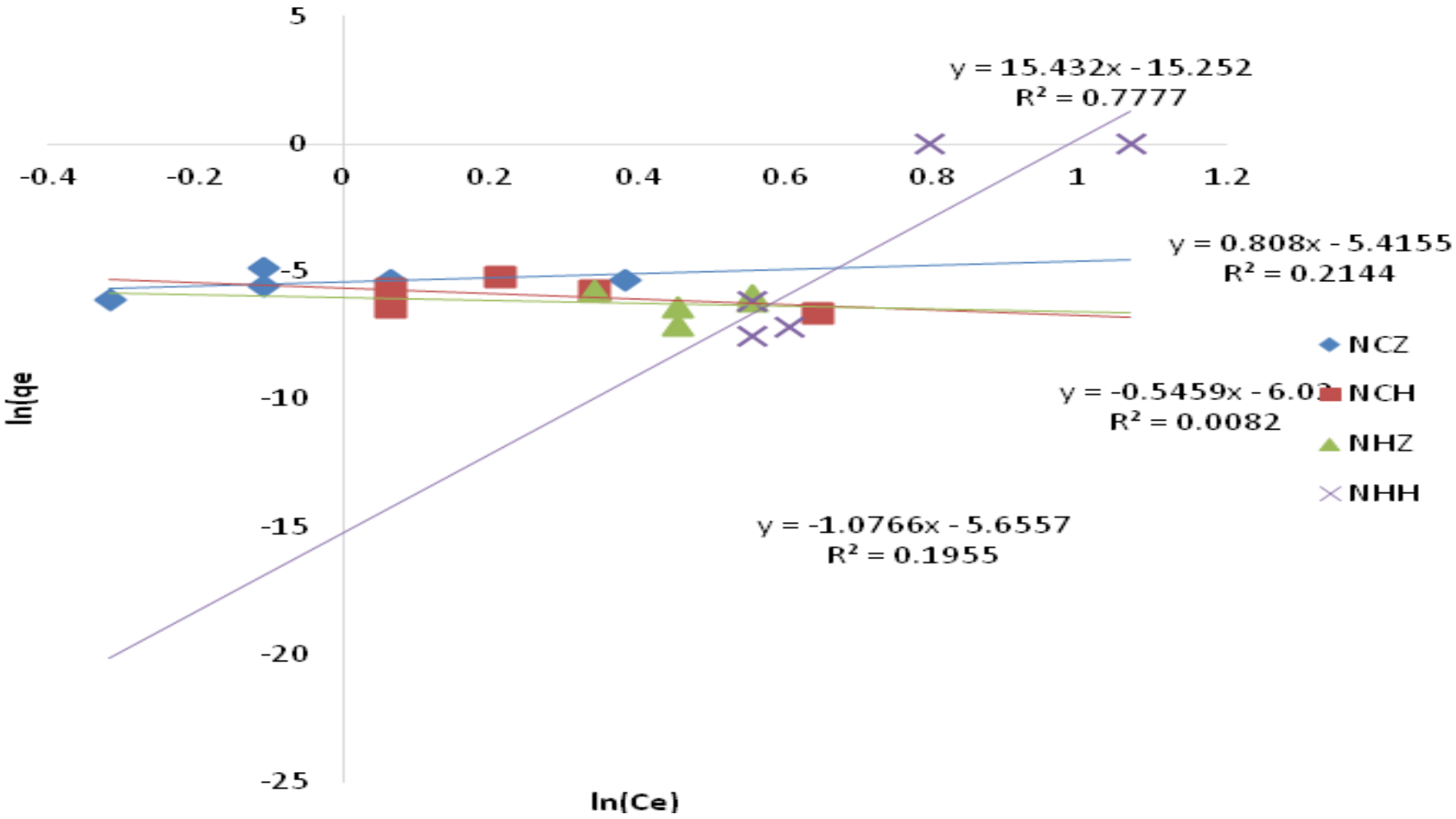


Figure 4. 94: Freundlich Isotherm models for nickel ion

Table 4. 8 Freundlich Isotherm model constants

	NCZ			NCH			NHZ			NHH		
	K_F	N	R^2	K_F	N	R^2	K_F	n	R^2	K_F	n	R^2
Nitrate	1.00	0.00	0.75	3.74	-0.20	0.87	1.00	0.00	0.01	247.60	-0.11	0.31
Phosphate	4.11	-0.37	0.39	1.00	0.00	0.00	1.00	0.00	0.00	0.45	-0.15	0.65
Chloride	0.78	-0.22	0.26	0.88	-0.23	0.07	0.65	-0.22	0.49	0.80	0.22	0.23
Cd	0.67	0.00	0.75	0.11	-0.20	0.89	1.22	-1.57	0.10	2.02	0.69	0.31
Cr	0.70	-16.42	0.29	2.19	-0.20	0.58	1.00	0.00	0.00	2.43	-0.23	0.44
Zn	1.87	-0.28	0.58	5.42	-0.97	0.78	2.94	-0.48	0.55	5.68	-1.36	0.80
Ni	2.24	-1.85	0.21	0.34	-0.18	0.20	0.58	-0.12	0.01	50×10^5	-0.07	0.78
Pb	1.48	-0.25	0.48	1.20	-0.19	0.03	1.78	-0.19	0.64	2.45	-0.19	0.54

Table 4. 9 Efficiency of regeneration and reuse of the activated carbon (NHH)

Parameters	**Cycle 1**	**Cycle 2**	**Cycle 3**	**Cycle 4**	**Cycle 5**
BOD	80.00%	80.00%	80.00%	80.00%	60.00%
COD	60.71%	46.43%	25.00%	17.86%	7.14%
Bacterial count	99.53%	98.13%	94.85%	94.38%	92.97%
Fungal count	91.67%	83.33%	75.00%	75.00%	75.00%
Cd	65.57%	60.66%	49.18%	40.16%	18.03%
Cr	81.99%	81.86%	41.06%	39.70%	5.32%
Zn	95.47%	85.28%	70.91%	55.56%	49.47%
Ni	57.25%	54.06%	52.09%	38.94%	36.33%
Pb	70.05%	63.96%	62.94%	52.28%	39.09%

Cycle number represents the sequence in which the neem carbon is regenerated and reused. The metals are Cd, Cr, Zn, Ni and Pb while the oxygen parameters are DO, BOD and COD. BC is Bacterial Count and FC is Fungal Count.

4.14 Bohart Adams Adsorption Model

The Bohart Adams adsorption model was used to determine the effect of breakthrough time and bed height on the adsorption of nickel ion in the wastewater. NHH was selected because it happens to have the least surface area among the four neem carbons. Nickel ion was also selected due to it high concentration in the wastewater and its implication on human health especially as it relates to causes of lung cancer, respiratory failure, asthma and chronic bronchitis and heart disorder Lars *et al.* (1997). The Bohart Adams parameters and correlation coefficient on the adsorption of nickel ion in wastewater by NHH is presented in Table 4.10.

Breakthrough time (t_b) was the time taken when the effluent concentration (C_t) of Ni (II) reached 50% of the feed concentration (Co). The plot of the ratio of effluent and inlet concentrations (C_t/C_o) and time (min) for varying operating conditions is presented in Figure 4.95. The result showed a direct relationship between (C_t/C_o) and time. The plot of adsorption capacity against bed height is presented in Figure 4.96. The graph showed a decreased adsorption capacity with increased bed height with a correlation coefficient of 0.9987. The effect of bed height on breakthrough time is presented in Figure 4.97. A direct correlation was observed between the breakthrough time and bed height.

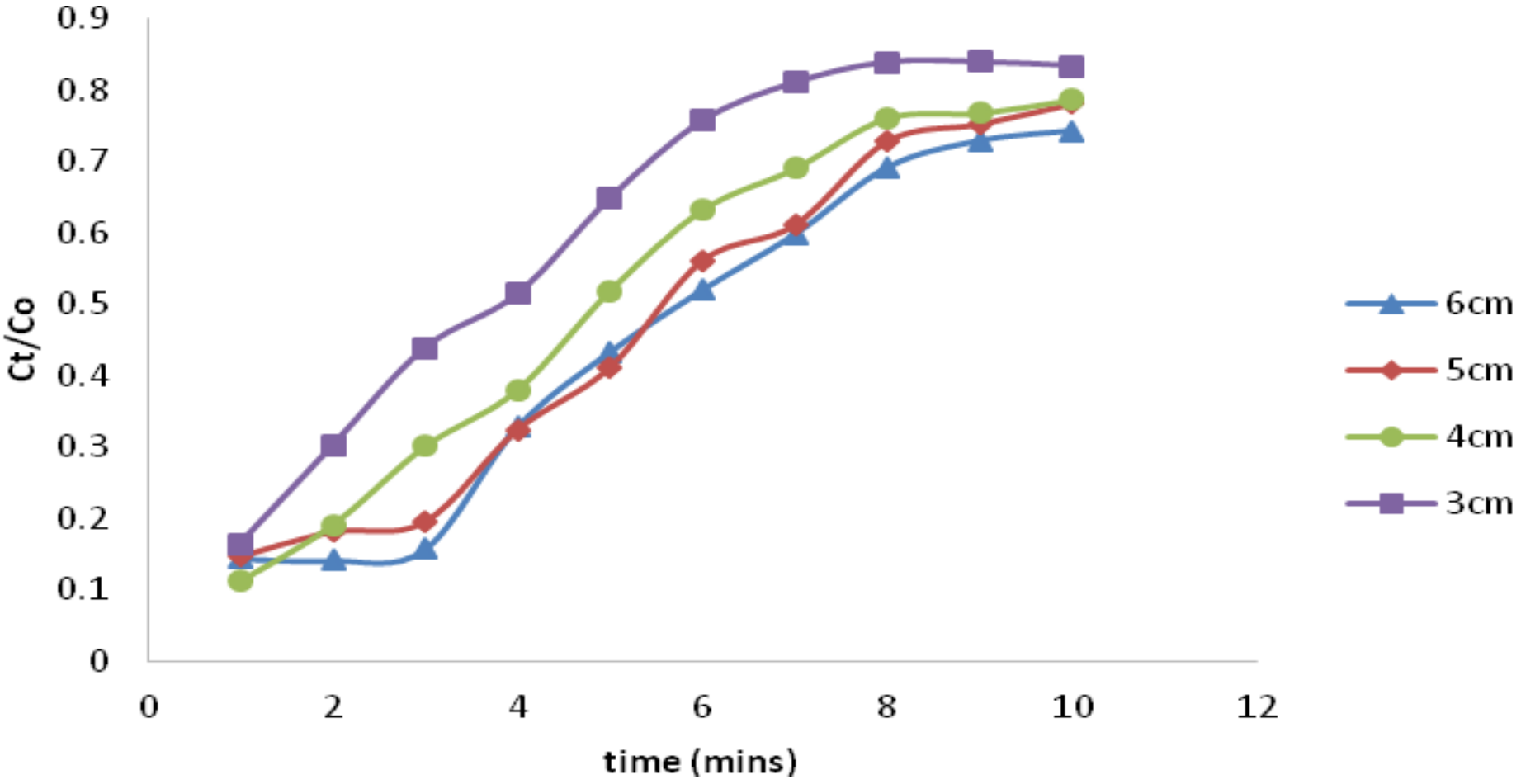


Figure 4. 95: The Breakthrough curve for nickel ion adsorption on NHH

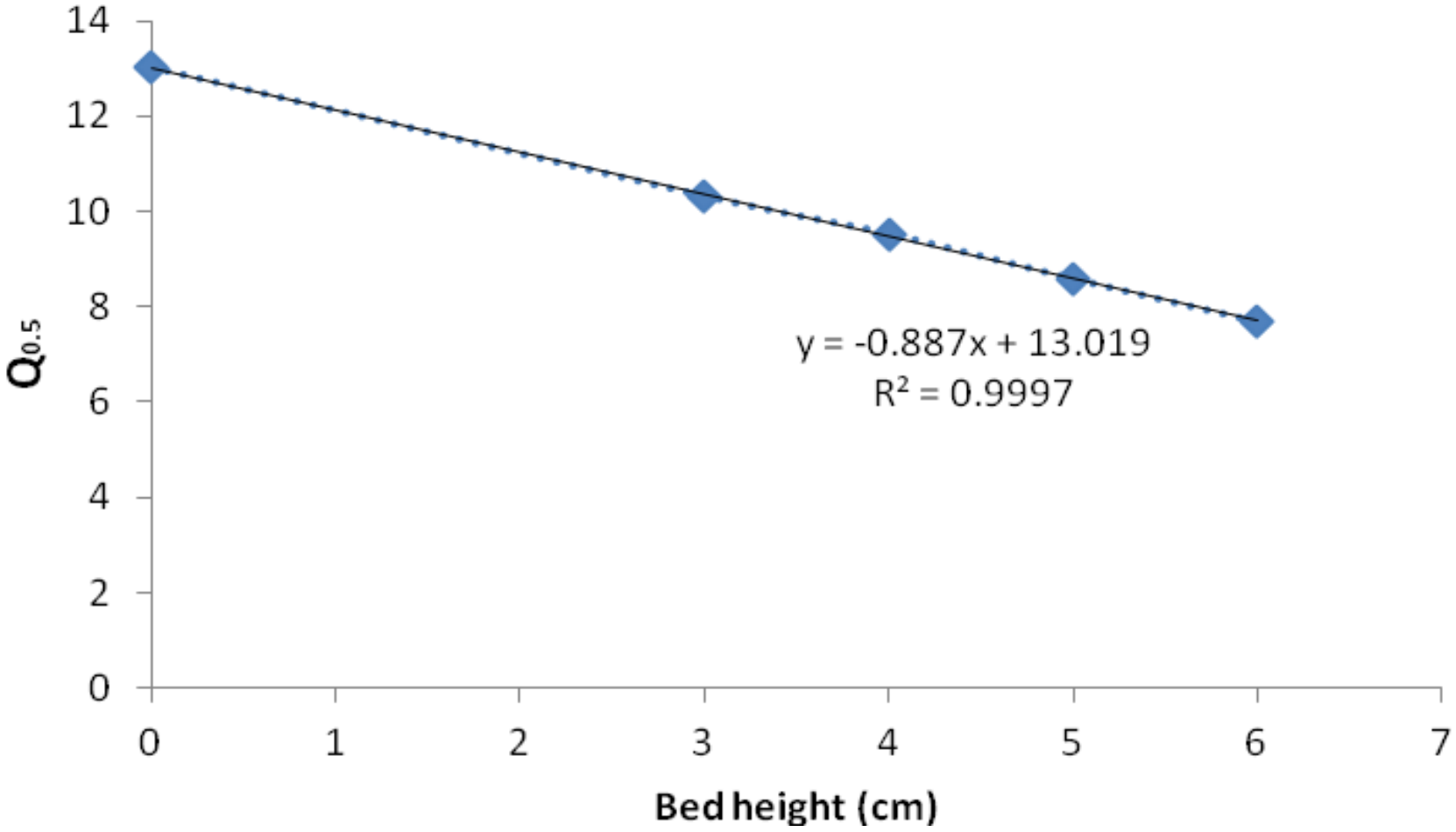


Figure 4. 96: The effect of bed height on the adsorption capacity ($Q_{0.5}$)

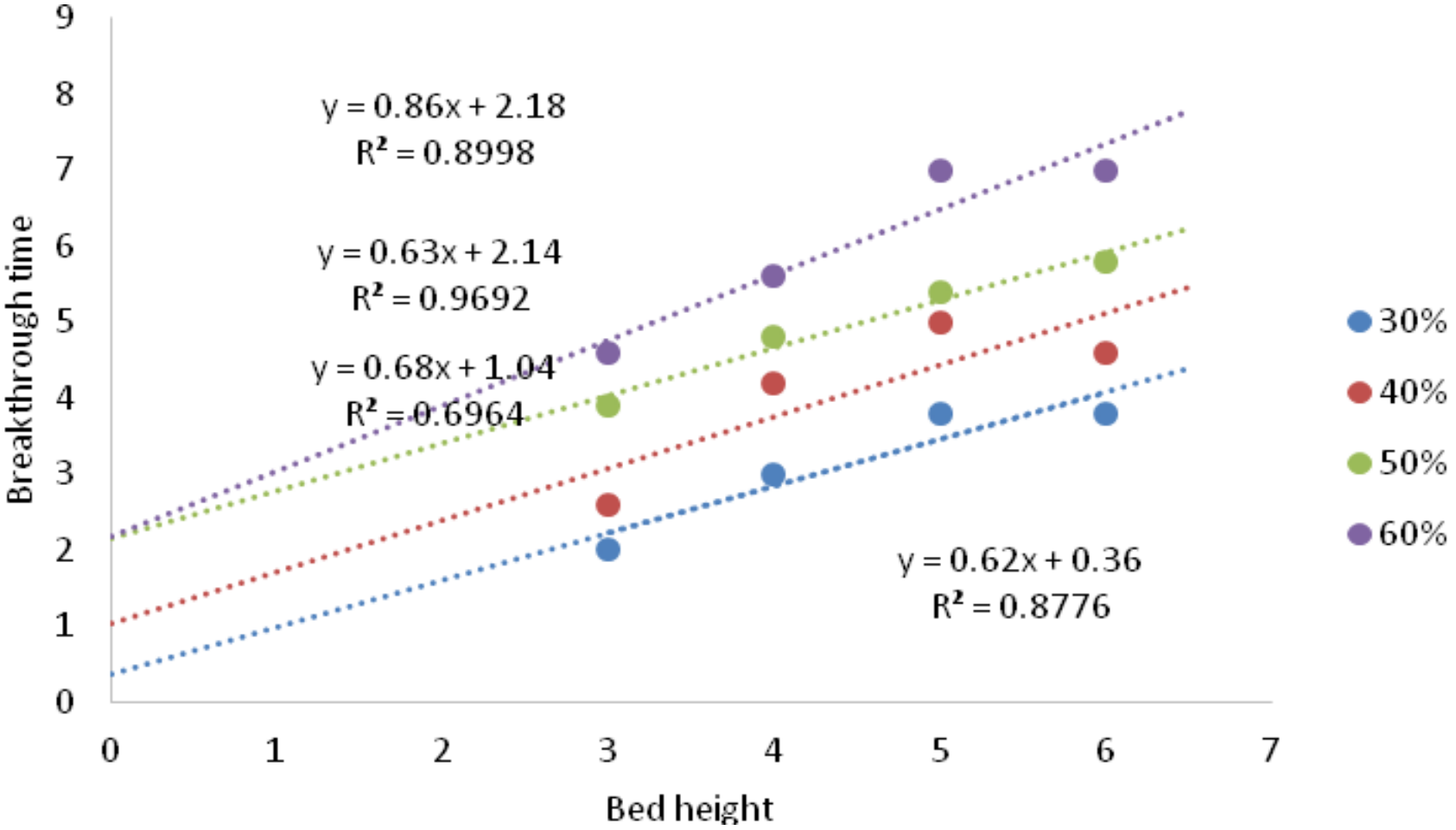


Figure 4. 97: Effect of bed height on the breakthrough time

Table 4. 10 Bohart Adams Parameters from Ni (II) adsorption in wastewater

Breakthrough %	C_t/C_o	a	b	N_o	R^2	K
30	0.3	0.62	-0.36	18.8058	0.8779	0.87987
40	0.4	0.68	-1.04	20.6258	0.6964	0.23179
50	0.5	0.63	-2.14	19.1092	0.9692	0.08522
60	0.6	0.88	-2.18	26.6921	0.8998	0.06165

CHAPTER FIVE

5.0 DISCUSSION

5.1 Physicochemical properties of raw neem and the prepared activated carbons

The results of the physicochemical properties of the raw and modified neem husks and cakes are summarized in Table 4.1. The physicochemical investigations were carried out before and after carbonization and activation of the raw neem husk and cake with $ZnCl_2$ and H_3PO_4. The parameters investigated included moisture content, dry matter content, ash content, the bulk density, % carbon yield and pH. Generally, the results indicate significant improvement in the properties of the activated neem husk and cake relative to the raw neem samples.

The bulk density of the RNH (0.95 g/ml) was higher than that of the RNC (0.87 g/ml). The bulk density of the RNH decline from 0.95 g/ml to 0.76 g/ml and 0.82 g/ml for NHZ and NHH respectively while the RNC declined from 0.87 g/ml to 0.77 g/ml and 0.83 g/ml respectively for NCZ and NCH. Higher density provides greater volume and normally indicates better quality activated carbon Elliott *et al*., 1989. Tsai *et al.*, 2001 reported a higher density range of 1.20 - 1.35g/ml; Tripathi and Chapman (2003) reported a density as high as 0.7g/ml; Hazard Mater (2006) reported a bulk density of 0.509 – 0.748 from Pomace-An Olive industry waste; Itodo *et al.*, 2009 reported a linear relationship between porosity and bulk density of nut shells biosorbent for textile waste water treatment.

The moisture content of the RNH and RNC were found to be 4.45% and 8.95% respectively while that of the activated samples were lower. This is an indication that the activation process was successful. This is also in agreement with the moisture content of other carbons materials reported in literature which ranges from 3.80% -

10.01% (Gary *et al.,* 2003). The commercial adsorbent contain about 5 - 8% moisture content (Gary *et al.,* 2003). The low moisture contents of the RNH and RNC suggests that the materials would make good adsorbent (US EPA, 2008).

Similar trends were observed in the volatile matter content, where the RNH and RNC values were higher than that of the activated samples. The volatile matter content are within the range of 3.89% -54.44%. Selvi *et al.* (2001) reported a volatile matter content as high as 87.8%. High fixed carbon and volatile matter content makes the adsorbent material good precursors for production of activated carbon (Demirbas *et al.,* 2002). These imply that the adsorbent had the potentials of a good precursor.

Ash content of a sample is the inorganic residue left after the organic matter has been burnt off (Allen *et al.,* 1974). It is also the measure of the mineral content of the sample (Allen *et al.,* 1974). The ash content of the neem carbon ranges from 6.56% – 20.11%. Demirbas *et al.,* 2002 reported that low ash content signifies better precursor material since high ash content would interfere with pore structure development of the adsorbent and hence adsorption will be less. OMRI (2002) reported that the lower the ash content the better the adsorptive material. This implies that low ash content would give high purity activity and would not add to contamination load of adsorbate. Tsai *et al.,* 2001 reported ash content range of 9.35 - 43.57% for different coal samples. The ash content of the raw and activated neem carbon fell within this category. This is an indication that the neem carbon produced would be a good adsorbent.

5.2 Carbonization of Neem Husk and Cake

The effect of temperature on the carbonization of the raw neem husk was studied within the temperature range of 150^{o}C to 500^{o}C as presented in Figure 4.1. The graph shows a gradual increase in the adsorption of methylene blue which is used as model adsorbate for studying organic contaminant (Abechi, 2011). The optimum carbonization

temperature was observed at a temperature of 400^{o}C. Beyond this temperature, the adsorption of the methylene blue declined with increase in temperature as depicted in Figure 4.1, implying that all the cellulosic materials have been converted to carbon char (Mattson and Mark, 1971). Heating beyond this temperature would lead to the collapse of some of the orifices and cavities and at higher temperature of carbonization and prolong heating time, there would be further conversion of the char carbon to CO and CO_2 in the presence of oxygen, thus decreasing the weight of the carbon at equilibrium as presented in Equations 2.2 and 2.3 (Loo, 1974).

5.3 Activation of Neem Husk and Cake

The effect of temperature (between 450 – 650^{o}C) on the activation of neem carbon with H_3PO_4 and $ZnCl_2$ was studied. The optimum activation temperature for H_3PO_4 was found to be at 550^{o}C (450-600^{o}C) while $ZnCl_2$ was at 500^{o}C (450-550^{o}C) as shown in Figure 4.2. The possible reasons for the drop in adsorption of methylene blue beyond the optimum activation temperature could be as a result of the closure in the orifices of the neem carbon and the unavailability of vacant surface area for adsorption (Bansal and Goyal, 2005). Activation increases the adsorptive capacity of the carbonized materials. It is mostly done at a temperature higher than the carbonization temperature (Diaz-Teran *et al.,* (2001). Gimba (2001) reported a carbonization temperature of 600°C for coconut shell while activation was achieved at a higher temperature of 900°C.

5.4 BET Surface Area and Pore Characterization of the Prepared Activated Carbon

The BET surface area, pore volume and pore size values of the activated neem samples (NCH, NCZ, NHZ and NHH) are presented in Table 4.2. The BET surface area for NHH, NHZ, NCH and NCZ were 230.79, 238.56, 352.00 and 252.18 m^2/g respectively.

The average pore sizes for NHH, NHZ, NCH and NCZ were 22.22, 22.46, 34.26 and 24.16Å respectively. The International Union of Pure and Applied Chemistry (IUPAC) classified pores as follows; micropores (<20 Å), mesopores (20–500 Å) and macropores (>500 Å). Based on the IUPAC classification, the pore diameter of the neem activated neem carbon was found to be between 22Å - 34Å, indicating that the activated carbon was in the mesopores region. Rivera-Utrilla *et al.,* 2001 reported a pore diameter between 5.7 – 72.5 Å from Sorbo-Morit and Merck commercial activated carbon. Dada *et al.*, (2012) reported pore diameter of 19.82 Å from rice husk activated carbon. Devi *et al.*, 2012 reported pore diameter that ranges from 17.88 – 19.82 Å. Takeo *et al.,* 2003 reported pore diameter within the range of 13.3 – 72.6 Å from charcoal from coffee. According to Bansal and Goyal, (2005) the mesopore account for about 5% of the internal surface area while the micropores account for about 95% of the internal surface area.

5.5 Fourier Transform Infrared (FTIR) Analysis

Fourier transform infrared spectroscopy (FTIR) was used to determine the functional groups on the surface of the raw and activated carbon. The spectra of the raw and activated carbons were measured within the range of 400–4000 cm^{-1} with a resolution of 4cm^{-1}. Spectra plots for the adsorbents are shown in Figures 4.7- 4.12. Table 4.3 lists the fundamental frequencies of the raw neem samples and activated samples indicating their band frequencies in the FTIR spectrum. The FTIR of the raw neem husk, displayed major absorption bands at 3,400 – 3,900 cm^{-1}, 2,200 – 2,400 cm^{-1}, 1,400 – 1,700 cm^{-1}, 1,000 – 1,200 cm^{-1}, 500-800 $cm^{-1}$and 400-483 cm^{-1}. The bands at 400-483 cm^{-1} and 500-800 $cm^{-1}$are associated with the inplane and out-of-plane aromatic ring deformation C-H bending mode (Sahira *et al.,* 2013). The broad band between 700 and 800cm^{-1} represents bounded O–H groups in the carbon structure (Sahira *et al.,* 2013).

In the raw samples the strong peak seen at 1420-1460 cm^{-1} has been assigned to stretching vibrations of C-C bonds. The disappearance of bands at 2,929.79 cm^{-1}, 1,723.45 cm^{-1}, 1,425.44 cm^{-1} and 1,246 cm^{-1} and appearance of new bands between 700 – 970 cm^{-1} is evident of the successful carbonization and activation process. On the other hand, C–H stretch could be ascribed to the band that appeared at 1000-1100 cm^{-1}. The band at 1500 cm^{-1} may be attributed to the aromatic rings carbon–carbon stretching vibration enhanced by polar functional groups (Ahmad and Hameed, 2009). The strong peak around 1600 cm^{-1} refers to stretching vibrations of bonds in the aromatic ring coupled to that of highly conjugated carbonyl groups (C=O) (Sahira *et al.,* 2013). The strong band around 1720 cm^{-1} observed in the raw samples shows the presence of stretching vibration of C=O bonds in ketones, aldehyde, lactone, and carboxyl (Sahira *et al.,* 2013). These groups are abundant in the raw samples. Disappearance of these peaks in the activated carbon samples is indicative of complete carbonization.

The peaks at 2250-2400 cm^{-1} denotes C-O stretching from ketones, aldehydes or carboxylic groups in the raw samples and the interaction between oxygen and carbon during pyrolysis in the activated carbon samples. Oxygen containing surface functional groups plays important role in influencing the surface properties and adsorption behaviour of the sample (Bansal and Goyal, 2005). The nature of activating agents does not have much effect in the type of oxygenated surface functional groups (Sahira *et al.,* 2013). The weak peak in the raw samples around 2900 cm^{-1} is attributed to C-H (stretching vibration in methyl group) interaction with the surface of the carbon since the groups disappear after pyrolysis. The band around 3450 cm^{-1} is due to the absorption of water molecules as result of an O-H stretching mode of hydroxyl groups and adsorbed water. Likewise, weak band around 3740 cm^{-1} is assigned to stretching vibration of O-H bonds in hydroxyl groups (Ahmad and Hameed, 2009; Sahira *et al.,*

(2013). The location of hydrogen-bonded OH groups, usually in the range of 3200–3750 cm^{-1} for alcohols and phenols, involved in hydrogen bonding may be due to adsorbed water.

The FTIR spectra obtained was in agreement with results reported in literature on activated carbon. Some of the activated carbon used in conformity to the findings from neem include; activated carbons prepared from rice straws (Dada *et al.*, 2012), Oak sawdust (Abd El-Latifa *et al*., 2010) and palm kernel shell (Abechi, 2011). From the spectra of activated carbon samples, it was noted that all the carbons contain oxygenated surface functional groups such as hydroxyl, carbonyl, carboxyl and lactones (Sahira *et al.*, 2013). These acidic surface functional groups are favourable for removal of colour (Ahmad and Hameed, 2009). There are changes in the intensity of the absorption bands in the raw material compared with activated carbon product. This show that the carbonization and activation process were successful.

5.6 Scanning Electron Microscope (SEM)

Figures 4.13 to 4.16 show the SEM micrographs of the neem cake and neem husk derived activated carbon. The SEM enables the direct observation of the changes in the surface microstructures of the carbons due to the modifications (Walker *et al.*, 2001). Large pores in a honeycomb shape were clearly found on the surface of the activated neem carbon as presented in Figures 4.13 to 4.16. The well-developed pores had led to the large surface area and porous structure of the activated carbon (Ahmad and Hameed, 2009). There is clear demarcation in the surface morphology of AC treated with $ZnCl_2$ and H_3PO_4. The monographs of NHZ and NCZ as observed in Figures 4.13 and 4.16, clearly showed developed honey comb like, highly defined cylindrical pores and cavities and rough surfaces on the carbon samples. The largely isolated cylindrical units have walls made up of layers of relatively thick sheets. This demonstrated that $ZnCl_2$

was effective to create well developed pores with uniform distribution leading to large surface area and porous structure.

The morphology of NHH and NCH appear sponge-like with large surfaces and narrow pores widths. The narrowing of the pore widths suggest a kind of deformation where the matrix softens and walls of the pores give way and close in on each other. For NHH and NCH, the phosphoric acid incorporated into the interior of the precursor particle restricted the formation of tar as well as other liquids such as acetic acid and methanol, present in the raw neem material, and inhibited the particle shrinkage or volume contraction during heat treatment (Bansal and Goyal 2005). Another important feature of the NCH micrographs is the cracks in the carbon matrix probably developed as a result of thermal stress on the carbon matrix due to temperature changes in the activation process. Such cracks contribute to the overall surface of the activated carbon and as such are important. The cavities on the surfaces of carbons resulted from the evaporation of the activating agent (phosphoric acid) during carbonization, leaving the space previously occupied by the activating agent (Bansal and Goyal 2005). On one hand, the restricted shrinkage and limited volatile released might facilitate the conservation of porous structures present in the precursor. On the other hand, after washing the final product, the extraction of deeply penetrated acid led to the creation of tremendous porosity (Bansal and Goyal 2005).

5.7 Thermoanalytical Studies

The thermal stability of the activated carbon samples were tested by measuring the mass loss within a heating ramp rate. The descending TGA thermal curves shown in Figures 4.18 to 4.20 indicate the occurrence of weight loss. The details of the thermograms are presented in Table 4.4. Two stages of thermal decomposition behaviour were observed and revealed two derivative peaks in temperature in the TG curve of each samples. The

mid-points for the first derivative peak temperatures were 87.00°C , 85.64°C , 88.35°C and 86.86°C for NCZ, NCH, NHZ and NHH respectively while the corresponding weight loss are 3.62%, 3.67%, 3.05% and 3.02% respectively (Table 4.4). The value of the zinc chloride activated carbon samples show that the samples tend to be more resistant to heat than their corresponding phosphoric acid activated carbon samples. The weight loss at this range was due to moisture being dried off in the material. The mid-points for the second derivative peak temperatures were 450.01, 449.55, 465.23 and 466.19°C for the activated carbon samples NSZ, NSH, NHZ and NHH respectively, resulting to an overall mass loss of 9.81, 10.14, 12.06 and 3.89% respectively. This mass loss corresponds to the volatile matter content of the samples. The huge weight loss observed at temperatures ranging from 350°C to 500°C could be attributed to the decomposition of organic components in the raw material, such as cellulose, hemicelluloses, and lignin. At higher temperatures, condensable fragments of the cellulosic structure in neem husk material are likely to be lost by volatilization (Gimba, 2001). The total weight loss in the NHH sample proved it to be the most thermally stable material as presented in Table 4.4.

5.8 Physicochemical Characteristics of the Hospital Wastewater Before Treatment

The mean values of the parameters that characterized the Raw Waste Water (RWW) sample are presented in Appendix ll. The raw water showed a characteristic pH of 6.4, indicating the existence of a slightly acidic environment. The mean pH values recorded fell within the WHO pH tolerance limit (6.00 - 8.00) for discharged wastewater (Wyasu an Okereke, 2012). A conductivity value of 77µS/cm indicates the presence of mineral substances in moderate concentrations. Turbidity of 56 NTU and high total dissolved solids (TDS) of 40.36 mg/ml was recorded, indicating the presence of highly coloured substances in the water. The COD in the wastewater was 280 mg/ml which is higher

than the permissible limit of 100 mg/ml for wastewater discharge as recommended by Federal Environmental Protection Agency (FEPA, 1991). The dissolved oxygen (DO) in the wastewater was 39 mg/ml while BOD is 15mg/ml. This indicate the high ecotoxicity of the wastewater (Escher, 2011; Yadav and Kumar, 2011; Wyasu and Okereke, 2012). After treating the wastewater with the different adsorbents from neem carbon, NCH and NHZ had the highest percent reduction of COD followed by NHH with 25% while NCZ is the least with 23.2% as shown in Figure 4.21. For BOD, NCZ and NHH were the most effective in reducing BOD by 53.3% while NCH and NHZ both had 26.7% as depicted in Figure 4.21.

The concentrations of chloride, nitrite and phosphate ions in the wastewater were 1.76, 9.72 and 1.26mg/ml respectively which were lower than the discharge limit for wastewater. This implies that that less of this ions sources were discharged from the hospital waste supporting higher microbial content in the wastewater. All the heavy metal ion contents of the wastewater studied were of relatively high values with respect to the recommended discharge limit for wastewater except zinc ion. This values maybe influenced by the volume, the number and intensity of services provided in the hospitals, especially from the use of X-ray films containing lead and other heavy metals in radiology, pharmaceutical services, laboratory and laundry activities (Prayitno *et al.,* 2013). The bacterial and fungal counts were 4,270 and 4,800 CFU/100 ml respectively. The high load of fungal/bacterial flora can be attributed to the presence of more sewage that contributed to microbial load than there are drugs and disinfectants in the wastewater supporting the low concentration of chloride in the wastewater.

5.9 Physicochemical parameters of the treated Water

The hospital wastewater was treated with the Neem Cake activated with $ZnCl_2$ (NCZ), Neem Cake activated with H_3PO_4 (NCH), Neem Husk activated with $ZnCl_2$ (NHC) and

Neem Husk activated with H_3PO_4 (NHH). A comparison of the investigated parameters in the raw and treated effluents is presented in Figures 4.21 to 4.23. All the studied parameters were below the recommended discharge limit for wastewater except cadmium, chromium, nickel and lead.

5.9.1 pH

pH is a measure of the intensity of acidity or alkalinity in water (Kumar *et al.*, 2010). The pH values of the wastewater treated with NCZ, NCH, NHZ and NHH were 5.78, 5.47, 5.27 and 5.07 respectively indicating a decrease in pH by 9.7, 10.3, 17.7 and 20.8% respectively. A comparison of the pH values of the four treated water samples is presented in Figures 4.22. The permissible limit of pH for discharge wastewater is 6.0 to 8.0 (FEPA, 1991). pH affects the dissolved oxygen level in the water which has direct effect on photosynthesis of aquatic plants, metabolic rates of aquatic organisms and the sensitivity of these organisms to pollution, parasites and disease (FWPCA, 1968).

5.9.2 Electrical Conductivity (EC)

EC is a measure of total salt content in water and a determination of levels of inorganic constituents in water (Morrison *et al.,* 2001; Awofolu, 2007). Figure 4.22 shows a decrease in the EC values of the treated wastewater samples. NCZ decreased EC by 30.6 %, NCH decreased EC by 78.2%, a 74.7% decreased in EC was achieved by NHZ while NHH showed a 61.0% decrease in EC. The high percentage decreased recorded was an indication of the efficiency of the activated carbon samples in removing salt and other inorganic constituent in the wastewater.

5.9.3 Turbidity

Turbidity is a measure of water clarity and indicates the degree to which light entering a column of water is scattered by suspended solids (Kumar *et al.*, 2010). The results show turbidity of 56 NTU in wastewater is below the permissible limit of discharge of wastewater. After treatment with the four different adsorbents, turbidity decreased to between 0 and 5 NTU which depicted the effectiveness of the adsorbent in clearing the highly coloured wastewater. The treated water samples showed a reduction in values by 100, 91.1, 91.1 and 100% for wastewater treated with samples NCZ, NCH, NHZ and NHH respectively.

5.9.4 Total Hardness (TH)

NIS (2007) has specified the maximum permissible limits of TH to be within 150 mg/ml of $CaCO_3$ while the USEPA guidelines are within 500 mg/ml of $CaCO_3$. The wastewater contained high amount of $CaCO_3$ which made it to have a hardness of 3939 mg/ml of $CaCO_3$. The adsorbents were efficient in reducing the hardness of the wastewater to 1,402 mg/ml of $CaCO_3$. The adsorbents treated with $ZnCl_2$ had better reduction of the hardness in the wastewater. This could be as a result of the characteristics of the zinc metal in the $ZnCl_2$ as a transition metal that supported the reduction of $CaCO_3$ in the wastewater. All treated samples were above the recommended limit of 150 mg/ml by NIS (2007). Though the hardness of water is not a pollution parameter and has no adverse effect on human health, it indicates water quality (Kumar *et al.*, 2010; Yadav and Kumar, 2011).

5.9.5 Chemical Oxygen Demand (COD)

COD is a measure of the oxygen required for the chemical oxidation of organic matter (Satone *et al.,* 2011). The permissible limit of COD for discharge wastewater is 100 mg/ml (Escher *et al.,* 2011). The values obtained for COD after treatment were higher than the permissible limit of COD for discharge wastewater. The neem carbons reduced the COD level in the wastewater from 280 mg/ml to 190 mg/ml. The high COD observed in the wastewater depicted the high microbial load of the wastewater. This could be allotted to the high nitrates concentration of 9.72 mg/ml, bacterial load of 4,270CFU/100ml and fungal load of 4,800 CFU/100ml.

5.9.6 Biochemical Oxygen Demand (BOD)

BOD is the amount of oxygen required by bacteria in stabilizing the decomposable organic or biologically oxidizable matter (Kumar *et al.,* 2010; Yadav and Kumar, 2011). BOD gives an idea about the extent of pollution in water and wastewaters. Rani and Dahiya (2008) reported that the desirable limit for BOD in wastewater is 20.0 mg/ml and permissible limit is 30.0 mg/ml. Kumar *et al.,* (2010) also reported a permissible limit 4.0 mg/ml. The permissible discharge limit for BOD according to FEPA is 50 mg/ml. Based on FEPA recommended standard for wastewater discharge, all treated wastewater samples had BOD values below the wastewater desirable limits. The BOD of the treated wastewater samples were reduced by 53.3% (7 mg/ml) for NCZ and NHH samples and 26.7% (11 mg/ml) for NCH and NHZ. Kumar *et al.* (2010) reported that the presence of nitrates and phosphates in water can contribute to high BOD levels. Because they are nutrients and can cause plant life and algae to grow quickly. When plants grow quickly, they also die quickly. This contributes to the organic waste in the

water. However, the neem carbons reduced BOD from 15.0 mg/ml in the wastewater to 7.0 mg/ml.

5.9.7 Dissolved Oxygen (DO)

DO is a measure of the degree of pollution by organic matter, the destruction of organic substance as well as the self-purification capacity of the water body (Kumar *et al.,* 2010). The permissible limit for DO ranges from 30 to 39 mg/ml (Rani and Dahiya, 2008). It is expected as BOD levels increases, DO levels should decrease because the oxygen that is available in the water is being consumed by the bacteria. However, as the high BOD of 15 mg/ml in the wastewater was reduced by the neem carbons DO remains almost constant except for NCZ that declined by 23%. This could be as a result of the presence of organic waste in the wastewater that is still undergoing decomposition process by bacterial.

5.9.8 Nitrate

The mean nitrate concentration of the treated wastewater samples were found to be 0.006, 0.118, 0.108 and 0.033 mg/ml, for samples treated with NCZ, NCH, NHZ and NHH respectively. The permissible limit for the discharge of nitrate in wastewater as recommended by the Federal Environmental Protection Agency (FEPA) is 20 mg/ml. The activated carbon samples have shown excellent reduction of nitrates in wastewater. Ajibola and Ladipo (2009) conducted a study on the quality of water runoff discharged from some industries into the Isolo Canal, Lagos and reported a mean nitrate concentration as high as 58.5 mg/ml.

5.9.9 Phosphates

The mean phosphate concentration in the treated wastewater samples were found to be 0.14, 7.52, 0.06 and 3.48mg/ml, for samples treated with NCZ, NCH, NHZ and NHH respectively (Figure 4.24). The phosphate contents were reduced only for samples NCZ and NHZ by 88.9% and 96.0% respectively. NCH and NHH did not show efficiency in reducing phosphates in the wastewater samples rather release more phosphate ions from the surface of the activated carbon. This is in conformity with the findings reported by Gimba (2001) that even after thorough washing of the adsorbent with acids or water, the salts were not completely removed from the carbons. This shows that complete removal is seldom if ever accomplished, because the salts of these metals are strongly held by carbon and only a small portion is released with each extraction with acid.

The permissible limit for the discharge of phosphate ion in wastewater as recommended by the Federal Environmental Protection Agency (FEPA) is 5 mg/ml. The concentrations of the treated wastewater were all below the FEPA permissible limit except for NCH. Ajibola and Ladipo (2009) reported a mean phosphate concentration of 1.58 mg/ml in Isolo, Lagos state.

5.9.10 Chloride

The FEPA permissible limit for the discharge of chloride ions in wastewater is 500 mg/ml. The concentration of chloride ions in the wastewater was 1.76 mg/ml, which is below the threshold for wastewater discharge. After treating the wastewater with the NCZ, NCH, NHZ and NHH, the mean chloride concentrations in the treated wastewater are 0.31, 1.33, 0.07 and 0.0 mg/ml respectively. The chloride ion concentration was all below the permissible limit for the discharge of chloride ion in wastewater as

recommended by the Federal Environmental Protection Agency (FEPA). The activated carbon samples have shown excellent reduction of chloride ion in wastewater.

5.9.11 Heavy metals

The heavy metal concentration of the wastewater samples after treatment with the neem activated carbons are shown in Figure 4.25. The concentrations of cadmium ion in the wastewater after treatment with the four different adsorbents were all below the FEPA permissible limit for discharge of wastewater except for NCZ (Appendix XI).

The neem adsorbents were effective in reducing the chromium ion in the wastewater though the chromium ion concentrations in the treated wastewater were all above the FEPA permissible limit for discharge wastewater. NCZ adsorbed 57.4% (0.312 mg/ml) of the chromium ion, NCH adsorbed 28.2% (0.526 mg/ml), and NHZ adsorbed 81.6% (0.133 mg/ml) of the chromium ion while NHH reduced the chromium ion concentration in the wastewater by 47.3% (0.386 mg/ml). Emine *et al.*, (2006) conducted studies on adsorption of chromium (VI) on Pomace - An olive oil industry waste and reported the adsorption of chromium to be within the range of 4.68 – 21.74%.

The concentrations of zinc ion in the treated wastewater were all below the permissible limit as recommended by FEPA for discharge wastewater except for the NCZ and NHZ. NCH and NHH reduced the zinc ion concentration by 59.0% and 43.3% respectively. However, the concentration of zinc ion increased in NCZ and NHZ. This can be attributed to the release of excess Zn ions from the surface of the activated carbon from the activating agent. Again, this could be the same reason as observed by Gimba, (2001) that even after thorough washing of the adsorbent with acids or water, the salts were not completely removed from the carbons.

The level of nickel ion in the treated wastewater was above the permissible limit as recommended by FEPA for discharge wastewater. Though, the adsorbent were efficient in reducing the nickel ion concentration in the wastewater. NCZ adsorbed 61.37% (1.468 mg/ml) of Ni ion in wastewater, NCH adsorbed 49.8% (1.907 mg/ml), NHZ adsorbed 54.0% (1.746 mg/ml) while NHH adsorbed 41.7% (2.215 mg/ml).

The Pb ion content of the treated wastewater was above the permissible limit as recommended by FEPA for discharge wastewater. Though, the adsorbent were efficient in reducing the lead ion concentration in the wastewater. NCZ reduced the lead ion concentration by 70.1% (1.59 mg/ml).

5.10 Microbial load reduction activities of Neem Activated Carbon

Microbial populations are indicators for pathogenic organisms. Outbreaks of diseases can occur as a result of hospital wastewater polluted by a combination of different microorganism species discharging into streams and groundwater (Rhodes, 2000). They should not be found in drinking water but are usually present in surface/ receiving water, soil, sewage and feces of humans and animals (Adekunle *et al.*, 2007). The NIS limits for bacterial and fungal count is 0 CFU/100ml while the permissible limit for discharge of bacterial and fungal count in wastewater is 10,000 CFU/100ml. The bacteriological and fungal count of the raw wastewater was exceedingly high at 4,270 and 2,400 CFU/100ml respectively. The excellence of the activated carbon was demonstrated in the microbial load reduction. Though, the wastewater samples were not completely rid off its microbe. However, the bacterial load was greatly reduced by 99.4%, 99.3%, 99.3% and 99.3% for NCZ, NCH, NHZ and NHH samples respectively (Figure 4.26). The fungal loads were decreased significantly by 88.8%, 90.0%, 85.8% and 90.4% for NCZ, NCH, NHZ and NHH samples respectively.

5.11 The Pseudo-Second-Order Rate Kinetic Model

From the kinetic plots in Figures 4.27 – 4.44 the studied parameters were mostly influenced during the initial 10 minutes of adsorption and thereafter, no significant change was observed. This may be due to the fast attainment of equilibrium between the adsorbent and adsorbate because of the availability of unoccupied active sites (Kulkarni, 2013). These results are in agreement with the works of other researchers (Kazemipour, *et al.*, 2008; Abedi-Koupaia and Mohri-Esfahania, 2012). For few other parameters like conductivity, phosphate, chromium, nickel and lead greater adsorption were observed beyond 10 minutes. This could be as a result of greater ionic potential (ratio of charge to ionic radius) or the most electronegative ones would be removed first and if the sites were still undersaturated, then those having lower ionic potential or lower electronegativity would be removed in the sequence (Ucer *et al.* 2006; Kaushik *et al.*, 2007).

The data for the time dependence on the removal of some of the tested parameters by the neem activated carbon samples were subjected to the linearized pseudo-second-order rate model equation of Ho and McKay (1998). The value of the adsorption capacity of the activated carbons q_e, the pseudo-second-order rate constant k_2 (g/mg min), the initial adsorption rate constant h (mg/g min), and the coefficient of determination R^2 were evaluated from the slope and intercept of the linear plot as presented in Table 4.5. A straight line in the plot proves a good agreement of experimental data with the pseudo-second-order kinetic model and that the adsorption process may be described as chemisorption (Ho and McKay 1998). From the results Table 4.5, it can be seen that the kinetics of adsorption of all the studied parameters onto neem activated carbons follow this model with coefficient of determination greater than 0.80 except for nickel and zinc. These results imply that chemisorption mechanism

plays an important role on the adsorption of the studied parameters onto the neem activated carbons.

5.12 The Weber-Morris Intraparticle Diffusion Model

The pseudo-second-order models may not be sufficient to give the certainty of the adsorption mechanism and cannot identify the diffusion mechanism, the kinetic results were further analysed using the intra-particle diffusion model. The possibility that the diffusion mechanism might be the rate limiting stage in regard to the entire process was evaluated by the linear dependence on the Weber-Morris Intraparticle Diffusion Model Weber and Morris (1963). The intraparticle diffusion model has therefore been integrated to explain the diffusion and describe the adsorption process occurring within the internal pores of the adsorbent. The kinetic data were fed into the linear equation of the diffusion model developed by Weber and Morris (1963).

The rate constant k_{id} (gg^{-1} $min^{-1/2}$) and intraparticle diffusion rate coefficient C_i (g/g) were calculated from the slope and intercept of the plot of the amount adsorbed against the square root of the time. Larger k_{id} values indicate better adsorption which is related to improved bonding between adsorbate and adsorbent particles and may simply be due to the fact that higher adsorbate concentration adds to a greater driving force for diffusion of adsorbate molecules into the pores (Sunil and Arti, 2010). According to Itodo *et al.,* (2009), the adsorption mechanism assumes intraparticle diffusion if the following conditions are met:

(i) High R^2 values to ascertain applicability (R^2>0.7); (ii) Straight line which passes through the origin for the plot area q_t vs. $t^{1/2}$; (iii) Intercept $C_i < 0$. A validity test which deviates from (ii) and (iii) above shows that the mode of transport is affected by more than one process which means that two or more stages occur. From Figures 4.53 to 4.60, it was observed that none of the straight lines passed through the origin and most of the

C_i values were greater than 0, suggesting that intra-particle diffusion was not the only rate-controlling step. According to Sunil and Arti (2010), when the plots do not pass through the origin, it is indicative of some degree of boundary layer control and this further show that the intra-particle diffusion is not the only rate-limiting step, but also other kinetic models may control the rate of adsorption, all of which may be operating simultaneously. The R^2 values of the WMIDM and the poor K_{id} values, as listed in Table 4.6 show that the straight lines do not pass through the origin implying that the process of adsorption was not by diffusion. The packing density of the activated carbon can be responsible for this phenomenon owing to the fact that the effect of initial contact time indicated that the contact with the surface directly affected the sorption procedure. Probably, the initial stages were controlled by external mass transfer or surface diffusion, followed by chemical reaction or a constant-rate stage, and diffusion causing gradual decrease of the process rate. It is therefore unlikely that a number of ion/molecules diffuse into the pore before being adsorbed.

5.13 Equilibrium Adsorption Studies

5.13.1 Effect of initial wastewater volume on physicochemical parameters of the wastewater

The results of variation of initial wastewater volume on the pH of the treated wastewater showed that the bulk of the change in the pH of the material occurs within the first 10 ml of wastewater, beyond which no further increase was observed. This could be due to the availability of active adsorption sites and surface area at the initial wastewater volume but as the volume increases the available active sites for adsorption decreases until the adsorbent becomes saturated (Kaushik *et al.*, 2007).

The result on initial wastewater volume on conductivity values as presented in Figure 4.62 also showed that the optimum reduction occurred in the first 10 ml of wastewater then remained constant and later increased at an initial volume of 30 - 40 ml. This might be as a result of more available sites for adsorption at the initial volume but as the volume increased the available sites on the adsorbent tend to be saturated with the adsorbates. The increase observed at higher volumes might be as a result of ion transfer on the surface of the adsorbent by the adsorbate. A similar trend was observed for total dissolve solids as shown in Figure 4.63. The optimum reduction was observed at the initial volume of 10 ml of wastewater, thereafter no significant increase was observed until at an initial volume of 30 - 40 ml. The order of efficiency of the adsorbents on reduction of conductivity and total dissolve solid was in this order; NCZ>NCH>NHZ>NHH. Figure 4.64 shows the effect of initial volume on turbidity of the treated water. NCH and NHH show a constant decrease in turbidity values till it reached equilibrium at 30 ml while NCZ, NHZ show a maximum reduction at the initial volume of 10 ml thereafter an increase in turbidity values was observed at initial volume of 20 ml.

The effect of initial volume on hardness of wastewater (Figure 4.65) showed maximum reduction in hardness at the initial volume of 10 ml after which the efficiency of the activated carbon gradually reduced and consequently the hardness values. This could be attributed to the fact that the adsorption sites on the surface of the activated carbon get saturated as wastewater volume increases.

The value of chloride and nitrate ions concentration reduce significantly at the 10ml initial wastewater volume and reduce steadily up to the initial 30 ml (Figures 4.69 and 4.70). Figures 4.72, 4.73, 4.75 and 4.76 present the effect of initial volume on the adsorption of cadmium, chromium, nickel and lead ions in wastewater respectively. A

significant reduction of the ions concentration was recorded at the initial 10 ml. This pattern indicates the formation of monolayer coverage at the outer interface of the adsorbents at the early stage (Ahmad and Hameed, 2009). The result of the effect of initial volume on phosphate and zinc ion adsorption showed an increase in phosphate and zinc ion concentration in the neem samples activated with $ZnCl_2$ and H_3PO_4 as presented in Figures 4.71 and 4.74). This could be attributed to the release of phosphate and zinc ions from the surface of the activated carbon into the wastewater sample.

5.14 The Langmuir Sorption Isotherm

The adsorption equilibrium data for the studied parameters were analysed using the Langmuir isotherm model as presented in Figures 4.79 to 4.86. The Langmuir constants related to energy of adsorption and adsorption capacity were calculated from the slope and intercept of the plot and summarized in Table 4.7. The higher the R^2 value, the better the fitness of the isotherm to the model (Itodo *et al.,* 2009). Based on the mean R^2 values for the adsorption isotherm, nitrate, phosphate, chloride, nickel and zinc ion best fed into the Langmuir adsorption model. These imply that the adsorption does not proceed beyond monolayer coverage and each adsorption site is equivalent in terms of energy of adsorption and uniform and there is no interaction between adjacent adsorbate molecules (Langmuir, 1918). The essential characteristic of the Langmuir isotherm was further expressed in terms of a dimensionless constant separation factor or equilibrium parameter (R_L) which indicates the adsorption nature. R_L values between 0 and 1 indicate favourable absorption, R_L values equal to zero indicate irreversible absorption while R_L value that is equal to one indicate a linear adsorption and R_L greater than one depict an unfavourable adsorption. From Table 4.7, most of the studied parameters R_L values were between 0 and 1 except for cadmium, chromium and zinc ions which showed that the adsorption process was favourable.

5.15 Freundlich Adsorption Isotherm

The Freundlich isotherm was used to estimate the adsorption intensity of the adsorbent towards the adsorbate. Apart from a homogeneous surface, the Freundlich equation is also suitable for a highly heterogeneous surface and an adsorption isotherm lacking a plateau, indicating a multi-layer adsorption (Freundlich, 1906). The Freundlich constants were calculated from the slope and intercept of the plot of log q against log C_{eq} and summarized in Table 4.8. According to Kadirvelu and Namasivayam (2000), an n value between 1 and 10 represents beneficial adsorption. Also, Igwe and Abia (2007) reported that a negative n value indicates an unfavourable adsorption. The values of n for all the studied parameters were found to be less than 1 and are negative. These imply that the adsorption pattern does not fit to the Freundlich model relative to the Langmuir model.

5.16 Regeneration and Reuse Studies

A regeneration study was conducted in order to verify the possibility of activated carbon reutilization and to determine its pollutant adsorption capacity within five consecutive cycles of adsorption–desorption. The first cycle was the most efficient cycle of the adsorbent in reducing all of the investigated parameters. As the cycle progresses, the performance of the adsorbent decreased for all the parameters as presented in Table 4.9. The drop in the performance of the adsorbent as the cycle increases might be due to saturation of available active sites. Interestingly, the neem carbons showed excellent reduction of the following parameters even at the fifth cycle; BOD (60%), bacterial count (93%), fungal count (75%), zinc (50%), lead (39%) and nickel (36%). Generally, the regeneration process was very effective and that the adsorbent could be exploited for use several time before its life span exhausted (Dwivedi *et al.* 2008). The regeneration process was successful up to the fifth cycle for most of the studied parameters.

5.17 Bohart Adams Model

Adams–Bohart model based on the surface reaction theory assumes that equilibrium is not instantaneous; therefore, the rate of the adsorption is proportional to the adsorption capacity which still remains on the sorbent (Bohart and Adams, 1920). This model established the fundamental equations describing the relationship between C_t/C_o and time (t) in a continuous system. The breakthrough curves was plotted by varying the bed heights (6.0, 5.0, 4.0 and 3.0 cm) at constant influent concentration (C_o =50 mg/l), constant flow rate of 0.133 ml/min and at the initial nickel concentration of 3.801 mg/l. The result showed a breakthrough concentration of 10.32, 9.53, 8.58 and 7.68 mg/l respectively at bed height 6.0, 5.0, 4.0 and 3.0 cm with a coefficient of determination (R^2) of 0.9987. It was seen that with increased column bed height, a higher removal efficiency of nickel ion was observed. The increased nickel ion adsorption could be as a result of increased contact time with the NHH activated carbon. Another reason for the higher uptake of Ni ion at the highest bed height could be due to increased surface area of the adsorbent, which provided more binding sites for the sorption (Goel *et al.*, 2005). Reza *et al.*, (2012) reported similar result on the study of anionic dyes on aqueous solution using sawdust. The main Bohart Adams parameters were calculated from the plot of time versus bed height on column operation under constant experimental conditions (at flow rate of 0.133 ml/min, bed heights; 3.0, 4.0, 5.0 and 6.0 cm and influent Ni concentration of 3.801 mg/l) as presented in Figure 4.97. It was observed that the breakthrough time at desired breakthrough concentrations exhibit linearity with bed depth.

CHAPTER SIX

6.0 SUMMARY, CONCLUSION AND RECOMMENDATION

6.1 Summary

The summaries of the key findings are:

i. The raw neem cake and husk were successfully carbonized at 400^{o}C and activated using $ZnCl_2$ and H_3PO_4 as activating agents at 500 ^{o}C and 550 ^{o}C respectively.

ii. The following physiochemical properties of the raw and activated neem husk and cake were determined; Moisture Content (3.02 – 8.95%), Dry matter (91.05 – 96.98%), Volatile Matter Content (3.89 – 54.44%), Ash Content (6.56 – 20.11) and Bulk Density (0.76 – 0.95g/ml).

iii. The BET surface area and pore size of the prepared neem husk and cake were found to be between 230 – 352 m^2/g and 22 - 34 Å respectively. The SEM further confirmed the well defined pore structure of the neem carbon.

iv. The changes on the surface functional groups of the raw and activated neem carbons as shown by the FTIR results are evident that the carbonization and activation process were successful.

v. The thermal–analytical studies showed the thermal stability of the prepared neem carbon up to 450^{o}C.

vi. The hospital wastewater was evaluated to assess DO, BOD, COD, microbial content, heavy metals and mineral contents.

vii. The effectiveness and efficiency of the prepared neem carbons was proven in reducing the following parameters/pollutants in a multi-component system: Nitrates (100%), chloride (100%), turbidity (100%), phosphate (95%), BOD (53%), COD (32%), bacterial load (99.94%), fungal load (90.42%), chromium (82%), lead (70%), nickel (61%), zinc (59%) and cadmium (36%).

viii. The kinetics studies showed that the adsorption pattern followed the pseudo-second-order rate model more than the Weber and Morris intraparticle diffusion model.

ix. The adsorption model best fit into the Langmuir adsorption model than Freundlich.

x. The economy of regeneration and reuse of the carbon showed that the adsorbent can be regenerated and reused up to 5 cycles.

6.2 Conclusion

Neem husk and cake are readily available bio resource materials and are usually classified as waste materials (Alau *et al.,* 2010). The carbonization of neem husk and cake and subsequent activation with zinc chloride and phosphoric acid to produce neem activated carbon suitable for the treatment of hospital wastewaters was successful when compared with the raw sample. The neem husk and cake were carbonized to remove volatile organic matter and subsequently activated with $ZnCl_2$ and H_3PO_4 which had been recommended as efficient and cost effective activating agents (Guzel and Uzun, 2002; Gimba *et al.*, 2004; Alau *et al.,* 2011; Abechi, 2011). The results of the nitrogen gas adsorption analysis showed that the activation process produced high surface area materials with well developed pores and volume. The surface areas and pore size of the four different neem carbons are in this order; NCH ($352m^2g$; 34.26Å)> NCZ

(252.18m^2g; 24.16Å) > NHZ (238.56m^2g; 22.46Å) >NHH (230.79m^2g; 22.22Å). This is in conformity with the BET and SEM results which showed the microstructure of the activated carbon samples with large honey-like pores and thick surfaces. FTIR showed the changes on the surface functional groups between the raw and activated neem carbons. This further confirmed that the activation process was successful. The Results of the TGA showed that the produced activated carbon were hydrophobic and thermally stable up to 450^{o}C.

The wastewater collected contained relatively large amount of pollutants (fungi, bacterial, nitrates, phosphates, chlorides, lead, nickel, cadmium, chromium and zinc). The effects of time and initial wastewater volume on the investigated parameters (metals, physicochemical parameters, oxygen parameters and bacterial and fungal count) in the multi component system were studied. The kinetic data were analysed using the pseudo-second-order rate and the Weber and Morris intraparticle diffusion models. The results showed that the adsorption pattern followed the pseudo-second-order rate model more than the Weber and Morris intraparticle diffusion model, implying that the mechanism of removal of pollutants was by chemisorptions and intraparticle diffusion was not the only rate determining step in the process. The Equilibria results fed into the Langmuir and Freundlich isotherm models. The results show that the adsorption pattern fitted into the two models but more favourable in the Langmuir isotherm than the Freundlich isotherm, suggesting monolayer pattern of adsorption between the adsorbent and the adsorbates (Langmuir, 1918). Column studies showed that the adsorption of nickel ion onto NHH activated carbon increased with increased bed height of the adsorbent.

The adsorbents (NCH, NCZ, NHZ and NHH) had excellent adsorption capacities for nitrates (100% adsorption), chloride (100% adsorption), phosphate (95% adsorption)

and turbidity (100% adsorption). For the oxygen demand parameters, BOD was reduced by 53%, COD was reduced by 32% and DO by 23%. The activated carbon demonstrated an excellent adsorption of the high microbial load in the wastewater. Though the wastewater samples were not completely rid of its microbial load but the bacterial load was greatly reduced by 99.94% while the fungal load was reduced by 90.42%. The adsorbents reduced chromium ion by 82%, lead ion by 70%, nickel ion by 61%, zinc ion by 59% while the least adsorbed in the multi component system is cadmium by 36%.

The regeneration and reuse studies show that the adsorbent is effective up to the fourth cycle of regeneration for most of the studied parameters. The economy of regeneration of the adsorbent is high and that the regeneration process is a successful way to cut cost of preparation activated carbon from Neem husk.

6.3 Recommendation

The following recommendations are made from the study of wastewater treatment using neem activated carbon:

i. Further studies could be used to treat industrial and other municipal waste water with the neem activated carbon.
ii. Other activating agents and activating methods could be used to further modify the neem carbon to treat waste water or other effluents.
iii. Studies on combining neem activated carbon and other bio waste activated carbons in varied proportions can be undertaken.
iv. Studies on the pollution levels of farm produce and aquatic animals around the hospital treatment plant and water ways can be under taken.
v. Further studies on removal of the excess zinc ion and phosphate ion from the activated carbon can be undertaken.

REFERENCES

Abah, S.O. and Ohimain, E.I. (2010). Assessment of Dumpsite Rehabilitation Potential using the Integrated Risk Based Approach: A case study of Eneka, Nigeria. *World Applied Science Journal*, **8**(4): 436-442.

Abd El-Latifa, Mona Mahmoud and Amal Mozarei Ibrahim (2010). Removal of reactive dye from aqueous solutions by adsorption onto activated carbons prepared from oak sawdust. *Desalination and Water Treatment*, **20** (1): 1-3.

Abechi, E.S., Gimba, C.E., Uzairu, A. and Kagbu, J.A. (2011). Kinetics of adsorption of methylene blue onto activated carbon prepared from palm kernel shell. Arc modified Nigerian nanoclay ash. *Applied Science Research*, **3** (1):154-156.

Abedi-Koupaia, J. and Mohri-Esfahania, E. (2012). *Desalination of Water Using nanoparticles of Husk Ashes in Sand Filter*. Proceedings of the 4th International Conference on Nanostructures (ICNS4), Kish Island, I.R. Iran, pp. 1150-1152.

Abram, J.C. (1973). Paper presented at a conference on *Activated carbon in water treatment*. Organized by the Water Research Association held at the University of Reading, pp. 1-29.

Adamson, A.W. (1960*). Physical Chemistry of Surface*. Inter school publisher, pp. 457 - 458.

Adekunle I. M., Adetunji M. T., Gbadebo A. M and Banjoko O. B. (2007). Assessment of Groundwater Quality in a Typical Rural Settlement in Southwest Nigeria. *International Journal Environment Research.* **4**(4): 307-318.

Ademoroti, C.M.A (1996). *Standard Method for Water and Effluent Analysis*. Foludex press limited, Ibadan, Nigeria, pp. 22 - 54.

Adesemoye, A. O., Opere, B. O., & Makinde, S. C. O. (2006). Microbial content of abattoir wastewater and its contaminated soil in Lagos, Nigeria. *African Journal of Biotechnology*, **5** (1): 20 – 22.

Ahmad A.L. and Hameed (2009). Batch adsorption of methylene blue from aqueous solution by garlic peel, an agricultural waste biomass. *Journal of Hazardous Materials*, **164**(2), 870-875.

Ajibola, V.O. and Ladipo, M.K. (2009). Quality of Water Runoff Discharged from Some Industries into the Isolo Canal, Lagos. *Environmental Research Journal*, **3**(1): 107-112.

Akinwale, C., Mynepalli, K. C. and Sridhar (2010). Increase in healthcare facilities and rapid environmental degradation: A technological paradox in Nigeria's urban centres. *African Journal of Environmental Science and Technology*, **4**(9): pp. 577-585.

Aksu, Z. and Gonen F. (2004). Biosorption of phenol by immobilized activated sludge in a continuous packed bed: prediction of breakthrough curves, *Journal of Process Biochemistry*, **39**(1): 599–613.

Akter, N., Kazi, N. M. and Chowdhury, S. A. (1999). Environmental investigation of medical waste management system in Bangladesh with special reference to Dhaka City. BRAC. *Research and Evaluation Division*, *75*.

Alagoz, B.A.Z. and Kocasoy, G. (2007). Treatment and disposal alternatives for health-care wastes in developing countries – A case study in Istanbul, Turkey. *Waste Management. Research*, **25**(1): 83-89.

Alau, K. K., Gimba, C. E., Kagbu, J. A. and Nale, B. Y. (2011). Preparation of Activated Carbon from Neem (Azadirachta indica) husk by Chemical Activation with H_3PO_4, KOH and $ZnCl_2$. *Archives of Applied Science Research*, **2**(5), 451-455.

Al-Khatib, I.A., Al-Qaroot, Y.S. and Ali-Shtayeh, M.S. (2009). Management of healthcare waste in circumstances of limited resources: A case study in the hospitals of Nablus city, Palestine. *Waste Management Research*, **27**(4): 305-312.

Allen, S.E., Grimsham, J.A. and Quarmby, C. (1974). *Chemical Analysis of Ecological Materials*. Blackwell scientific publications, Oxford London, pp. 80 – 81.

Aloko, D. F. and Adebayo, G. A. (1997). Production and characterization of activated carbon from agricultural wastes (Rice husk and corn cob). *Journal of Engineering and Applied Sciences*, **2**(2): 440-444.

American Public Health Association, and American Water Works Association. (1998). Standard methods for the examination of water and wastewater: selected analytical methods approved and cited by the United States Environmental Protection Agency. American Public health association

Helrich, K. C. (1990). *Official methods of Analysis of the AOAC. Volume 2* (No. Ed. 15). Association of Official Analytical Chemists Inc..

Association of Official Analytical Chemists (AOAC) (1990). 15th Editions. Washington. D.C

Atkins, W. (2003). *Physical Chemistry Text Book*. Oxford University Press. Pp 988 - 989.

Awofolu, O.R. Duplessis, R. and Rampedi, I. (2007). Influence of Discharge Effluent on Water Quality of Surface Water Utilized for Agricultural Purposes. *African Journal of Biotechnology*, **6**(1): 2251-2258.

Babarinde, A.A.N. (2002). Adsorption of Zn (ll) and Cd (ll) by coconut husk and goat hair. *Journal of Pure and Applied Sci*ence, **5**(1): 81 – 85.

Bansal, R.P. and Goyal, M. (2005). *Activated Carbon Adsorption*. CRC Press, Taylor & Francis Group, 6000 Broken Sound Parkway NW, Suite 300 Boca Raton, FL, USA, pp. 3 –36.

Bansode, R.R., Losso, J.N, Marshall, W.E., Rao, R.M. and Portier, J.R. (2003). Adsorption of metal ions by Pecan Shell-based GACs. *Journal of Bioresource Technology*. **89**(1)**:** 115 – 119.

Bass, M.C., Cerrella, E.G. and Cukierman, A.L. (2002). Activated Carbon Developed from a Rapidly Renewable Biosource for Removal of Cadmium (ll) and Nickel (ll) ions from Dilute Aqueous Solution. *Industrial and Engineering Chemistry Research American Chemical Society*, **41** (2):180 – 189.

Bohart G.S. and Adams, E.Q. (1920) Behavior of charcoal towards chlorine. *Journal of Chemical Society* **42**(1): 523-529

Cheremisinoff, P. and Ellerbusch, F. (1978). *Carbon Adsorption Handbook*. Ann Arbor Science Published Inc, pp. 72, 689 – 690.

Christen, J. (1996). *Solid Waste Management in Developing Countries*. Sweden Icon Publishers, pp 55 -56.

Clescerl, Leonore S., Greenberg, Arnold E., and Eaton, Andrew D. (2010). *Standard Methods for the Examination of Water and Wastewater*. (Ed) American Public Health Association, Washington, DC.

Coker (2009). Medical waste management in Ibadan, Nigeria: Obstacles and Prospects. *Journal of Waste Manag*ement, **29**(2): 804- 811.

Dabrowski, A. (1998). Studies in Surface Science and Catalysis, *Elsevier Science*, **120**(1): 3–68.

Dada, A.O., Olalekan, A.P., Olatunya, A.M. and Dada, O. (2012). Langmuir, Freundlich, Temkin and Dubinin–Radushkevich Isotherms Studies of Equilibrium Sorption of Zn^{2+} Unto Phosphoric Acid Modified Rice Husk. *Journal of Applied Chemistry*. **3**(1): 38-45.

Daintith, J. (2000). A Dictionary of Chemistry. 4th (ed). Oxford University Press, pp 15.

Da Silver, C.E., Hoppe, A.E., Ravanello, M.M., Mello, N. (2005). Medical waste management in the south of Brazil. *Journal of Waste Management*, **25**(1): 600-605.

David, N. O., Alex, C. and Ndubuisi, U (2012). Waste management options for health care wastes in Nigeria. A case study of Port Harcourt hospitals. *Journal of Public Health and Epidemiology*. **4**(6): pp.156-169.

Demirbas, E., Kobya, M., Oncel, S., and Sencan, S. (2002). Removal of Ni (ll) From Aqueous Solution by Adsorption onto Hazelnut Shell Activated Carbon: *Bioresource Technology*, **84**(1): 291 – 293.

Devi, B. Veena, Jahagirdar, A. A., Zulfiqar, A. M.N. (2012). Adsorption of Chromium on Activated Carbon Prepared from Coconut Shell. *International Journal of Engineering Research and Applications (IJERA)*, **2**(5): pp. 364-370.

Diaz-Teran, J.D.M., Nevskaia, A.J. Lopez-Peinado and A. Jerez (2001). Porosity and adsorption properties of an activated charcoal colloids and surface. *A physiochem and engineering aspects*, 187 – 188; 167-175.

Dwivedi, C.P., Sahu, J.N., Mohanty, C.R., Mohan, B.R. and Meikap, B.C. (2008). Column performance of granular activated carbon packed bed for Pb(II) removal. *Journal of Hazardous Materials*, **156**(1): 596–603.

Ekpete, O. A. and Horsfall, M. J. N. R. (2011). Preparation and characterization of activated carbon derived from fluted pumpkin stem waste (Telfairia occidentalis Hook F). *Research Journal Chemical Science,* **1**(3): 10-17.

Elliott, C., Colby, T. And Iticks, H. (1989). Activated carbon obliterans alter aspiration of activated charcoal. *Chest*, **96**(3), 672-674.

Emine Malkoc, Yasar Nuhoglu and Murat Dundar (2006). Studies Adsorption of chromium(VI) on pomace - An olive oil industry waste: Batch and column studies. *Journal of hazardous materials*. **138** (1): 142-151.

Escher, B.I., Baumgartner, R., Koller, M., Treyer, K., Lienert, J. and. McArdel, C.S. (2011). Environmental toxicology and risk assessment of pharmaceuticals from hospital wastewater. *Journal of* w*ater research,* **45**(1): 75-92.

Federal Environmental Protection Agency (1991)

Ferreira, A.P. and Veiga, M.M. (2003). Hospital waste operational procedures: A case study in Brazil. *Waste Management Research*, **21**(1): 377-382.

Freundlich, M. F. (1906). Uber die adsorption in losungen. *Physical Chemical Journal*, **57**(A): 385–470.

FWPCA (Federal Water Pollution Control Administration) (1968). Water Quality Criteria: Report of the National Technical Advisory Committee to the Secretary of the Interior. U. S. coastal Cities, pp. 32-34.

Gary, V.K., Gupta, R., Yadav, A. and Kumar, K., (2003). Dye Removal from Aqueous Solution by Adsorption on Treated Sawdust. *Bioresource Technology*, **89**(1)**:** 121-124.

Gauntlett, R.B. and Packman, R.F. (1973). *The use of activated carbon in water treatment*. A paper presented at a conference on Activated Carbon in Water Treatment, organized by the Water Research Association held at the University of Reading. Pp. 31 -51.

Gimba, C.E. (2001). *Preparation and Adsorption of Activated Carbon from Coconut Shell.* A Ph. D Dissertation, Department of Chemistry, Ahmadu Bello University, Zaria, Nigeria.

Gimba, C.E., Olayemi, J.Y., Okunnu, S.T. and Kagbu, J.A., (2001). Adsorption of ethylene Blue by Activated carbon from Coconut Shell. *Global Journal of Pure and Applied Sciences*, **7**(2):265-267.

Gimba, C. Ocholi and O. Nok, A. (2004). Preparation of Activated Carbon from Agricultural wastes II Cyanide binding with activated carbon matrix from groundnut shell. *Nigeria journal of scientific research,* **4** (2): 106-110.

Goel Jyotsna, Krishna Kadirvelu, Chitra Rajagopal, and Vinod Kumar (2005). Removal of Lead (II) by Adsorption Using Treated Granular Activated Carbon: Batch and Column Studies. *Journal of Hazardous Materials*,**125**(1): 211–220.

Greenberg, A. E., Clesceri, L.S and Eaton, A.D. (1980). *Standard Methods for the Examination of Water and Wastewater*. American Waster Environment Federation, Washington, pp. 195-239.

Guzel, F. and Uzun, İ. (2002). Determination of the micropore structures of activated carbons by adsorption of various dyestuffs from aqueous solution. *Turkish Journal of Chemistry*, **26**(3): 369-378.

Hajira, H. and Muhammed, S. (2008). Removal of Fast Green Dye from an Aqueous solution Using Azairachta Indica Leaf Powder As Low Cost Adsorbent. *African Journal of Biotechnol*. **7**(21): 3906-3911.

Hassler, J. W. (1974). Purification with Activated Carbon; industrial, commercial, environmental.

Hazard, J. Mater. (2006). Adsorption of chromium (VI) on Pomace-An Olive industry waste: Batch and column studies. *Journal of hazardous materials*. **138** (1), 142-151.

Hendricks, D. W. (2006). *Water treatment unit processes: physical and chemical*. CRC press.

Ho, Y. S. and McKay, G. (1998). A Comparison of Chemisorption Kinetic Models Applied to Pollutant Removal on Various Sorbents. *Transitional Inorganic Chemical Journal*, **76** (B): 332-340.

Hung, Y.T., Lo, H.H., Wang, L.K., Taricska, J.R., and Li, K.H. (2005) Granular activated carbon adsorption, in Physicochemical Treatment Processes, Handbook of Environmental Engineering.

Igwe, J. C. and Abia, A. A. (2007). Adsorption isotherm studies of Cd (II), Pb (II) and Zn (II) ions bioremediation from aqueous solution using unmodified and EDTA-modified maize cob. *Eclética Química*, **32** (1), 33-42.

Inglezakis, V. and Poulopoulos, S. (2006). Adsorption, ion exchange and catalysis: design of operations and environmental applications. *Elsevier*, (3),

Itodo, A.U., Abdulrahman, F. W., Hassan, L. G., Maigandi, S.A. and Abubakar, M. N. (2009). Activation Chemistry and kinetic studies nut shells biosorbent for textile

waste water treatment. *Journal of research in Science, Education, Information and Communication Technology,* **1**(1):168-177.

Jaroniec, M. and Madey, R. (1988). Physical adsorption on heterogeneous solids. Studies in physical and theoretical chemistry, *59*.

John, L. Rose (1998). Advanced waste treatment of secondary effluent with activated carbon pp. 65 – 72.

Jovanović, D. S. (1969). Physical adsorption of gases. *Kolloid-Zeitschrift und Zeitschrift für Polymere*, **235**(1), 1214-1225.

Kadirvelu, K. and Namasivayam, C. (2000). Agricutural by-product as metal adsorbent: Sorption of lead (II) from aqueous solution onto coirpith carbon.*Environmental Technology*, **21**(10), 1091-1097.

Kadirvelu, K., Kavipriya, M., Karthika, C., Radhika, M., Vennilamani, N. and Pattabhi, S. (2003). Utilization of various agricultural wastes for activated carbon preparation and application for the removal dyes and metal ions. From aqueous solutions. *Bioresource Technology*, **87**(1):129-132.

Kagbu, J.A., Amupitan, J.O., Oyedeji, J.O. and Elaigwu, P. (2001). Evaluation of Yankassa sheep wool as an adsorptive matrix for bleaching textile effluents. *Journal Chemical Society Nigeria*. **26** (1): 14-16.

Kannan, N. and Meenakshisundaram, M., (2001). Adsorption of Congo Red on Activated Carbon: A Comparative Study. *Water, air and soil pollution*. **138**(1): 289 – 305

Kaushik, N., Gor, J.P., Shah, P.N. and Modi, K. (2007). Physicochemical parameters, isotherms, sorption kinetics and column operations for adsorption of copper (II) from wastewater using fly ash. *Journal of Scinetific and Industrial research*, **66**(1): 170-177.

Kazemipour, M., Ansari, S., Tajrobehkar, M., Majdzadeh, H. and Reihani, K. (2008). Removal of lead, cadmium, zinc, and copper from industrial wastewater by carbon developed from walnut, hazelnut, almond, pistachio shell, and apricot stone. *Journal of Hazardous Materials*, **150**(1): 322-327.

Khan, A. R., Ataullah, R. and Al-Haddad, A. (1997). Equilibrium adsorption studies of some aromatic pollutants from dilute aqueous solutions on activated carbon at different temperatures. *Journal of colloid and interface science*,**194**(1), 154-165.

Kulkarni, S.J. (2013). Removal of organic matter from domestic waste water by adsorption, *International Journal of Science, Engineering and Technology Research.* **2(**10): 1836-1839.

Kumar, A., Bisht, B. S., Joshi, V. D., Singh, A. K. and Talwar, A. (2010). Physical, chemical and bacteriological study of water from rivers of Uttarakhand. *Journal of Human Ecology*, **32**(3), 169-173.

Lafi, W.K., (2001). Production of activated carbon from a corns and olive seed. *Journal of Biomass and Bioenergy*, **20**(1):57-62.

Langmuir, I. (1918). The sorption of gases on plane surfaces of glass, mica and platinum. *Journal of America Chemical Society*, **40**(9): 1361-1403.

Lars Stixrude, Evgeny Waserman and Ronald Cohen . (1997). Composition and temperature of Earth's inner core. *Journal of Geophysical Research* (American Geophysical Union), **102** (B11): 24729–24740.

Lartey, R. B., Acquah, F. and Nketia, K. S. (1999). Developing national capability for manufacture of activated carbon from agricultural wastes. *Ghana Eng*, **19**(1), 1-2.

Liao, X., Zhang and M., Shi, B. (2004). Collagen-fiber-immobilized tannins and their adsorption of Au(III*). Industrial and Engineering Chemistry Research*, **43**(1): 2222–2227

Longe, E. O. and Williams, A. (2006). A preliminary study of medical waste management in Lagos metropolis, Nigeria. *Iranian Journal of Environmental Health Science and Engineering*, **3**(2), 133-139.

Loo, T.G. (1974). *Activated carbon carbon from coconut shells*. Royal tropical Institute. Publication, the Neitherlands. Pp. 1-2.

Mattson, J. S. and Mark, H. B. (1971). *Activated carbon: surface chemistry and adsorption from solution*. Pp. 23 – 35.

McDougall, G.J., Handcock, R.D., Nicol, M.J., Washington, O.I. and Copperthwatyh, R.G. (1982). The mechanism of adsorption of goal cyanide on activated carbon. *Journal South African Institute Mining Metal*, **80**(1): 344-356.

Menendez-Diaz, J.A. and Gullon, I.M. (2006). *Types of carbon adsorbents and their production, in Activated Carbon Surfaces in Environmental Remediation*. T.J. Bandosz, *Elsevier*, Printed in the Netherlands, pp. 1–47.

Mesfin, K.D., Gelaye, K. A., Alamdo, A. G. and Trifa, Z. M. (2013). Assessment of the health care waste generation rates and its management system in hospitals of Addis Ababa, Ethiopia, *BMC public health*, **13**(1), 28-29.

Morrison, G., Fatoki, O. S., Persson, L. and Ekberg, A. (2001). Assessment of the impact of point source pollution from the Keiskammahoek Sewage Treatment Plant on the Keiskamma River-pH, electrical conductivity, oxygen-demanding substance (COD) and nutrients. *Water SA*, **27**(4), 475-480.

Mozammel, H.M., Masahiro, O. and B., S.C. (2002). Activated charcoal from coconut shell using $ZnCl_2$ activation. *Biomass and Biomass and Bioenergy,* **22**(1):397–400

Mumtaz, H. and Mirza, M. M. (2014). Awareness about Hospital Wastes and its effects on the Health of Patients in District Dera Ghazi Khan. *Asian Journal of Applied Science and Engineering*, **3**(3), 301-308.

Ndidi, N., Nelson, O., Patricia, O., John, S. A. (2009). Waste management in healthcare establishments within Jos Metropolis, Nigeria, *African Journal of Environmental Science and Technology*. **3**(12) 459-465.

Ngwuluka, N., Ochekpe, N., Odumosu, P. and John, S. A. (2009). Waste management in healthcare establishments within Jos Metropolis, Nigeria.*African Journal of environmental science and technology,* **3**(12): 459-465.

Nigerian Industrial Standard (NIS) (2007). *Requirements, Nigerian Standard for Drinking Water Quality*, NIS 554. pp 15-22.

Ocholi, O. (2006). Studies on the Preparation and Adsorption of activated Carbon Matrices from Delonix regia Pods and Khaya senegalensis Fruits. Unpublished M.Sc. Thesis, AhmaduBello Universiy, Zaria.

Ogunlowo, O.O., Coker, A.O. and Sangodoyin, A.Y. (1991). Managing Hospital Waste in Nigeria. 24th WEDC Conference: Sanitation and Water for All.

OMRI (2002). Activated Carbon Processing. National Organic Standards Board Technical Advisory Panel Review for the USDA National Organic Program. Pp. 1-14.

Parfitt, G.D. and Sing, K.S.W. (1976). Characterization of Powdered Surfaces, Academic Press pp. 15-51.

Patil, V. G. and Pokhrel, K. (2004). Biomedical solid waste management in an Indian hospital: a case study. *Journal waste management*. **25**(1): 592–599.

Prayitno, Zaenal K, Bagyo Y. and Rudy W. L. (2013). Study of Hospital Wastewater Characteristic in Malang City. *International Journal of Engineering and Science* **2**(2): 13-16.

Pruss, A., Kay, D., Fewtrell, L., & Bartram, J. (2002). Estimating the burden of disease from water, sanitation, and hygiene at a global level. *Environmental health perspectives*, **110**(5), 537-542.

Purcell, P.J. (2006). Milestones in the development of municipal water treatment science and technology in the 19th and early 20th centuries: part I. *Water and Environment Journal*, **19**(3): 230–237.

Qasem, S. M. (1997). *Production of activated carbon by chemical activation of jift using a fluidized bed reactor* (Doctoral dissertation, M. Sc. Thesis, University of Jordan).

Rani, D. and Dahiya, R.P. (2008). COD and BOD removal from domestic wastewater generated in decentralised sectors. *Journal* r*esource Technology*, **99**(1): 344–349.

Redlich, O. J. D. L. and Peterson, D. L. (1959). A useful adsorption isotherm. *Journal of Physical Chemistry*, **63**(6), 1024-1024.

Reza, A., Seyghali, B., Mohammad-Khah, A. And Zanjanchi, M. A. (2012). Highly efficient adsorption of anionic dyes from aqueous solutions using sawdust

modified by cationic surfactant of cetyltrimethylammonium bromide.*Journal of Surfactants and Detergents*, **15**(5), 557-565.

Rhodes, G., Huy, G., Swings, J., McGann, P., Hiney, M., Smith, P. and Pickup, W.R. (2000). Distribution of oxytetracycline resistance plasmids between Aeromonads in hospital and aquaculture environments: Implications of Tn172 in dissemination of the tetracycline resistance determinant Tet A. *Applied Environmental and Microbiology*. **66**(9): 3883-3890.

Rivera-Utrilla, J., Bautista-Toledo, I., Ferro-Garcı´a, M. A. and Moreno-Castilla, C. (2001). Activated carbon surface modifications by adsorption of bacteria and their effect on aqueous lead adsorption. *Journal chemical Teachnol Biotechnol*, **76**(1):1209–1215.

Sahira Joshi, Adhikari Mandira, Pokharel Bhadra Prasad and Pradhananga Raja Ram (2013). Effects of Activating Agents on the Activated Carbons Prepared from Lapsi Seed Stone. *Research Journal of Chemical Sciences*, **3**(5): 19-24.

Sandhya Babel and Tonni Agustiono Kurniawan (2003). Cr(VI) removal from synthetic wastewater using coconut shell charcoal and commercial activated carbon modified with oxidizing agents and/or chitosan. *Chemosphere* **54**(1): 951–967.

Satone, A.K., Bajoria, J.R., Tekade, P.V. and Mohabansi, N.P. (2011). Monitoring of drinking water quality of M.I.D.C. of Wardha city, Maharashtra. *Rasayan Journal of Chemistry* **4**(4): 910-913.

Selvi, K., Pattabhi, S., Kadirvelu, K., (2001). Removal of Cr (Vl) from Aqueous Solution by Adsorption Onto Activated carbon. *Bioresource Technology*, **80**(1): 87-89.

Sontheimer, H., Crittenden, J., and Summers, R.S. (1988). Activated Carbon for Water Treatment, Forschungstelle Engler – Bunte- Institute, Universita¨t Karlsruhe, Karlsruhe, Germany.

Shrihari, V., Babu, M. and Das, A. (2005). Kinetics of phenol sorption raw agro-based wastes. *Journal of Applied Sciences*, **6**(1): 47–50.

Shrihari, V. and Das, A. (2009). Adsorption of phenol from aqueous media by an agro-waste (Hemidesmus Indicus) based activated carbon. *Applied Ecology and Environmental Research*, **7**(1): 13–23.

Stephen, O. and Elijah, I.O. (2011). Healthcare waste management in Nigeria: A case study. *Journal of Public Health and Epidemiology* **3**(3): 99-110.

Sun, J., Hippo, H., Marsh, H., O'Brien, W.S.O. and Crelling, J.C. (1997). Activated Carbon produced from an Illinois Basin Coal Carbon. *Elsevier*, **35**(3): 341–352

Sunil K. B. and Arti J. (2010). Removal of copper (II) from aqueous solution using spent tea leaves (STL) as a potential sorbent. *Water SA* **36**(3): 0378 – 4738.

Takeo Nakamura, Toshimitsu Tokimota, Takamichi Tamura, Naohilo Kawasaki and Seiki Tanada (2003). Decolorization of Acidic Dye by Charcoal from Coffee. *Journal of Health Science*, **49**(6): 520 – 523.

Tchnohanoglous, G., Theisen, H. and Eliassen, R. (1979). Solid Waste Engineering Principles and Management Issues, McGraw-Hill Book Co., USA.

Thomas, J.W. and Crittenden, B. (1998). Adsorption Technology and Design, Butterworth Heinemann pp.1-51.

Townend, W.K. and Cheeseman, C.R. (2005). Guidelines for the evaluation and assessment of the sustainable use of resources and of wastes management at healthcare facilities. *Waste Management Research*, **23**(1): 398- 408

Tripathi, S., Chapman, W.G. (2003). A density functional approach to chemical reaction equilibria in confined systems: Application to dimerization. *Ournal of Chemical and Physics*, **118**(17): 118, 7993.

Tsai, W.T., Chang, C.Y., Wang, .S.Y., Chang, C.F., Chien, S.F. and Sun, H.F. (2001). Cleaner production of carbon adsorbents by utilizing agricultural waste corn cob. Elsevier. **32**(1): 43–53.

Tudor, T.L., Noonan, C.L. and Jenkin, L.E.T. (2005). Healthcare waste management: A case study from the Cornwall NHS, UK. *Waste Management Journal*, **25**(1): 606-615

Turoti, M., Gimba, C.E., Ocholi, O. and Nok, A.J. (2007). *ChemClass Journal CSN* Zaria. **31**(7): 24-31.

United State Environmental Protection Agency, Washington, D.C. (2008). "Septic Systems Fact Sheet." EPA publication no. 832-F-08-057.

Uzoigwe, C. I. and Okpokwasili, G. C. (2012). Biodegradation of oil spill dispersants in natural aquatic ecosystem. *International Journal of Physical Sciences,* **7**(38): 5477-5484.

Uzunova S., Uzunov, I. and Angelova D. (2013). Liquid-phase sorption of oil by carbonized rice husks: impact of grain size distribution on the sorption kinetics. *Journal of Chemical Technology and Metallurgy*, **48**(5): 505-512.

Walker, J. T., Verran, J., Boyd, R. D. and Percival, S. (2001). Microscopy methods to investigate structure of potable water biofilms. *Methods in enzymology*, *337*, 243-255.

Weber, W. and Morris, J. (1963). Kinetics of adsorption on carbon from solution. *Journal of Sanitery Engineering Division ASCE*, 89 (SA2): 31-59

Weber, W.J.Jr (1973). 'The prediction of the performance of activated carbon for water treatment'. A paper presented at a conference on, Activated carbon in water treatment', organized by the Water Research Association held at the University of Reading, (3^{rd} – 5^{th} April, 1973), pp. 53-71.

Wentz, C. W. (1995). Hazadous Waste Management, Second Edition, McGraw-Hill, New York, pp. 201-202.

World Health Organisation. (1999). *Unsafe injection practices and transmission of blood borne patogens. Bull*. World Health Organization, **77**: 787-819.

Wyasu, G. and Okereke, N.Z (2012). The influence of hospital wastewater and food samples grown within Ahmadu Bello University teaching hospital, Zaria-Nigeria on its receiving environment. *Advances in Applied Science Research*, **3**(3):1686-1690.

Yadav, S.S. and Kumar, R. (2011). Monitoring Water quality of Kosi River in Rampur District, Uttar Pradesh, India. *Applied Science Research*, **2**(2): 197-201.

Yehaskel, A. (1978). *Activated carbon: Manufacture and regeneration*. Park Ridge, New Jersey, USA: Noyes Data Corporation. Pg.1, 66-67

APPENDICES

Appendix I: Ethical Approval

UNIVERSITY OF ABUJA TEACHING HOSPITAL

P.M.B. 228, ABUJA - F.C.T. NIGERIA
07040045614, 09-2905535, 09-2904040
www. uath. ng.org.

Chief Medical Director
Dr. Peter Alabi
BM. BCH, FMCP

Chairman, Board of Management
Valentine I. Attah Ph D

Director of Administration
Musa Abdullahi
MPA, AHAN

Chairman Medical Advisory Committee
Dr. A.S. Haruna
MBBS, FWACP

Our: FCT/UATH/HREC/PR/386

Your Ref: _____

Date: 24/7/14

Kenneth Alau Kukhiyep
Dept. of Chemistry
A B U, Zaria

RE: Modification of Neem (Azadirachta Indica) Husk and Neem Cake Activated Carbon for the Treatment of hospital Wastewater

I am happy to inform you that approval has been given to conduct the above named study.

The approval is for one year and will lapse on 23/7/15. It can be renewed on request. If for any reason the study is not commenced as per the expected date, the committee should be appropriately informed.

Any changes to the protocol would necessarily require an approval from committee.

Best wishes.

Edith Akanya (Mrs
Secretary, UATH HREC

Appendix II: Physicochemical Properties of Hospital wastewater before and after treatment with adsorbents

Parameters	Before Treatment RWW	After treatment with NCZ	NCH	NHZ	NHH	SDW
pH	6.40±0.05	5.78±0.08	5.74±0.09	5.27±0.07	5.07±0.02	6-8.00
Conductivity (µS/cm)	77.0±6.74	53.4±8.75	17.0±7.08	19.5±4.12	28.9±8.25	-
TDS (g/L)	40.5±5.20	30.9±4.41	8.8±3.12	10.2±5.74	15.8±6.94	100.00
Turbidity (NTU)	56.0±1.30	1.0±0.34	5.0±1.09	5.0±1.94	1.0±0.32	300.00
Nitrite (mg/L)	9.72±0.02	0.01±0.01	0.12±0.03	0.11±0.01	0.03±0.01	20.00
Phosphate (mg/ml)	1.26±0.64	0.14±0.06	7.52±1.63	0.06±0.02	3.48±0.40	5.00
Chloride (mg/ml)	1.76±0.03	0.31±0.02	1.33±0.01	0.07±0.02	0.01±0.00	500.00
COD (mg/ml)	280±6.34	215±7.20	190±4.92	190±5.32	210±4.12	100.00
BOD (mg/ml)	15±2.20	7±1.30	11±2.11	11±3.47	7±2.79	50.00
DO (mg/ml)	39±5.12	30±3.49	38±7.63	39±4.87	38±6.87	-
Hardness (g/ml $CaCO_3$)	3939±21.20	1423±15.20	1621±17.08	1402±8.12	1505±17.22	150.00
Bacterial count (CFU/100ml)	4.27*10^5±70.12	2600±25.12	3000±24.25	3100±26.65	2800±24.12	10,000
Fungal count (CFU/100ml)	24,000±12.00	2700±4.00	2400±4.00	3400±11.12	2300±19.71	10,000
Cadmium, Cd (mg/ml)	0.12±0.02	0.10±0.06	0.10±0.01	0.08±0.01	0.09±0.01	0.10
Chromium, Cr (mg/ml)	0.73±0.02	0.31±0.01	0.53±0.01	0.13±0.01	0.39±0.02	0.05
Zinc, Zn (mg/ml)	4.24±0.92	7.02±0.64	1.74±0.03	7.35±1.04	2.40±0.20	5.00
Nickel, Ni (mg/ml)	3.80±0.20	1.47±0.10	1.91±0.10	1.75±0.20	2.23±0.20	1.00
Lead, Pb (mg/ml)	1.97±0.30	0.59±0.10	1.59±0.20	1.59±0.20	1.34±0.30	0.10

RWW represents Raw WasteWater; *NCZ* and *NCH* represent Neem cake activated with $ZnCl_2$ and H_3PO_4 respectively; *NHZ* and *NHH* represent Neem husk activated with $ZnCl_2$ and H_3PO_4 respectively; C*OD* represents the Chemical Oxygen demand; *DO* is the dissolved Oxygen and *BOD* is the Biological Oxygen Demand: S*DW* represent Standard of Discharge of Wastewater as listed in NIS (2007); [a]Escher , (2011); [b]Kumar *et al.* (2010)

Appendix III: Effect of bed height on breakthrough time

Mass of NHH used	Bed height (X)	Breakthrough time (t)	Adsorption capacity, $Q_{0.5}$
11.46	3	3.9	10.32
15.28	4	4.8	9.53
19.1	5	5.4	8.58
22.92	6	5.8	7.68

Appendix IV: Federal Environmental Protection Agency (Maximum Permissible Limit)

1. 1,1,1, -trichloroethane ---------- 3.0 mg/1
2. 1,1,2.- dichloroethyelene ---------- 0.2 mg/1
3. 1,1, 2,- Trichloroethne ---------- 1.06 mg/1
4. 1,2- Dichloroethane ---------- 0.04 mg/1
5. 1,3- dichloropropene ---------- 0.2 mg/1
6. Aluminum ---------- 0.5 mg/1
7. Ammonia Nitrogen ---------- 10 mg/1
8. Arsenic ---------- 0.2 mg/1
9. Barium ---------- 10 mg/1
10. Benzene ---------- 0.2 mg/1
11. BOD5 ---------- 50 mg/1
12. Boron ---------- 5 mg/1
13. Cadmium ---------- 0.1 mg/1
14. Calcium ---------- 100 mg/1
15. Chloride ---------- 500 mg/11
16. Chlorine ---------- 1 mg/1
17. Chromium (total) ---------- 1.0 mg/1
18. Chromium (VI) ---------- 0.05 mg/1
19. Cirrus- 1,2 - dichloroethylene -- mg/1
20. Cobalt ---------- mg/1
21. COD ---------- 100
22. Clifford Organisms---------- 10,000 counts/100 ml
23. Color ---------- 300 TCU
24. Copper ---------- 1.0 mg/1
25. Cyanide ---------- 0.1 mg/1
26. Detergents ---------- 10 mg/1
27. Dichloromethane ---------- 0.2 mg/1
28. Iron ---------- 10 mg/1
29. Lead ---------- 0.1 mg/1
30. Magnesium ---------- 100mg/1
31. Manganese ---------- 1.0 mg/1
32. Mercury ---------- 0.01 mg/1
33. Nickel ---------- 1.0 mg/1

34. Nitrite - N ---------- 20 mg/1
35. Nitrite - N ----------2.0 mg/1
36. Nitrogen total ---------- 10 mg/1
37. Oil and Grease ---------- 10 mg/1
38. pH ---------- 6.0-8.0
39. Phenols ---------- 0.2 mg/1
40. Phosphate (total) ---------- 10 mg/1
41. Phosphate (soluble) ---------- 5.0 mg/1
42. Selenium ----------1.0 mg/1
43. Silver ----------0.5 mg/1
44. Sulfate ----------500 mg/1
45. Sulfide ---------- 1.0 mg/1
46. TDS ---------- 1200 mg/1
47. Temperature ---------- 20-350C
48. Tetra Cholera ethylene -------- 0.1 mg/1
49. Tetrachloromethananc --------- 0.02 mg/1
50. Tin ---------- 5 mg/1
51. Total Suspended Solids ------- 100 mg/1
52. Tricholoroethylene ---------- 0.3 mg/1
53. Turbidity ---------- 300 NTU
54. Zinc ---------- 5 mg/1

Federal Environmental Protection Agency (FEPA), 1991